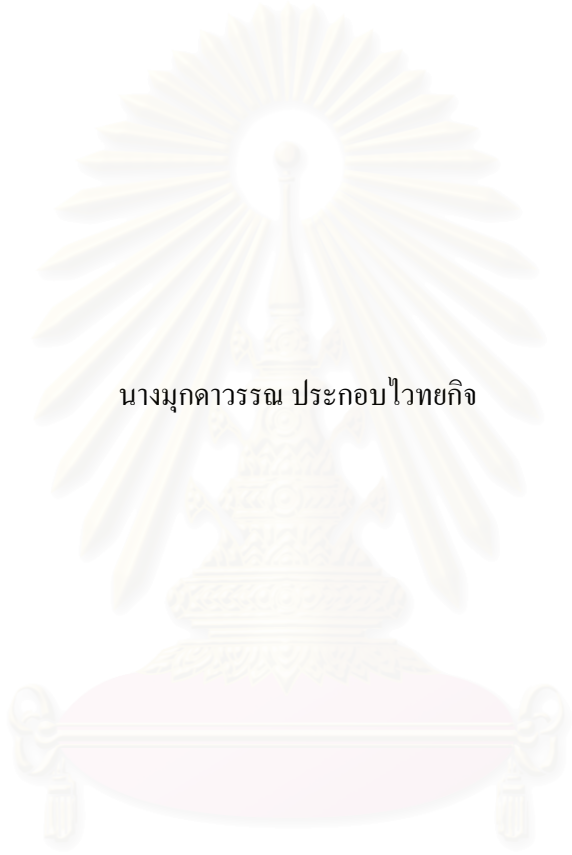การศึกษาเปรียบเทียบนาโนพาร์ทิเคิลที่บรรจุไอทราโคนาโซลโดยใช้พอลิไอโซบิวทิลไซยาโนอไครเลต

และพอลิ (ดีแอล-แลคไทด์-โค-ไกลโคไลด์)เป็นตัวพายา

นางมุกดาวรรณ ประกอบไวทยกิจ

COMPARATIVE STUDY OF ITRACONAZOLE-LOADED NANOPARTICLES USING POLYISOBUTYLCYANOACRYLATE AND POLY (DL-LACTIDE-CO-GLYCOLIDE) AS DRUG CARRIERS

Mrs. Mukdavan Prakobvaitayakit

Thesis Title   Comparative Study of Itraconazole-Loaded Nanoparticles Using Polyisobutylcyanoacrylate and Poly (DL-Lactide-Co-Glycolide) As Drug Carriers

By   Mrs. Mukdavan Prakobvaitayakit

Field of Study   Pharmaceutics

Thesis Advisor   Associate Professor Ubonthip Nimmannit, Ph.D.

Accepted by the Faculty of Pharmaceutical Sciences, Chulalongkorn University in Partial Fulfillment of the Requirements for the Doctor's Degree

……….…………………….Dean of the Faculty of Pharmaceutical Sciences
(Associate Professor Boonyong Tantisira, Ph.D.)

THESIS COMMITTEE

…………………………………………….. Chairman
(Associate Professor Garnpimol C. Ritthidej, Ph.D.)

………………………………………….……. Thesis Advisor
(Associate Professor Ubonthip Nimmannit, Ph.D.)

…………………………………………….. Member
(Associate Professor Supol Durongwatana, Ph.D.)

…………………………………………….. Member
(Associate Professor Parkpoom Tengamnuay, Ph.D.)

…………………………………………….. Member
(Assistant Professor Panida Vayumhasuwan, Ph.D.)

…………………………………………….. Member
(Narueporn Sutanthavibul, Ph.D.)

…………………………………………….. Member
(Saisampun Suwachrungoon)

มุกดาวรรณ ประกอบไวทยกิจ : การศึกษาเปรียบเทียบนาโนพาร์ทิเคิลที่บรรจุไอทราโคนาโซลโดยใช้
พอลิไอโซบิวทิลไซยาโนอครีเลตและพอลิ (ดีแอล-แลคไทด์-โค-ไกลโคไลด์) เป็นตัวพายา
(COMPARATIVE STUDY OF ITRACONAZOLE-LOADED NANOPARTICLES USING
POLYISOBUTYLCYANOACRYLATE AND POLY (DL- LACTIDE- CO-GLYCOLIDE) AS DRUG
CARRIERS) อ. ที่ปรึกษา : รศ.ดร. อุบลทิพย์ นิมมานนิตย์, 326 หน้า.   ISBN 974-17-5068-4

งานวิจัยนี้ได้ถูกออกแบบเพื่อหาความเหมาะสมของนาโนพาร์ทิเคิลที่บรรจุยาไอทราโคนาโซลที่เตรียม
จากพอลิไอโซบิวทิลไซยาโนอครีเลต (PIBCA) และพอลิ (ดีแอล-แลคไทด์-โค-ไกลโคไลด์) (PLGA) โดยใช้ การ
ออกแบบแบบแฟคทอเรียล (factorial design) และ ระเบียบวิธีเรสพอนซ์ เซอรเฟส (response surface
methodology)   ในงานวิจัยนี้ยังได้ตรวจสอบความคงตัวและความเป็นพิษต่อเซลล์ของนาโนพาร์ทิเคิลทั้งสอง
ชนิดด้วย โมเดลที่ได้ทดสอบถูกต้องทางสถิติที่มีตัวเลขนัยสำคัญ (P<0.05) ได้ถูกพัฒนาขึ้น โดยเป็นฟังก์ชั่น
ระหว่างขนาดของอนุภาค, การกระจายของขนาดอนุภาค, จำนวนไอทราโคนาโซลที่ถูกจับในนาโนพาร์ทิเคิล
และประสิทธิภาพในการหุ้มรอบตัวยากับพอลิเมอร์หรือโมโนเมอร์, เบนซิล เบนโซเอต และ ไอทราโคนาโซล
ออพติไมเซชันแบบใช้ตัวตอบสนองหลายตัว (Multiple response optimizations) ทำโดยใช้รูปกราฟคอนทัวร์
(contour plots) ของตัวตอบสนองหลายๆตัวมาทับกัน   และ วิธีการให้เข้าถึงวัตถุประสงค์ (desirability
approach) ทำให้ได้สูตรที่เหมาะสมของนาโนพาร์ทิเคิลที่มีไอทราโคนาโซล   500 ไมโครกรัมต่อมิลลิลิตร
ส่วนประกอบของนาโนพาร์ทิเคิล ที่บรรจุไอทราโคนาโซลที่เตรียมจากพอลิ (ดีแอล-แลคไทด์-โค-ไกลโคไลด์) ประ
กอบด้วย PLGA 10 มิลลิกรัมต่อมิลลิลิตร, เบนซิล เบนโซเอต 16.94 ไมโครกรัมต่อมิลลิลิตร และ ไอทราโค-
นาโซล 1001.01 ไมโครกรัมต่อมิลลิลิตร ในขณะที่ นาโนพาร์ทิเคิลที่บรรจุไอทราโคนาโซลที่เตรียมจากพอลิไอ-
โซบิวทิลไซยาโนอครีเลต ประกอบด้วย ไอโซบิวทิลไซยาโนอครีเลต 8.09 ไมโครลิตรต่อมิลลิลิตร, เบนซิล
เบนโซเอต 10.19 ไมโครกรัมต่อมิลลิลิตร และไอทราโคนาโซล 1200.77 ไมโครกรัมต่อมิลลิลิตร

การนำการออกแบบแบบแฟคทอเรียลและระเบียบวิธีเรสพอนซ์ เซอรเฟสมาใช้นั้นประสบผลสำเร็จใน
การสร้างโมเดลทางสถิติของขนาดของอนุภาค, การกระจายของขนาดอนุภาค, จำนวนไอทราโคนาโซลที่ถูกจับ
ในนาโนพาร์ทิเคิล และประสิทธิภาพในการหุ้มรอบตัวยาที่เป็นฟังก์ชั่นของตัวแปรที่ใช้ในสูตรตำรับ สูตรตำรับที่
เหมาะสมของนาโนพาร์ทิเคิลที่บรรจุไอทราโคนาโซลที่เตรียมจากพอลิไอโซบิวทิลไซยาโนอครีเลตมีความคงตัว
มากกว่านาโนพาร์ทิเคิลที่บรรจุไอทราโคนาโซลที่เตรียมจากพอลิ (ดีแอล-แลคไทด์-โค-ไกลโคไลด์) ทางกลับกัน
ความเป็นพิษต่อเซลล์ของนาโนพาร์ทิเคิลเปล่าที่เตรียมจากพอลิ (ดีแอล-แลคไทด์-โค-ไกลโคไลด์) และ นาโน-
พาร์ทิเคิลที่บรรจุไอทราโคนาโซลที่เตรียมจากพอลิ (ดีแอล-แลคไทด์-โค-ไกลโคไลด์) มีน้อยกว่านาโนพาร์ทิเคิล
เปล่าที่เตรียมจากพอลิไอโซบิวทิลไซยาโนอครีเลต และ นาโนพาร์ทิเคิลที่บรรจุไอทราโคนาโซลที่เตรียมจากพอลิ
ไอโซบิวทิลไซยาโนอครีเลตอย่างเด่นชัด   ค่า IC_{50} โดยประมาณของนาโนพาร์ทิเคิลที่เตรียมจากพอลิ (ดีแอล-
แลคไทด์-โค-ไกลโคไลด์)   และ   นาโนพาร์ทิเคิลที่เตรียมจากพอลิไอโซบิวทิลไซยาโนอครีเลตเท่ากับ   79.2
มิลลิกรัมต่อมิลลิลิตร และ 114 ไมโครกรัมต่อมิลลิลิตรตามลำดับ

ภาควิชา   เภสัชกรรม   ลายมือชื่อนิสิต ....
สาขาวิชา   เภสัชกรรม   ลายมือชื่ออาจารย์ที่ปรึกษา...............................
ปีการศึกษา   2546   ลายมือชื่ออาจารย์ที่ปรึกษาร่วม...........................

MUKDAVAN PRAKOBVAITAYAKIT : COMPARATIVE STUDY OF ITRACONAZOLE-LOADED NANOPARTICLES USING POLYISOBUTYLCYANOACRYLATE AND POLY (DL-LACTIDE-CO-GLYCOLIDE) AS DRUG CARRIERS. THESIS ADVISOR : ASSOC. PROF. UBONTHIP NIMMANNIT, Ph.D. 326 pp. ISBN 974 -17-5068-4

This research was designed to optimize itraconazole-loaded polyisobutyl-cyanoacrylate (PIBCA) nanoparticles and itraconazole-loaded poly (lactide-co-glycolide) (PLGA) using factorial designs and response surface methodology. In this study the stability and cytotoxicity of both nanoparticles were also investigated. A validated statistical model having significant coefficient figures ($P < 0.05$) for the particle size, particle size distribution, amount of itraconazole entrapped in the nanoparticles, and encapsulation efficiency as function of the polymer or monomer, benzyl benzoate, and itraconazole were developed. Multiple response optimizations by using the overlay contour plot for the responses and the desirability approach allowed the selection of the optimum formulation ingredients for nanoparticles containing itraconazole of 500 µg/mL. The composition of itraconazole-loaded PLGA nanoparticles contained 10 mg/mL of PLGA, 16.94 µg/mL of benzyl benzoate and 1001.01 µg/mL of itraconazole whereas the composition of itraconazole-loaded PIBCA nanoparticles contained 8.09 µL/mL of IBCA, 10.19 µg/mL of benzyl benzoate and 1200.77 µg/mL of itraconazole.

Factorial designs and response surface methodology have been successfully used to construct a statistical model for the particle size, polydispersity index and encapsulation efficiency as a function of the formulation variables. The optimized formula of itraconazole-loaded PIBCA nanoparticles was more stable than the optimized formula of itraconazole-loaded PLGA nanoparticles. On the contrary, the cytotoxicity of plain and itraconazole-loaded PLGA nanoparticles was less prominent than that of plain and itraconazole-loaded PIBCA nanoparticles. The estimated IC_{50} values of PLGA nanoparticles and PIBCA nanoparticles were 79.2 mg/mL and 114 µg/mL, respectively.

Department	PHARMACEUTICS	Student's signature	………………..
Field of study	PHARMACEUTICS	Advisor's signature	…………………
Academic Year	2003	Co-advisor 's signature	…………………

CONTENTS

LIST OF TABLES

LIST OF TABLES (CONT.)

LIST OF TABLES (CONT.)

LIST OF TABLES (CONT.)

LIST OF TABLES (CONT.)

LIST OF TABLES (CONT.)

LIST OF TABLES (CONT.)

LIST OF TABLES (CONT.)

LIST OF TABLES (CONT.)

LIST OF TABLES (CONT.)

LIST OF TABLES (CONT.)

LIST OF TABLES (CONT.)

LIST OF FIGURES

LIST OF FIGURES (CONT.)

LIST OF FIGURES (CONT.)

LIST OF FIGURES (CONT.)

FIGURE   PAGE

LIST OF FIGURES (CONT.)

LIST OF FIGURES (CONT.)

LIST OF FIGURES (CONT.)

FIGURE   PAGE

LIST OF FIGURES (CONT.)

LIST OF FIGURES (CONT.)

LIST OF ABBREVIATIONS

Adj R-Squared	Adjusted R-Squared
Adeq Precision	Adequate Precision
°c	degree celsius
g	gram
HPLC	high-performance liquid chromatography
h	hour
IBCA	isobutylcyanoacrylate
mg	milligram
min	minute
mL	milliliter
nm	nanometer
PBS	phosphate buffer saline
PACA	polyalkylcyanoacrylate
PCS	photon correlation spectroscopy
PIBCA	polyisobutylcyanoacrylate
PLA	poly (lactic acid)
PLGA	poly (lactide-co-glycolide)
Pred R-Squared	Predicted R-Squared
PVA	poly vinyl alcohol
R	correlation coefficient
R-Squared	determination coefficient
rpm	revolution per minute
SEM	scanning electron microscopy

LIST OF ABBREVIATIONS (CONT.)

SLS   sodium lauryl sulphate

TEM   transmission electron microscopy

μg   microgram

CHAPTER I

INTRODUCTION

Fungal infections remain a major therapeutic problem in immunocompromised patients. Since the 1960s, amphotericin B has been the drug of choice for the treatment of almost all endemic mycoses, but its use is limited by various severe side effects, including chills, fever, hypotention, azotemia, renal tubular damage and hypokalaemia. To overcome the failures of conventional antifungal therapy caused by a lack of activity against deep fungal infections or problem of toxicity of the active substance, extensive studies have been carried out in the field of colloidal drug carriers, especially liposomes (Bakker-Woudenberg and Roerdink, 1986; Bakker-Woudenberg et al., 1993, 1994; Lopez-Berestein, 1987; Wansan and Lopez-Berestein, 1995). At the same time a new azole antifungal compounds have been synthesized and evaluated in vivo, alone (Clemons et al., 1995; Como and Dismukes, 1994; Dismukes, 1988; Fromtling, 1988) or associated with liposomes (Brasseur et al., 1991; Le Conte et al., 1991; Singh et al., 1993) or cyclodextrins (Hostetler et al., 1992; Van Doorne et al.,1988). Particular interest has been focused on the new triazole derivative itraconazole, in the light of its specific advantages: broad spectrum of activity including aspergillosis and lower toxicity than amphotericin B, implying a better therapeutic index. Since it is effective against aspergillosis, itraconazole is under extended and intensive investigations in view to optimize its use in human clinical therapy.

However, itraconazole is a weakly basic (pKa = 3.7) and highly hydrophobic (octanol/water partition coefficient at pH = 8.1, log P = 5.66) drug (Chasteigner et al., 1996). It is insoluble in water so the first route of administration is oral route. Large

interindividual as well as intraindividual variations of its oral bioavailibility have been reported (Heykants et al., 1989). In particular, gastric acidity and food intake influence absorption. Moreover, in immunocompromised patients, itraconazole absorption through the infected gastro-intestinal mucosa is greatly altered. The route of administration is one factor that has a significant impact on the therapeutics outcomes of drug. The development of an injectable dosage form would be extremely useful to overcome this drawback and to offer a dosage form that would allow the necessary therapeutic dose to be achieved. This implies a liquid preparation containing not less than 0.500 mg/mL of itraconazole (Heykants et al., 1989).

Parenteral route is one approach to take the sustained and controlled drug delivery systems into the body. The drug can be directed to the intended site of action, and must be able to avoid interactions with other sites within the body. It can produce effects at a site of injection or being absorbed into the circulating systems and the target sites, respectively, depending on sites of injection and the properties of drug delivery carriers. The intravenous, subcutaneous, intramuscular, intraperitoneal, and intrathecal routes are all examples of parenteral routes of drug administration (Leung, Robinson, and Lee, 1987).

Colloidal drug carriers are currently under investigation including polymeric nanoparticles, liposomes, and lipid emulsions. There are, however, a number of drawbacks with respect to toxicity, product reproducibility, stability on storage, incorporation of drugs and their controlled release behaviors, which so far have prevented the widespread clinical application of these systems (Couvreur et al., 1995; Prankerd and Stella, 1990; Siekmann and Westesen, 1995; Thunemann and General, 2001). Nanoparticles made of well characterized biodegradable polymers such as

polyalkylcyanoacrylate or poly (lactic acid) could be easily manufactured in a reproducible manner and represented an attractive alternative for improving the modulation of drug delivery, shelf life and stability in biological fluids. Polyalkylcyanoacrylate nanoparticles are often used as colloidal carriers in controlled drug delivery systems (Kreuter, 1991). Their physico-chemical characterizations by evaluation of the particle size, zeta potential, surface hydrophobicity, density and specific surface area (Kreuter, 1983; Muller et al., 1992) as well as by the determination of the sorption behavior of drugs were the objective of a number of publications (Leu, 1983; Harmia et al., 1986). But to date little is known regarding to the effect of formulation variables on preparation of oily nanoparticles by interfacial polymerization of itraconazole. Poly (lactide-co-glycolide) (PLGA) polymers have been studied extensively for many years. PLGA have the advantage of being well characterized and already commercially used for microparticulate drug delivery systems (Allemann and Leroux, 1999). PLGA are biocompatible, biodegradable and bioresorbable (Wise et al., 1979). PLGA nanoparticles can be formed by interfacial deposition following solvent displacement technique (Fessi et al., 1989). Several compounds such as indomethacin (Cauchetier et al., 2003), and muramyl dipeptide MDB-B30 (Barichello et al., 1999) have been incorporate in this technique. Chasteigner et al. (1996) studied the association of itraconazole with colloidal drug carriers except PLGA and polyisobutylcyanoacrylate.

The application of an optimization technique consisting of statistical design in pharmaceutical formulation development would provide an efficient and economical method to acquire the necessary information to understand relationship between controllable (independent) variables and performance or quality (dependent) variables or responses (Stetsko, 1986). In addition, the optimization process provides a method

to develop an empirical model equation to characterize the response as a function of the different independent variables. The technique of optimization is well reported in the literature for the development of tablet formulations (Ceschel, Maffei and Badiello, 1999; Dawoodbhai, 1991; Bos, Bolhuis and Lerk, 1991), microcapsules (Arica et al., 2002; Zaghloul et al., 2001), media component (Adinarayana and Ellaiah, 2002), a hydrocolloid dressing (Nangia, Lam and Hung, 1990) and suspension (Elkheshen et al.,1996).

Several procedures have been described involving cell culture techniques for preliminary biocompatibility evaluation of materials intended for medical application (Pizzoferrato et al., 1994). To harmonize in vitro cytotoxicity test methods, an ISO norm was created by the International Standard Organization (1992). This document classifies the in vitro cytotoxicity test methods into three categories based on the preparation of the test material as follows:

(1) Test of extracts prepared from polymer;

(2) Indirect contact methods, where cells and the test material are separated by a protective layer, for example an agar layer

(3) Direct contact methods where the cells are put directly in contact with the test material.

Cell viability was measured using the crystal violet assay which is extensive used in many studies (Fang et al., 2001; Kaido et al., 2002; Park et al., 2002; Shatrov, 1999; Thumwanit and Kedjarune, 1999; Yamamoto et al., 2001).

The purposes of this study were to investigate the utility of a factorial design and optimization process to develop and improve formulation of itraconazol-loaded PLGA nanoparticles and itraconazol-loaded polyisobutylcyanoacrylate (PIBCA) nanoparticles to use as an injectable dosage form. The optimization process was used

to generate a model equation that provides a means of evaluating changes in response due to changes in the independent variable levels. Since it was important to have information about toxicity of the drug carrier to determine if these results did not prohibit the use of nanocapsules in human medicine, the other purposes of this study were to study the stability and cytotoxicity of itraconazole-loaded nanoparticles and plain (nondrug-bound) nanoparticles made from PIBCA and PLGA.

The Objectives of This Study:

1. To evaluate the solubility of itraconazole in four different oils consisting of benzyl benzoate, caprylic/capric triglycerides, soybean oil and corn oil.

2. To study the effect of stirring rate and surfactant concentration on the particle size, size distribution and zeta potential of itraconazole-loaded PIBCA nanoparticles and itraconazole-loaded PLGA nanoparticles.

3. To study the influence and interaction of certain factors; concentration of polymer/ monomer, benzyl benzoate and itraconazole in inorganic phase; on morphometrical parameters and encapsulation efficiency.

4. To characterize the property of itraconazole- loaded PIBCA nanoparticles and itraconazole loaded PLGA nanoparticles.

5. To optimize process of itraconazole-loaded PIBCA nanoparticles and itraconazole loaded PLGA nanoparticles.

6. To study the in vitro drug release of itraconazole-loaded PIBCA nanoparticles and itraconazole-loaded PLGA nanoparticles.

7. To investigate the stability of itraconazole-loaded PIBCA nanoparticles and itraconazole-loaded PLGA nanoparticles during storage for 30, 60 and 90 days at 4 °C.

8. To determine the cytotoxicity of itraconazole-loaded PIBCA nanoparticles, plain (nondrug-bound) PIBCA nanoparticles, itraconazole-loaded PLGA nanoparticles and plain (nondrug-bound) PLGA nanoparticles towards cell in culture.

CHAPTER II

LITERATURE REVIEWS

1. Itraconazole

Itraconazole is a synthetic triazole antifungal agent. It is a 1:1:1:1 racemic mixture of four diastereomers (two enantiomeric pairs), each possessing three chiral centers. It may be represented by the following structural formula and nomenclature (Figure 1) (FOI, 1990).
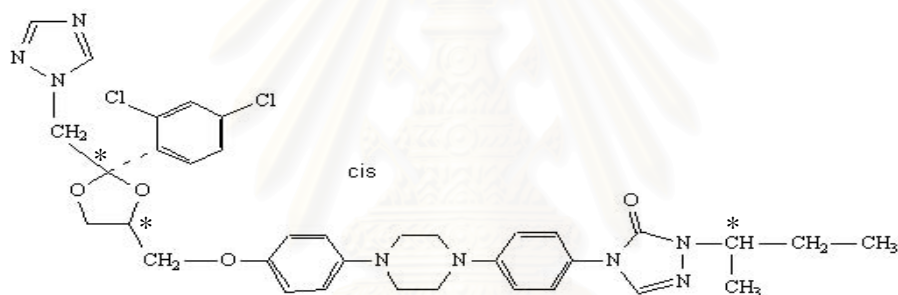
(±)-1[$\underline{R}$*-$\underline{sec}$-butyl]-4-[$\underline{p}$-[4-[$\underline{p}$-[[2$\underline{R}$*,4$\underline{S}$*)-2-(2,4-dichlorophenyl)-2-(1$\underline{H}$-1,2,4-triazol-1-ylmethyl)-1,3-dioxolan-4-yl]methoxy]phenyl]-1-piperazinyl]phenyl]-Δ^2-1,2,4-triazolin-5-one mixture with (±)-1-[($\underline{R}$*)-$\underline{sec}$-butyl]-4-[$\underline{p}$-[4-[$\underline{p}$-[[(2 $\underline{S}$*,4$\underline{R}$*)-2-(2,4-dichlorophenyl)-2-(1$\underline{H}$-1,2,4-triazol-1-ylmethyl)-1,3-dioxolan-4-yl]methoxy] phenyl] -1-piperazinyl]phenyl]- Δ^2-1,2,4-triazolin-5-one

Figure 1 Structural formula and nomenclature of itraconazole (FOI, 1990).

Itraconazole has a molecular formula of $C_{35}H_{38}C_{12}N_8O_4$ and a molecular weight of 705.64. It is a white to slightly yellowish powder. It is insoluble in water, very slightly soluble in alcohols, and freely soluble in dichloromethane. It has a pKa

of 3.70 (based on extrapolation of values obtained from methanolic solutions) and a log (n-octanol/water) partition coefficient of 5.66 at pH 8.1.

1.1 Antimicrobial Action

Itraconazole is a potent antifungal drug with activity against histoplasmosis, blastomycosis and onchomyosis. The pharmacological mechanism is the same as the structural analogues ketoconazole and micronazole,which interfere with the synthesis of ergosterol of the fungal membrane by inhibition of 14α-demethylase, a CYP 450 *iso*-enzyme (Barone et al., 1993). It has slightly wider spectrum of activity than ketoconazole. It is active against *Aspergillus* spp., *Blastomyces dermatitidis, Candida* spp., *Coccidioides immitis, Cryptococcus neoformans, Epidermophyton* spp., *Histoplasma capsulatum, Malassezia furfur, Micro-sporum* spp., *Paracoccidioides brasiliensis*, Sp*orothrix schenckii,* and *Trichophyton* spp.

1.2 Pharmacokinetics

Itraconazole is well absorbed when given by mouth after food. Mean peak plasma concentrations can be reached within 4 hours and for a 100-mg daily dose can range from 400 to 600 ng/mL at steady state which can be reached within 14 days. Bioavailability increases with doses of 100 to 400 mg in such a manner as to suggest that itraconazole undergoes saturable metabolism. Itraconazole is highly protein bound; only 0.2% circulates as free drug. Itraconazole is widely distributed but only small amounts diffuse into the cerebrospinal fluid. Concentrations attained in the skin,

sebum, pus, and female genital tissues are several times higher than simultaneous plasma concentrations. Therapeutic concentrations of itraconazole remain in the skin and mucous membrane, for 1 to 4 weeks after the drug is discontinued (Cauwenbergh et al., 1988).

Itraconazole is metabolised in the liver to inactive compounds, which are excreted in the bile or urine; 3 to 18% is excreted in the feces as unchanged drug. Small amounts are eliminated in the stratum corneum and hair. Itraconazole is not removed by dialysis (Prentice et al., 1994).

The elimination half-life following a single 100-mg dose has been reported as 20 hours; the half-life increases to 30 hours with continued administration (Heykants et al., 1987).

1.3 Uses and Administration

Itraconazole is used for the treatment of oropharyngeal and vulvovaginal candidiasis, pityriasis versicolor, and of dermatophytoses such as tinea pedis, tinea cruris, and tinea corporis. It is also used for aspergillosis, blastomycosis, and histoplasmosis. Itraconazole has also been reported to be effective in systemic candidiasis, chromoblastomycosis, coccidioidomycosis, cryptococcosis, paracoccidioidomycosis and sporotrichosis.

The dose of itraconazole in oropharyngeal candidiasis is 100 mg (or 200 mg in patients with AIDS or neutropenia) daily by mouth for 15 days. Vulvovaginal candidiasis may be treated with itraconazole 200 mg by mouth twice daily for one day. Pityriasis versicolor may be treated with itraconazole 200 mg daily for 7 days. For dermatophytoses the dose is 100 mg daily for 15 days in tinea corporis or tinea cruris or

for 30 days in tinea pedis or tinea manuum; for nail infections a dose of 200 mg daily for 3 months has been suggested. For blastomycosis or histoplasmosis an initial dose of 200 mg daily may be increased by 100-mg increments to a maximum of 200 mg twice daily. Aspergillosis may be treated with 200 to 400 mg daily. In life-threatening infections, a loading dose of 200 mg three times a day for three days has been suggested.

1.4 Report on Itraconazole Preparation Study

Chateigner et al. (1996) evaluated the association of itraconazole with intravenously compatible drug carriers (liposomes, cholesterol complexs, nanospheres) and the different association yields were compared. The highest association yield, 4.1 % (0.510 mg/mL), were obtained with nanoshere composed of the most hydrophobic polymer tested, poly-ε-caprolactone, and a negative charged steroidal surfactant, sodium deoxycholate.

Chowdary and Srinivasa (2000a, 2000b) studied the development of dissolution media for itraconazole (2000a) and the effects of surfactants on solubility and dissolution rate of itraconazole (2000b). Different approaches usually used in the design of dissolution media for poorly soluble drugs to maintain sink conditions (i.e., a large difference in the dissolved drug concentration and saturation drug concentration) included a) increasing the volume of the aqueous media or removing the dissolved drug. b) increasing solubility of the drug by adding co-solvents such as anionic or non-ionic surfactants to the dissolution medium and c) alteration of pH to enhance the solubility of ionizable drug molecule. The solubility of itraconazole in purified water (pH 6.4), 0.1 N hydrochloric acid (pH 1.2) and phosphate buffer (pH 7.4) was 1.2, 5.0, and 0.77 μg/mL respectively (Chowdary and Srinivasa, 2000a,

2000b). These results suggested that itraconazole is poorly soluble at both acidic and alkaline pH. Hence, adjusting pH of the dissolution fluid cannot be applied to maintain sink conditions for itraconazole. Unlike surfactants, such as Tween 20 and sodium lauryl sulfate (SLS), both greatly increased the solubility of itraconazole in 0.1 N hydrochloric acid. A 76 and 164 fold increase in the solubility of itraconazole in 0.1 N hydrochloric acid was observed at 0.5% and 1.0% SLS concentrations respectively (Chowdary and Srinivasa, 2000a, 2000b). SLS not only increased itraconazole solubility but also enhanced the dissolution rate of itraconazole by 26.5 fold at 1.0% concentration of SLS (Chowdary and Srinivasa, 2000b).

Chowdary and Srinivasa (2000c) investigated how to enhance the dissolution rate of itraconazole from tablet formulations by using solid dispersion of itraconazole in lactose, microcrystalline cellulose (MCC) and three superdisintegrants (Primogel, Kollidon CL, and Ac-Di-Sol). The order for the excipients to enhance the dissolution rate was Ac-Di-Sol > Kollidon CL > Primogel > microcrystalline cellulose > lactose. Micronization and conversion of the drug into the amorphous form and the fast disintegrating and dispersing action of the superdisintegrants contributed to the enhancement of dissolution rate of itraconazole. Itraconazole solubility and initial dissolution rate has been improved according to transformation of crystalline forms of drugs into high energy amorphous forms in solid dispersions (Jung, 2002).

Yoo et al. (2000) used tablets containing itraconazole manufactured by wet granulation of solid dispersion particles prepared by spray-drying with polyvinylacetal diethylaminoacetate (Asd tablets). The dissolution rate of itraconazole from Asd tablets was fast, with more than 90% release within 10 min, compared to less than 20 % for a market product, Sporanox® capsules.

2. Nanoparticles

Drug carrier systems are being developed with the aim of changing the distribution of an active substance within the body and thus increasing its pharmacological efficacy and/or reducing its toxicity. In this respect, colloidal particles (25 nm to 1 µm in diameter) have shown some very promising results. Liposomes, which are composed of one or more phospholipid bilayers enclosing an aqueous phase, have been intensively studied over the last 25 years (Puisieux et al., 1995) and some liposome-based pharmaceuticals are now on the market. Similarly sized systems based on biodegradable polymers, referred to as nanoparticles, were developed slightly later and show some advantages over liposomes in terms of stability both during storage and in vivo study (Puisieux et al., 1993; Couvreur et al., 1995). Nanoparticles can be defined as solid colloidal particles containing an active substance that are produced by mechanical or chemical means. In terms of size alone, the lower limit of nanoparticles is generally taken to be in the neighborhood of 5-10 nm and the upper size limit of ~1000 nm (1 µm). Nanoparticles are used as the collective name to describe both nanospheres and nanocapsules (Kreuter, 1994; Bouwstra et al., 1994; Allemann et al., 1993; Speiser, 1991). The difference between these two forms lies in their morphology and body architecture. Nanospheres are formed by a dense polymeric matrix, whereas nanocapsules are composed of an oil core surrounded by a polymeric membrane (Rollot et al, 1986; Puglisi et al., 1995; Kouhri Fallouh et al., 1986) (Figure 2).
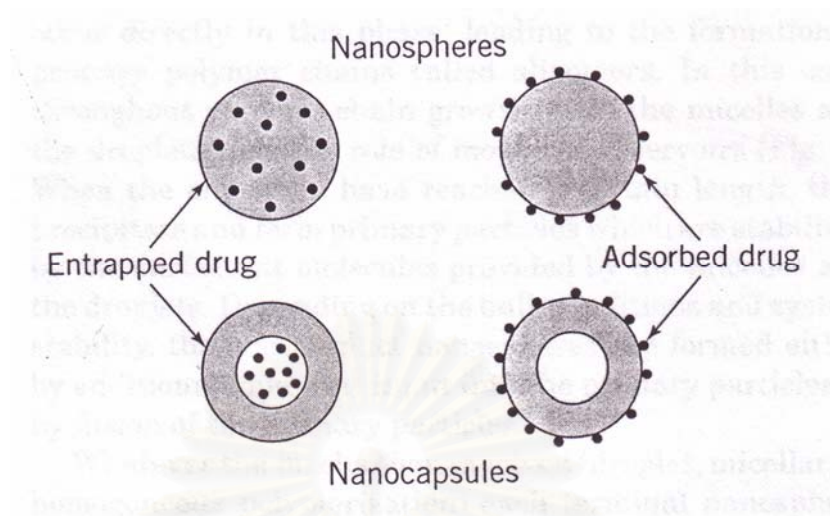
Figure 2   Nanoparticles (Allemann et al., 1993).

2.1 Nanoparticles Prerpared from Preformed Polymers

Preformed polymers commonly used for the preparation of nanoparticles include   poly (lactic acid), poly (glycolic acid), poly (lactide-co-glycolide), poly (ε-caprolactone), poly (alkylcyanoacrylate), and nonbiodegradable polymers such as poly (methyl methacrylate), poly (vinylchloride-co-acetate) and poly (styrene) (Couvreur et al., 1996).   The methods for preparing nanoparticle   from preformed polymers can be classified into four categories: emulsion evaporation, solvent displacement, salting-out, and emulsification diffusion.   These techniques are similar in that they involve an organic solution containing the nanoparticle components that functions as an internal phase during preparation and an aqueous solution containing stabilizers that constitute the dispersion medium for the nanoparticles.   Another similarity between the techniques is the poor encapsulation efficiency of moderately water-soluble and freely water-soluble drugs (including peptides and proteins), which partition out from the organic phase into the aqueous continuous phase.   Despite considerable attempts, the techniques remain efficient only

for lipophilic drugs. It is worth noting that although all the methods enable the preparation of nanospheres, only solvent diplacement (Fessi et al., 1987) and, more recently, the emulsification-diffusion technique (Quintanar-Guerrero et al., 1997) have enabled the preparation of nanocapsules.

2.1.1 Emulsification Evaporation

Emulsification evaporation is a well-established method based on the classical procedure patented by Vanderhoff et al. (Vanderhoff et al., 1979) for the preparation of pseudolatexes or artificial latexes. The preformed polymer is dissolved together with the drug in a water-immiscible organic solvent such as chloroform or methylene chloride, which is then emulsified into an aqueous phase using either ultrasonication or homogenization (high-pressure homogenizers or micro-fluidizers) to achieve the formation of a sub-micron emulsion. The subsequent removal of the organic solvent by heating or reduced pressure evaporation results in the formation of nanoapheres. Disadvantages of this technique are associated with the toxicity of the solvent used, the relatively low entrapment of water- soluble drugs, including peptides and proteins, and the use of high input of energy to achieve formation of sub-micron emulsions. The low entrapment of water soluble drugs is due to the rapid diffusion of the drugs from the organic phase into the aqueous phase during the emulsification process. To overcome this problem, nanoparticles of poly (lactide-co-glycolide) (Blanco and Alonso, 1997) and poly (lactic acid) (Zambaux et al., 1998) with a particle size ranging from 300-600 nm were prepared from double emulsions (water-in –oil – in water) by sonication. Protein (human serum albumin) was dissolved in the internal aqueous phase and methylene chloride was used as an organic solvent. The authors found that the entrapment efficiency of protein varied

from 40-90% depending on type of polymers and the volume fraction of the internal aqueous phase containing protein.

Some typical examples of nanoparticles were prepared by emulsification evaporation. In most cases, chlorinated solvents (chloroform and methylene chloride) were used because of their water insolubility, easy emulsification, solubilizing properties, and low boiling point. However, the disadvantage of these solvents in their toxicity (class 2 in the International Conference on Harmonization [ICH] guidelines for residual solvents, 1996), and their use should be limited to protect patients from potential adverse effects. Poly vinyl alcohol (PVA) and albumin have been preferentially used as colloidal stabilizers. PVA has been shown to be an excellent stabilizer to prepare biodegradable nanoparticles, not only by emulsification evaporation but also with all techniques discussed here. Furthermore, it is one of the few stabilizers that avoids nanoparticle aggregation during postpreparative steps (e.g., purification and freeze drying), enhancing the yield of dry nanoparticle product without addition of other adjuvants (Quintanar-Guerrero et al., 1998a). Nevertheless, PVA has the disadvantage of not being accepted for i.v. administration. Although its i.v. safety has been revised recently and compared with that of poly (ethyleneglycol) (Yamaoka et al., 1995), use of PVA for this route is not recommended.

2.1.2 Solvent Displacement

This technique was first described and patented by Fessi et al. (1987). In this process, polymer, drug, and optionally a lipophilic stabilizer (e.g., phospholipids) are dissolved in a semipolar water-miscible solvent, such as acetone or ethanol. This solution is poured or injected into and aqueous solution containing a

stabilizer (e.g., PVA or poloxamer 188) under magnetic stirring. Nanoparticles are formed instantaneously by rapid solvent diffusion, which is then eliminated from the suspension under reduced pressure. The mechanism of formation of nanoparticle by this technique has been explained by the interfacial turbulence generated during the solvent displacement (Fessi et al., 1989; Quintanar-Guerrero et al., 1997). This technique has been successfully applied to preparation of nanoparticles from various types of preformed biodegradable polymers including poly (lactic acid), poly (glycolic acid), poly (lactide-co-glycolide), poly (ε-caprolactone), poly (alkylcyano-acrylate), and nonbiodegradable polymers such as poly (methyl methacrylate), poly (vinylchloride-co-acetate) and poly (styrene) (Couvreur et al., 1996). Nanocapsules of these polymers can be prepared by the introduction of the fourth component, an oil, which is miscible with the solvent (acetone or ethanol) but immiscible with the solvent-aqueous mixture. Such oils include medium chain triglycerides and benzyl benzoate (Fessi et al., 1989; Kreuter, 1994; Couvreur et al., 1995). The preformed polymer is deposited at the interface between the oily dispersed droplets and the water continuous phase resulting in the formation of oily cored nanocapsules with high encapsulation efficiency for lipophilic drugs (Fessi et al., 1989; Santos-Magalhaes et al., 1995). Nanoparticles prepared from poly (lactic acid) in which acetone was used as a solvent and benzyl benzoate as the oil compartment have been successfully prepared to encapsulate lipophilic drugs such as indomethacin, taxol, vitamin K and clofibrate with encapsulation rates of up to 100 % (Fessi et al.,1989; Santos-Magalhaes et al., 1995; Quintanar–Guerrero et al., 1998a). Hydrophilic drugs including peptides are not efficiently entrapped using the solvent displacement methods as the drug again rapidly diffuses into the aqueous phase during the preparation process (Niwa et al., 1993).

2.1.3 Salting – out

This technique is based on the separation of a water-miscible solvent from aqueous solutions via a salting out effect. Acetone is generally chosen as the water-miscible solvent because of its solubilizing properties and its well-known separation from aqueous solutions by salting-out with electrolytes (Matkovich, 1973). Polymer and drug are dissolved in acetone, and this solution is emulsified under vigorous mechanical stirring in an aqueous gel containing the salting-out agent and a colloidal stabilizer. This oil-in-water emulsion is diluted with a sufficient volume of water or aqueous solutions to enhance the diffusion of acetone into the aqueous phase, thus inducing the formation of nanospheres. Solvent and salting-out are then eliminated by cross-flow filtration (Quintanar-Guerrero et al., 1998).

2.1.4 Emulsification Diffusion

This technique is base on the removal of a partially water-miscible solvent, such as benzyl alcohol or ethyl acetate, used to solubilise preformed polymers from the emulsified droplets of polymer by dilution with water (Leroux et al., 1995; Quintanar- Guerrero et al., 1996). Preformed polymers such as poly (D, L, -lactic acid) or poly (ε-caprolactone), and lipophilic drugs are dissolved in an organic phase which is emulsified under vigorous mechanical stirring to form oil-in-water emulsions. The system is then diluted with a sufficient amount of water to induce the diffusion of the solvent into the aqueous continuous phase resulting in the precipitation of the polymer and the formation of nanoapheres. The solvent can then be removed by cross-flow filtration. Nanocapsules with an oily core can be prepared by this technique if water-immiscible oil such as medium chain triglycerides is dissolved in the water-saturated solvent prior to emulsification (Quintanar-Guerrero et

al., 1998b). This technique reportedly results in a high entrapment of lipophilic drugs but entrapment of peptides is low. Low entrapment has been attributed to the leakage of the peptide into the aqueous phase during the preparation process (Quintanar-Guerrero et al., 1997).

2.2 Nanoparticles Prepared from Polymerization of

Monomers

Various methods have been used to prepare nanoparticles from polymerization of monomers including, micellar polymerization (emulsification polymerization) and interfacial polymerization using sub-micron emulsions and microemulsions.

2.2.1 Emulsification Polymerization

Nanoparticles have been prepared by emulsification polymerization of monomers which are dissolved or emulsified in water containing surfactant prior to polymerization (Kreuter and Speiser, 1976; Couvreur et al., 1979). The polymerization of the monomer is started by introducing an initiator (Couvreur et al., 1996). For example, nonospheres have been prepared from methyl methacrylate and alkyl cyanoacrylates by this technique which has subsequently been used as polymeric drug carriers (Kreuter and Speiser, 1976; Couvreur et al., 1979). For methyl methacrylate, polymerization is initiated either by input of high-energy radiation (γ-rays produced by a ^{60}Co source) or by addition of an initiator such as ammonium or potassium peroxodisulfate (Kreuter, 1983). Alkyl cyanoacrylates were first used for the preparation of nanospheres by Couvreur et al. (1979). Droplets of

liquid monomers were added to an acidic solution (pH<3.0) containing surfactant. The low pH was used to regulate the polymerization reaction. Nanospheres having a matrix core with a particle size of less than 200 nm were performed by this method (Couvreur et al., 1979). Poly (alkylcyanoacrylate) (PACA) constitutes a group of biodegradable, bioerodible polymers. They have been extensively used as degradable tissue adhesives in surgery (Florence et al., 1979). These properties render them suitable for the fabrication of biodegradable drug delivery systems. The advantage of the alkyl cyanoacrylate monomer is that neither high-energy radiation nor chemical initiators, which can affect the stability of entrapped drug, are required for the polymerization process (Couvreur et al., 1995). Alkyl cyanoacrylates undergo base-catalyzed anionic polymerization (Kreuter, 1994). The polymerization of PACA can be initiated by OH^- from the dissociation of water in a polymerization medium.

Entrapment of drug within PACA nanospheres was achieved by incorporating the drug during the polymerization process or alternatively adsorbing it onto the surface of preformed nanospheres (Couvreur et al., 1979; Grangier et al., 1991; Damge et al., 1997). It is unlikely that a high entrapment of peptides can be achieved by either of these methods due to the aqueous nature of the continuous phase, although a high association has been reported when insulin is adsorbed onto preformed nanoparticles (Grangier et al., 1991; Damge et al., 1997).

2.2.2 Interfacial Polymerization of Oil-in– Water Sub- micron Emulsions

Polymerization of monomers utilizing the interface of oil-in-water dispersions was first used to prepare oily cored poly (iso-butyl cyanoacrylate) (PIBCA) nanocapsules which efficiently entrapped lipophilic compounds (Al Khouri

Fallouh et al., 1986) . Iso-butyl cyanoacrylate monomers, drug and oil (medium chain triglycerides, benzyl benzoate or ethyl oleate) were dissolved in a water-miscible solvent such as ethanol (Al Khouri Fallouh et al., 1986). This mixture was slowly injected (0.5 mL/min) through a wide-bore syringe needle or a micropipette tip into an aqueous phase (pH between 4 and 10) containing nonionic surfactants such as poloxamer 188, phospholipid, polysorbate 80 or Triton^{TM} X-100 (Couvreur et al., 1979; Puglisi et al., 1995; Couvreur et al., 1996). The polymerization of alkyl cyanoacrylate monomer occurred at the oil/water interface of the oil-in-water dispersions that formed following the diffusion of the water-miscible solvent into the aqueous phase. The interfacial polymerization of the monomer results in the formation of oily cored nanocapsules having a particle size between 200 and 300 nm with a narrow size distribution. The water-miscible organic solvent is then removed under reduced pressure. The presence of the surfactants in the aqueous phase is necessary to prevent the aggregation of nanocapsules on storage (Al Khouri Fallouh et al., 1986).

A number of studies have shown that lipophilic drugs can be successfully encapsulated within the oily core of nanocapules due to their solubility in this phase (Al Khouri Fallouh et al., 1986; Fresta et al., 1996). Hydrophilic drugs are unlikely to be efficiently encapsulated within oily cored nanocapsules prepared by this technique due to their affinity for the continuous phase. However it has been reported that this technique can successfully encapsulate insulin and calcitonin up to 90 % (Damge et al., 1990; Lowe and Temple, 1994). How the peptides incorporate into the nanocapsules is not known, but insulin and calcitonin have hydrophobic domains in their structure which may enable them to associate with the oil phase (Lowe and Temple, 1994). The preparation of nanocapsules having an aqueous core

however would seem more suitable for high entrapment of hydrophilic bioactives including peptides (Vranckx et al., 1996; Fattal et al., 2000).

Disadvantage of polymerization using sub-micron emulsion, however, are associated with the requirement of a high input of energy either by ultrasonication (El-Samaligy et al., 1986), vigorous stirring (Vranckx et al., 1996) or homogenization (Fattla et al., 2000); which may not be suitable to individual scale up. Further it is difficult to obtain nanocapsules with a size below 200 nm and a narrow polydispersity unless a high concentration of suitable surfactants together with a high input of energy is used (Vranckx et al, 1996). The use of a high input of energy to form nanocapsules can be overcome by the use of water-in-oil microemulsion (Gasco and Trotta, 1986).

2.3 Polyalkylcyanoacrylate (PACA) Nanoparticles

Polyalkylcyanoacrylate (PACA) nanoparticles have been prepared using several methods. Nanospheres of PACA have been prepared by the micellar polymerization of alkyl cyanoacrylate in an acidic aqueous medium containing surfactant (Couvreur et al., 1979). Drug could either be incorporated into the matrix of these nanoparticles or adsorbed onto their surface (Couvre et al., 1996). Nanocapsules of PACA having an oily core for the entrapment of lipophilic drugs have been prepared by mixing an organic phase containing monomer, oil, and drug into an aqueous dispersion medium. Polymerization at the oil/water interface results in oily cored nanocapsules (Al Khouri Fallouh et al., 1986). The interfacial polymerization of water-in-oil submicron emulsions (El-Samaligy et al., 1986; Vranckx et al., 1996) or water-in-oil microemulsions (Gasco and Trotta, 1986)

following the addition of alkyl cyanoacrylate monomers into oil continuous phase results in the formation of aqueous cored nanocapsules. These aqueous cored nanocapsules were shown to be suitable for the entrapment of peptides and oligonucleotides (Vranckx et al., 1996; Fattal et al., 2000). These and other studies have shown that the type and concentration of alkyl cyanoacrylate monomer, type of the organic phase (if present) and pH of the aqueous phase used in the preparation of PACA nanoparticles effect the particle size and size distribution, yield, molecular weight entrapment efficiency of drug and the release of drug from nanoparticles (Kreuter, 1994; Couvreur et al., 1996; Fresta et al., 1996). The influence of these variables on the preparation of PACA nanoparticles prepared by the various techniques are reviewed and discussed in the topic of nanospheres, oily cored nanocapsules, and aqueous cored nanocapsules prepared from water-in-oil sub micron emulsions.

2.3.1 Nanospheres

The particle size and size distribution of PACA nanospheres produced by micellar polymerization of aqueous solutions containing surfactant and stabilizers (e.g. dextran) was found to be affected by the pH of the polymerization medium, monomer concentration, type and concentration of surfactant / stabilizer used (Krause et al., 1986; Seijo et al., 1990; Das et al., 1995). Das et al. (1995) reported that at pH 4 and above, the polymerization reaction was very rapid and as such the nanoparticles formed were not stabilized which resulted in the formation of an amorphous polymer mass rather than nanoparticles. They successfully prepared nanospheres when the pH of the aqueous medium was 2.0. Seijo et al. (1990) also investigated the effect of pH on the physicochemical characteristics of nanoparticles

prepared by the same micellar polymerization technique. They investigated the effect of pH over the range of 1 to 3. Mean diameter of PIBCA nanospheres produced increased with increasing the [H_3O^+] from a mean of 34 nm at pH 3 to greater than 80 nm at pH 1. Seijo et al. (1990) also investigated the effect of varying the mass of monomer used for polymerization on the characteristics of nanospheres. Increasing the monomer concentration resulted in a slight increase in particle size and size distribution when it was polymerized in an aqueous medium having a pH of 2.

Seijo et al. (1990) and Das et al. (1995) also investigated the effect of surfactant concentration on the characteristics of the nanospheres produced by micellar polymerization. Seijo et al. (1990) using Pluronic^{TM} F68, showed the concentration of surfactant used significantly influenced particle size, with a reduction in size being observed with increasing concentration of surfactant (0.2-10.0%)from 160 to around 300 nm. Das et al. (1995) studied the effect of concentration of two surfactants on characteristics of nanospheres, namely Pluronic^{TM} F68 and Tween^{TM} 20. Again increasing concentration of surfactant resulted in a reduction of particle size. However, particles produced using Pluronic^{TM} were smaller and non-aggregated, whereas particles formed with Tween^{TM} were larger and showed evidence of aggregation and a significantly lower yield. Krause et al. (1986) also commented on the problem of particle aggregation leading to a reduced yield of nanoparticles (resulting from the removal of these aggregates by filtration) when Tween^{TM} 20 was used as a surfactant. The superior performance of Pluronic^{TM} was proposed to be a result of the formation of a thicker hydration sheath around the nanoparticles, compared to Tween^{TM} 20, which effectively increased the thickness of the Stern layer resulting in particle stabilization (Das et al., 1995).

Das et al. (1995) also investigated the effect of several formulation variables, particularly pH, on the molecular weight of the resulting PACA.   Alkylcyanoacrylate undergoes a base-catalyzed anionic polymerization. The mechanism of polymerization is shown in Figure 3.

(a)

(b)
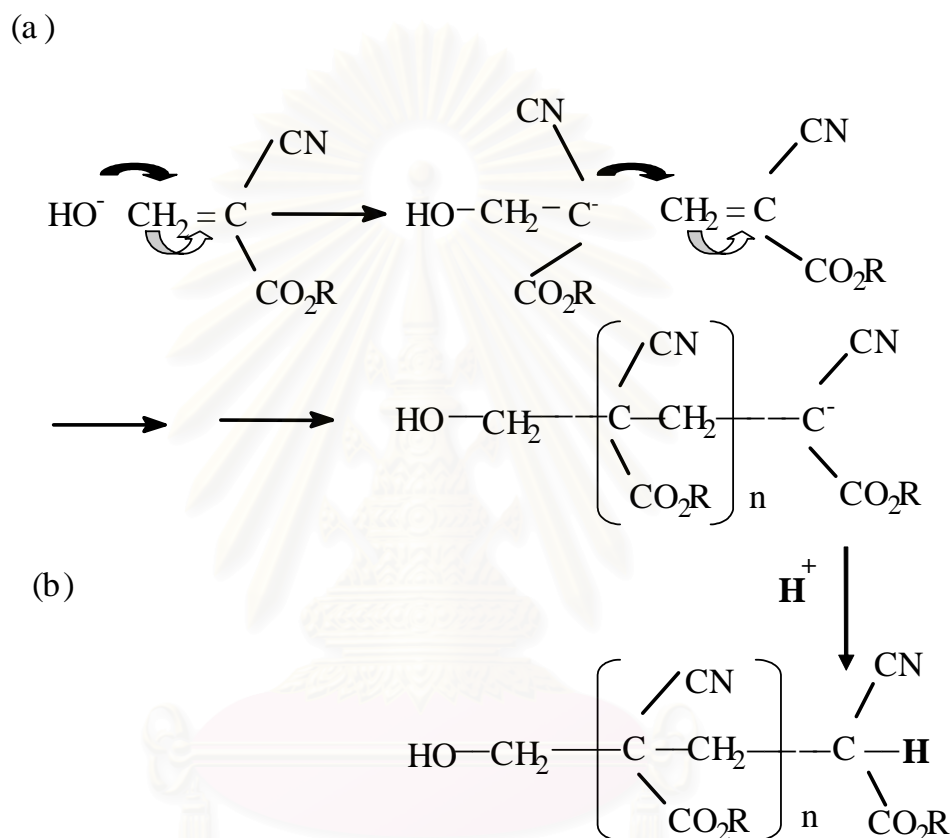
Figure 3 Polymerization (a) and termination (b) mechanism of PACA

(R is alkyl functional group) (Das et al., 1995).

Dissociation of water generates initiating OH^- ions and terminating H_3O^+ ions. The molecular weight of PACA would thus be expected to be influenced by the relative concentration of these initiating and terminating species. As expected from the polymerization mechanism, the molecular weight of PACA prepared by micellar polymerization of monomer was found to decrease with

decreasing pH (increasing concentration of the terminating species) of the polymerization medium (Vansnick et al., 1985; Das et al., 1995). The anionic polymerization mechanism of alkylcyanoacrylates also raises the possibility of other compounds including bioactives having anionic residues, inducing or becoming involved in the polymerization reaction. Grangier et al. (1991) reported the formation of a heavier polymeric fraction of PIBCA when growth hormone releasing factor was added at the beginning of the polymerization process. This was proposed to be a result of the intervention of the peptide in the polymerization reaction. Similar findings were reported by Vansnick et al. (1985) and Damge et al. (1990) for insulin and doxorubicin.

Nanospheres prepared by micellar polymerization can be loaded with bioactive either by addition of drug to the aqueous solution prior to, or at the same time as the monomer (entrapment) or by its addition at a time following initiation of polymerization (adsorption). For poorly water-soluble bioactives, the amount of drug, which can be entrapped, is limited by the solubility of the bioactive in the aqueous polymerization vehicle. However, despite the low amount of bioactive, which can be incorporated, the entrapment efficiency for a poorly water-soluble drug added prior to polymerization has been reported to be good (Krause et al., 1986). Addition of bioactive to the system before initiation of polymerization, however, can lead to the intervention of the bioactive in the polymerization process leading to the covalent binding of the bioactive in the polymerization process leading to the covalent binding of the bioactive to the polymer (Tassedt et al.,1995). For this reason, researchers have investigated the possibility of loading drug by its addition to the polymerizing vehicle following initiation of polymerization (Grangier et al., 1991; Tassset et al., 1995; Damge et al., 1997).

These researchers have demonstrated the importance of the time at which bioactive is added to the polymerization medium in avoiding covalent binding of drug to polymer. The time interval at which bioactive is added to the system following initiation of the polymerization also has a significant effect on the amount of bioactive, which becomes associated with the nanospheres (Grangier et al., 1991; Damge et al., 1997). Association of bioactive to nanospheres appears to be greatest if added soon after initiation of polymerization and becomes progressively less if added after an optimized time. This was reported to be 15 and 60 minutes for the adsorption of growth hormone releasing factor and insulin onto isobutyl-cyanoacrylate respectively resulting in association efficiencies of greater than 80%. Addition of the bioactive before this optimum time resulted in a significant amount of the peptide being covalently linked to the polymer. Since alkylcyanoacrylates of different alkyl chain lengths polymerize at different rates, the optimum time of bioactive addition following polymer initiation must be determined for each alkyl-cyanoacrylate and bioactive. For example, the optimum time for the addition of growth hormone releasing hormone to poly (isohexylcyanoacrylate) nanospheres was reported to be 5 hours (Grangier et al., 1991)

2.3.2 Oily Cored Nanocapsules

A number of studies have investigated the effect of formulation variables on the physico-chemical characteristics of oily cored nanocapsules prepared by the interfacial polymerization of oil in water dispersions. This technique usually requires the oil component to be mixed with a water-miscible organic solvent which diffused into the continuous aqueous phase upon mixing, allowing polymerization / precipitation at the oil / water interface. To this effect, the oil acts as a monomer

support.   This technique has been proposed as a method for the preparation of nanocapsules that allows for a high level of entrapment of lipophilic compounds (Al Khouri Fallouh et al., 1986).

Al Khouri Fallouh et al. (1986) investigated the effect of the pH of the aqueous phase, temperature of preparation, concentration of surfactant and ethanol on the characteristics of the oily cored nanocapsules.   Only pHs between 4 and 10 allowed for the formation of nanocapsules of uniform size.   Greater polydispersity occurred below pH 4.   Temperature had an effect on resultant size of nanocapsules with an increase in size being observed with increasing the temperature of the system.   Pluronic^{TM} F68 was used as surfactant but varying the concentration had little effect on the characteristics of the nanoparticles although the authors reported that the presence of surfactant was necessary to overcome aggregation during storage.   The concentration of ethanol used to dissolve the oily phase and monomer however, had a significant effect on nanocapsule size.   The authors reported that a minimum concentration of 15% of ethanol in the oil phase was necessary to successfully prepare nanoparticles.   Below 15%, the monomer polymerized as flakes without formation of nanoparticles.   Above 15%, nanocapsule formed and size was found to decrease with increasing ethanol content of the oily mixture.   In contrast, Gallardo et al. (1993) reported that in the absence of ethanol, nanospheres having a size of less than 80 nm were formed when isobutylcyanoacrylate was mixed with the medium chain triglyceride, Miglyol^{TM} 812 and emulsified in a pH 3 aqueous phase containing Pluronic^{TM} F68.   Addition of ethanol to this system resulted in the formation of nanocapsules having a size of around 300 nm.   At certain oil : ethanol ratios, two populations of nanoparticles ; nanospheres of a size around 90 nm and nanocapsules having a size of about 200 nm ; were observed.   The molecular weight

of the resulting PIBCA of the nanocapsules formed in this study was found to increase with increasing amount of ethanol added to the oil phase, ranging from 30,000 to in excess of 100,000 when the ethanol : oil ratio was increased from 50 : 1 to 1250 : 1 respectively.

The type of water-miscible solvent also has an influence on the characteristics of PACA nanoparticles formed by this technique (Puglisi et al., 1995; Fresta et al., 1996). Protic water-miscible solvents such as ethanol, n-butanol and iso-propanol result in the formation of a mixture of nanospheres and nanocapsules as previously reported by Gallardo et al. (1993). However, aprotic water-miscible solvents such as acetone and acetonitrile result in the formation of only nanocapsules. This led to the speculation of the mechanism of nanocapsule formation, with interfacial precipitation of preformed polymers being proposed as a mechanism in the presence of protic solvents and interfacial polymerization being proposed as a mechanism in the presence of aprotic solvents. The dual population of nanospheres and nanocapsules formed by protic water-miscible solvent / oil mixture resulted from precipitation of the preformed polymers (nanospheres) or interfacial precipitation of preformed polymers around an oil droplet (nanocapsules) (Chouinard et al., 1994; Puglisi et al., 1995; Fresta et al., 1996).

The type of surfactant used to emulsify the oil in water system has also been shown to affect the size and size distribution of oily cored nanocapsules prepared by this technique using aprotic solvents (Puglisi et al., 1995). The effect of different surfactants on size was attributed to the emulsifying properties of the surfactant, leading to changes in size of the oil droplets, which act as the polymer template.

Another factor, which has been investigated with regards to its effect on the characteristics of oily cored nanocapsules, is the mass of monomer used for polymerization (Puglisi et al., 1995; Fresta et al., 1996). In this regard, increasing the amount of monomer added to the oil/water-miscible solvent mix dose not appear to influence the size of the resulting nanocapsules, which is in contrast to its apparent effect on nanospheres formed by micellar polymerization. Instead, increasing the mass of monomer used for polymerization appears to increase the thickness of the polymer wall. This would suggest that monomer polymerization occurs from the interface inwards i.e. polymer initiation occurs at the oil/water interface as a result of nucleophilic attack by $[OH^-]$ and once initiated, continues through the monomer-rich oil phase as a result of the presence of the carbanion on the polymer terminus. In this case, $[OH^-]$ and the terminating $[H_3O^+]$ are excluded from the oil phase. Fresta et al. (1996) attempted to measure the wall thickness of the nanocapsules from freeze fracture TEM images. They reported that the wall thickness of nanocapsules increased form 52 to 65 nm upon increasing the mass of ethyl cyanoacrylate from 140 to 320 μL. However, closer inspection of the micrographs of oily cored nano-capsules presented in their report shows that the oil droplets are rarely central and often lie very close to the particle periphery. The reported wall thickness is thus, the mean of the wall thickness observed either side of the droplet, which varied form around 180 nm to as little as 4 nm.

Oily cored nanocapsules were first proposed as a means to efficiently encapsulate lipophilic bioactives (Al Khouri Fallouh et al., 1986). Fresta et al. (1996) later demonstrated that the efficiency of entrapment is related to the drug's affinity for the oil phase. For example, the observed lower encapsulation efficiency of carbamazepine compared to ethosuximide correlated with their solubilities in the

oil phase (medium chain triglycerides, of 26.2 and 108.3 mg/mL, respectively). Surprisingly, reports have also documented the efficient entrapment of hydrophilic compounds within oily cored nanocapsules being in excess of 90% for the peptides, insulin and calcitonin (Damge et al., 1990; Lowe and Temple, 1994). The solubility of these peptides in the disperse phase to be encapsulated was facilitated by the presence of a large percentage of ethanol, a water-miscible solvent. Lowe and Temple (1994) proposed that the peptides, however, were encapsulated within the oily cores of these nanocapsules, but rather were entrapped in the polymer wall of the nanocapsules as the water-miscible solvent diffused into the bulk. In view of the reports relating to the efficient entrapment of peptides within nanospheres produced by micellar polymerization by adsorbing the bioactive onto the particles following initiation of polymerization, adsorption may also play a role in the association of peptides within oily cored nanocapsules. It is conceivable that when anionic bioactives are dispersed in the protic water-miscible solvents, that they may also initiate the polymerization reaction leading to their covalent binding to the resultant polymer. Damge et al. (1990) reported that the high molecular weight fraction of polyisobutylcyanoacrylate increased in the presence of insulin as a result of this association.

2.3.3 Aqueous Cored Nanocapsules Prepared from Water-in-Oil Sub-micron Emulsions

Aqueous cored nanocapsules have been proposed as a means of efficiently encapsulating hydrophilic bioactives. In this technique, a water-in-oil sub micron emulsion is prepared by ultrasonication or vigorous stirring and the monomer is subsequently added to the oil continuous phase. Polymerization at the water/oil

interface results in the formation of aqueous cored nanocapsules (El-Samaligy et al., 1986). These authors studied the effect of monomer concentration and type on the characteristics of nanocapsules prepared by this technique. Increasing the amount of monomer used for polymerization was believed to be the result of the formation of a thicker polymer wall. The wall thickness, however, was not determined. The *in vitro* release of fluorescein was found to be reduced upon increasing monomer concentrations suggesting the formation of a thicker polymer wall. The increase in nanocapsule size with increased wall thickness would suggest that in the case of interfacial polymerization of alkylcyanoacrylates using water in oil systems, polymerization proceeds from the interface outwards. This is in contrast to the direction of polymerization for oil in water systems but it would appear that polymerization always proceeds into the organic phase.

The type of surfactant used to stabilize the water-in-oil emulsion also influences the size of nanocapsules produced by this technique. Vranckx et al. (1996) reported that the size of nanocapsules prepared when sodium lauryl sulphate was used as surfactant was approximately 220 nm, while nanocapsules prepared with polyoxyethylene 23 lauryl ether (Brij^{TM} 35) had an approximate size of 57 nm. This may be a result of the difference in the emulsifying properties of these surfactants, influencing the particle size of the disperse phase.

Nanocapsules prepared by this technique, however, have been reported to have a broad particle size distribution (El-Samaligy et al., 1986; Fattal et al., 2000). El-Samaligy et al. (1986) reported that particle size ranged from 500-1500 nm when PACA nanocapsules were prepared by this technique. The low yield of nanocapsules which has been reported for this technique has been attributed to this

broad size distribution as loss of the larger particles, the aggregates occurs upon isolation of nanocapsules by filtration (Krause et al., 1986).

3. Nanoparticle Characterizations

3.1 Particle Size Measurements

The most significant characteristics of colloidal dispersions are the size and the shape of the particles. Particle size of the lipid particles has a direct effect on both toxicity and stability. Particles greater than 4-6 μm are known to increase the incidence of emboli and blood pressure changes. For intravenous injections, particles should be less than 1 μm in diameter. For subcutaneous or intramuscular injections, the particle should preferably be less than 250 μm in diameter. Larger particle sizes can be used for oral formulations. Submicron particles are needed for target drug delivery (Domb, 1993). Particle size measurements are useful in that they allow aggregation or crystal growth to be evaluated. They are technically very difficult because the particle sizes usually extend beyond the limit of detection of any one given instrument. Thus, at least two complementary techniques should be employed. Many advanced instruments for determining particles size are available. Electron microscopy, laser inspection system and coulter counter methods are used to determine the particle size over than 1 μm. For particle size determinations below 1 μm, photon correlation spectroscopy (PCS) or quasi-elastic laser light scattering (QELS) is useful (Haskell, 1998; Prankerd and Stella, 1990).

Photon correlation spectroscopy (PCS) is a laser light scattering method suitable for the measurement of particles ranging from 5 nm to 5 μm. The

PCS device consists of a laser, a temperature controlled cell, and a photomultiplier. The light scattered from a colloidal dispersion is detected on a photomultiplier and transferred to a correlator for the calculation of a correlation function. This function is then processed to calculate the mean size of the particles. Powerful modern equipment allows the determination of the size distribution of mono- and multimodal populations of particles. The advantage of this technique is the ease of sample preparation. To be analyzed, the particles only need to be sufficiently diluted in a solvent, which is generally filtered water.

Scanning electron microscopy is widely used in the field of nanocarriers. It has high resolution and the sample preparation is relatively easy. However, to be analyzed, the samples must withstand a high vacuum. To visualize the particles, they have to be conductive and, therefore, coating of the surface of the sample with gold is required. The thickness of this coating is at least 20 nm. This must be taken into account in the size determination, especially for small nanoparticles (e.g., <200 nm). Removal of stabilizing agents added during the preparation of the particles is essential. Otherwise, depending on the amount of these additives, the particles are partially or completely hidden in a matrix of additives.

For size determination, transmission electron microscopy is not as widely used as PCS and SEM, but it is still a powerful method for determining the morphology of particles. With this technique, Fessi et al. (1989) estimated the wall thickness of PLA nanocapsules. Krause et al. (1985) described the highly porous structure of PLA nanospheres prepared by the emulsion-evaporation procedure.

3.2 Zeta Potential

It is clear that the surface properties of colloidal systems are critical in determining their drug carrier potential, since they will control their interactions with plasma proteins. Zeta potential measurements will give information about the overall surface charge of the particles and how this is affected by changes in the environment (e.g. pH, presence of counter-ions, and adsorption of proteins). Charge shielding by polyethyleneglycol or other hydrophilic groups can be used to predict the effectiveness of the barrier function against opsonisation in vivo. Zeta potential can also be used to determine the type of interaction between the active substance and the carrier; i.e. whether the drug is encapsulated within the body of the particle or simply adsorbed on the surface. This is important because adsorbed drug may not be protected from enzymatic degradation, or may be released very rapidly after administration. (Barratt, 2000)

The zeta potential is determined by measuring the migration velocity of the suspension particles with respect to the net effective charges on the surface, called electrophoretic mobility.   The Zeta meter[®] is a microelectrophoretic mobility apparatus used to measure them.   Furthermore, zeta potential measurements are typically performed using a Doppler electrophoresis apparatus such as the Zetasizer[®] . A new technique for measuring zeta potential, electric sonic analysis or ESA, can be performed using a Matec[®] ESA 8000. This technique allows the zeta potential to be determined for a concentrated dispersion without the typical necessary dilutions that could affect the dispersion stability.   The other instrument can be used to measure them is an amplitude weighted phase structuration (Floyd and Jain, 1996).

4. In Vitro Drug Release

During the last decade there has been a considerable increase in interest in the use of disperse systems as drug carriers. Dissolution characteristic of drugs from these dosage forms is important factor for absorption and bioavailability. Several studies have shown that the dissolution rate is a rate-limiting step for absorption and bioavailability of drugs administered in suspension formulations (Banakar, 1992a).

In vitro release studies should in principle be useful for quality control as well as for the prediction of in vivo kinetics. Unfortunately, due to the very small size of the particles, the release rate observed in vivo can differ greatly from the release obtained in a buffer solution. However, in vitro release studies remain very useful for quality control as well as for evaluation of the influence of process parameters on the release rate of active compounds. In vitro drug release from microdispersed systems has been extensively reviewed by Washington (1990) Drug release from nanoparticles can take place through several processes, of which the following appear to be the most important: (1) The drug may diffuse out of the carrier through the solid matrix; to allow complete release from the carriers, (the concentration of drug in the release medium should remain infinitely low, which condition is known as sink condition); (2) The solvent may penetrate the nanoparticles and dissolve the drug, which then diffuses out into the release medium. Depending on the physico-chemical characteristics of the particles, water can enter the particles through narrow pores or by hydration. Once the drug is dissolved, the drug diffuses out of the particles. Here again, since diffusion is driving the release, sink conditions are required to obtain meaning information; (3) The carrier may be degraded by its surrounding; as long as this process is faster than diffusion, the release is said to be erosion-controlled.

The USP paddle method is one method used to study dissolution of solid lipid nanoparticle (Muller, Mehnert et al., 1995). However, sampling is one problem due to interference of the smaller particles, which often get through the sampling probe. Flow-through apparatus has also been employed frequently to determine the dissolution characteristics of suspension (United States Pharmacopeial Convention, 1995). This dissolution cell allows fresh dissolution medium to be circulated continuously, at a known velocity, surrounding the dissolving particles. However, this method is rather complicate compare to the other methods.

Membrane diffusion technique is the most popular method for studying the dissolution characteristic of microdisperse systems (Kinget and de Greef, 1995; Levy and Benita, 1990; Lostritto, Goei, and Silvestri, 1987; Saarinen-Savolainen et al., 1997; Tukker and de Blaey, 1983; Washington, 1990). In this approach the carrier disperse phase, suspended in a small volume of continuous phase, is separated form a large bulk of sink phase by a dialysis membrane which is permeable to the drug. The sample and sink are well stirred. The drug diffuses out of the carrier and through the membrane to the sink, wherein it is periodically assayed. Thus, the accumulation of the drug in the sink is controlled by the consecutive rate processed of (non-sink) partition and diffusion of the drug across the membrane.

The measurement of release profiles requires good sink condition, implying that release must occur into a large volume of sink medium. It has been recom-mended as a rule of thumb that the drug concentration in the sink phase in dissolution experiments must be kept below 10% of saturation (Washington, 1990). This poses a problem since the drug must be assayed in the sink medium, and as the sink volume is increased the concentration of drug being measured decreases. Especially for

insoluble drugs, a method of assay is required which is very sensitive to less quantity of drug in solution

5. Cytotoxicity Assay

There are many applications in cytotoxicity assays. The choice of assay will depend on the agent under study, the nature of the response, and the particular target cell. Assays can be divided into two major classes : (1) an immediate or short-term response such as an alteration in membrane permeability or a perturbation of a particular metabolic pathway, and (2) long-term survival, either absolute, usually measured by the retention of self-renewal capacity, or survival in alter state, e.g., expressing genetic mutation(s) or malignant transformation.

Traditional assays have involved either counting total viable cells; using hemocytometer chamber or electronic particle counter or colony counting. The need to process large numbers of samples has led to attempt to introduce assays which can be automated. Radionuclide incorporation assays have been intensively studied and widely used but usually include steps which are relatively time consuming. The introduction of multiwell plates revolutionized the approach to replicate sampling in tissue culture. They are economical to use, lend themselves to automated handling, and can be of good optical quanlity. (Freshney, 1987)

5.1 Crystal Violet Staining

Crystal violet staining is a simple, rapid method.   There are so many researches using this technique to evaluate cytotoxicity of chemical substances in this

decade. In October 1992, The Japaneses Society of Alternatives to Animal Experiments (JSAAE) organized an inter-laboratory validation study on cytotoxicity assays for development of an alternative(s) to the in vivo Draize eye irritation test. The five assays were colony formation assay, crystal violet staining assay, lactate dehydrogenase release assay, neutral red uptake, and MTT assay. The results show that colony formation assay, crystal violet staining assay, neutral red uptake, and MTT assay are recommendable (Ohno et al., 1998).

Thumwanit et al. (1999) tested cytotoxicity of polymerized commercial cyanoacrylate adhesive on cultured human oral fibroblasts. Cell viability testing using MTT and crystal violet staining methods showed that cyanoarylate-coated filter paper released substances that were toxic to cells,while wax-coated filter paper gave the same result as the control. Cytotoxicity testing using MTT test and crystal violet staining systems gave a similar result. The MTT test is a very sensitive method for the assessment of biocompatibility but this method takes more time compared with crystal violet staining.

Yamamoto et al. (2001) studied cytoxicity and apoptosis produced by troglitazone in human hepatoma cells. After incubation with troglitazone, its metabolites, pioglitazone, or rosiglitazone for 48 h., cells were fixed with 3.7% formaldehyde and stained with 0.2% crystal violet. The absorbance of the extracts wit 2% sodium dodecyl sulfate at 620 nm was measures. It was found that troglitazone exhibited time-and concentration-dependent cytotoxicity. Traglitazone induced apoptotic cell death characterized by internucleosomal DNA fragmentation and nuclear condensation which it may be one of the factors of liver injury in human.

Fang et al. (2001) used crystal violet staining method to test cytotoxicity of tumor necrosis factor α (TNFα). The viable cells were stained with

staining buffer (22.3% ethanol containing 0.5% crystal violet, 8% methanol, 7 g/L NaCl) for 1-2 h. The dye was eluted with 33% citric acid, and absorbance was measured at 595 nm.

Kaido et al. (2002) compared the cytotoxic and mutagenic effect of 213-nm and 193-nm laser radiation on primary cultures of human corneal fibroblasts. After irradiation the cells were incubated for 7 days, then fixed and stained with 0.5% crystal violet in 100 % methanol. The results showed that the 213-nm Nd:YAG laser was more cytotoxic and mutagenic than the 193-nm excimer laser on cultured mammalian cells .

Park et al. (2002) used the crystal violet method to test cytotoxicity. Cells were stained with 0.2% crystal violet in 20% ethanol for 5 min. The microplates were rinsed with water and 0.1 mL of water: methanol: ethanol (5:1:4 by volume) solution was added to each well to solubilized the stained cells. The absorbance of each well was read at 570 nm using a 96-well ELISA reader.

5.2 Cytotoxicity of Polyalkylcyanoarylate Nanoparticle.

Kante et al. (1982) investigated toxicity of polyalkylcyanoarylate nanoparticle.   Membrane integrity of the incubated cell was regularly controlled using both the erythrosin B exclusion test and the leakage of lactic dehydrogenase. The 1% final concentration in incubated medium, the polybutylcyanoacrylate nanoparticles greatly affected the integrity of the hepatocytes; the 0.5% in culture medium, on the other hand, exerted no effect.

Gonzlez-Martin et al. (2000) studied the cytotoxicity by increasing concentration of unloaded nanoparticles ranging from 1.10 μg/mL to 2366.70 μg/mL.

After a 24-h incubation period, Vero cell-line viability was determined by ionic intensified fluorecien diacetate method (Yang et al., 1995). The concentration that killed 50% cells was 200 μg/mL.

CHAPTER III

MATERIALS AND METHODS

Materials

1. Isobutylcyanoacrylate (IBCA) was a gift from Loctite (Dublin, Ireland).

2. Polylactide-co-glycolide (PLGA) with different ratios (Birmingham Polymers Inc., USA).

    - 50:50 PLGA copolymers (MW 10800)

    - 65:35 PLGA copolymers (MW 12400)

    - 75:25 PLGA copolymers (MW 11200)

    - 85:15 PLGA copolymers (MW 11200)

3. Itraconazole (Tricon Enterprises PVT Ltd., Batch no. IT0080900, India).

4. Caprylic/capric triglycerides (Crodamol GTCC^{TM}) (Croda Surfactants, New Zealand).

5. Benzyl benzoate (Sigma, USA).

6. Corn oil (Sigma, USA).

7. Soybean oil (E.Merck, UK).

8. Poloxamer F68 (BASF, Germany).

9. Acetone (HPLC grade) (Mallinckrodt Baker, Inc, Paris).

10. Acetonitrile (HPLC grade) (BDH, UK).

11. Methanol (HPLC grade) (BDH, UK).

12. Potassium dihydrogen orthophosphate (Merck, Germany).

13. Disodium hydrogen orthophosphate (Merck, Germany).

14. Sodium Chloride (Merck, Germany).

15. Ketoconazole (Janssen, USA).

16. Sodium lauryl sulphate (SLS) (Kao, Japan).

17. Vero Cell-line was a gift from GPO (Bangkok, Thailand).

18. Crystal violet (BDH, UK).

19. Trypan blue (BDH, UK).

20. Dulbecco's Modified Eagle Medium (DMEM) powder(low glucose) (Gibco, USA).

21. Fetal Bovine Serum, Qualified   (Gibco, USA).

22. HEPES Buffer Solution (1M) (Gibco, USA).

Equipments

1. Analytical balance (Model A200S, Satorius analytic, Germany).

2. Balance (Model PB3002, Mettler Toledo, Switzerland).

3. High-performance liquid chromatography (HPLC) instruments equipped with the following

- a constant flow pump (Model 600E, Waters, USA)

- a tunable absorbance detector (Model 484, Waters, USA)

- an auto-injector (Model 712 WISP, Waters, USA)

- an integrator (Model 746 Data Module, Waters, USA)

- C18 column (Lichrospher 60 RP-select B (5 micron) 4.6 x 120 mm, Merck, Germany).

4. Magnetic stirrer (Model MR 3001, Heidolph, Germany).

5. Photon correlation spectroscopy (Malvern 4700 laser spectrometer®, Malvern Instruments Ltd., UK).

6. pH meter (Model 232, Pye Unicam ltd., England).

7. Scanning electron microscopy (Model JSM-541OLV, JOEL®, Japan).

8. Shaker (Model TBVS Hetomix® and DT Hetotherm®, Heto, Denmark).

9. Ultracentrifuge® (Model L80, Beckman, USA).

10. Ultrapure Water® equipped with filter system (Balston®, Balston Inc., USA), Boost pump, Option 3 water purifier, Maximum ultrapure water, and Reservoir (ELGA, USA).

11. Zetasizer 4® (Malvern Instruments Ltd., UK).

12. Dissolution tester (Model VK 7000®, Vankel Industries, Inc, USA).

13. Micro titer plate(96 wells plate) and tissue culture flask (Nunc,Denmark)

14. Centrifuge (Universal 30 RF, Hettich)

15. Autoclave (MC-30L,ALP, Japan)

16. CO_2 incubator (Forma Scientific,3862,USA)

17. Inverted microscopy (Axiovert 35 M, Zeiss, Germany)

18. Microplate Reader (Kinetic-QuL, Bio Whittaker , Germany)

19. Water bath with shaker (Model TBVS HETOMIX, Heto, Allerod, Denmark)

20. Vertical Laminar Airflow (NUAIRE, NU4525-400, USA)

21. Vortex – Geniez (G-560E, Scientific Industries, USA)

22. Hemocytometer (Improved Neubauer, BOECO, Germany)

23. Minitab Statistical Software Release 13 (Minitab, Inc., USA)

24. Design-Expert, version 5 (Stat-Ease Corporation, USA)

Methods

1 Solubility of Itraconazole

1.1 Solubility of Itraconazole in Different Oils

Excess amount of itraconazole was put into each of four different oils consisting of benzyl benzoate, corn oil, caprylic/capric triglycerides, and soybean oil. After sonication for 30 minutes, the samples were shaken at 30 °C for 1, 3, 5, and 7 days. The solubility of itraconazole in different oils was analyzed by HPLC in different conditions, which have been calibrated as describe in section 4.3.

The objective of this part was to evaluate the solubility of itraconazole in four different oils consisting of benzyl benzoate, caprylic/capric triglycerides, soybean oil and corn oil. To answer the basic question which was "do the type of oil and shaking day affect itraconazole solubility and if so, how?", the experimental protocol was as follows:

I. Design Structure

The two-way analysis of variance (ANOVA) design was used to evaluate the solubility of itraconazole in four different oils consisting of benzyl benzoate, caprylic/capric triglycerides, soybean oil and corn oil. The independent variables as two treatment factors were "type of oil" at four levels; benzyl benzoate, caprylic/capric triglycerides, soybean oil and corn oil; and "day" at four levels; 1, 3,5 and 7 days, giving a total 16 treatment combinations. Since there were three replicates, then total observations were 48 as shown in Table 1. The observed response was the solubility of itraconazole in this experiment. y_{ijk} was the observed

response when factor A (Type of oil) was at i th level (i =1,2,3,.4) and factor B (day)
was at j th level (j =1,2,3,4) for the k th replicate (k =1,2,3).

Table 1 General arrangement for a two-way analysis of variance (ANOVA) design
for testing solubility of itraconazole in different oils.

		Factor B (day)			
		Level 1 (1day)	Level 2 (3 days)	Level 3 (5 days)	Level 4 (7days)
Factor A (Type of oil)	Level 1 benzyl benzoate	$y_{111}, y_{112}, y_{113}$	$y_{121}, y_{122}, y_{123}$	$y_{131}, y_{132}, y_{133}$	$y_{141}, y_{142}, y_{143}$
	Level 2 caprylic/capric triglyceride	$y_{211}, y_{212}, y_{213}$	$y_{221}, y_{222}, y_{223}$	$y_{231}, y_{232}, y_{233}$	$y_{241}, y_{242}, y_{243}$
	Level 3 soybean oil (3)	$y_{311}, y_{312}, y_{313}$	$y_{321}, y_{322}, y_{323}$	$y_{331}, y_{332}, y_{333}$	$y_{341}, y_{342}, y_{343}$
	Level 4 corn oil (4)	$y_{411}, y_{412}, y_{413}$	$y_{421}, y_{422}, y_{423}$	$y_{431}, y_{432}, y_{433}$	$y_{441}, y_{442}, y_{443}$

II. Response Model

$$y_{ijk} \quad = \quad \mu + \tau_i + \beta_j + (\tau\beta)_{ij} + \varepsilon_{ijk} \tag{1}$$

Where μ was the overall mean effect, τ_i was the effect of the ith level of the row
factor A or the effect of type of oil on itraconazole solubility, β_j was the effect of the
jth level of the column factor B or the effect of shaking day on itraconazole solubility,

$(\tau\beta)_{ij}$ was the effect of the interaction between τ_i and β_j or the interaction effect of type of oil and day on itraconazole solubility and ε_{ijk} was a random error component.

III. Hypotheses

Hypotheses about the equality of row treatment (type of oil) effects were as follows,

H_0 : no type of oil effect on itraconazole solubility or

H_0 : $\tau_1 = \tau_2 = \tau_3 = \tau_4 = 0$

H_1 : at least one $\tau_i \neq 0$ **(2)**

And the equality of column treatment (day) effects were as follows,

H_0 : no shaking day effect on itraconazole solubility or

H_0 : $\beta_1 = \beta_2 = \beta_3 = \beta_4 = 0$

H_1 : at least one $\beta_j \neq 0$ **(3)**

IV. Statistical Test

F test was carried out to test the effect of factor A (type of oil) and factor B (day).

V. Decision Rule

If P value exceeded the specified significant level of the test, expressed as a probability, then the null hypothesis was accepted. Small F values and large P values would signify acceptance of the null hypothesis of no effect.

VI. Multiple Comparisons

If the analysis of variance indicated that row (type of oil) or column (day) means differ, in which the null hypothesis had been rejected (P< 0.05). It was usually of

interest to make comparisons between the individual row (type of oil) or column (day) means to discover the specific differences. The hypothesis to be tested in multiple comparisons were as follows,

$$H_0 : \text{ no difference between compared treatments or}$$

$$H_0 : \mu_i = \mu_j$$

$$H_1 : \mu_i \neq \mu_j \tag{4}$$

1.2 Solubility of Itraconazole in Different Aqueous Media

Excess amount of itraconazole was put into each of seven different aqueous media consisting of water, phosphate buffer saline (PBS), 0.25% poloxamer in water, 0.25% poloxamer in PBS, 0.25% SLS in PBS (Leroux, 1996), 4% cyclodextrin in water and simulated gastric fluid (SGF). After sonication for 30 minutes, the samples were shaken at 30°C for 1, 3, 5, and 7 days. The solubility of itraconazole in different media was analyzed by HPLC in different conditions, which have been calibrated as describe in section **4.3**.

Since itraconazole solubility in water, phosphate buffer saline (PBS), 0.25% poloxamer in water, 0.25% poloxamer in PBS were very low and could not be measured by HPLC in this study. To assess the solubility of itraconazole in three remaining aqueous media consisting of 0.25% SLS in PBS, 4% cyclodextrin in water and SGF, the experimental protocol was as follows:

I. <u>Design Structure</u>

The two-way analysis of variance (ANOVA) design was used to evaluate the solubility of itraconazole in three different aqueous media. The independent variables

as two treatment factors were " medium" at three levels; 0.25% SLS in PBS, 4% cyclodextrin in water and SGF ; and "day" at four levels; 1, 3,5 and 7 days, giving a total 12 treatment combinations. Since there were three replicates, then total observations were 36 as shown in Table 2. The observed response was the solubility of itraconazole in this experiment. y_{ijk} was the observed response when medium was at ith level (i =1,2,3) and day was at j th level (j =1,2,3,4) for the kth replicate (k =1,2,3).

Table 2 General arrangement for a two-way analysis of variance (ANOVA) design for testing solubility of itraconazole in different aqueous media

		Factor B (day)			
		Level 1 (1day)	Level 2 (3 days)	Level 3 (5 days)	Level 4 (7days)
Factor A (Medium)	Level 1 0.25% SLS in PBS	$y_{111}, y_{112}, y_{113}$	$y_{121}, y_{122}, y_{123}$	$y_{131}, y_{132}, y_{133}$	$y_{141}, y_{142}, y_{143}$
	Level 2 4% cyclodextrin in water	$y_{211}, y_{212}, y_{213}$	$y_{221}, y_{222}, y_{223}$	$y_{231}, y_{232}, y_{233}$	$y_{241}, y_{242}, y_{243}$
	Level 3 SGF	$y_{311}, y_{312}, y_{313}$	$y_{321}, y_{322}, y_{323}$	$y_{331}, y_{332}, y_{333}$	$y_{341}, y_{342}, y_{343}$

The response model, the hypotheses, statistical test, decision rule and multiple comparisons was as described in section **1.1**.

1.3 Statistical Analysis

The two-way analysis of variance (ANOVA) followed by Tukey's pairwise comparisons at a 95 % confidence interval was used to test for significant difference among different oils and media at each time point with regards to the solubility. The two-way analysis of variance (ANOVA) and Tukey's pairwise comparisons were performed using the Minitab statistical analysis program assuming normal distribution.

2 Preparation of Nanoparticles

2.1 Preparation of Nanoparticles Prepared from Isobutyl cyanoacrylate (IBCA)

Itraconazole-loaded polyisobutylcyanoacrylate (PIBCA) nanoparticles were prepared according to the interfacial polymerization technique described by Al-Khouri et al. (1986). The accurate concentration of 5.5 µL/mL of IBCA monomer, 12.5 µg/mL of benzyl benzoate, and 1050 µg/mL of itraconazole were dissolved in 10 mL of acetone. The organic phase was added under mechanical stirring at a constant flow rate of 0.3 mL/min into 25 mL of an aqueous phase containing 0.25% of nonionic surfactant (poloxamer). The nanoparticles were formed immmediately by polymerization of monomers on the water/oil interface. After completed polymeri-

zation (1h) the colloidal suspension of nanoparticles was concentrated by evaporation under vacuum and the final volume (10 mL) was filtrated through a sintered glass filter (porosity 4, mesh size 5-15 μm).

2.1.1 Effect of Stirring Rate during Pouring Organic Phase into Water Phase

The same procedure as described in section **2.1** was prepared with different stirring rate ranging from 500, 650 to 800 rpm respectively. The effect of stirring rate was investigated on the particle size, the polydispersity index (PI) and the zeta potential.

To study the effect of stirring rate on the particle size, size distribution and zeta potential of itraconazole-loaded PIBCA nanoparticles, the experimental protocol was as follows:

I. <u>Design Structure</u>

The one-way analysis of variance (ANOVA) design used in this study. The independent variables as the one factor was " stirring rate" at three levels; 750, 1000 and 1500 rpm. Since there were two replicates, then total observations were 6 as shown in Table 3. Table 3 represents the j th observation taken under factor level or treatment i. The observed responses were the particle size, size distribution and zeta potential of itraconazole-loaded PIBCA nanoparticles.

Table 3 Typical data for a one-way analysis of variance (ANOVA) design.

Treatment (level) Stirring rate	observations	
Level 1 750 rpm	y_{11}	y_{12}
Level 2 1000 rpm	y_{21}	y_{22}
Level 3 1500 rpm	y_{31}	y_{32}

II. Response Model

$$y_{ij} \quad = \quad \mu + \tau_i + \varepsilon_{ij} \tag{5}$$

Where μ was the overall mean effect, τ_i was the effect of the ith level of the stirring

rate   and ε_{ij} was a random error component.

III. Hypotheses

Hypotheses about the equality of treatment (stirring rate) effects were as follows,

H_0 : no stirring rate effect on the response or

H_0 : $\tau_1 = \tau_2 = \tau_3 = 0$

H_1 : at least one $\tau_i \neq 0$ $\qquad$ (6)

IV. Statistical Test

$$SS_T = SS_{treatment} + SS_E \tag{7}$$

$$F_0 = \frac{MS_{treatment}}{MS_E} \tag{8}$$

F test was carried out to test the effect of treatment (stirring rate).

V. Decision Rule

The P-value approach to hypothesis testing was to reject H_0 if the P-value for the statistic F_0 is less than α.

2.1.2 Effect of Surfactant Concentrations in the Water Phase

The same procedure as described in section **2.1** was prepared with different concentration of poloxamer. The concentration of poloxamer was varied from 0.25 % (Valero, 1996), 0.50% (Chouinard, 1991), 0.75% to 1% (Rollot, 1986) respectively at the constant stirring rate of 750 rpm. The effect of surfactant concentration was investigated on the particle size, the polydispersity index (PI) and the zeta potential.

To study the effect of surfactant concentrations, the experimental protocol was as described in section **2.1.1**.

The independent variable was the surfactant concentration at four levels as follows, 0.25%, 0.50%, 0.75% and 1%. Since there were two replicates, then total observations were 8.

The response variables were the particle size, size distribution and zeta potential of itraconazole-loaded PIBCA nanoparticles.

2.1.3 The Factorial Design Study for Preparation of Itraconazole - Loaded PIBCA Nanoparticles

A factorial design is frequently employed for the planning of a research because it provides the maximum of information, requiring the least experiments (Erden and Celebi, 1996; Vandervoort and Ludwig, 2002). Itraconazole-

loaded PIBCA nanoparticles were prepared using method as described in section **2.1**. The concentration of poloxamer was fixed at 0.25% and the stirring rate was fixed at 750 rpm.

I. Design Structure

The range of a factor must be chosen in order to adequately measure its effects on the response variable. Furthermore, ranges must be chosen so that they encompass all of the preparation conditions likely to be encountered during nanoparticle formation. The range of IBCA monomer concentration (X_1) was chosen from 1 μL/mL to 10 μL/mL, benzyl benzoate concentration (X_2) was chosen from 5 μg/mL to 20 μg/mL and itraconazole concentration (X_3) ranged from 200 μg/mL to 1900 μg/mL as shown in Table 4

Table 4 Level of the investigated variables of itraconazole-loaded PIBCA nanoparticles.

Code unit	Independent Variables		
	IBCA (μL/mL) (X_1)	Benzyl benzoate (μg/mL) (X_2)	Itraconazole (μg/mL) (X_3)
-1	1	5	200
0	5.5	12.5	1050
1	10	20	1900

A 3^3 full factorial design with two replicates was used in this study. A 3^3 full factorial design has three factors, each at three levels. High and low levels of each factor were coded as 1 and -1, respectively, and the mean value was coded as zero. The coded variable, x_i, can be defined using equation

$$x_i = \frac{(X_i - X_i^x)}{\Delta X_i} \tag{9}$$

Where x_i is the coded value of the ith independent variable, which is usually defined to be dimensionless with mean zero and the same spread or standard deviation, X_i is the actual value of the ith independent variable, X^x_i is the actual value of the ith independent variable at the center point and ΔX_i is the step change value.

The three independent variables investigated were the concentration of IBCA monomer, benzyl benzoate (X_2) and itraconazole (X_3). The treatment combinations for a 3^3 factorial design was 27 observations as shown in Figure 4. Fifty-four observations were required to complete this 3^3 experimental design with two replications. In coded form, {1,1,1} represented the observation where each factor was at its highest level. Similarly, {1,0,-1} represented the observation where IBCA monomer concentration was set high, benzyl benzoate concentration was at its mean value and itraconazole concentration was set low, and so on. The design points for the investigated variables which have randomly runs are presented in Table 5. The four responses of interest were the particle size (nm), the polydispersity index (PI), the amount of itraconazole entrapped in nanoparticles (ITRAe) and the encapsulation efficiency (ITRAe [%]).

Figure 4 Three-dimensional region defined by the combination of coded variables.

● denotes the cube vertices and ○ denotes the centre of the cube faces and the design

origin (McCarron et al., 1999).

Table 5 Design points for the investigated variables of itraconazole-loaded PIBCA nanoparticles.

Formula	Random #	Level of variables					
		X_1 (µL/mL)		X_2 (µg/mL)		X_3 (µg/mL)	
		Actual variable	Code Variable	Actual variable	Code variable	Actual variable	Code variable
1a	1	1	-	5	-	200	-
26a	2	10	+	20	+	1050	0
13a	3	5.5	0	12.5	0	200	-
15a	4	5.5	0	12.5	0	1900	+
23a	5	10	+	12.5	0	1050	0
19a	6	10	+	5	-	200	-
24a	7	10	+	12.5	0	1900	+
20a	8	10	+	5	+	1050	0
19b	9	10	+	5	-	200	-
7a	10	1	-	20	+	200	-
22a	11	10	+	12.5	0	200	-
17a	12	5.5	0	20	+	1050	0
22b	13	10	+	12.5	0	200	-
5a	14	1	-	12.5	0	1050	0
21a	15	10	+	5	-	1900	+
1b	16	1	-	5	-	200	-
3a	17	1	-	5	-	1900	+
21b	18	10	+	5	-	1900	+
17b	19	5.5	0	20	+	1050	0
27a	20	10	+	20	+	1900	+
10a	21	5.5	0	5	-	200	-
11a	22	5.5	0	5	-	1050	0
16a	23	5.5	0	20	+	200	-
24b	24	10	+	12.5	0	1900	+
11b	25	5.5	0	5	-	1050	0
25a	26	10	+	20	+	200	-
10b	27	5.5	0	5	-	200	-
15b	28	5.5	0	12.5	0	1900	+
16b	29	5.5	0	20	+	200	-
8a	30	1	-	20	+	1050	0
25b	31	10	+	20	+	200	-
2a	32	1	-	5	-	1050	0
12a	33	5.5	0	5		1900	+
5b	34	1	-	12.5	0	1050	0
20b	35	10	+	5	-	1050	0

Table 5 Design points for the investigated variables of itraconazole-loaded PIBCA nanoparticles (continued).

Formula	Random #	Level of variables					
		X_1 (µL/mL)		X_2 (µg/mL)		X_3 (µg/mL)	
		Actual variable	Code Variable	Actual variable	Code variable	Actual variable	Code variable
26b	36	10	+	20	+	1050	0
2b	37	1	-	5	-	1050	0
6a	38	1	-	12.5	0	1900	+
23b	39	10	+	12.5	0	1050	0
14a	40	5.5	0	12.5	0	1050	0
8b	41	1	-	20	+	1050	0
18a	42	5.5	0	20	+	1900	+
27b	43	10	+	20	+	1900	+
13b	44	5.5	0	12.5	0	200	-
6b	45	1	-	12.5	0	1900	+
18b	46	5.5	0	20	+	1900	+
12b	47	5.5	0	5	-	1900	+
4a	48	1	-	12.5	0	200	-
14b	49	5.5	0	12.5	0	1050	0
9a	50	1	-	20	+	1900	+
7b	51	1	-	20	+	200	-
9b	52	1	-	20	+	1900	+
4b	53	1	-	12.5	0	200	-
3b	54	1	-	5	-	1900	+

II. Response Model

A second order model equation was employed for fitting the response surface in the form:

$$y = \beta_0 + \sum_{i=1}^{k} \beta_i x_i + \sum_{i=1}^{k} \beta_{ii} x_i^2 + \sum_{i \langle j=2}^{k} \beta_{ij} x_i x_j + \varepsilon \qquad (10)$$

Where y is the measured response of the particle size (nm), the polydispersity index (PI), the amount of itraconazole entrapped in the nanoparticles (ITRAe) (µg/mL), and the encapsulation efficiency (ITRAe [%])(%), β is called the regression coefficient, β_0, intercept term, β_i, β_{ij} and β_{ii} are, respectively, the measures of the effects of

variables x_i, $x_i x_j$, and x_i^2. The variable $x_i x_j$ represents the first order interactions

between x_i and x_i $(i<j)$.

III. Hypotheses

The hypotheses for testing the significance of any individual regression coefficient,

say β_i, are

$$H_0 : \beta_i = 0 , \beta_{ii} = 0, \beta_{ij} = 0$$

$$H_1 : \beta_i \neq 0 , \beta_{ii} \neq 0, \beta_{ij} \neq 0 \qquad (11)$$

If the parameter estimate is zero, then its associated factor plays no significant role in

the model.

IV. Statistical Test

Using an F-test, it is possible to test for lack of fit within each model, thereby

identifying which of the linear, quadratic or cubic terms in the models best described

the data.

V. Decision Rule

The P-value approach to hypothesis testing was to reject H_0 if the P-value for the

statistic F_0 is less than α.

2.2 Preparation of Nanoparticles Prepared from Poly

(lactic-co-glycolic acid)(PLGA)(85:15)

Itraconazole-loaded PLGA nanoparticles were prepared according to

the method already described by Fessi et al.(1989). Briefly, the accurate concentration

of 55 mg/mL of of PLGA (85:15), 12.5 µg/mL of benzyl benzoate, and 1000 µg/mL of itraconazole were dissolved in 10 mL of acetone. The organic phase was pour into 25 mL of the aqueous phase containing 0.25 % of poloxamer at a constant stirring rate at 750 rpm.   The organic solvent was finally removed under reduced pressure and the final volume was filtrated through a sintered glass filter (porosity 4, mesh size 5-15 µm).

2.2.1 Effect of Stirring Rate during Pouring Organic Phase into Water Phase

The same procedure as described in section **2.2** was prepared with different speed of homogenizer ranging from 750, 1000, to 1500 rpm. The effect of stirring rate was investigated on the particle size, the polydispersity index (PI) and the zeta potential.

To study the effect of stirring rate, the experimental protocol was as described in section **2.1.1** .

The independent variable was the stirring rate at three levels as follows, 750, 1000 and 1500 rpm.   Since there were two replicates, then total observations were 6.

The response variables were the particle size, size distribution and zeta potential of itraconazole-loaded PLGA nanoparticles.

2.2.2 Effect of Surfactant Concentrations in the Water Phase

The same procedure as described in **2.2** was prepared with different concentration of poloxamer ranging from 0.25 %, 0.50%, 0.75% to 1%

respectively at the constant stirring rate of 750 rpm. The effect of surfactant concentration was investigated on the particle size, the polydispersity index (PI) and the zeta potential.

To study the effect of surfactant concentration, the experimental protocol was as described in **2.1.1 .**

The independent variable was the surfactant concentration at four levels as follows, 0.25 %, 0.50%, 0.75% and 1%. Since there were two replicates, then total observations were 8.

The response variables were the particle size, size distribution and zeta potential of itraconazole-loaded PLGA nanoparticles.

2.2.3 The Factorial Design Study of Itraconazole - Loaded PLGA Nanoparticles

Itraconazole- loaded PLGA nanoparticles were prepared using method as described in **2.2**. The concentration of poloxamer was fixed at 0.25% and the stirring rate was fixed at 750 rpm.

In order to reach the objective of this research, the experimental protocol was as follows,

I. <u>Design Structure</u>

A 2^3 full factorial design with 2 replicates was used in this study. The 3 independent variables investigated were the concentrations of PLGA (A), benzyl benzoate (B), and itraconazole (C) each at two levels. The range of PLGA concentration (A) was chosen from 1 mg/mL as low level to 10 mg/mL as high level, benzyl benzoate concentration (B) was chosen from 5 μg/mL as low level to 20 μg/mL as high level

and itraconazole concentration (C) ranged from 200 µg/mL as low level to 1800

µg/mL as high level (Table 4). The treatment combinations for this design are $2^3 = 8$

as shown in Figure 5. Five replicates at the center of the design were investigated to

allow for an independent estimation of the experimental error and to check the

linearity of the factor effects (Montgomery, 2001). The concentration of PLGA,

benzyl benzoate and itraconazole at the center of the design was 55 mg/mL, 12.5

µg/mL and 1000 µg/mL, respectively. Twenty-one observations are required to

complete this 2^3 experimental design with two replicates including the addition of

five replicates at the center of the design and the random design points for the

investigated variables are presented in Table 7.
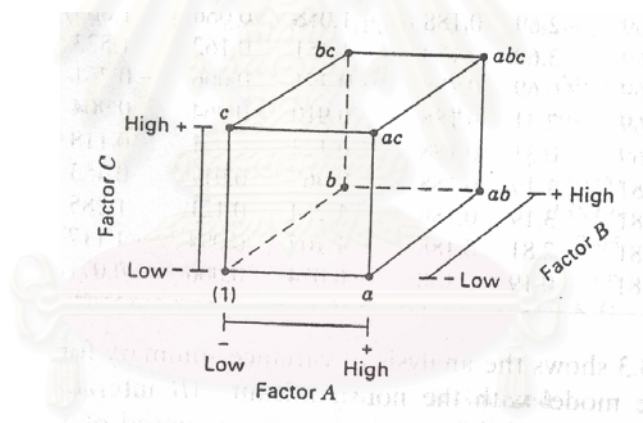
Figure 5 The geometric view of the 2^3 factorial design (Montgomery, 2001).

In developing the regression equation the test factors were coded according to

the equation **9**.

The effect of the previously mentioned variables was

investigated on the following responses: the particle size (nm), the polydispersity

index (PI), the amount of itraconazole entrapped in nanoparticles (ITRAe) and the

encapsulation efficiency (ITRAe [%]).

Table 6 Level of the investigated variables of itraconazole-loaded PLGA nanoparticles.

| Code Unit | Independent Variables | | |
	PLGA (A) (mg/mL)	Benzyl Benzoate (B) (µg/mL)	Itraconazole (C) (µg/mL)
-1	10	5	200
1	100	20	1800

Table 7 Design points for the investigated variables of itraconazole-loaded PLGA nanoparticles.

| Formula | Random No. | Level of Variables | | |
		A (mg/mL)	B (µg/mL)	C (µg/mL)
1a	1	10	5	200
4a	2	10	20	1800
4b	3	10	20	1800
6a	4	100	5	1800
3a	5	10	20	200
5a	6	100	5	200
2a	7	10	5	1800
3b	8	10	20	200
1b	9	10	5	200
2b	10	10	5	1800
8a	11	100	20	1800
8b	12	100	20	1800
7a	13	100	20	200
7b	14	100	20	200
6b	15	100	5	1800
9a	16	55	12.5	1000
9b	17	55	12.5	1000
9c	18	55	12.5	1000
9d	19	55	12.5	1000
9f	20	55	12.5	1000
5b	21	100	5	200

II. Response Model

A linear regression model equation was employed for fitting the response surface in the following equation:

$$y = \beta_0 + \sum_{i=1}^{k} \beta_i x_i + \sum_{i \langle} \sum_{j=2}^{k} \beta_{ij} x_i x_j + \varepsilon \qquad \text{(12)}$$

where y is the measured response of the particle size (nm), the polydispersity index (PI), the amount of itraconazole entrapped in the nanoparticles (ITRAe) (µg/mL), and the encapsulation efficiency (ITRAe [%]), β is called the regression coefficient, β_0, intercept term, β_i and β_{ij} are, respectively, the measures of the effects of variables x_i and $x_i x_j$. The variable $x_i x_j$ represents the first order interactions between x_i and x_j ($i < j$).

III. Hypotheses

The hypotheses for testing the significance of any individual regression coefficient, say β_i, are

$$H_0 : \beta_i = 0 \ , \ \beta_{ij} = 0$$

$$H_1 : \beta_i \neq 0 \ , \ \beta_{ij} \neq 0 \qquad \text{(13)}$$

One important reason for adding the replicate runs at the design center is that center points do not effect the usual effect estimates in a 2^k design. The error mean square was calculated according to the following equation:

$$MS_E = \frac{SS_E}{n_c - 1} \qquad \text{(14)}$$

$$MS_E = \frac{\sum_{Center\ points} \{Y_i - \overline{Y}\}^2}{n_c - 1} \qquad \text{(15)}$$

Where Y_i is the response of the i th replicates at the center of the design, $\overline{Y}$ is the mean, and n_c is the number of the replicates.

The curvature sum of squares is calculated according to the following equation:

$$SS_{curvature} = \frac{n_f n_c \{\overline{Y_f} - \overline{Y_c}\}^2}{n_f + n_c} \tag{16}$$

Where n_f and n_c are the number of the factorial experiments and the experiments at the center, respectively; $\overline{Y_f}$ and $\overline{Y_c}$ are the means of the corresponding observations.

$SS_{curvature}$ with 1 degree of freedom was compared with the error mean square to check any curvature in the response surface as a function of different factors effect.

IV. Statistical Test

Using an F-test, it is possible to test for lack of fit within each model, thereby identifying which of the linear model, quadratic model or cubic model best described the data.

V. Decision Rule

The P-value approach to hypothesis testing was to reject H_0 if the P-value for the statistic F_0 is less than α.

2.3 Statistic Analysis

2.3.1 Test for Stirring Rate and Surfactant Concentration

Statistical analysis of the effect of speed and surfactant concentration was carried out by the one-way analysis of variance (ANOVA) with a level of significance of P< 0.05. The one-way analysis of variance was performed using the Minitab statistical analysis program assuming normal distribution.

2.3.2 Response Surface Analysis for the factorial design Study of Itraconazole-Loaded IBCA Nanoparticles and Itraconazole-Loaded PLGA Nanoparticles

Data was analysed using Design-Expert software with a level of significance of P< 0.05. Statistical analysis was provided within the package by constructing an ANOVA table, where the variation explained by the fitted model is compared to the variation unaccounted for by the model. From this ratio, an F statistic can be derived allowing rejection of the null hypothesis at the chosen level of significance and inference that the variation accounted for in the model is significantly greater than the unexplained variation.

2.3.3 Multiple response Optimization

Optimization is obtained by establishing a relationship among the various types of variables; the values for the independent variables should be fixed, while the values of the dependent variables are linked immediately to the former by means of a mathematical model. Optimization techniques for pharmaceutical formulation and processing, as well as theoretical and practical aspects, can be found in the pharmaceutical literature (Davis, 1978; Schartz, 1990; Renoux et al., 1996)

A relatively straightforward approach to optimizing several factor responses that works well when there are only a few process variables is to overlay the contour plots for each response. When there are more than three design variables, overlaying contour plots becomes awkward, because the contour plot is two-dimensional, and k - 2 of the design variables must be held constant to construct the graph. Often a lot of trial and error is required to determine which

factors to hold constant and what levels to select to obtain the best view of the surface.

A popular approach is to formulate and solve the problem as a **constrained optimization problem**. There are many numerical techniques that can use to solve this problem. Sometimes these techniques are referred to as nonlinear programming methods. The Design-Expert software package solves this version of the problem using a direct search procedure. In search methods the response surfaces, as defined by the appropriate equations, are searched by various methods to find the combination of independent variables yielding the optimum. A search method of optimization was applied to a pharmaceutical system and was reported by Schwartz et al. (1990). It takes five independent variables into account and is computer assisted. It was proposed that the procedure described could be set up such that persons unfamiliar with the mathematics of optimization and with no previous computer experience could carry out an optimization study.

Another useful approach to optimization of multiple responses is to use the simultaneous optimization technique popularized by Derringer and Suich (1980). Their procedure makes use of desirability functions. The general approach is to first convert each response Y_i into an individual desirability function d_i that varies over the range

$$0 \leq d_i \leq 1$$

when the response Y_i is at its goal or target, then $d_i = 1$, and when the response is outside an acceptable region, $d_i = 0$. Then the design variables are chosen to maximize the overall desirability

$$D = (d_1 * d_2 * \ldots \ldots * d_m)^{1/m} \qquad \textbf{(17)}$$

The individual desirability functions are structured as shown in Figure 6. If the objective or target T for the response y is a maximum value,

$$d = \begin{cases} 0 & y < L \\ (\dfrac{y - L}{T - L})^r & L \leq y \leq T \\ 1 & y > T \end{cases} \qquad \textbf{(18)}$$

when the weight r = 1, the desirability function is linear. Choosing r > 1 places more emphasis on being close to the target value, and choosing 0 < r < 1 makes this less important. If the target for the response is a minimum value,

$$d = \begin{cases} 1 & y < T \\ (\dfrac{U - y}{U - T})^r & T \leq y \leq U \\ 0 & y > U \end{cases} \qquad \textbf{(19)}$$

The two-sided desirability shown in Figure 6(c) assumes that the target is located between the lower (L) and upper (U) limits, and is defined as

$$d = \begin{cases} 0 & y < L \\[2ex] \left(\dfrac{y-L}{T-L}\right)^r & L \le y \le T \\[2ex] \left(\dfrac{U-y}{U-T}\right)^r & T \le y \le U \\[2ex] 0 & y > U \end{cases} \qquad \textbf{(20)}$$
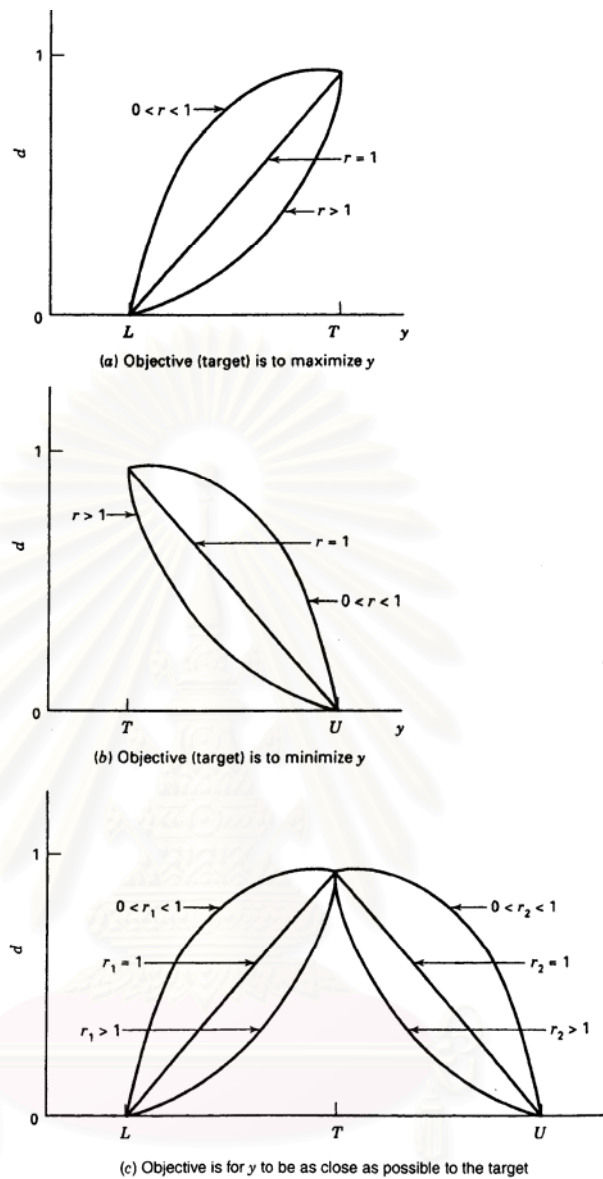
Figure 6   Individual desirability functions for simultaneous optimization

(Myers and Montgomery, 2002).

In order to optimization, the Design-Expert software was used for this purpose.

(a) Overlay the contour plots for each response.

(I) Itraconazole- loaded PIBCA nanoparticles

To compare the multiple response optimizations, the contour plots for the four responses with different conditions were overlaid. Firstly, the contour plots for the four responses; $160 < Y_1$ (the particle size) < 190, $0.044 < Y_2$ (PI) < 0.077, $450 < Y_3$ (ITRAe) < 550, and $40 < Y_4$ (ITRAe [%]) < 50 were overlaid. Secondly, the contour plots for the four responses; $160 < Y_1$ (the particle size) < 190, $0.044 < Y_2$ (PI) < 0.077, $450 < Y_3$ (ITRAe) < 550, and $50 < Y_4$ (ITRAe [%]) < 60 were overlaid.

(II) Itraconazole- loaded PLGA nanoparticles

To compare the multiple response optimization, the contour plots for the four responses with different conditions were overlaid. Firstly, the contour plots for the four responses; $300 \leq Y_1$ (the particle size) ≤ 400, $0.452 < Y_2$ (PI) < 0.632, $450 \leq Y_3$ (ITRAe) ≤ 550, and $60 \leq Y_4$ (ITRAe [%]) ≤ 70 were overlaid. An overlay plot for the four responses: $200 \leq Y_1$ (the particle size) ≤ 300, $0.452 < Y_2$ (PI) < 0.632, $450 \leq Y_3$ (ITRAe) ≤ 550, and $60 \leq Y_4$ (ITRAe [%]) ≤ 70 was performed.

(b) Constrained optimization and simultaneous optimization technique

To perform the constrained optimization and simultaneous optimization technique using desirability function , the optimized

conditions of itraconazole- loaded PIBCA nanoparticles and itraconazole- loaded PLGA nanoparticles were given as follows,

(I) Itraconazole- loaded PIBCA nanoparticles

The target of ITRAe was chosen to be 500 µg/mL, while the lower limit was equal to 450 µg/mL, and the upper limit was 550 µg/mL. The particle size ranged from 160 nm to 190 nm. The polydispersity index ranged from 0.044 to 0.077, and the ITRAe [%] ranged from 40% to 60%.

(II) Itraconazole- loaded PLGA nanoparticles

The target of ITRAe was chosen to be 500 µg/mL, while the lower limit was equal to 450 µg/mL, and the upper limit was 550 µg/mL. The particle size was set equal at the minimum between 300 and 400 nm. The polydispersity index ranged from 0.452 to 0.632. , and the ITRAe [%] ranged from 60 % to 70%.

(c) Model and Optimization Verification

Verification of the predicted value was made by preparing itraconazole- loaded PIBCA nanoparticles (Table8) and itraconazole- loaded PLGA nanoparticles (Table 9) with different formula compositions including optimized conditions. The particle size and the encapsulation efficiency were used as the measured response.

Table 8 Formula composition of itraconazole-loaded PIBCA nanoparticle for the

model and optimization verification.

Formula	Concentration		
	IBCA (μL/mL)	Benzyl benzoate (μg/mL)	Itraconazole (μg/mL)
1	8.09	10.19	1200.77
2	7.68	10.14	1224.58
3	8.43	10.16	1188.87
4	7.89	10.10	12.17.02

Table 9 Formula composition of itraconazole-loaded PLGA nanoparticles for the

model and optimization verification.

Formula	Concentration		
	PLGA (mg/mL)	Benzyl benzoate (μg/mL)	Itraconazole (μg/mL)
1	55	20.00	1000.00
2	10	12.50	1000.00
3	100	12.50	200.00
4	10	16.94	1001.01

3 Characterization of nanoparticles

3.1 Particle size and size distribution

The physicochemical characteristics of nanoparticles were studied

within 5 days for all preparations. The particle size and size distribution (defined as

polydispersity index (PI)) of nanoparticles were determined by photon correlation

spectroscopy (Malvern 4700 laser spectrometer, Malvern Instruments Ltd.).   For

particle size analysis, the nanoparticles were dispersed in ultrapure water filtrated

through 0.22 μm nylon membrane for minimizing dust. Measurements were carried out at 30°C using a 632.8 nm laser at an angle of 90°.

3.2 Surface Morphology

The external surface morphology of nanoparticles was visualized by Scanning Electron Microscopy (SEM). The samples were dried either by liquid nitrogen or freeze drying. Samples were then sputter coated with gold prior to viewing at an acceleration voltage of 40 kV.

3.3 Zeta Potential

The Zeta potential of the nanoparticles was determined by Zetasizer 4 (Malvern Instruments Ltd.). The nanoparticles were dispersed in ultrapure water filtrated through 0.22 μm nylon membrane. The measurements were carried out at 30°C.

3.4 The Amount of Itraconazole Entrapped in Nanoparticles (ITRAe) and the Encapsulation Efficiency (ITRAe[%]

The amount of itraconazole entrapped in nanoparticles (ITRAe) in the suspension was assayed by HPLC developed in section **4** after filtration through a sintered glass filter (porosity 4, mesh size 5-15μm). This filtration step retained the unassociated itraconazole that precipitated in the aqueous phase just after preparation because of its insolubility. Three replications of one mL of sample solution were mixed with 5 mL of the internal standard solution equivalent to 2.5 mg of ketoconazole in a 100 mL volumetric flask and diluted with methanol. The coating

material was dissolved in methanol. A portion of solution was appropriate diluted with methanol. The amount of itraconazole was calculated from calibration curve, multiplied with dilution factors.

The encapsulation efficiency (ITRAe [%]) was calculated by using the following formula,

$$ITRAe[\%] \quad = \frac{M_{actual}}{M_{theoretical}} \times 100 \qquad\qquad \textbf{(21)}$$

where M_{actual} was the actual amount of itraconazole determined by the above experiment and $M_{theoretical}$ was the theoretical amount of itraconazole calculated from the quality added in the fabrication process.

4. High - Performance Liquid Chromatographic Technique for Drug Analysis

The determination of itraconazole by reverse phase HPLC assay with UV detection was modified from the method described by Law et al. (1994). The procedure was developed as follows:

Column : Lichrosper 60 RP-select B $^{®}$5 μ(4.6 x 120 mm)

Mobile phase : Acetonitrile:water:diethylamine(50:50:0.05)

Mobile phase was prepared freshly and filtered through a 0.45 μm membrane filter. It was then degassed by sonication for about 1 hour prior to use.

Flow rate : 1.1 mL/minute

Detector wavelength : 263 nm

Injection volume   : 30 μL

Internal standard   : ketoconazole

Temperature   : ambient

 Attenuation   : 64

Chart speed   : 0.25 cm/minute

Retention time   : Itraconazole   6.29 – 6.37 minutes

                                 Ketoconazole   3.49- 3.84 minutes

4.1 Validation for the Quantitative Determination of Itraconazole

The typical analytical parameters considered in the validation of the quantitative determination of itraconazole by HPLC method were as follows: (United States Pharmacopeial Convention, 1995).

4.1.1 Specificity

The specificity of the HPLC method used to determine itraconazole quantity was evaluated by comparing the chromatograms of itraconazole and the peaks of other components in the nanoparticle systems. The blank preparation that had the same component as itraconazole- loaded nanoparticles was prepared and the peaks of other components in the sample must not interfere with the peak of itraconazole.

4.1.2 Precision

(a) Within Run Precision

The within run precision was evaluated by analyzing peak area ratios of drug to internal standard of three repetitions of each concentration of standard solution on the same day. The mean, the standard deviation (SD) and the percentage coefficient of variation (%CV) of each concentration were determined.

(b) Between Run Precision

The between run precision was evaluated by analyzing peak area ratios of drug to internal standard of three repetitions of each concentration of standard solution on 3 different days. The mean, the standard deviation and the percentage coefficient of variation of each concentration were determined.

4.1.3 Accuracy

The accuracy of itraconazole assay was evaluated by analyzing percent recoveries of each concentration of itraconazole standard solution. Percent recovery of each injection was calculated by comparing the concentration fitted from a calibration curve with the known concentration.

4.1.4 Linearity

The linearity was evaluated by plotting the standard curve between the peak area ratios of itraconazole to internal standard and the concentrations of itraconazole. Linear regression analysis was performed. The equation and the coefficient of determination (R-square) were calculated.

4.2 Preparation of Standard Solutions

The internal standard solution was prepared by completely dissolving 100 mg of ketoconazole in a 200-mL volumetric flask and diluted to volume with methanol. Fifty mg of itraconazole was accurately weighed into a 200-mL volumetric flask; the drug was dissolved and diluted with methanol.

Itraconazole solutions with volume of 0.5, 1, 2, 3, 4, 5 mL were mixed with 5 mL of the internal standard solution in a 100-mL volumetric flask and diluted with same solvent to obtain standard solutions with various concentrations of itraconazole ranging from 1.25 to 12.5 µg/mL. These solutions were assayed by HPLC method.

The standard solutions were also prepared from plain nanoparticles with different components containing ketoconazole as internal standard and different added concentration of itraconazole ranging from 1.25 to 12.5 µg/mL. The percent recovery was calculated.

For drug solubility analysis, the standard solutions were prepared from 1 mL of each oil containing ketoconazole and itraconazole ranging from 1.25 to 12.5 µg/mL. The percent recovery was calculated.

4.3 Analysis of Itraconazole Content in Preparation, Different Oils and Different Aqueous Media

One mL of sample solution was mixed with 5 mL of the internal standard solution in a 100 mL volumetric flask and diluted with methanol. This solution was assayed by HPLC method. The ratio of the peak area of itraconazole to that of the internal standard was used to calculate the itraconazole concentration. The

amount of drug was calculated from calibration curve, multiplied with dilution factors.

A portion of the solution under drug solubility testing was appropriately diluted with methanol and was determined by HPLC at 263 nm. The amount of drug solubility was calculated from calibration curve and multiplied with dilution factors.

5 In Vitro Release Study

Release of itraconazole from of itraconazole-loaded PIBCA nanoparticles (using 8.09 µL/mL of IBCA monomer, 10.19µg/mL of benzyl benzoate ,and 1200.77 µg/mL of itraconazole) and itraconazole-loaded PLGA nanoparticles (using 10 mg/mL of PLGA with different ratio [85:15, 75:25, 65:35 and 50:50] , 16.94 µg/mL of benzyl benzoate, and 1001.01 µg/mL of itraconazole) were investigated. The dissolution method was followed as stated in the USP XXIII (1995). The dissolution apparatus II was operated using constant temperature at 37± 0.5 °C with constant stirring rate of 50 rpm/min. Nine hundred milliliters of PBS with 2% sodium lauryl sulphate was used as dissolution medium (degassed and maintained). The medium was chosen to avoid precipitation of itraconazole released in the dissolution medium and to reach sink condition. A sufficient amount of nanoparticles (corresponding to 2.5 mg of itraconazole) was placed in dissolution medium (n = 6). Five milliliters of each sample was withdrawn after the dissolution apparatus was operated at 0.25, 0.5, 0.75, 1, 2,4, 6,12,24, 48, 72, 96, 120,144 and 168 hours, respectively. The equivalent amount of dissolution medium equilibrated at 37± 0.5 °C was added immediately

after each sampling to maintain a constant volume of dissolution medium. Samples were filtered through 5 µm filters and centrifuged at 50,000 rpm for 20 minutes at 4°C. The precipitated was discarded and the supernatant was used to assay the amount of drug release as described in section **4.3**.

6 Physical Stability Study

The stability studies were performed on itraconazole-loaded PIBCA nanoparticles and itraconazole-loaded PLGA nanoparticles with three replicate samples during 3 months storage at 4 °C. The integrity of the nanoparticles was evaluated by the particle size, the encapsulation efficiency and the zeta potential. The experimental protocol was similar as described in section **1.1**.

The two-way analysis of variance (ANOVA) design was used to evaluate the stability study The independent variables as two treatment factor were " polymer" at two levels; PIBCA and PLGA ; and "day" at three levels; 30, 60 and 90 days, giving a total 6 treatment combinations. Since there were three replicates, then total observations were 18. The observed response was the particle size, the encapsulation efficiency and the zeta potential.

The two-way analysis of variance (ANOVA) followed by Tukey's pair wise comparisons at a 95 % confidence interval was used to test for significant difference among different types at each time interval with regards to the the particle size, the encapsulation efficiency and the zeta potential. The two-way analysis of variance (ANOVA) and Tukey's pair wise comparisons were performed using the Minitab statistical analysis program assuming normal distribution.

7 Cytotoxic Determination

Vero cell-line were cultured at 37 °C in an atmosphere of 5% CO_2 and 95% relative humidity in Dulbecco's Modified eagle's Medium (DMEM) with 10 % fetal bovine serum previously inactivated at 56 °C for 30 min. The cells were washed twice and resuspended in a DMEM medium with 10 % fetal bovine serum. A 12 X 8 microtiter plate (Nunc, InterMed Denmark) was used for cytotoxicity assay. Each well was injected with 100 μL containing 4 $X10^5$ cell/mL. After incubation at 37° C for 18 hr in a 5% CO_2 atmosphere, non-adhering cells were removed by rinsing them with cold medium. One hundred microlitres of various types and concentrations of test preparations were injected into each well containing cell lines. All concentrations were used in 8 replications. After incubation period, cell viability was determined by the crystal violet staining technique. The supernatant was discarded and the remaining, viable, adherent cells were stained with 100 μL of 0.1% crystal violet in 25% methanol for 15 min. The microtiter plates were rinsed with running water and air dried. The absorbance of each well was read at 620 nm using 96-well Microplate Reader (Bio Whittaker, Germany). The absorbance of the control wells which contained no test material was regarded as 100 percent. Cytotoxicity activity was calculated as follows:

$$\text{Viability (\% of control)} = \frac{\text{A620 of test sample}}{\text{A620 of control sample}} \text{ x } 100 \qquad \textbf{(22)}$$

The results were plotted between the percent viability against the concentrations of test preparations, and the cytotoxicity assay was determined for the IC_{50} from the curve. The IC_{50} was defined as the concentration which caused 50% cell death (Yamamoto et al., 2001).

7.1 Influence of Incubation Times on Cytotoxicity

The various preparations were used to investigate the influence of incubation times on Vero cell line cytotoxicity. The 0.5 % of 0.25% poloxamer in water in incubation medium, 0.5% of plain PLGA nanoparticles in incubation medium , 0.5 % of itraconazole- loaded PLGA nanoparticles in incubation medium , 0.5% of plain PIBCA nanoparticles in incubation medium, and 0.5 % of itraconazole-loaded PIBCA nanoparticles in incubation medium were incubated at 1, 2, 3 and 4 h. The 1 % of 0.25% poloxamer in water in incubation medium, 1% of plain PLGA nanoparticles in incubation medium, 1 % of itraconazole-loaded PLGA nanoparticles in incubation medium, 1% of plain PIBCA nanoparticles in incubation medium, and 1 % of itraconazole- loaded PIBCA nanoparticles in incubation medium were also incubated at 1, 2, 3 and 4 h. The diagram of cytotoxicity assay is shown in Figure 7.

The two-way analysis of variance (ANOVA) design was used to evaluate the influence of incubation time on cytotoxicity. The independent variables as two treatment factor were "test preparation" at five levels; 0.5 % of 0.25% poloxamer in water in incubation medium, 0.5% of plain PLGA nanoparticles in incubation medium, 0.5 % of itraconazole- loaded PLGA nanoparticles in incubation medium, 0.5% of plain PIBCA nanoparticles in incubation medium, and 0.5 % of itraconazole- loaded PIBCA nanoparticles in incubation medium; and "time" at four levels; 1, 2, 3 and 4 h,, giving a total 20 treatment combinations. Since there were eight replicates, then total observations were 160.   The observed response was the viability. The design protocol was similar to the design described in section **1.1**.

7.2 Influence of Concentration on Cytotoxicity

Various concentrations of itraconazole- loaded PIBCA nanoparticles, plain PIBCA nanoparticles ranging from 0.2% to 100% of preparations which corresponded, respectively, to, 30.8 µg/ mL and 15.4 mg/mL were incubated at 4 h. Various concentrations of itraconazole-loaded PLGA nanoparticles and plain PLGA nanoparticles ranging from 0.2% to 100% of preparations which corresponded, respectively, to,2.4 mg/mL and 1.2 g/mL were incubated at 4 h. The diagram of cytotoxicity assay is shown in Figure 7.

The two-way analysis of variance (ANOVA) design was used to evaluate the influence of concentration on cytotoxicity. The independent variables as two treatment factor were "test preparation" at four levels; itraconazole- loaded PIBCA nanoparticles, plain PIBCA nanoparticles, itraconazole-loaded PLGA nanoparticles and plain PLGA nanoparticles ; and "concentration" at nine levels; 0.2%, 0.4%, 0.6%, 0.8%, 1%, 5%,10% 20% and 40%, giving a total 36 treatment combinations. Since there were eight replicates, then total observations were 288. The observed response was the viability. The design protocol was similar to the design described in section **1.1**.

7.3 Statistical Analysis

The two-way analysis of variance (ANOVA) followed by Tukey's pair wise comparisons at a 99 % confidence interval was used to test for significant difference among different types at each time interval with regards to the viability.

The two-way analysis of variance (ANOVA) and Tukey's pair wise comparisons were performed using the Minitab statistical analysis program assuming normal distribution.

Figure7 Diagram of cytotoxicity assay.

	1	2	3	4	5	6	7	8	9	10	11	12
A	◯	◯	◯	◯	◯	◯	◯	◯	◯	◯	◯	◯
B	◯	◯	◯	◯	◯	◯	◯	◯	◯	◯	◯	◯
C	◯	◯	◯	◯	◯	◯	◯	◯	◯	◯	◯	◯
D	◯	◯	◯	◯	◯	◯	◯	◯	◯	◯	◯	◯
E	◯	◯	◯	◯	◯	◯	◯	◯	◯	◯	◯	◯
F	◯	◯	◯	◯	◯	◯	◯	◯	◯	◯	◯	◯
G	◯	◯	◯	◯	◯	◯	◯	◯	◯	◯	◯	◯
H	◯	◯	◯	◯	◯	◯	◯	◯	◯	◯	◯	◯

1. The concentration of 0.5 % or 1% of 0.25% poloxamer in water in incubation medium was (1), 0.5% or 1% of plain PLGA nanoparticles in incubation medium was (2), 0.5 % or 1% of itraconazole- loaded PLGA nanoparticles in incubation medium was (3), 0.5% or 1% of plain PIBCA nanoparticles in incubation medium was (4) and 0.5% or 1 % of itraconazole- loaded PIBCA nanoparticles in incubation medium was (5) .

| E** | E** | E** | 1 | 2 | 3 | 4 | 5 | C * | E** | E** | E** |

Figure7 Diagram of cytotoxicity assay (continued).

2. Various concentrations of itraconazole- loaded PIBCA nanoparticles , plain

PIBCA nanoparticles , itraconazole- loaded PLGA nanoparticles and plain PLGA

nanoparticles   ranging from 0.2% to 100% of preparations were incubated at   4 h .

C*	0.2	0.4	0.6	0.8	1	5	10	20	40	80	100

C*: Control (cells + medium)   E **: empty

CHAPTER IV

RESULTS AND DISCUSSION

1 Solubility of Itraconazole

1.1 Solubility of Itraconazole in Different Oils.

Itraconazole was associated with several properties that made it difficult to formulate especially into parenteral preparations, such as very poor water solubility (~1 ng/mL at neutral pH) and a high log P(estimated log P_{oct} = 6.2) (Peeters et al., 2002). One approach, which had been applied to produce pharmaceutically acceptable parenteral dosage forms of the drug, was the use of nanoparticle preparation. Oil selection was one of the factors to incorporate maximum itraconazole to nanoparticles. Benzyl benzoate, corn oil, caprylic/capric triglycerides, and soybean oil were selected because they could be used in parenteral preparation. The solubility of itraconazole in different oils is shown in Table 10. It was found that itraconazole solubility in different oils was ranked in the order of soybean oil < caprylic/capric triglycerides < corn oil < benzyl benzoate. The highest solubility of itraconazole was 1036.69 ± 43.61 µg/mL in benzyl benzoate. Therefore, benzyl benzoate was used for further study. The solubility of itraconazole in different oil among 1,3,5, and 7 days did not show significant difference (P > 0.05) but the solubility of itraconazole in different oils among benzyl benzoate, corn oil, caprylic/capric triglycerides, and soybean oil showed significant difference (P< 0.05) as shown in Table 11.

Using Tukey's pairwise comparisons, all pairwise between benzyl benzoate, corn oil, caprylic/capric triglycerides and soybean oil showed significant

difference of each other in solubility (P< 0.05). The details of Tukey's pairwise comparisons are shown in Table 12.

Table 10 Solubility of itraconazole in different oils (values represent means ± S.D., n=3).

Type of oil	Solubility (µg/mL)			
	1 day	3days	5 days	7 days
Benzyl benzoate	972.21±30.26	988.46±12.94	1036.69±43.61	994.39±5.44
Corn oil	777.05±19.35	768.78±14.27	755.07±7.53	779.17±16.11
Caprylic/capric triglycerides	165.61±0.86	170.60±1.21	175.55±2.97	178.29±2.70
Soybean oil	41.88±0.92	43.44±1.48	45.23±0.94	49.76±1.37

Table 11 ANOVA Table for solubility of itraconazole in different oils.

Source of variable	DF	SS	MS	F	P
day	3	957	319	1.61	0.207
oil	3	7666331	2555444	1.3E+04	0.000
Interaction	9	5330	592	2.99	0.011
Error	32	6349	198		
Total	47	7678967			

Table 12 P-value obtained from Tukey's pairwise comparisons among levels of oil.

Oil	Benzyl benzoate	Corn oil	Caprylic/capric triglycerides	Soybean oil
Benzyl benzoate	-	0.0000	0.0000	0.0000
Corn oil	0.0000	-	0.0000	0.0000
Caprylic/capric triglycerides	0.0000	0.0000	-	0.0000
Soybean oil	0.0000	0.0000	0.0000	-

1.2 Solubility of Itraconazole in Different Aqueous Media

The solubility of itraconazole in different aqueous media is shown in Table 13. Itraconazole solubility in different media was ranked in the order of 4% cyclodextrin in water < SGF < 0.25% SLS in PBS whereas the solubility of itraconazole in water, PBS, 0.25% Poloxamer in PBS and 0.25% Poloxamer in water were less than 1.25 µg/mL. These results were in agreement with Chowdary and Srinivasa (2000a, 2000b) that itraconazole solubility in purified water and phosphate buffer was 1.2 and 0.77 µg/mL, respectively. Chowdary and Srinivasa (2000a, 2000b) found that the solubility of itraconazole in 0.1 N hydrochloric acid was greatly increased when SLS was added. A 76 and 164 fold increase in the solubility of itraconazole in 0.1 N hydrochloric acid was observed at 0.5% and 1.0% SLS concentrations, respectively. The same result was found in this study when 0.25% SLS in PBS was used to test the solubility of itraconazole. The highest solubility of itraconazole was 31.29±1.27 µg/mL in 0.25% SLS in PBS. Therefore, 0.25% SLS in PBS was used as a medium for *In vitro* release study. The solubility of itraconazole in water, PBS, 0.25% Poloxamer in PBS, and 0.25% Poloxamer in water were less than 1.25 µg/mL which was less than limit of quantitation so only the solubility of itraconazole in 4% cyclodextrin, 0.25% SLS in PBS and SGF were analyzed by ANOVA. The solubility of itraconazole in each of 4% cyclodextrin, 0.25% SLS in PBS and SGF among 1, 3, 5 and 7 days were not significant difference (P > 0.05) but the solubility of itraconazole among 4% cyclodextrin in water, 0.25% SLS in PBS and SGF were significant difference (P< 0.05) as shown in Table 14.

Using Tukey's pairwise comparisons, 4% Cyclodextrin in water showed significant difference in itraconazole solubility with 0.25% SLS in PBS (P<

0.05). The itraconazole solubility in 0.25% SLS in PBS and SGF were significant difference (P < 0.05). There was no significant difference in itraconazole solubility between 4% cyclodextrin in water and SGF (P > 0.05). The details of Tukey's pairwise comparisons are shown in Table 15.

Table 13 Solubility of itraconazole in different aqueous media (values represent means ± S.D., n=3).

Type of aqueous medium	Solubility (µg/mL)			
	1 day	3days	5 days	7 days
Water	< 1.25	< 1.25	< 1.25	< 1.25
PBS	< 1.25	< 1.25	< 1.25	< 1.25
0.25% Poloxamer in water	< 1.25	< 1.25	< 1.25	< 1.25
0.25% Poloxamer in PBS	< 1.25	< 1.25	< 1.25	< 1.25
0.25%SLS in PBS	31.06±1.80	31.29±1.27	31.08±1.15	30.76±1.76
4% Cyclodextrin in Water	8.71±0.56	8.61±0.65	8.91±0.57	9.05±0.37
Simulated Gastric Fluid	9.40±0.80	9.66±0.79	9.36±0.80	9.50±0.67

Table 14 ANOVA Table for solubility of itraconazole in different aqueous media.

Source of variable	DF	SS	MS	F	P
Aqueous medium	2	3839.02	1919.51	1802.84	0.000
Day	3	0.08	0.03	0.02	0.995
Interaction	6	0.87	0.14	0.14	0.990
Error	24	25.55	1.06		
Total	35	3865.52			

Table 15 P-value obtained from Tukey's pairwise comparisons among levels of aqueous medium.

Aqueous medium	4% Cyclodextrin in Water	0.25%SLS in PBS	Simulated Gastric Fluid (SGF)
4% Cyclodextrin in Water	-	0.0000	0.2833
0.25%SLS in PBS	0.0000	-	0.0000
Simulated Gastric Fluid (SGF)	0.2833	0.0000	-

2 Preparation of Nanoparticles

2.1   Preparation of Nanoparticles Prepared from IBCA

2.1.1 Effect of Stirring Rate During Pouring Organic Phase into Water Phase

Table App.B.1, Table App.B.2 and Table App. B.3 show the effect of stirring rate during pouring organic phase into water phase on the particle size, the polydispersity index (PI) and the zeta potential of the nanoparticles formed, respectively.   The one-way analysis of variance (ANOVA) demonstrated that the stirring rate did not significantly affect the particle size (Table 16), the polydispersity index (PI) (Table 17), and the zeta potential (Table 18) of the nanoparticles formed. Since there was no significant difference among the stirring rate of 750, 1000 and 1500 rpm ($P > 0.05$); then the stirring rate of 750 rpm was suitable to use in further study. This stirring rate gave the less energy consuming condition which had advantage on cost effective for industrial production.

Table 16 ANOVA Table for particle size of itraconazole-loaded PIBCA nanoparticles comparing among different stirring rates.

Source of variables	df	SS	MS	F	P
Stirring rate	2	0.063	0.032	0.04	0.959
Error	3	2.245	0.748		
Total	5	2.308			

Table 17 ANOVA Table for polydispersity index (PI) of itraconazole-loaded PIBCA nanoparticles comparing among different stirring rates.

Source of variables	df	SS	MS	F	P
Stirring rate	2	0.0000013	0.0000007	0.50	0.650
Error	3	0.0000040	0.0000013		
Total	5	0.0000053			

Table 18 ANOVA Table for zeta potential of itraconazole-loade PIBCA nanoparticles comparing among different stirring rates.

Source of variables	df	SS	MS	F	P
Stirring rate	2	40.2	20.1	1.01	0.462
Error	3	59.8	19.9		
Total	5	100.0			

2.1.2 Effect of Surfactant Concentrations in the Water Phase

Table App.B.4, Table App.B.5 and Table App.B.6 show the effect of surfactant concentration in the water phase on the particle size, the polydispersity index (PI) and the zeta potential of the nanoparticles formed, respectively. The one-way analysis of variance (ANOVA) demonstrated that there

was no significant difference of the surfactant concentration on the particle size ($P >$ 0.05, Table 19), polydispersity index ($P > 0.05$, Table 20) and the zeta potential ($P >$ 0.05, Table 21). The suitable surfactant concentration used in the 3^3 factorial design was 0.25% because this concentration was the lowest concentration which gave the same size, polydispersity index and zeta potential as the other surfactant concentrations. The lower concentration of surfactant used, the safer gained.

Table 19 ANOVA Table for particle size of itraconazole-loaded PIBCA nanoparticles comparing among different surfactant concentrations.

Source of variables	df	SS	MS	F	P
Concentration	3	1.094	0.365	0.47	0.721
Error	4	3.125	0.781		
Total	7	4.219			

Table 20 ANOVA Table for polydispersity index (PI) of itraconazole-loaded PIBCA nanoparticles comparing among different surfactant concentrations.

Source of variables	df	SS	MS	F	P
Concentration	3	0.0000025	0.0000008	1.11	0.443
Error	4	0.0000030	0.0000008		
Total	7	0.0000055			

Table 21 ANOVA Table for zeta potential of itraconazole-loaded PIBCA nanoparticles comparing among different surfactant concentrations.

Source of variables	df	SS	MS	F	P
Concentration	3	43.1	14.4	0.45	0.731
Error	4	127.6	31.9		
Total	7	170.6			

2.1.3 The Factorial Design Study for Preparation of Itraconazole - Loaded PIBCA Nanoparticles

The application of one-way ANOVA design as a means to optimize nanoparticle characteristics has previously been reported by Seijo et al. (1990) and Lescure et al. (1992). The classical approach used in these studies, where one factor was varied whilst the others remained constant, was unlikely to reveal the possible presence of factor interactions (Armstrong and James, 1990). Therefore, in this study the interactions of input factors with each other was emphasized, in that the effect of changing one factor would depend on the magnitude of one or more of the other factors.

Several measured responses from the design were chosen for investigation, namely, the particle size, the polydispersity index, the amount of itraconazole entrapped in nanoparticle (ITRAe) and the encapsulation efficiency (ITRAe [%]) of itraconazole-loaded PIBCA nanoparticles. These responses represented significant properties of the particles which had impact on their physiological fate. A factorial design of type 3^n was used, where n is the number of factors, three in this study and 3 indicated that each factor had three levels of interests. Thus, 27 experimental trials were required to complete the design. Since there were two replicates, then 54 observations would be obtained.

Three factors were considered important for this study. Concentration of IBCA monomer added to the medium was considered important, as it constituted the primary building block of the formed particle and, ultimately, the nanoparticle. The benzyl benzoate was chosen because itraconazole was highly dissolved in benzyl benzoate, thus it could enhance the amount of itraconazole

entrapped in nanoparticles. The itraconazole concentration was included as the third design factor because it could enhance encapsulation efficiency.

Influence of Preparation Factors on Particle Size of Itraconazole-Loaded PIBCA Nanoparticles

The particle size is an important parameter, as the biopharmaceutical properties of a nanoparticle formulation can be influenced by its physicochemical properties. For example, smaller particles possess a larger surface area, which in turn can lead to a faster release of the drug incorporated. In this way, the size and release properties of the nanoparticles are interrelated (Yoncheva et al.,2003). The size can also play an important role in endocytosis possibilities of nanoparticles (Zimmer et al., 1991; Calvo et al., 1996)

Table App. B.7 shows the particle size of itraconazole-loaded PIBCA nanoparticles obtained from the 3^3 factorial design study. Model adequate checking of itraconazole- loaded PIBCA nanoparticles in factorial design study is shown in Figure 8, where particle size was used as response variable. Figure 8 (a) is the normal probability plot of the studentized residuals to check for normality of residuals. The normal probability plot did not reveal anything particularly troublesome. This plot resembled a straight line which indicated that the underlying error distribution was normal. Figure 8 (b) shows the plot of studentized residuals versus predicted values to check for constant error. No unusual structure was apparent. Figure 8 (c) is the plot of outlier t versus run order to look for outliers, i.e., influential values. All of standardize residuals (d_i) laid in the interval $-3 \leq d_i \leq 3$ conformed that there was no outlier in this study. Figure 8 (d) shows Box-Cox plot for power transformations. Generally, transformations are used for three purposes; stabilizing response variance,

making the response variable closer to the normal distribution, and improving the fit

of the model to the data. The Box- Cox method showed that the tranformation

Figure 8 Model adequate checking of itraconazole-loaded PIBCA nanoparticles in

factorial design study; response: size.

(a) Normal probability plot of the studentized residuals

(b) Studentized residuals versus predicted values

(c) Outlier t versus run order   (d) Box-Cox plot

(a)

(b)

(c)

(d)
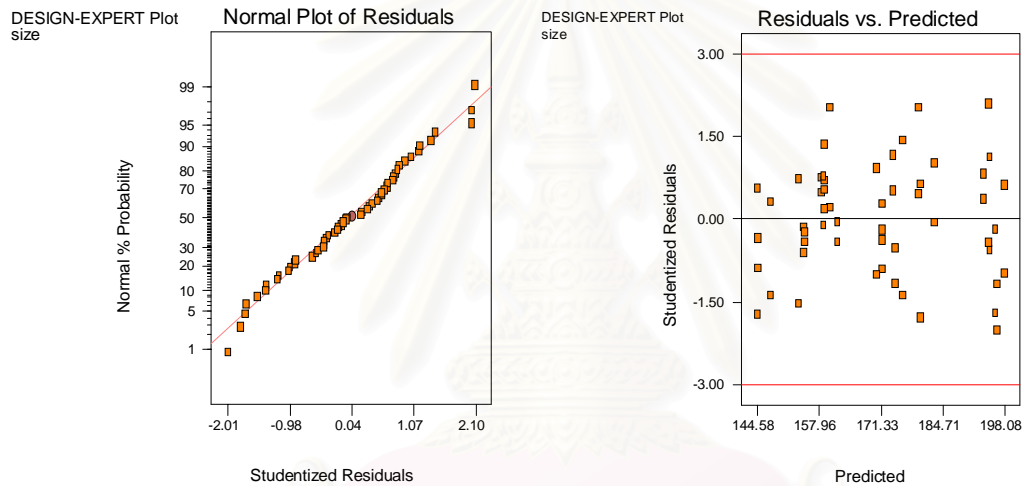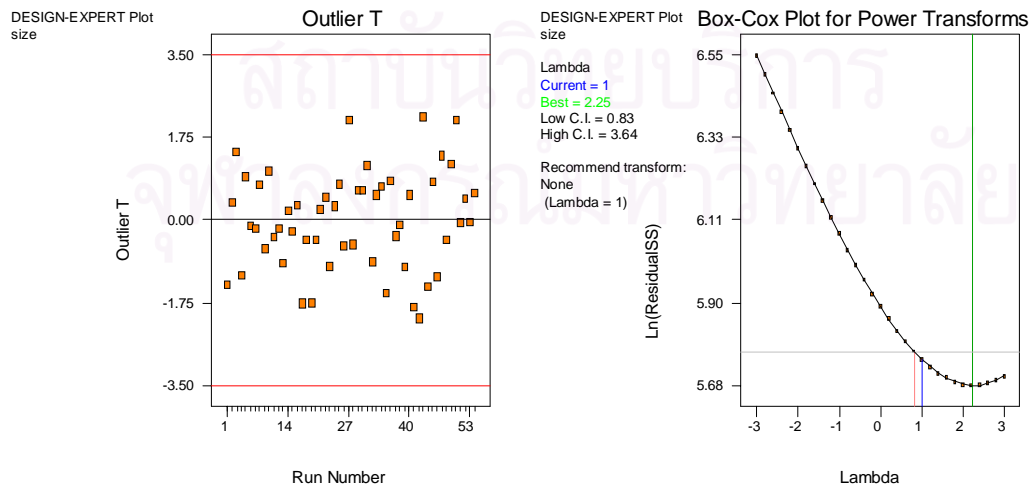
parameter λ was equal to 1, this implied that the data did not need transformation. All the diagnostic plots in Figure 8 were in agreement with the assumption of analysis of variance.

Table 22 shows Design-Expert output analyzing particle size data of itraconazole-loaded PIBCA nanoparticles. From examining this table, The Design-Expert software first computed the sequential or extra sums of squares for the linear, quadratic and cubic terms in the model (there was warning message concerning aliasing in the cubic model because the 3^3 factorial design did not contain enough runs to support a full cubic model). Based on the small P-value for the quadratic term, it was used to fit to the particle size response. Table 22 also shows the final model in terms of both the coded variables and the actual factor levels.

The values of the coefficients of X_1, X_2 and X_3 are related to the effect of these variables on the response. Coefficients with more than one factor term and those with higher order terms represent interaction terms and quadratic relationships. A positive sign represents a synergistic effect, while a negative sign indicates an antagonistic effect. The significance of each coefficient is determined by P values. The smaller the P-value, the more significant is the corresponding coefficient (Box et al., 1978).

The equation in terms of coded factors obtained from Table 22 was as follows, size $= 173.98 + 5.60 * X_1 + 18.82 * X_2 - 0.72 * X_3 - 9.28 * X_1^2 + 3.24 * X_2^2 + 1.23 * X_3^2 + 1.22 * X_1X_2 + 0.75 * X_1X_3 - 0.083* X_2X_3$. This equation could be used to predict the particle size at any point in the space spanned by the factors in the design.

Table 22 Design-Expert output analyzing particle size data of itraconazole-loaded PIBCA nanoparticles.

Response: Size

Sequential Model Sum of Squares for Particle Size of PIBCA Nanoparticles

Source	Sum of Squares	DF	Mean Square	F Value	Prob > F
Mean	1.575E+006	1	1.575E+006		
Linear	13905.15	3	4635.05	150.39	< 0.0001
2FI	49.59	3	16.53	0.52	0.6700
Quadratic	1178.52	3	392.84	55.23	< 0.0001
Cubic	114.27	7	16.32	3.04	0.0125
Residual	198.67	37	5.37		
Total	1.590E+006	54	29451.09		

Lack of Fit Tests for Particle Size of PIBCA Nanoparticles

Source	Sum of Squares	DF	Mean Square	F Value	Prob > F
Linear	1378.13	23	59.92	9.93	< 0.0001
2FI	1328.54	20	66.43	11.01	< 0.0001
Quadratic	150.03	17	8.83	1.46	0.1836
Cubic	35.76	10	3.58	0.59	0.8057
Pure Error	162.91	27	6.03		

Table 22 Design-Expert output analyzing particle size data of itraconazole-loaded PIBCA nanoparticles (continued).

Model Summary Statistics

Source	S.D.	R-Squared	Adjusted R-Squared	Predicted R-Squared	PRESS
Linear	5.55	0.9002	0.8942	0.8851	1774.47
2FI	5.63	0.9034	0.8911	0.8789	1871.23
Quadratic	2.67	0.9797	0.9756	0.9692	476.26
Cubic	2.32	0.9871	0.9816	0.9720	432.04

ANOVA for Response Surface Quadratic Model

Analysis of Variance Table [Partial Sum of Squares]

Source	Sum of Squares	DF	Mean Square	F Value	Prob > F
Model	15133.26	9	1681.47	236.42	< 0.0001
X_1	1128.96	1	1128.96	158.74	< 0.0001
X_2	12757.70	1	12757.70	1793.78	< 0.0001
X_3	18.49	1	18.49	2.60	0.1140
X_1^2	1034.16	1	1034.16	145.41	< 0.0001
X_2^2	126.10	1	126.10	17.73	0.0001
X_3^2	18.25	1	18.25	2.57	0.1163
$X_1 X_2$	35.77	1	35.77	5.03	0.0300
$X_1 X_3$	13.65	1	13.65	1.92	0.1729
$X_2 X_3$	0.17	1	0.17	0.023	0.8790
Residual	312.94	44	7.11		
Lack of Fit	150.03	17	8.83	1.46	0.1836
Pure Error	162.91	27	6.03		
Cor Total	15446.19	53			

S.D.	2.67		R-Squared	0.9797
Mean	170.78		Adj R-Squared	0.9756
C.V.	1.56		Pred R-Squared	0.9692
PRESS	476.26		Adeq Precision	46.618

Table 22 Design-Expert output analyzing particle size data of itraconazole-loaded PIBCA nanoparticles (continued).

Factor	Coefficient Estimate	DF	Standard Error	95% CI Low	95% CI High	VIF
Intercept	173.98	1	0.96	172.05	175.92	
X_1-IBCA	5.60	1	0.44	4.70	6.50	1.00
X_2-Benzyl benzoate	18.82	1	0.44	17.93	19.72	1.00
X_3-itraconazole	-0.72	1	0.44	-1.61	0.18	1.00
X_1^2	-9.28	1	0.77	-10.83	-7.73	1.00
X_2^2	3.24	1	0.77	1.69	4.79	1.00
X_3^2	1.23	1	0.77	-0.32	2.78	1.00
$X_1 X_2$	1.22	1	0.54	0.12	2.32	1.00
$X_1 X_3$	0.75	1	0.54	-0.34	1.85	1.00
$X_2 X_3$	-0.083	1	0.54	-1.18	1.01	1.00

Final Equation in Terms of Coded Factors:

size $=173.98+5.60* X_1+18.82 * X_2-0.72 * X_3 -9.28 * X_1^2+3.24 * X_2^2+1.23 * X_3^2+1.22 * X_1 X_2+0.75 * X_1 X_3 -0.083 * X_2 X_3$

Final Equation in Terms of Actual Factors:

size $= 137.12208+5.62806*$ IBCA$+0.88403*$ Benzyl benzoate$-5.34894E-003*$ itraconazole$-0.45844*$ IBCA$^2+0.057630*$ Benzyl benzoate$^2+1.70704E-006*$ itraconazole$^2+0.036173*$ IBCA $*$ Benzyl benzoate$+1.97168E-004 *$ IBCA $*$ itraconazole$-1.30719E-005 *$ Benzyl benzoate $*$ itraconazole

Diagnostics Case Statistics

Standard Order	Actual Value	Predicted Value	Residual	Leverage	Student Residual	Cook's Distance	Outlier t	Run Order
1	148.10	147.36	0.74	0.255	0.322	0.004	0.319	16
2	144.20	147.36	-3.16	0.255	-1.372	0.06	-1.386	1

Table 22 Design-Expert output analyzing particle size data of itraconazole-loaded PIBCA nanoparticles (continued).

Diagnostics Case Statistics

Standard Order	Actual Value	Predicted Value	Residual	Leverage	Student Residual	Cook's Distance	Outlier t	Run Order
3	165.20	160.27	4.93	0.171	2.032	0.085	2.110	27
4	160.80	160.27	0.53	0.171	0.220	0.001	0.217	21
5	154.30	154.61	-0.31	0.255	-0.134	0.001	-0.132	6
6	153.20	154.61	-1.41	0.255	-0.612	0.013	-0.607	9
7	160.80	161.80	-1.00	0.171	-0.414	0.004	-0.410	48
8	161.70	161.80	-0.10	0.171	-0.043	0.000	-0.042	53
9	172.50	175.93	-3.43	0.130	-1.380	0.028	-1.395	44
10	179.50	175.93	3.57	0.130	1.434	0.031	1.451	3
11	170.60	171.50	-0.90	0.171	-0.369	0.003	-0.365	11
12	169.30	171.50	-2.20	0.171	-0.90	0.017	-0.903	13
13	185.10	182.73	2.37	0.255	1.028	0.036	1.029	10
14	182.60	182.73	-0.13	0.255	-0.058	0.000	-0.057	51
15	199.60	198.08	1.52	0.171	0.625	0.008	0.620	29
16	195.70	198.08	-2.38	0.171	-0.982	0.020	-0.981	23
17	197.50	194.87	2.63	0.255	1.144	0.045	1.148	31
18	193.60	194.87	-1.27	0.255	-0.550	0.010	-0.546	26
19	142.60	144.74	-2.14	0.171	-0.880	0.016	-0.878	32
20	143.90	144.74	-0.84	0.171	-0.345	0.002	-0.341	37
21	160.30	158.40	1.90	0.130	0.764	0.009	0.760	25
22	159.60	158.40	1.20	0.130	0.482	0.003	0.478	22
23	155.30	153.50	1.80	0.171	0.743	0.011	0.739	8
24	149.80	153.50	-3.70	0.171	-1.522	0.048	-1.546	35
25	159.60	159.10	0.50	0.130	0.201	0.001	0.199	14

Table 22 Design-Expert output analyzing particle size data of itraconazole- loaded PIBCA nanoparticles (continued).

Diagnostics Case Statistics

Standard Order	Actual Value	Predicted Value	Residual	Leverage	Student Residual	Cook's Distance	Outlier t	Run Order
26	160.90	159.10	1.80	0.130	0.723	0.008	0.719	34
27	176.90	173.98	2.92	0.130	1.172	0.020	1.177	49
28	175.30	173.98	1.32	0.130	0.529	0.004	0.525	40
29	172.60	170.30	2.30	0.130	0.924	0.013	0.923	5
30	167.80	170.30	-2.50	0.130	-1.005	0.015	-1.005	39
31	175.60	179.95	-4.35	0.171	-1.790	0.066	-1.838	41
32	181.50	179.95	1.55	0.171	0.640	0.008	0.636	30
33	195.60	196.05	-0.45	0.130	-0.181	0.000	-0.179	12
34	191.80	196.05	-4.25	0.130	-1.708	0.043	-1.748	19
35	194.50	193.59	0.91	0.171	0.376	0.003	0.372	2
36	195.60	193.59	2.01	0.171	0.829	0.014	0.826	36
37	140.60	144.58	-3.98	0.255	-1.730	0.102	-1.772	17
38	145.90	144.58	1.32	0.255	0.572	0.011	0.567	54
39	160.30	159.00	1.30	0.171	0.535	0.006	0.531	33
40	162.30	159.00	3.30	0.171	1.359	0.038	1.373	47
41	154.30	154.85	-0.55	0.255	-0.239	0.002	-0.236	15
42	153.90	154.85	-0.95	0.255	-0.413	0.006	-0.409	18
43	158.60	158.86	-0.26	0.171	-0.108	0.000	-0.107	38
44	160.80	158.86	1.94	0.171	0.798	0.013	0.795	45
45	171.60	174.50	-2.90	0.130	-1.166	0.020	-1.170	4
46	173.20	174.50	-1.30	0.130	-0.523	0.004	-0.518	28
47	172.30	171.57	0.73	0.171	0.300	0.002	0.297	24
48	171.10	171.57	-0.47	0.171	-0.194	0.001	-0.192	7

Table 22 Design-Expert output analyzing particle size data of itraconazole-loaded PIBCA nanoparticles (continued).

Diagnostics Case Statistics

Standard Order	Actual Value	Predicted Value	Residual	Leverage	Student Residual	Cook's Distance	Outlier t	Run Order
49	184.30	179.63	4.67	0.255	2.030	0.141	2.108	50
50	180.70	179.63	1.07	0.255	0.467	0.007	0.463	52
51	191.60	196.48	-4.88	0.171	-2.011	0.084	-2.087	42
52	193.60	196.48	-2.88	0.171	-1.188	0.029	-1.193	46
53	193.80	194.78	-0.98	0.255	-0.423	0.006	-0.419	20
54	199.60	194.78	4.82	0.255	2.096	0.150	2.183	43

On the particle size, the Fisher F-test with a very low probability value ($P_{model} > F$ less than 0.0001) demonstrated a very high significance for the regression model (Montgomery, 2001). The goodness of fit of the model was checked by the determination coefficient (R-Squared). In this case, the value of the determination coefficient (R-Squared = 0.9797) indicated that only 2.13% of the total variations were not explained by the model. The value of the determination coefficient (R-Squared = 0.9797) was as high as the value of the adjusted determination coefficient (Adj. R-Squared = 0.9756), which indicated a high significance of the model (Box et al., 1978). At the same time a relatively low value of the coefficient of variation (C.V. = 1.56) indicated improved precision and reliability of the conducted experiments (Box and Wilson, 1951).

The second order main effect of IBCA monomer was significant, as is evident from its respective P-value ($Px_1^2 < 0.0001$) as well as its first order main

effect ($Px_1 < 0.0001$). The positive coefficient value ($\beta_1 = 5.60$) of the main effect of IBCA monomer (X_1) was less dominant than the negative quadratic effect ($\beta_{11} = -9.28$) of the same factor. These values suggested that the concentration of IBCA monomer had quadratic relationship on the particle size of the nanoparticles (Figure9 (a)). Figure 9 (a) shows a significant increase in the particle size observed when the IBCA concentration was increased from 1.0 µL/mL to 6.75 µL/mL. The particle size decreased when the concentration of IBCA added was higher than 6.75 µL/mL. This behavior can be explained because two types of particles: nanospheres and nanocapsules, were obtained in the final suspension as reported by Gallardo et al. (1993). The increase in IBCA concentration produced an increase in the particle size, probably due to a growing of wall thickness nanocapsules. When the concentration of IBCA was higher than 6.75 µL/mL, the nanospheres having lesser diameter were developed which resulted in decreasing the average size of the final colloidal system.

.   The second order main effect of benzyl benzoate was significant, as was evident from its respective P-value ($Px_2^2 = 0.0001$) as well as its first order main effect ($Px_2 < 0.0001$) (Figure 9 (b)). The positive coefficient value ($\beta_2 = 18.82$) indicated the dominant main effect of IBCA coefficient (X_1), because the positive quadratic effect ($\beta_{22} = 3.24$) of the same factor was less dominant. These values suggested that the concentration of benzyl benzoate had significantly effect on particle size. Figure 9 (b) shows the increasing effect of benzyl benzoate on the particle size of the nanoparticles. This result also agreed with Al Khouri et al. (1986) that oil type and concentration were the important factor.

         The particle size was predominantly influenced by benzyl benzoate and IBCA monomer while itraconazole had no significantly effect ($P = 0.114$).

Mccarron et al. (2000) reported that particle size was not influenced by the concentration of 5-fluorouracil. On the contrary, Illum et al. (1986) found that the particle size increased when the rose bengal concentration was increased.

A significant synergistic interaction between IBCA and benzyl benzoate ($P < 0.05$) was observed. This interaction was reflected by the pattern of the lines of Figure 10 (a), Figure 11(a) and Figure 12(a). The two-factor interaction graph, shown in Figure 10 (a) was helpful in the practical interpretation of the results. This graph was constructed by plotting average particle size versus the concentration of IBCA for each concentration of benzyl benzoate and connecting the points for the low- and high-concentration of benzyl benzoate to give the two curves shown in figure. Inspection of the interaction graph indicated that changes in the concentration of IBCA produced a much larger change in the particle size at the high concentration of benzyl benzoate than at the low concentration of benzyl benzoate. The higher concentration of benzyl benzoate produced the larger particle size. Figure 11 (a), and Figure 12 (a) are a response surface plot and contour plot of the particle size as a function of the concentration of IBCA and benzyl benzoate. These plots were obtained from the fitted model. The effect of the strong interaction on this process was very clear because that the response surface was a twisted plane.

There was no significant difference interaction between IBCA monomer and itraconazole as shown in Figure 10(b), Figure 11(b), and Figure 12(b) ($P>0.05$). There was also no significant interaction between benzyl benzoate and itraconazole as shown in Figure 10 (c), Figure 11 (c), and Figure 12 (c) ($P > 0.05$).

Figure 9 One factor plots of itraconazole-loaded PIBCA nanoparticles in factorial design study; response: size.

(a) IBCA

(b) Benzyl benzoate
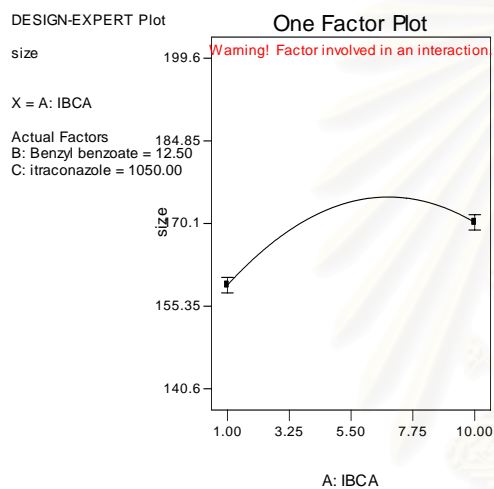
(c) Itraconazole

(a)

(b)

(c)

Figure 10 Interaction plots of itraconazole-loaded PIBCA nanoparticles in factorial design study; response: size.

(a) Interaction of IBCA and benzyl benzoate

(b) Interaction of IBCA and itraconazole

(c) Interaction of benzyl benzoate and itraconazole

(a)

(b)

(c)

Figure 11 Contour plots of itraconazole-loaded PIBCA nanoparticles in factorial design study; response: size.

  (a) Contour plot of IBCA and benzyl benzoate

  (b) Contour plot of IBCA and itraconazole

  (c) Contour plot of benzyl benzoate and itraconazole

(a)

(b)

(c)

Figure 12 Response surface plots of itraconazole-loaded PIBCA nanoparticles in factorial design study; response: size.

(a) Response surface plot of IBCA and benzyl benzoate

(b) Response surface plot of IBCA and itraconazole

(c) Response surface plot of benzyl benzoate and itraconazole

(a)

(b)

(c)
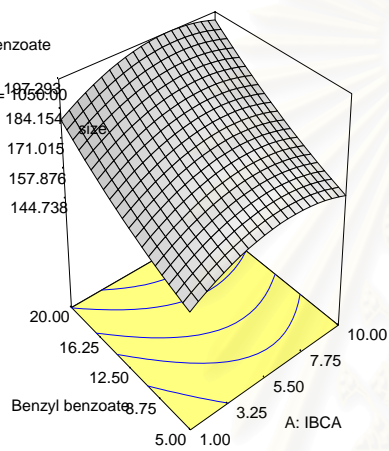
Influence of Preparation Factors on Particle Size Distribution of Itraconazole-Loaded PIBCA Nanoparticles

Table App. B.8 shows the particle size distribution (PI) of itraconazole-loaded PIBCA nanoparticles obtained from the 3^3 factorial design study. Design-Expert output analyzing particle size distribution (polydispersity index [PI]) data of itraconazole-loaded PIBCA nanoparticles is shown in Table 23. Based on the small P-value for the quadratic term, it was used to fit to the particle size distribution response.

Model adequate checking of PIBCA nanoparticles in factorial design study is shown in Figure 13, where particle size distribution (polydispersity index (PI)) was used as response variable. Figure 13(a) is the normal probability plot of the studentized residuals to check for normality of residuals. The normal probability plot did not reveal anything particularly troublesome. This plot resembled a straight line which indicated that the underlying error distribution was normal. Figure 13(b) shows the plot of studentized residuals versus predicted values to check for constant error. No unusual structure was apparent. Figure 13(c) is the plot of outlier t versus run order to look for outliers, i.e., influential values. All of standardize residuals (d_i) laid in the interval $-3 \leq d_i \leq 3$ conformed that there was no outlier in this study. Figure 13(d) shows Box-Cox plot for power transformations. The Box- Cox method showed that the tranformation parameter λ was equal to 1, this implied that the data did not need transformation. All the diagnostic plots in Figure 13 were in agree with the assumption of analysis of variance.

Figure 13 Model adequate checking of itraconazole-loaded PIBCA nanoparticles in factorial design study ; response: PI.

(a) Normal probability plot of the studentized residuals

(b) Studentized residuals versus predicted values

(c) Outlier t versus run order

(d) Box-Cox plot

(a)

(b)

(c)

(d)
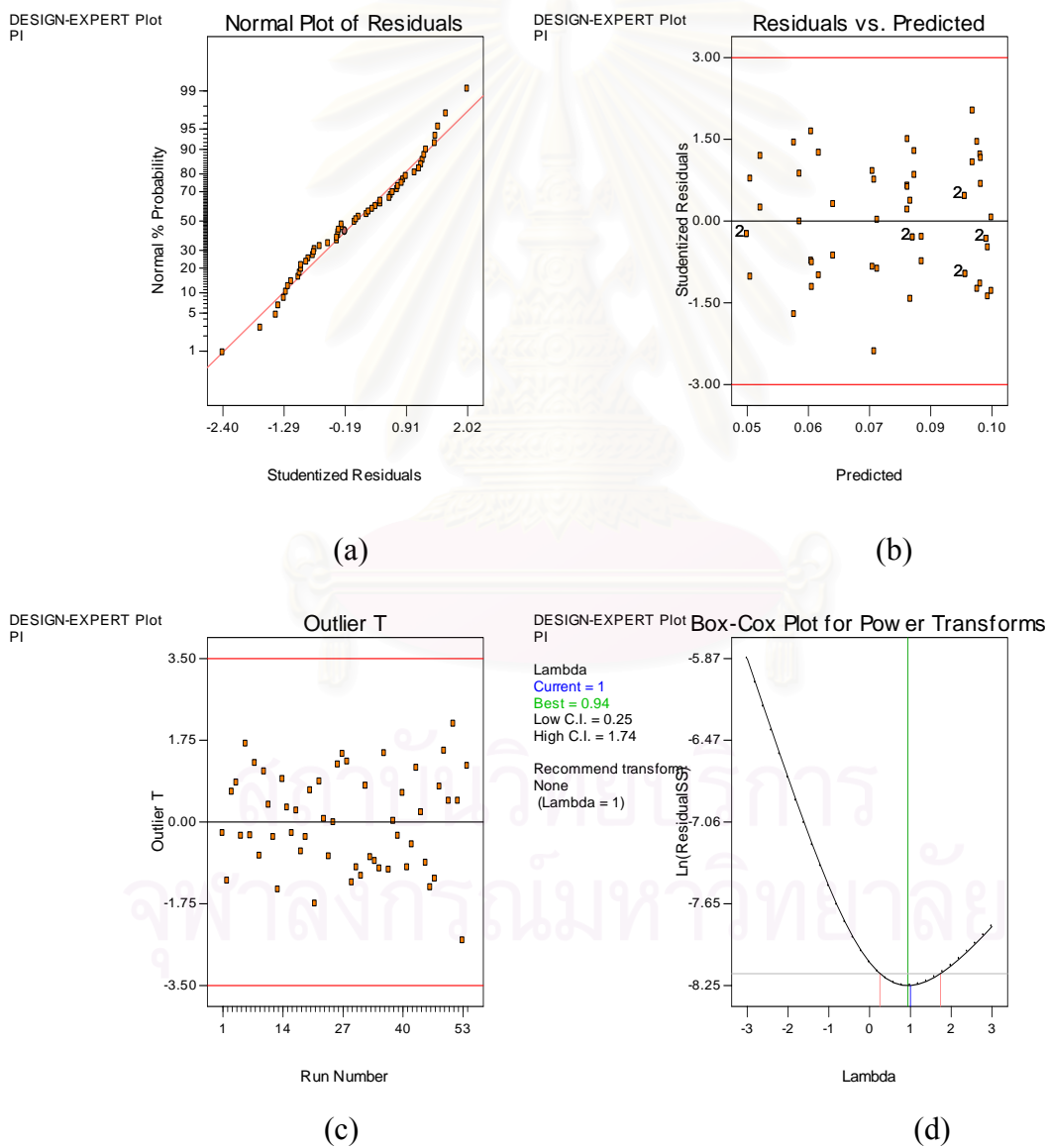
Table 23 Design-Expert output analyzing particle size distribution (polydispersity index [PI]) data of itraconazole-loaded PIBCA nanoparticles.

Response: PI

Sequential Model Sum of Squares

Source	Sum of Squares	DF	Mean Square	F Value	Prob > F
Mean	0.32	1	0.32		
Linear	0.016	3	5.213E-003	331.65	< 0.0001
2FI	2.659E-004	3	8.862E-005	8.01	0.0002
Quadratic	2.576E-004	3	8.588E-005	14.40	< 0.0001
Cubic	3.015E-005	7	4.307E-006	0.69	0.6830
Residual	2.323E-004	37	6.278E-006		
Total	0.33	54	6.196E-003		

Lack of Fit Tests

Source	Sum of Squares	DF	Mean Square	F Value	Prob > F
Linear	6.365E-004	23	2.767E-005	5.00	< 0.0001
2FI	3.706E-004	20	1.853E-005	3.35	0.0020
Quadratic	1.129E-004	17	6.644E-006	1.20	0.3274
Cubic	8.279E-005	10	8.279E-006	1.50	0.1950
Pure Error	1.495E-004	27	5.537E-006		

Model Summary Statistics

Source	S.D.	Adjusted R-Squared	Predicted R-Squared	R-Squared	PRESS
Linear	3.965E-003	0.9522	0.9493	0.9443	9.149E-004
2FI	3.326E-003	0.9683	0.9643	0.9610	6.414E-004
Quadratic	2.442E-003	0.9840	0.9808	0.9756	4.002E-004
Cubic	2.506E-003	0.9859	0.9797	0.9695	5.012E-004

Table 23 Design-Expert output analyzing the polydispersity index (PI) data of itraconazole-loaded PIBCA nanoparticles (continued).

ANOVA for Response Surface Quadratic Model
  Analysis of Variance Table [Partial Sum of Squares]

Source	Sum of Squares	DF	Mean Square	F Value	Prob > F
Model	*0.016*	*9*	*1.796E-003*	*301.10*	*< 0.0001*
X_1	*6.934E-004*	*1*	*6.934E-004*	*116.26*	*< 0.0001*
X_2	*0.015*	*1*	*0.015*	*2502.24*	*< 0.0001*
X_3	*2.178E-005*	*1*	*2.178E-005*	*3.65*	*0.0626*
X_1^2	*1.289E-004*	*1*	*1.289E-004*	*21.62*	*< 0.0001*
X_2^2	*1.225E-004*	*1*	*1.225E-004*	*20.53*	*< 0.0001*
X_3^2	*6.259E-006*	*1*	*6.259E-006*	*1.05*	*0.3112*
$X_1 X_2$	*2.282E-004*	*1*	*2.282E-004*	*38.25*	*< 0.0001*
$X_1 X_3$	*5.042E-006*	*1*	*5.042E-006*	*0.85*	*0.3629*
$X_2 X_3$	*3.267E-005*	*1*	*3.267E-005*	*5.48*	*0.0239*
Residual	*2.624E-004*	*44*	*5.965E-006*		
Lack of Fit	*1.129E-004*	*17*	*6.644E-006*	*1.20*	*0.3274*
Pure Error	*1.495E-004*	*27*	*5.537E-006*		
Cor Total	*0.016*	*53*			

S.D.	2.442E-003	R-Squared	0.9840	
Mean	0.077	Adj R-Squared	0.9808	
C.V.	3.18	Pred R-Squared	0.9756	
PRESS	4.002E-004	Adeq Precision	50.760	

Factor	Coefficient Estimate	DF	Standard Error	95% CI Low	95% CI High	VIF
Intercept	0.081	1	8.793E-004	0.079	0.082	
X_1-IBCA	4.389E-003	1	4.070E-004	3.569E-003	5.209E-003	1.00
X_2-Benzyl benzoate	0.020	1	4.070E-004	0.020	0.021	1.00
X_3-itraconazole	7.778E-004	1	4.070E-004	-4.256E-005	1.598E-003	1.00
X_1^2	-3.278E-003	1	7.050E-004	-4.699E-003	-1.857E-003	1.00
X_2^2	-3.194E-003	1	7.050E-004	-4.615E-003	-1.774E-003	1.00
X_3^2	7.222E-004	1	7.050E-004	-6.986E-004	2.143E-003	1.00
$X_1 X_2$	-3.083E-003	1	4.985E-004	-4.088E-003	-2.079E-003	1.00
$X_1 X_3$	4.583E-004	1	4.985E-004	-5.464E-004	1.463E-003	1.00
$X_2 X_3$	-1.167E-003	1	4.985E-004	-2.171E-003	-1.620E-004	1.00

Table 23 Design-Expert output analyzing the polydispersity index (PI) data of itraconazole-loaded PIBCA nanoparticles (continued).

Final Equation in Terms of Coded Factors:

$PI = + 0.081 + 4.389E - 003 * X_1 + 0.020 * X_2 + 7.778E-004 * X_3 - 3.278E-003 * X_1^2 - 3.194E-003 * X_2^2 + 7.222E-004 * X_3^2 - 3.083E-003 * X_1 X_2 + 4.583E-004 * X_1 X_3 - 1.167E-003 X_2 X_3$

Final Equation in Terms of Actual Factors:

$PI = + 0.019674 + 3.77199E-003 * IBCA + 4.82919E-003 * Benzyl\ benzoate + 4.44380E-007 * itraconazole - 1.61866E-004 * IBCA^2 - 5.67901E-005 * Benzyl\ benzoate^2 + 9.99616E-010 * itraconazole^2 - 9.13580E-005 * IBCA * Benzyl\ benzoate + 1.19826E-007 * IBCA * itraconazole - 1.83007E-007 * Benzyl\ benzoate * itraconazole$

Diagnostics Case Statistics

Standard Order	Actual Value	Predicted Value	Residual	Leverage	Student Residual	Cook's Distance	Outlier t	Run Order
1	0.045	0.046	-5.231E-004	0.255	-0.248	0.002	-0.245	16
2	0.045	0.046	-5.231E-004	0.255	-0.248	0.002	-0.245	1
3	0.059	0.056	3.185E-003	0.171	1.433	0.042	1.451	27
4	0.052	0.056	-3.815E-003	0.171	-1.716	0.061	-1.756	21
5	0.063	0.060	3.449E-003	0.255	1.636	0.091	1.669	6
6	0.058	0.060	-1.551E-003	0.255	-0.736	0.018	-0.732	9
7	0.075	0.073	1.671E-003	0.171	0.752	0.012	0.748	48
8	0.068	0.073	-5.329E-003	0.171	-2.397	0.119	-2.541	53
9	0.081	0.081	4.630E-004	0.130	0.203	0.001	0.201	44
10	0.082	0.081	1.463E-003	0.130	0.642	0.006	0.638	3
11	0.082	0.081	8.102E-004	0.171	0.364	0.003	0.361	11
12	0.078	0.081	-3.190E-003	0.171	-1.435	0.043	-1.453	13
13	0.097	0.095	2.255E-003	0.255	1.069	0.039	1.071	10
14	0.099	0.095	4.255E-003	0.255	2.018	0.139	2.094	51
15	0.096	0.099	-2.870E-003	0.171	-1.291	0.034	-1.301	29
16	0.099	0.099	1.296E-004	0.171	0.058	0.000	0.058	23
17	0.094	0.096	-2.440E-003	0.255	-1.157	0.046	-1.162	31
18	0.099	0.096	2.560E-003	0.255	1.214	0.050	1.221	26
19	0.048	0.046	1.713E-003	0.171	0.770	0.012	0.767	32
20	0.044	0.046	-2.287E-003	0.171	-1.029	0.022	-1.029	37
21	0.057	0.057	-3.704E-005	0.130	-0.016	0.000	-0.016	25
22	0.059	0.057	1.963E-003	0.130	0.862	0.011	0.859	22
23	0.064	0.061	2.769E-003	0.171	1.245	0.032	1.253	8

Table 23 Design-Expert output analyzing the polydispersity index (PI) data of itraconazole-loaded PIBCA nanoparticles (continued).

Standard Order	Actual Value	Predicted Value	Residual	Leverage	Student Residual	Cook's Distance	Outlier t	Run Order
24	0.059	0.061	-2.231E-003	0.171	-1.004	0.021	-1.004	35
25	0.075	0.073	2.074E-003	0.130	0.910	0.012	0.908	14
26	0.071	0.073	-1.926E-003	0.130	-0.845	0.011	-0.842	34
27	0.084	0.081	3.407E-003	0.130	1.495	0.033	1.517	49
28	0.082	0.081	1.407E-003	0.130	0.618	0.006	0.613	40
29	0.081	0.082	-7.037E-004	0.130	-0.309	0.001	-0.306	5
30	0.081	0.082	-7.037E-004	0.130	-0.309	0.001	-0.306	39
31	0.091	0.093	-2.176E-003	0.171	-0.979	0.020	-0.978	41
32	0.091	0.093	-2.176E-003	0.171	-0.979	0.020	-0.978	30
33	0.097	0.098	-7.593E-004	0.130	-0.333	0.002	-0.330	12
34	0.097	0.098	-7.593E-004	0.130	-0.333	0.002	-0.330	19
35	0.093	0.096	-2.787E-003	0.171	-1.254	0.032	-1.262	2
36	0.099	0.096	3.213E-003	0.171	1.445	0.043	1.464	36
37	0.049	0.048	5.046E-004	0.255	0.239	0.002	0.237	17
38	0.051	0.048	2.505E-003	0.255	1.188	0.048	1.194	54
39	0.058	0.060	-1.704E-003	0.171	-0.766	0.012	-0.763	33
40	0.057	0.060	-2.704E-003	0.171	-1.216	0.031	-1.223	47
41	0.065	0.064	6.435E-004	0.255	0.305	0.003	0.302	15
42	0.063	0.064	-1.356E-003	0.255	-0.643	0.014	-0.639	18
43	0.074	0.074	3.241E-005	0.171	0.015	0.000	0.014	38
44	0.072	0.074	-1.968E-003	0.171	-0.885	0.016	-0.883	45
45	0.084	0.082	1.907E-003	0.130	0.837	0.010	0.834	4
46	0.085	0.082	2.907E-003	0.130	1.276	0.024	1.285	28
47	0.082	0.084	-1.662E-003	0.171	-0.748	0.012	-0.744	24
48	0.083	0.084	-6.620E-004	0.171	-0.298	0.002	-0.295	7
49	0.094	0.093	9.491E-004	0.255	0.450	0.007	0.446	50
50	0.094	0.093	9.491E-004	0.255	0.450	0.007	0.446	52
51	0.097	0.098	-1.093E-003	0.171	-0.491	0.005	-0.487	42
52	0.095	0.098	-3.093E-003	0.171	-1.391	0.040	-1.406	46
53	0.098	0.097	1.421E-003	0.255	0.674	0.016	0.670	20
54	0.099	0.097	2.421E-003	0.255	1.148	0.045	1.153	43

On the particle size distribution defined as polydispersity index (PI), the size distribution of the nanoparticles was narrow in all formulas, having a PI of less than 0.1 as shown in Table 23 (Actual value in Diagnostics Case Statistics).

The second order main effect of IBCA monomer was significant, as was evident from its respective P-value ($Px_1^2 < 0.0001$) as well as its first order main effect ($Px_1 < 0.0001$). The positive coefficient value ($\beta_1 = 0.004389$) of the main effect of IBCA monomer (X_1) was more dominant than the negative quadratic effect ($\beta_{11} = -0.003278$) of the same factor. These values suggested that the concentration of IBCA monomer had quadratic relationship on the polydispersity index of the nanoparticles (Figure14 (a)).

The second order main effect of benzyl benzoate was significant, as was evident from its respective P-value ($Px_2^2 < 0.0001$) as well as its first order main effect ($Px_2 < 0.0001$) (Figure14 (b)). The positive coefficient value ($\beta_2 = 0.020$) indicated the dominant main effect of IBCA coefficient (X_1), because the positive quadratic effect ($\beta_{22} = -0.00319$) of the same factor was less dominant. These values suggested that the concentration of benzyl benzoate had significantly effect on the polydispersity index. Figure14 (b) shows the increasing effect of benzyl benzoate on the particle size of the nanoparticles. Itraconazole had no significantly effect (P=0.0626) as shown in Figure 14(c).

A significant antagonist interaction between IBCA and benzyl benzoate at $P < 0.05$ was observed. This interaction was reflected by the pattern of the lines of Figure 15 (a), Figure 16(a) and Figure 17(a). The two-factor interaction graph, shown in Figure 15 (a) was helpful in the practical interpretation of the results. Inspection of the interaction graph indicated that changes in the concentration of

IBCA produced a much larger change in the polydispersity index at the low concentration of benzyl benzoate than at the high concentration of benzyl benzoate. Figure 16 (a), and Figure 17 (a) are a contour plot and response surface plot of the particle size as a function of the concentration of IBCA and benzyl benzoate. These plots were obtained from the fitted model. The effect of the strong interaction on this process was very clear because the response surface was a twisted plane.

There was no significant interaction between IBCA monomer and itraconazole as shown in Figure 15(b), Figure 16(b), and Figure 17(b) (P > 0.05). A significant antagonist interaction between benzyl benzoate and itraconazole at P < 0.05 was observed. This interaction was reflected by the pattern of the lines of Figure 15 (c), Figure 16(c) and Figure 17(c). Inspection of the interaction graph (Figure 15 (c)) indicated that changes in the concentration of benzyl benzoate produced a much larger change in the polydispersity index at the low concentration of itraconazole than at the high concentration of itraconazole. Figure 16 (c), and Figure 17 (c) are a contour plot and response surface plot of the polydispersity index as a function of the concentration of benzyl benzoate and itraconazole. These plots were obtained from the fitted model. The effect of the strong interaction on this process was very clear because the response surface was a twisted plane. The effects of IBCA monomer and benzyl benzoate on the polydispersity index agreed with the effects of IBCA monomer and benzyl benzoate on the particle size.

Figure 14 One factor plots of itraconazole-loaded PIBCA nanoparticles in factorial design study; response: PI.
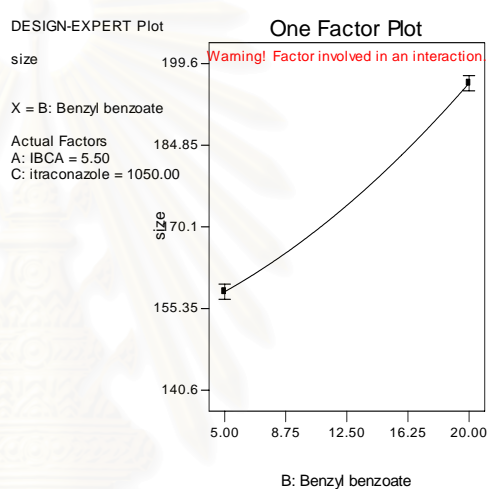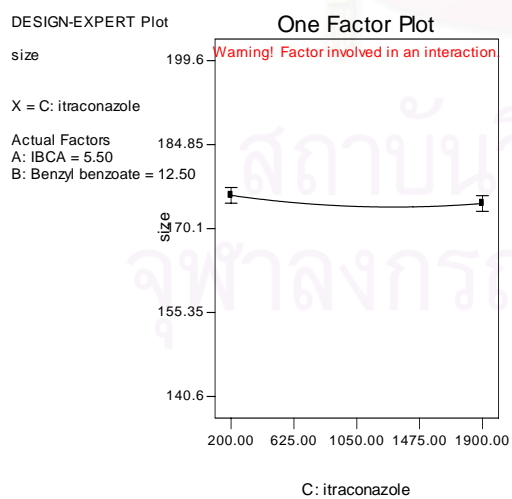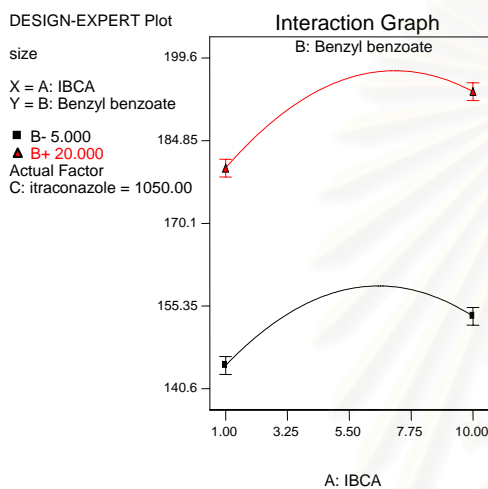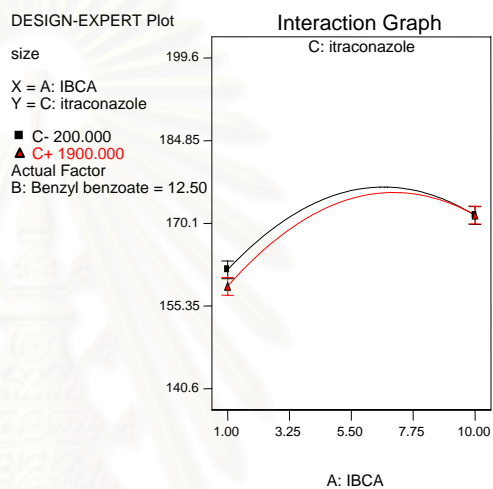
(a) IBCA

(b) Benzyl benzoate
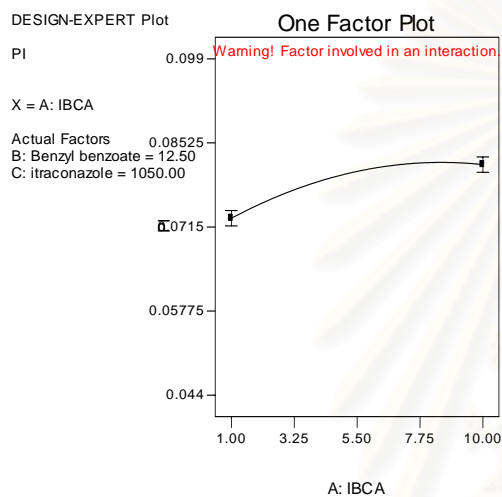
(c) Itraconazole

(a)
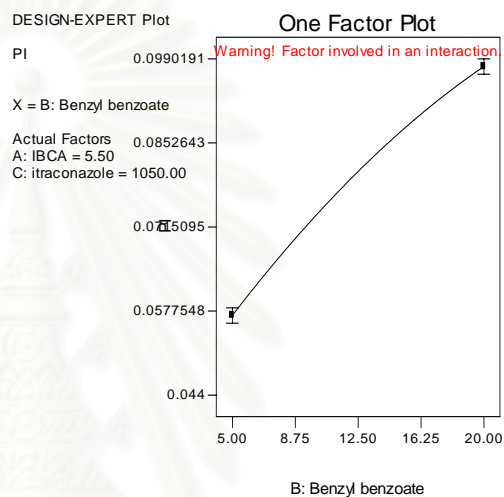
(b)
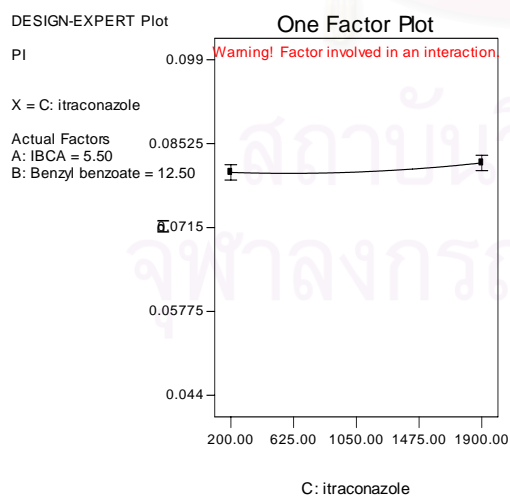
(c)

Figure 15 Interaction plots of itraconazole-loaded PIBCA nanoparticles in factorial design study; response: PI.
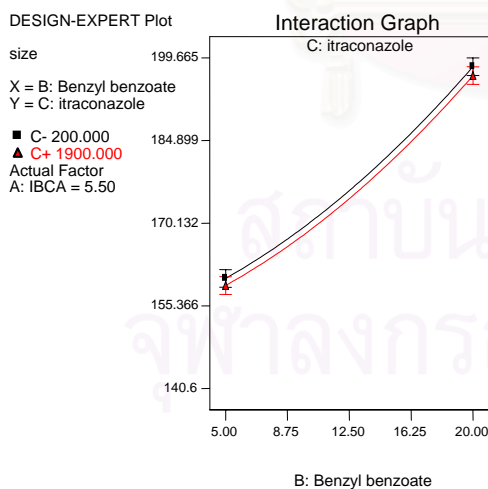
  (a) Interaction of IBCA and benzyl benzoate

  (b) Interaction of IBCA and itraconazole

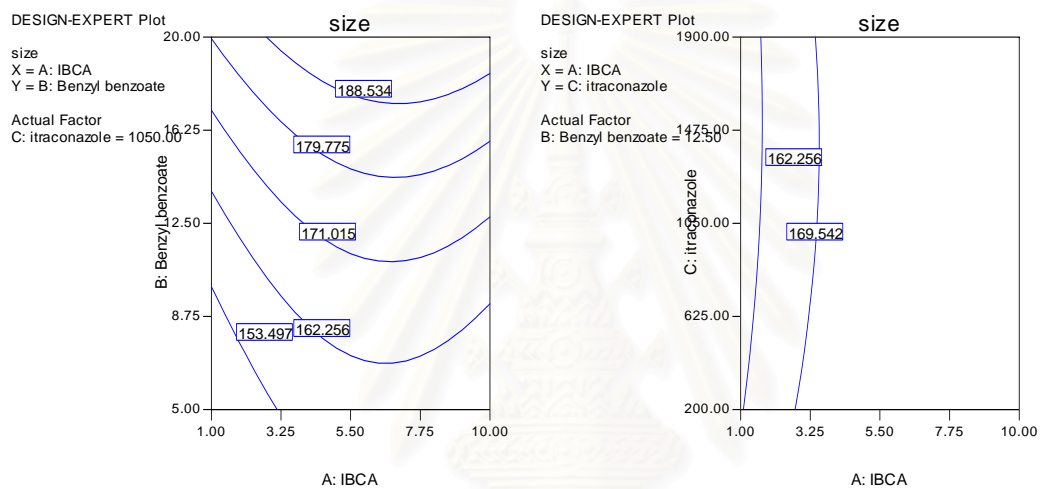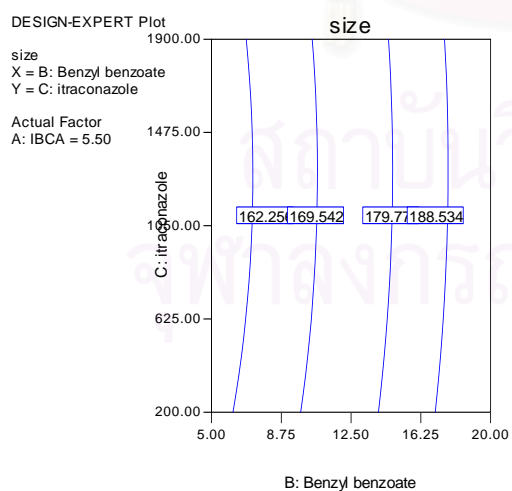 (c) Interaction of benzyl benzoate and itraconazole
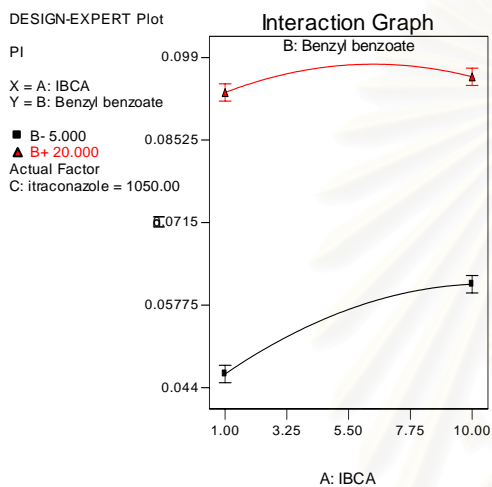
(a)

(b)

(c)

Figure 16 Contour plots of itraconazole-loaded PIBCA nanoparticles in factorial design study; response: PI.

(a) Contour plot of IBCA and benzyl benzoate

(b) Contour plot of IBCA and itraconazole

(c) Contour plot of benzyl benzoate and itraconazole
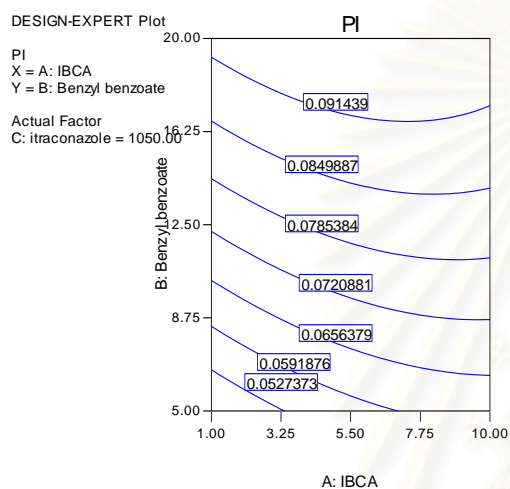
(a)
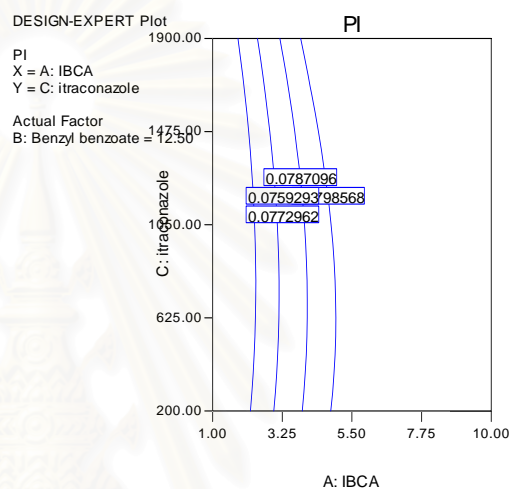
(b)

(c)

Figure 17 Response surface plots of itraconazole-loaded PIBCA nanoparticles in factorial design study; response: PI.

(a) Response surface plot of IBCA and benzyl benzoate

(b) Response surface plot of IBCA and itraconazole

(c) Response surface plot of benzyl benzoate and itraconazole

(a)

(b)

(c)
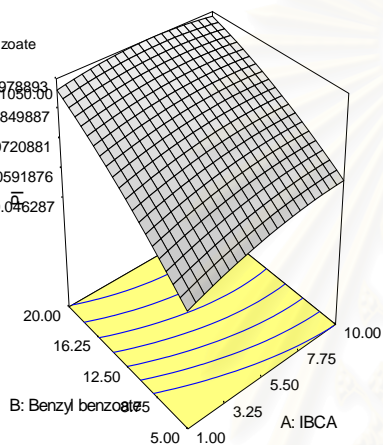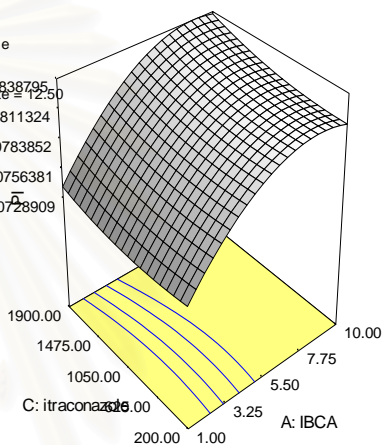
Influence of Preparation Factors on the Amount of Itraconazole Entrapped in Nanoparticles (ITRAe) of Itraconazole-Loaded PIBCA Nanoparticles

Table 24 shows Design-Expert output analyzing the amount of itraconazole entrapped in nanoparticles (ITRAe) data of itraconazole-loaded PIBCA nanoparticles while data is shown in Table App.B.9. Based on the small P-value for the quadratic term, it was used to fit to the ITRAe response. Model adequate checking of PIBCA nanoparticles in factorial design study is shown in Figure 18, where the amount of itraconazole entrapped in nanoparticles (ITRAe) was used as response variable. Figure 18(a) is the normal probability plot of the studentized residuals to check for normality of residuals. The normal probability plot did not reveal anything particularly troublesome. This plot resembled a straight line which indicated that the underlying error distribution is normal. Figure 18(b) shows the plot of studentized residuals versus predicted values to check for constant error. No unusual structure was apparent. Figure 18(c) is the plot of outlier t versus run order to look for outliers, i.e., influential values. All of standardize residuals (d_i) lie in the interval $-3 \leq d_i \leq 3$ conformed that there was no outlier in this study. Figure 18(d) shows Box-Cox plot for power transformations. The Box-Cox method showed that the tranformation parameter λ was equal to 1, this implied that the data did not need transformation. All the diagnostic plots in Figure 18 were in agree with the assumption of analysis of variance.

Figure 18 Model adequate checking of itraconazole-loaded PIBCA nanoparticles in factorial design study ; response: the amount of itraconazole entrapped in nanoparticles (ITRAe).

(a) Normal probability plot of the studentized residuals

(b) Studentized residuals versus predicted values

(c) Outlier t versus run order

(d) Box-Cox plot
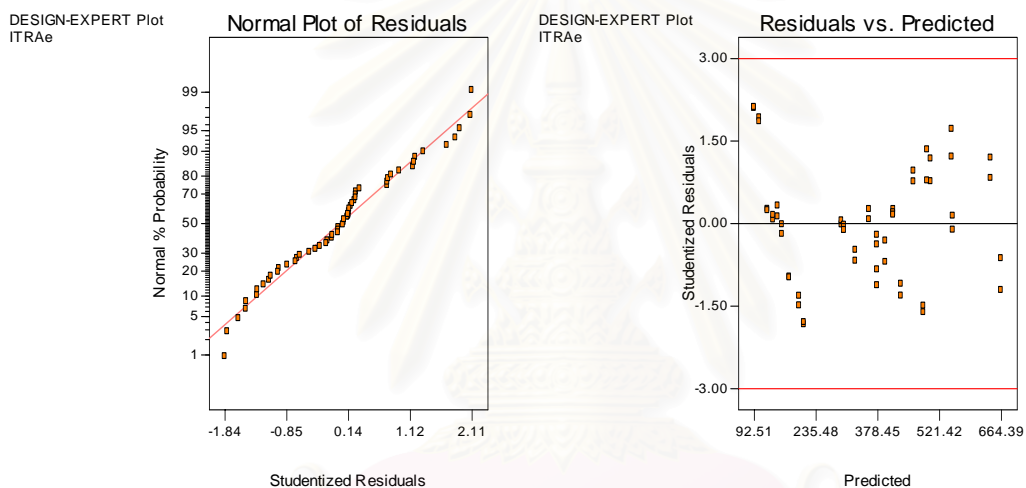
(a)

(b)
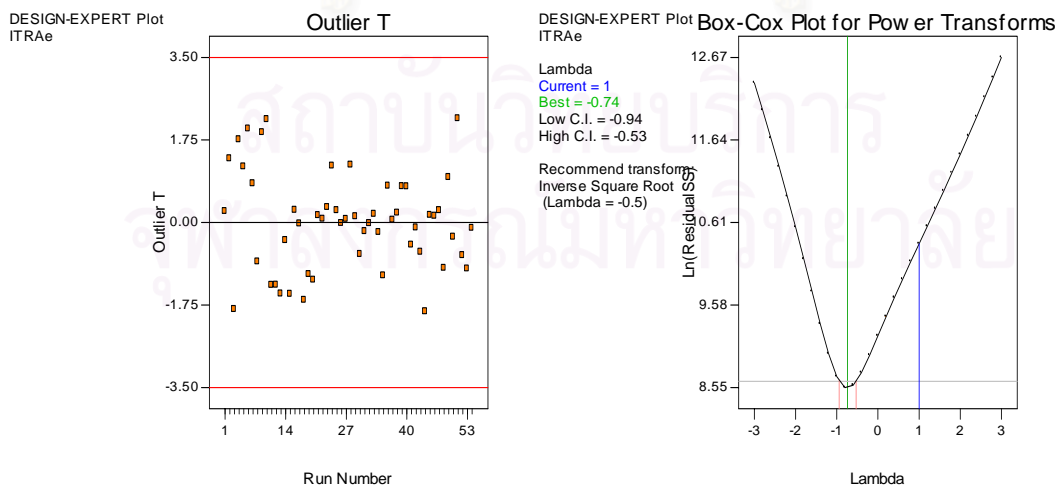
(c)

(d)

Table 24 Design-Expert output analyzing the amount of itraconazole entrapped in nanoparticles (ITRAe) data of itraconazole-loaded PIBCA nanoparticles.

Response: **ITRAe**

Sequential Model Sum of Squares

Source	Sum of Squares	DF	Mean Square	F Value	Prob > F
Mean	6.529E+006	1	6.529E+006		
Linear	1.242E+006	3	4.139E+005	77.25	< 0.0001
2FI	96400.71	3	32133.57	8.81	< 0.0001
Quadratic	1.404E+005	3	46790.38	66.15	< 0.0001
Cubic	22998.09	7	3285.44	14.96	< 0.0001
Residual	8125.03	37	219.60		
Total	8.039E+006	54	1.489E+005		

Lack of Fit Tests

Source	Sum of Squares	DF	Mean Square	F Value	Prob > F
Linear	2.674E+005	23	11624.41	588.21	< 0.0001
2FI	1.710E+005	20	8548.03	432.54	< 0.0001
Quadratic	30589.54	17	1799.38	91.05	< 0.0001
Cubic	7591.45	10	759.14	38.41	< 0.0001
Pure Error	533.58	27	19.76		

Model Summary Statistics

Source	S.D.	R-Squared	Adjusted R-Squared	Predicted R-Squared	PRESS
Linear	73.20	0.8225	0.8119	0.7932	3.122E+005
2FI	60.41	0.8864	0.8719	0.8519	2.235E+005
Quadratic	26.60	0.9794	0.9752	0.9681	48095.15
Cubic	14.82	0.9946	0.9923	0.9888	16884.23

Table 24 Design-Expert output analyzing the amount of itraconazole entrapped in nanoparticles (ITRAe) data of itraconazole-loaded PIBCA nanoparticles (continued).

ANOVA for Response Surface Quadratic Model
Analysis of Variance Table [Partial Sum of Squares]

Source	Sum of Squares	DF	Mean Square	F Value	Prob > F
Model	1.478E+006	9	1.643E+005	232.25	< 0.0001
X_1	1.392E+005	1	1.392E+005	196.82	< 0.0001
X_2	49538.89	1	49538.89	70.04	< 0.0001
X_3	1.053E+006	1	1.053E+006	1488.62	< 0.0001
X_1^2	6051.47	1	6051.47	8.56	0.0054
X_2^2	52270.24	1	52270.24	73.90	< 0.0001
X_3^2	82049.43	1	82049.43	116.00	< 0.0001
$X_1 X_2$	10548.33	1	10548.33	14.91	0.0004
$X_1 X_3$	61630.94	1	61630.94	87.13	< 0.0001
$X_2 X_3$	24221.45	1	24221.45	34.24	< 0.0001
Residual	31123.12	44	707.34		
Lack of Fit	30589.54	17	1799.38	91.05	< 0.0001
Pure Error	533.58	27	19.76		
Cor Total	1.510E+006	53			

S.D.	26.60	R-Squared	0.9794	
Mean	347.73	Adj R-Squared	0.9752	
C.V.	7.65	Pred R-Squared	0.9681	
PRESS	48095.15	Adeq Precision	49.968	

Factor	Coefficient Estimate	DF	Standard Error	95% CI Low	95% CI High	VIF
Intercept	461.82	1	9.58	442.53	481.12	
X_1-IBCA	62.19	1	4.43	53.25	71.12	1.00
X_2-Benzyl benzoate	37.10	1	4.43	28.16	46.03	1.00
X_3-itraconazole	171.02	1	4.43	162.09	179.96	1.00
X_1^2	-22.46	1	7.68	-37.93	-6.98	1.00
X_2^2	-66.00	1	7.68	-81.47	-50.53	1.00
X_3^2	-82.69	1	7.68	-98.16	-67.22	1.00
$X_1 X_2$	20.96	1	5.43	10.02	31.91	1.00
$X_1 X_3$	50.68	1	5.43	39.73	61.62	1.00
$X_2 X_3$	31.77	1	5.43	20.83	42.71	1.00

Final Equation in Terms of Coded Factors:

$$\text{ITRAe} = + 461.82 + 62.19 * X_1 + 37.10 * X_2 + 171.02 * X_3 - 22.46 * X_1^2 - 66.00 * X_2^2 - 82.69 * X_3^2 + 20.96 * X_1 X_2 + 50.68 * X_1 X_3 + 31.77 * X_2 X_3$$

Table 24 Design-Expert output analyzing the amount of itraconazole entrapped in nanoparticles (ITRAe) data of itraconazole-loaded PIBCA nanoparticles (continued).

Final Equation in Terms of Actual Factors:

ITRAe = - 45.70747 + 4.34253 * IBCA + 25.63003 * Benzyl benzoate+ 0.30639* itraconazole - 1.10896* $IBCA^2$ - 1.17331* Benzyl $benzoate^2$ - 1.14448E-004 * $itraconazole^2$ + 0.62117 * IBCA * Benzyl benzoate + 0.013248 * IBCA * itraconazole + 4.98327E-003* Benzyl benzoate * itraconazole

Diagnostics Case Statistics

Standard Order	Actual Value	Predicted Value	Residual	Leverage	Student Residual	Cook's Distance	Outlier t	Run Order
1	129.80	123.78	6.02	0.255	0.262	0.002	0.259	16
2	129.20	123.78	5.42	0.255	0.236	0.002	0.233	1
3	138.40	136.79	1.61	0.171	0.067	0.000	0.066	27
4	140.40	136.79	3.61	0.171	0.149	0.000	0.148	21
5	149.00	104.88	44.12	0.255	1.922	0.126	1.985	6
6	147.40	104.88	42.52	0.255	1.852	0.117	1.907	9
7	150.60	174.14	-23.54	0.171	-0.972	0.020	-0.972	48
8	150.30	174.14	-23.84	0.171	-0.985	0.020	-0.984	53
9	162.50	208.11	-45.61	0.130	-1.838	0.050	-1.891	44
10	163.50	208.11	-44.61	0.130	-1.798	0.048	-1.847	3
11	165.20	197.17	-31.97	0.171	-1.320	0.036	-1.332	11
12	161.00	197.17	-36.17	0.171	-1.494	0.046	-1.516	13
13	140.60	92.51	48.09	0.255	2.094	0.150	2.182	10
14	141.00	92.51	48.49	0.255	2.112	0.152	2.202	51
15	150.46	147.44	3.02	0.171	0.125	0.000	0.123	29
16	155.20	147.44	7.76	0.171	0.320	0.002	0.317	23
17	153.00	157.46	-4.46	0.255	-0.194	0.001	-0.192	31
18	157.00	157.46	-0.46	0.255	-0.020	0.000	-0.020	26
19	294.50	295.05	-0.55	0.171	-0.023	0.000	-0.022	32
20	296.30	295.05	1.25	0.171	0.052	0.000	0.051	37
21	365.10	358.73	6.37	0.130	0.257	0.001	0.254	25
22	360.50	358.73	1.77	0.130	0.071	0.000	0.071	22
23	357.20	377.50	-20.30	0.171	-0.838	0.015	-0.835	8
24	350.20	377.50	-27.30	0.171	-1.127	0.026	-1.131	35

Table 24 Design-Expert output analyzing the amount of itraconazole entrapped in

nanoparticles (ITRAe) data of itraconazole-loaded PIBCA nanoparticles (continued).

Diagnostics Case Statistics

Standard Order	Actual Value	Predicted Value	Residual	Leverage	Student Residual	Cook's Distance	Outlier t	Run Order
25	367.60	377.18	-9.58	0.130	-0.386	0.002	-0.382	14
26	371.90	377.18	-5.28	0.130	-0.213	0.001	-0.211	34
27	485.50	461.82	23.68	0.130	0.954	0.014	0.953	49
28	480.70	461.82	18.88	0.130	0.761	0.009	0.757	40
29	530.70	501.56	29.14	0.130	1.175	0.021	1.180	5
30	520.50	501.56	18.94	0.130	0.764	0.009	0.760	39
31	315.60	327.31	-11.71	0.171	-0.484	0.005	-0.480	41
32	310.80	327.31	-16.51	0.171	-0.682	0.010	-0.678	30
33	400.23	432.92	-32.69	0.130	-1.318	0.026	-1.329	12
34	405.60	432.92	-27.32	0.130	-1.101	0.018	-1.104	19
35	526.05	493.62	32.43	0.171	1.340	0.037	1.352	2
36	512.40	493.62	18.78	0.171	0.776	0.012	0.772	36
37	300.30	300.94	-0.64	0.255	-0.028	0.000	-0.028	17
38	298.10	300.94	-2.84	0.255	-0.124	0.001	-0.122	54
39	419.60	415.30	4.30	0.171	0.178	0.001	0.176	33
40	421.50	415.30	6.20	0.171	0.256	0.001	0.253	47
41	450.30	484.74	-34.44	0.255	-1.500	0.077	-1.522	15
42	447.60	484.74	-37.14	0.255	-1.617	0.089	-1.649	18
43	419.70	414.84	4.86	0.171	0.201	0.001	0.199	38
44	418.60	414.84	3.76	0.171	0.155	0.000	0.154	45
45	592.70	550.16	42.54	0.130	1.715	0.044	1.755	4
46	580.20	550.16	30.04	0.130	1.211	0.022	1.217	28
47	669.40	640.57	28.83	0.171	1.191	0.029	1.197	24
48	660.50	640.57	19.93	0.171	0.823	0.014	0.820	7
49	389.50	396.74	-7.24	0.255	-0.315	0.003	-0.312	50
50	380.60	396.74	-16.14	0.255	-0.703	0.017	-0.699	52
51	550.20	553.02	-2.82	0.171	-0.117	0.000	-0.115	42
52	556.30	553.02	3.28	0.171	0.135	0.000	0.134	46
53	636.50	664.39	-27.89	0.255	-1.215	0.050	-1.222	20
54	649.80	664.39	-14.59	0.255	-0.636	0.014	-0.631	43

On the amount of itraconazole entrapped in the nanoparticles (ITRAe),

the fisher F-test with a very low probability value ($P_{model} > F$ less than 0.0001)

demonstrated a very high significance for the regression model (Montgomery, 2001).

The value of the determination coefficient (R-Squared = 0.9794) was as high as the value of the adjusted determination coefficient (Adj. R-Squared = 0.9752), which indicated a high significance of the model (Box et al., 1978).

The second order main effect of IBCA was significant, as was evident from its respective P-value ($Px_1^2 = 0.0054$) as well as its first order main effect ($Px_1 < 0.0001$). The positive coefficient value ($\beta_1 = 62.19$) of the main effect of IBCA (X_1) was more dominant than the negative quadratic effect ($\beta_{11} = -22.46$) of the same factor. These values suggested that the concentration of IBCA monomer had direct relationship on the amount of itraconazole entrapped in the nanoparticles (ITRAe). Figure 19 (a) shows the increasing effect of IBCA monomer on the amount of itraconazole entrapped in the nanoparticles particle (ITRAe). This result was in accordance with Valero et al. (1996) that the amount of triamcinolone entrapped in the nanoparticles increased when the content of IBCA monomer was high. Chasteigner et al. (1996) reported that the hydrophobic interactions between itraconazole and the material network of nanoparticles played an important role in the stabilization of the associated drug. When more monomer content was used, the hydrophobic interaction resulted in an increase in the amount of itraconazole entrapped in the nanoparticles particle (ITRAe).

The second order main effect of benzyl benzoate was significant, as was evident from its respective P-value ($Px_2^2 < 0.0001$) as well as its first order main effect ($Px_2 < 0.0001$). The positive coefficient value ($\beta_2 = 37.10$) of main effect of benzyl benzoate (X_2) was less dominant than the negative quadratic effects ($\beta_{22} = -66.00$) of the same factor.

The second order main effect of itraconazole was significant, as was evident from its respective P-value ($Px_3^2 < 0.0001$) as well as its first order main effect ($Px_3 < 0.0001$). The positive coefficient value ($\beta_3 = 171.02$) of the main effect of itraconazole(X_3) was more dominant than the negative quadratic effect ($\beta_{33} = -82.69$) of the same factor. Figure 19 (c) shows an increasing effect of itraconazole on ITRAe The results were also agreed with Fresta et al. (1994) that the increase of drug concentration in the polymerization medium led to a slight enhancement of the drug content for both polymers and surfactants. McCarron et al. (2000) also reported that the increasing of 5-fluorouracil concentration increased the loading of PIBCA nanoparticles.

There were significant increasing effects of interactions: IBCA monomer and benzyl benzoate ($\beta_{12} = 20.96$), IBCA monomer and itraconazole ($\beta_{13} = 50.68$), and benzyl benzoate and itraconazole ($\beta_{23} = 31.77$) at $P < 0.01$ (Figure 21). It can be observed that different concentration of IBCA, benzyl benzoate and itraconazole produced different behavior in the encapsulation efficiency. These results agreed with Al Khouri et al. (1986) that oil type and concentration must be such that the dissolution of the monomer and that of the active ingredient were suitably guaranteed. If the oily phase content was too low in comparison with the IBCA monomer, flake polymerization will occur. If it was too low in comparison with the itraconazole, the latter will crystallize. These significant synergistic interactions are reflected by the pattern of the lines of Figure 20, 21, 22 [(a), (b), (c), respectively]. The two-factor interaction graph, shown in Figure 20 (a) was helpful in the practical interpretation of the results. Inspection of the interaction graph indicated that changes in the concentration of IBCA produced a much larger change in the

ITRAe at the high concentration of benzyl benzoate than at the low concentration of benzyl benzoate. Figure 21 (a), and Figure 22 (a) are a contour plot and response surface plot of the ITRAe as a function of the concentration of IBCA and benzyl benzoate. These plots were obtained from the fitted model. The effect of the strong interaction on this process was very clear because the response surface was a twisted plane. Inspection of the interaction graph shown in Figure 20(b) indicated that changes in the concentration of IBCA produced a much larger change in the ITRAe at the high concentration of itraconazole than at the low concentration of itraconazole. Figure 21 (b), and Figure 22 (b) are a contour plot and response surface plot of the ITRAe as a function of the concentration of IBCA and itraconazole. These plots were obtained from the fitted model. The effect of the strong interaction on this process was very clear because the response surface was a twisted plane. Figure 22(c) indicated that changes in the concentration of benzyl benzoate produced a much larger change in the ITRAe at the high concentration of itraconazole than at the low concentration of itraconazole. Figure 21 (c), and Figure 22 (c) are a contour plot and response surface plot of the ITRAe as a function of the concentration of benzyl benzoate and itraconazole. These plots were obtained from the fitted model. The effect of the strong interaction on this process was very clear because the response surface was a twisted plane.

Figure 19 One factor plots of itraconazole-loaded PIBCA nanoparticles in factorial design study; response: the amount of itraconazole entrapped in nanoparticles (ITRAe).

(a) IBCA

(b) Benzyl benzoate
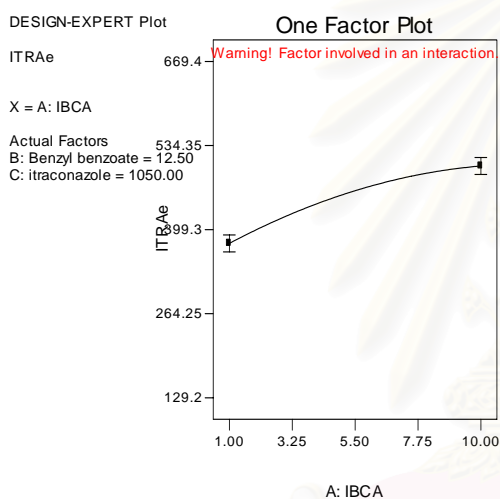
(c) Itraconazole

(a)
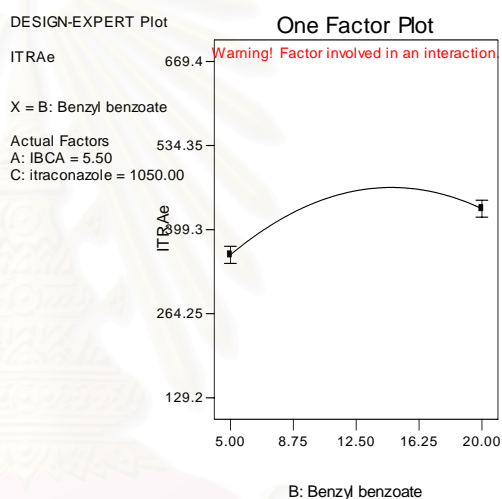
(b)
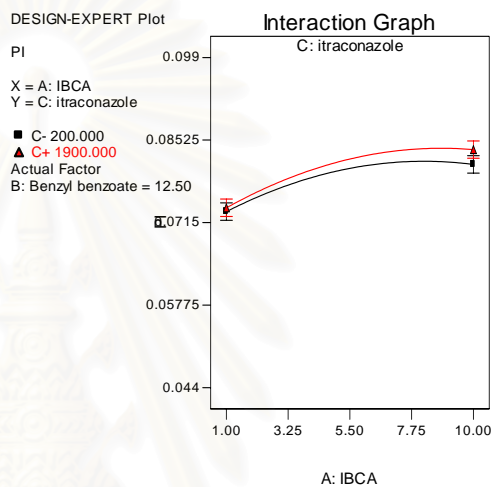

(c)

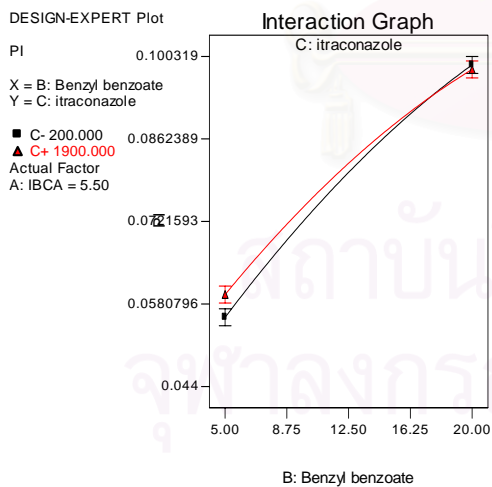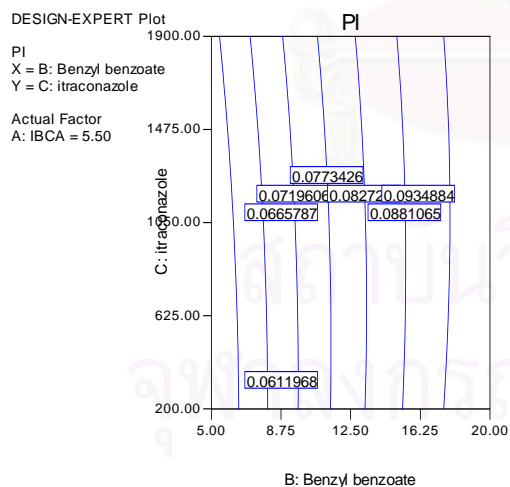Figure 20 Interaction plots of itraconazole-loaded PIBCA nanoparticles in factorial design study; response: the amount of itraconazole entrapped in nanoparticles (ITRAe).

- (a) Interaction of IBCA and benzyl benzoate
- (b) Interaction of IBCA and itraconazole
- (c) Interaction of benzyl benzoate and itraconazole
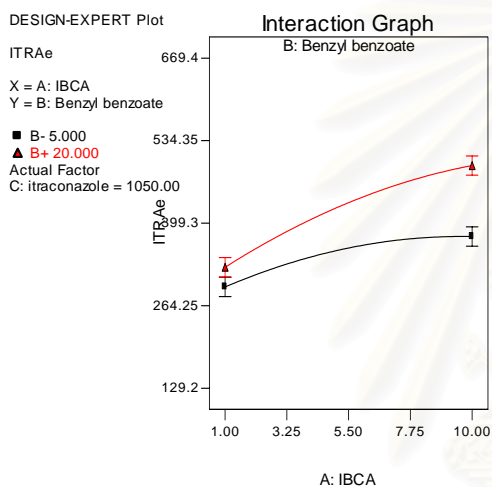
(a)
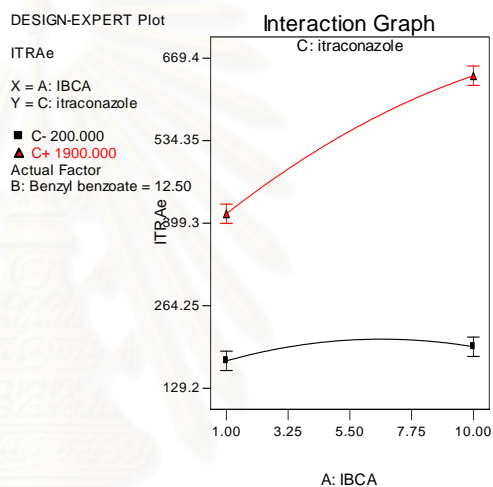
(b)
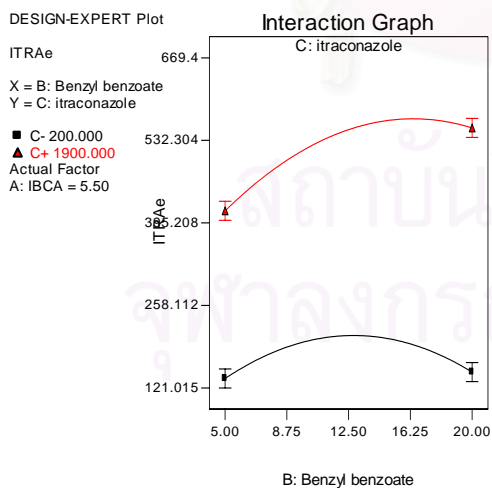
(c)

Figure 21 Contour plots of itraconazole-loaded PIBCA nanoparticles in factorial design study; response: the amount of itraconazole entrapped in nanoparticles (ITRAe).

(a) Contour plot of IBCA and benzyl benzoate

(b) Contour plot of IBCA and itraconazole

(c) Contour plot of benzyl benzoate and itraconazole
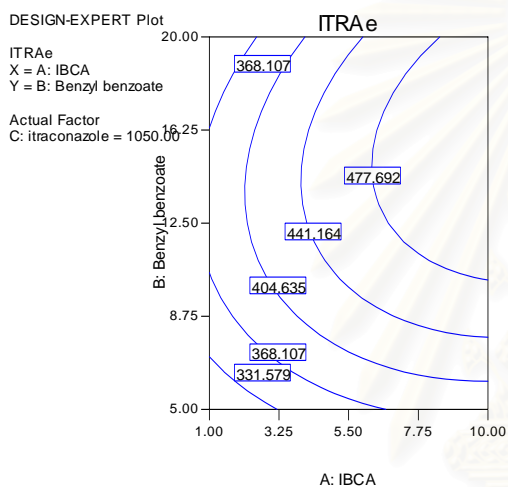
(a)
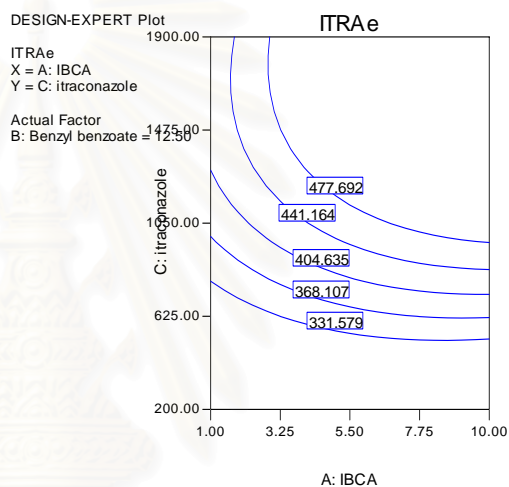
(b)
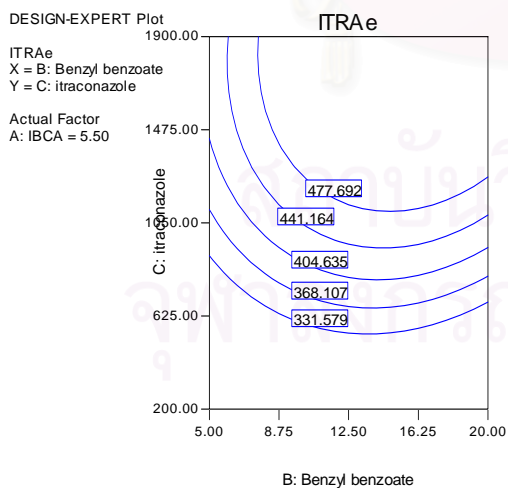
(c)

Figure 22 Response surface plots of itraconazole-loaded PIBCA nanoparticles in factorial design study; response: the amount of itraconazole entrapped in nanoparticles (ITRAe).

(a) Response surface plot of IBCA and benzyl benzoate

(b) Response surface plot of IBCA and itraconazole

(c) Response surface plot of benzyl benzoate and itraconazole

(a)

(b)

(c)

Influence of Preparation Factors on the Encapsulation Efficiency (ITRAe [%])
of Itraconazole-Loaded PIBCA Nanoparticles

Table App.B.10 shows the encapsulation efficiency (ITRAe [%]) of
itraconazole-loaded PIBCA nanoparticles obtained from the 3^3 factorial design study.
Design-Expert output analyzing the encapsulation efficiency (ITRAe [%]) data of
itraconazole- loaded PIBCA nanoparticles is shown in Table 25. Based on the small
P-value for the quadratic term, it was used to fit to the ITRAe [%] response. Model
adequate checking of itraconazole-loaded PIBCA nanoparticles in factorial design
study is shown in Figure 23, where the encapsulation efficiency (ITRAe [%]) was
used as response variable. Figure 23(a) is the normal probability plot of the
studentized residuals to check for normality of residuals. The normal probability plot
did not reveal anything particularly troublesome. This plot resembled a straight line
which indicated that the underlying error distribution was normal. Figure 23(b) shows
the plot of studentized residuals versus predicted values to check for constant error.
No unusual structure was apparent. Figure 23(c) is the plot of outlier t versus run
order to look for outliers, i.e., influential values. All of standardize residuals (d_i) laid
in the interval $-3 \leq d_i \leq 3$ conformed that there was no outlier in this study. Figure
23(d) shows Box-Cox plot for power transformations. The Box- Cox method showed
that the tranformation parameter λ was equal to 0.5. Responses raged from 15.68 to
82.6. Ratio of max to min was 5.26786. A ratio greater than 10 usually indicated a
transformation was required. All the diagnostic plots in Figure 23(a), (b), (c) and (d)
were in agree with the assumption of analysis of variance.

Figure 23 Model adequate checking of itraconazole-loaded PIBCA nanoparticles in factorial design study ; response: the encapsulation efficiency (ITRAe [%]).

(a) Normal probability plot of the studentized residuals

(b) Studentized residuals versus predicted values

(c) Outlier t versus run order

(d) Box-Cox plot
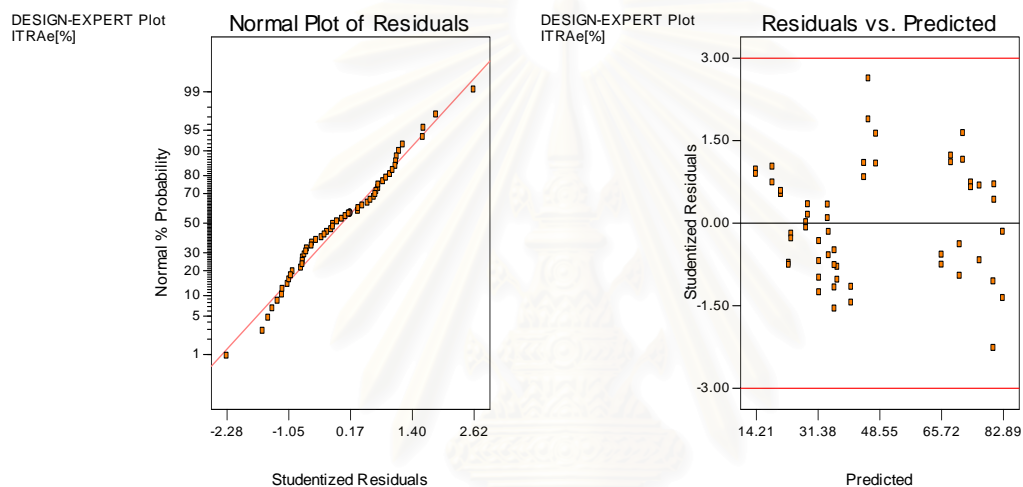
(a)

(b)
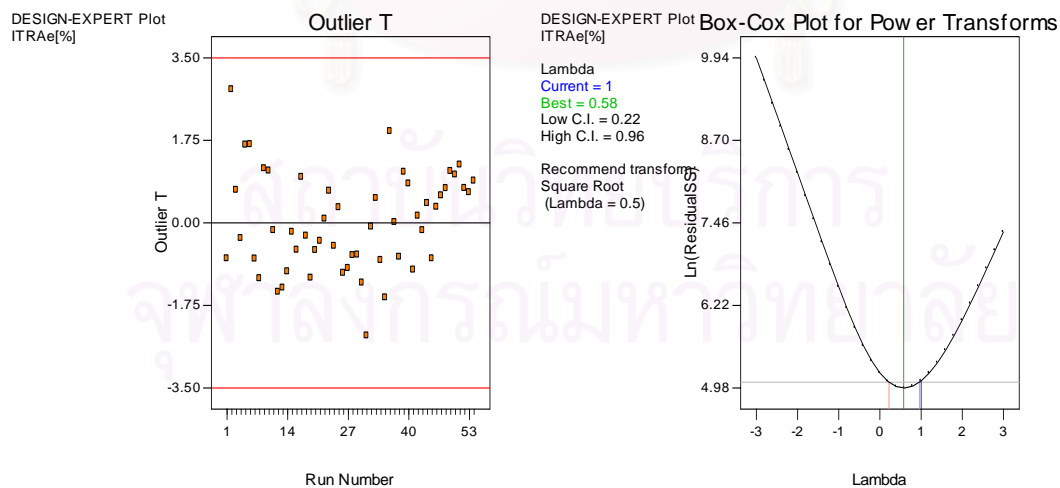
(c)

(d)

Table 25 Design-Expert output analyzing the encapsulation efficiency (ITRAe [%]) data of itraconazole-loaded PIBCA nanoparticles.

Response: ITRAe[%]

Sequential Model Sum of Squares

Source	Sum of Squares	DF	Mean Square	F Value	Prob > F
Mean	1.156E+005	1	1.156E+005		
Linear	22797.06	3	7599.02	149.67	< 0.0001
2FI	79.56	3	26.52	0.51	0.6794
Quadratic	2297.44	3	765.81	208.58	< 0.0001
Cubic	58.90	7	8.41	3.03	0.0127
Residual	102.64	37	2.77		
Total	1.409E+005	54	2609.39		

Lack of Fit Tests

Source	Sum of Squares	DF	Mean Square	F Value	Prob > F
Linear	2527.68	23	109.90	272.92	< 0.0001
2FI	2448.12	20	122.41	303.98	< 0.0001
Quadratic	150.67	17	8.86	22.01	< 0.0001
Cubic	91.77	10	9.18	22.79	< 0.0001
Pure Error	10.87	27	0.40		

Model Summary Statistics

Source	Std. Dev.	R-Squared	Adjusted R-Squared	Predicted R-Squared	PRESS
Linear	7.13	0.8998	0.8938	0.8852	2908.60
2FI	7.23	0.9029	0.8906	0.8808	3019.29
Quadratic	1.92	0.9936	0.9923	0.9903	246.57
Cubic	1.67	0.9959	0.9942	0.9912	223.45

Table 25 Design-Expert output analyzing the encapsulation efficiency (ITRAe [%])

data of itraconazole-loaded PIBCA nanoparticles (continued).

Analysis of Variance Table [Partial Sum of Squares]

Source	Sum of Squares	DF	Mean Square	F Value	Prob > F
Model	25174.07	9	2797.12	761.84	< 0.0001
X_1	1049.87	1	1049.87	285.95	< 0.0001
X_2	383.96	1	383.96	104.58	< 0.0001
X_3	21363.23	1	21363.23	5818.66	< 0.0001
X_1^2	50.42	1	50.42	13.73	0.0006
X_2^2	563.30	1	563.30	153.42	< 0.0001
X_3^2	1683.73	1	1683.73	458.59	< 0.0001
$X_1 X_2$	51.10	1	51.10	13.92	0.0005
$X_1 X_3$	22.54	1	22.54	6.14	0.0171
$X_2 X_3$	5.92	1	5.92	1.61	0.2108
Residual	161.55	44	3.67		
Lack of Fit	150.67	17	8.86	22.01	< 0.0001
Pure Error	10.87	27	0.40		
Cor Total	25335.62	53			

S.D.	1.92		R-Squared	0.9936
Mean	46.26		Adj R-Squared	0.9923
C.V.	4.14		Pred R-Squared	0.9903
PRESS	246.57		Adeq Precision	83.287

Factor	Coefficient Estimate	DF	Standard Error	95% CI Low	95% CI High	VIF
Intercept	44.30	1	0.69	42.91	45.69	
X_1-IBCA	5.40	1	0.32	4.76	6.04	1.00
X_2-Benzyl benzoate	3.27	1	0.32	2.62	3.91	1.00
X_3-itraconazole	-24.36	1	0.32	-25.00	-23.72	1.00
X_1^2	-2.05	1	0.55	-3.16	-0.93	1.00
X_2^2	-6.85	1	0.55	-7.97	-5.74	1.00
X_3^2	11.85	1	0.55	10.73	12.96	1.00
$X_1 X_2$	1.46	1	0.39	0.67	2.25	1.00
$X_1 X_3$	0.97	1	0.39	0.18	1.76	1.00
$X_2 X_3$	0.50	1	0.39	-0.29	1.28	1.00

Table 25 Design-Expert output analyzing the encapsulation efficiency (ITRAe [%])

data of itraconazole-loaded PIBCA nanoparticles (continued).

Final Equation in Terms of Coded Factors:

ITRAe[%] = + 44.30 + 5.40 * X_1 + 3.27 * X_2 - 24.36 * X_3 - 2.05 * X_1^2 - 6.85 * X_2^2
+ 11.85 * X_3^2 + 1.46* $X_1 X_2$ + 0.97 * $X_1 X_3$ + 0.50 * $X_2 X_3$

Final Equation in Terms of Actual Factors:

ITRAe[%] = + 63.78827 + 1.50701* IBCA + 3.16091* Benzyl benzoate - 0.065456
* itraconazole - 0.10122 * $IBCA^2$ - 0.12180 * Benzyl $benzoate^2$ + 1.63948E-005*
$itraconazole^2$ + 0.043235 * IBCA * Benzyl benzoate + 2.53377E-004* IBCA *
itraconazole + 7.79085E-005 * Benzyl benzoate * itraconazole

Diagnostics Case Statistics

Standard Order	Actual Value	Predicted Value	Residual	Leverage	Student Residual	Cook's Distance	Outlier t	Run Order
1	64.90	65.86	-0.96	0.255	-0.582	0.012	-0.578	16
2	64.60	65.86	-1.26	0.255	-0.763	0.020	-0.760	1
3	69.20	70.88	-1.68	0.171	-0.966	0.019	-0.965	27
4	70.20	70.88	-0.68	0.171	-0.392	0.003	-0.389	21
5	74.50	71.81	2.69	0.255	1.628	0.091	1.660	6
6	73.70	71.81	1.89	0.255	1.144	0.045	1.149	9
7	75.30	74.02	1.28	0.171	0.731	0.011	0.727	48
8	75.15	74.02	1.13	0.171	0.645	0.009	0.641	53
9	81.25	80.51	0.74	0.130	0.417	0.003	0.413	44
10	81.75	80.51	1.24	0.130	0.696	0.007	0.692	3
11	82.60	82.89	-0.29	0.171	-0.164	0.001	-0.162	11
12	80.50	82.89	-2.39	0.171	-1.368	0.039	-1.382	13
13	70.30	68.48	1.82	0.255	1.098	0.041	1.101	10
14	70.50	68.48	2.02	0.255	1.219	0.051	1.226	51
15	75.23	76.42	-1.19	0.171	-0.684	0.010	-0.680	29
16	77.60	76.42	1.18	0.171	0.675	0.009	0.671	23
17	76.50	80.26	-3.76	0.255	-2.275	0.177	-2.394	31
18	78.50	80.26	-1.76	0.255	-1.066	0.039	-1.068	26
19	28.04	28.19	-0.15	0.171	-0.087	0.000	-0.086	32
20	28.21	28.19	0.018	0.171	0.011	0.000	0.010	37
21	34.77	34.18	0.59	0.130	0.329	0.002	0.325	25

Table 25 Design-Expert output analyzing the encapsulation efficiency (ITRAe [%])

data of itraconazole-loaded PIBCA nanoparticles (continued).

Standard Order	Actual Value	Predicted Value	Residual	Leverage	Student Residual	Cook's Distance	Outlier t	Run Order
22	34.33	34.18	0.15	0.130	0.083	0.000	0.082	22
23	34.02	36.07	-2.05	0.171	-1.177	0.029	-1.183	8
24	33.35	36.07	-2.72	0.171	-1.562	0.050	-1.588	35
25	35.00	36.85	-1.85	0.130	-1.035	0.016	-1.036	14
26	35.42	36.85	-1.43	0.130	-0.800	0.010	-0.796	34
27	46.24	44.30	1.94	0.130	1.085	0.018	1.088	49
28	45.78	44.30	1.48	0.130	0.828	0.010	0.825	40
29	50.54	47.65	2.89	0.130	1.617	0.039	1.648	5
30	49.57	47.65	1.92	0.130	1.074	0.017	1.076	39
31	30.06	31.80	-1.74	0.171	-1.000	0.021	-1.000	41
32	29.60	31.80	-2.20	0.171	-1.264	0.033	-1.273	30
33	38.12	40.71	-2.59	0.130	-1.451	0.031	-1.470	12
34	38.63	40.71	-2.08	0.130	-1.166	0.020	-1.171	19
35	50.10	45.52	4.58	0.171	2.624	0.142	2.824	2
36	48.80	45.52	3.28	0.171	1.878	0.073	1.936	36
37	15.81	14.21	1.60	0.255	0.967	0.032	0.966	17
38	15.68	14.21	1.47	0.255	0.888	0.027	0.886	54
39	22.08	21.17	0.91	0.171	0.521	0.006	0.517	33
40	22.18	21.17	1.01	0.171	0.579	0.007	0.574	47
41	23.70	24.03	-0.33	0.255	-0.200	0.001	-0.198	15
42	23.56	24.03	-0.47	0.255	-0.285	0.003	-0.282	18
43	22.09	23.37	-1.28	0.171	-0.731	0.011	-0.727	38
44	22.03	23.37	-1.34	0.171	-0.766	0.012	-0.762	45
45	31.19	31.78	-0.59	0.130	-0.333	0.002	-0.329	4
46	30.54	31.78	-1.24	0.130	-0.696	0.007	-0.692	28
47	35.23	36.10	-0.87	0.171	-0.501	0.005	-0.497	24
48	34.76	36.10	-1.34	0.171	-0.771	0.012	-0.767	7
49	20.50	18.82	1.68	0.255	1.017	0.035	1.018	50
50	20.03	18.82	1.21	0.255	0.733	0.018	0.729	52
51	28.95	28.70	0.25	0.171	0.146	0.000	0.144	42
52	29.28	28.70	0.58	0.171	0.335	0.002	0.332	46
53	33.50	34.47	-0.97	0.255	-0.589	0.012	-0.585	20
54	34.20	34.47	-0.27	0.255	-0.166	0.001	-0.164	43

On the encapsulation efficiency (ITRAe [%]), the fisher F-test with a very low probability value ($P_{model} > F$ less than 0.0001) demonstrated a very high significance for the regression model (Montgomery, 2001). The value of the determination coefficient (R-Squared = 0.9936) was as high as the value of the adjusted determination coefficient (Adj. R-Squared = 0.9923), which indicated a high significance of the model (Box et al., 1978).

The second order main effect of IBCA was significant, as was evident from its respective P-value ($Px_1^2 = 0.0006$) as well as its first order main effect ($Px_1 < 0.0001$). The positive coefficient value ($\beta_1 = 5.40$) of the main effect of IBCA (X_1) was more dominant than the negative quadratic effect ($\beta_{11} = -2.05$) of the same factor. These values suggested that the concentration of IBCA monomer had direct relationship on the encapsulation efficiency (ITRAe [%]). Figure 24 (a) shows the increasing effect of IBCA monomer on the encapsulation efficiency (ITRAe [%]).

The second order main effect of benzyl benzoate was significant, as was evident from its respective P-value ($Px_2^2 < 0.0001$) as well as its first order main effect ($Px_2 < 0.0001$). The positive coefficient value ($\beta_2 = 3.27$) of main effect of benzyl benzoate (X_2) was less dominant than the negative quadratic effects ($\beta_{22} = -6.85$) of the same factor. Figure 24 (b) shows the effect of benzyl benzoate on the encapsulation efficiency (ITRAe [%]).

The second order main effect of itraconazole was significant, as was evident from its respective P-value ($Px_3^2 < 0.0001$) as well as its first order main effect ($Px_3 < 0.0001$). The negative coefficient value ($\beta_3 = -24.36$) of the main effect of itraconazole (X_3) was more dominant than the positive quadratic effect ($\beta_{33} = 11.85$)

of the same factor. Figure 24 (c) shows a decreasing effect of itraconazole on ITRAe [%].

There were significant increasing effects of interactions: IBCA monomer and benzyl benzoate (β_{12}= 1.46), and IBCA monomer and itraconazole (β_{13}= 0.97) at P< 0.05. The two-factor interaction graph, shown in Figure 25(a) was helpful in the practical interpretation of the results. Inspection of the interaction graph indicated that changes in the concentration of IBCA produced a much larger change in the ITRAe [%] at the high concentration of benzyl benzoate than at the low concentration of benzyl benzoate. Figure 26 (a), and Figure 27 (a) are a contour plot and response surface plot of the ITRAe [%] as a function of the concentration of IBCA and benzyl benzoate. These plots were obtained from the fitted model. The effect of the strong interaction on this process was very clear because the response surface was a twisted plane. Inspection of the interaction graph shown in Figure 25(b) indicated that changes in the concentration of IBCA produced a much larger change in the ITRAe [%] at the high concentration of itraconazole than at the low concentration of itraconazole. Figure 26 (b), and Figure 27 (b) are a contour plot and response surface plot of the ITRAe [%] as a function of the concentration of IBCA and itraconazole. These plots were obtained from the fitted model. The effect of the strong interaction on this process was very clear because the response surface was a twisted plane. There was no significant interaction between benzyl benzoate and itraconazole as shown in Figure 25(b), Figure 26(b), and Figure 27(b) (P > 0.05).

141

Figure 24 One factor plots of itraconazole-loaded PIBCA nanoparticles in factorial design study; response: the encapsulation efficiency (ITRAe [%]).
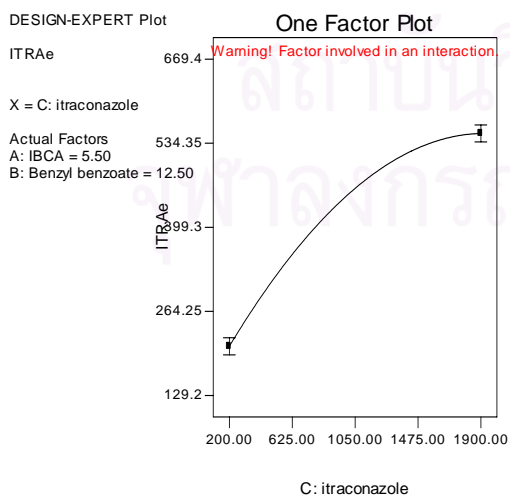
(a) IBCA

(b) Benzyl benzoate
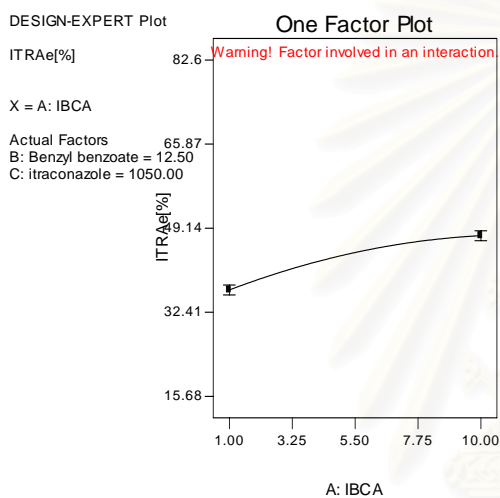
(c) Itraconazole

(a)
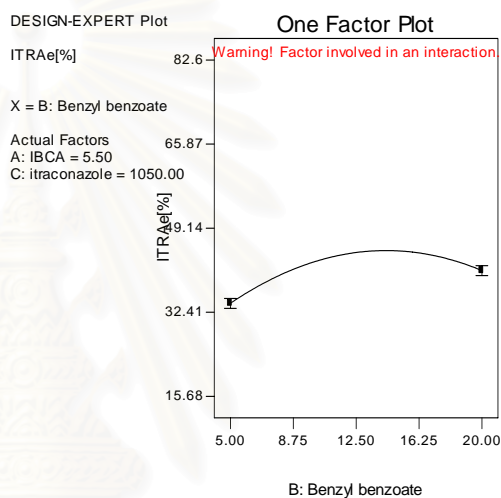
(b)
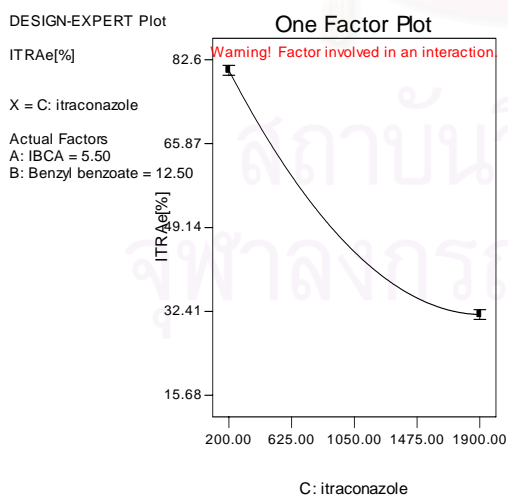
(c)

Figure 25 Interaction plots of itraconazole-loaded PIBCA nanoparticles in factorial
design study; response: the encapsulation efficiency (ITRAe [%]).

   (a) Interaction of IBCA and benzyl benzoate

   (b) Interaction of IBCA and itraconazole

   (c) Interaction of benzyl benzoate and itraconazole
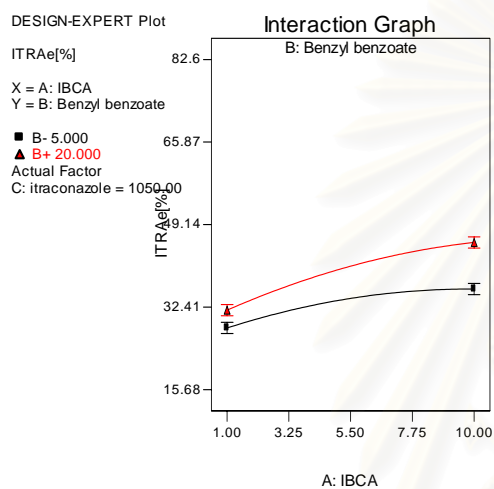
(a)
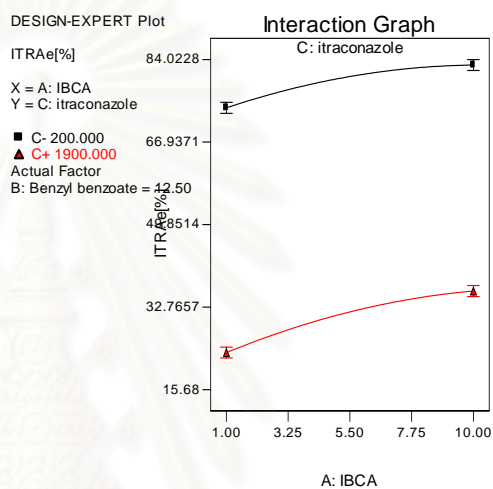
(b)
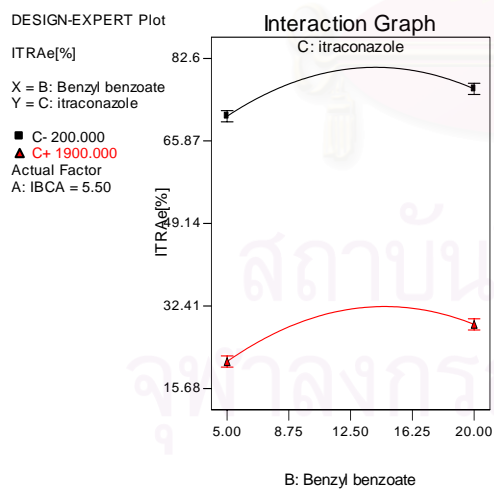
(c)

Figure 26 Contour plots of itraconazole-loaded PIBCA nanoparticles in factorial design study; response: the encapsulation efficiency (ITRAe [%]).

(a) Contour plot of IBCA and benzyl benzoate

(b) Contour plot of IBCA and itraconazole

(c) Contour plot of benzyl benzoate and itraconazole
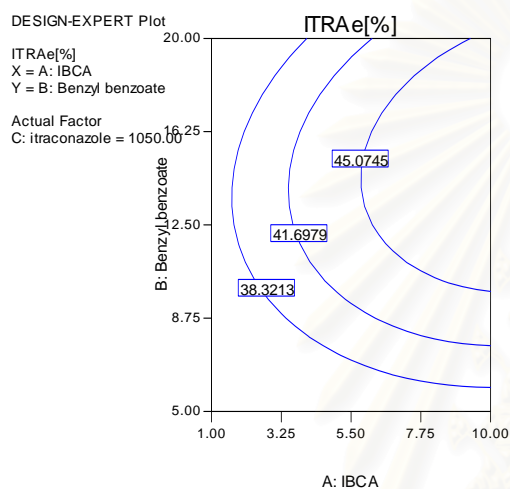
(a)
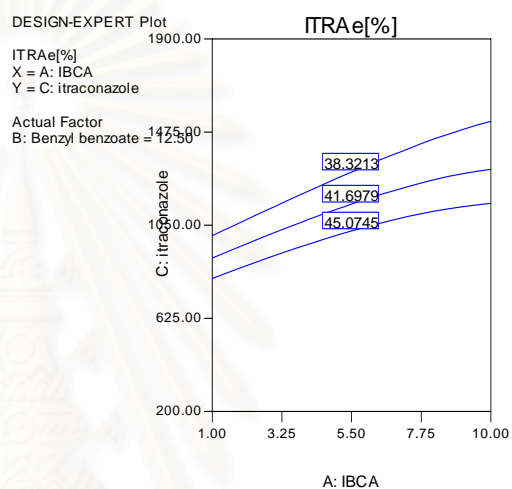
(b)
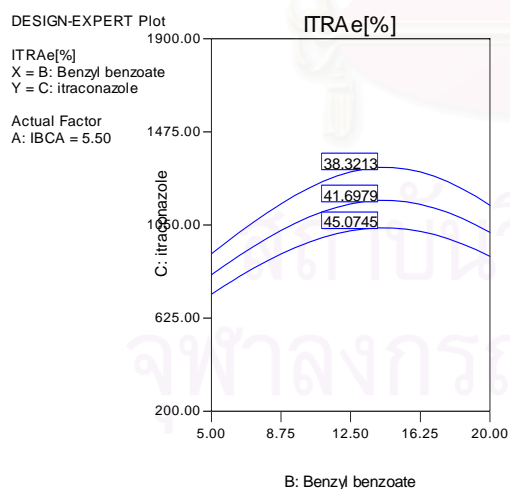
(c)

Figure 27 Response surface plots of itraconazole-loaded PIBCA nanoparticles in factorial design study; response: the encapsulation efficiency (ITRAe[%]).
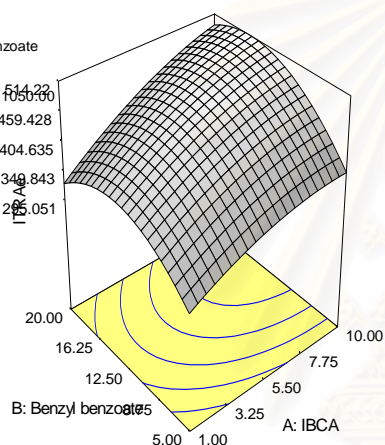
(a) Response surface plot of IBCA and benzyl benzoate

(b) Response surface plot of IBCA and itraconazole

(c) Response surface plot of benzyl benzoate and itraconazole

(a)

(b)
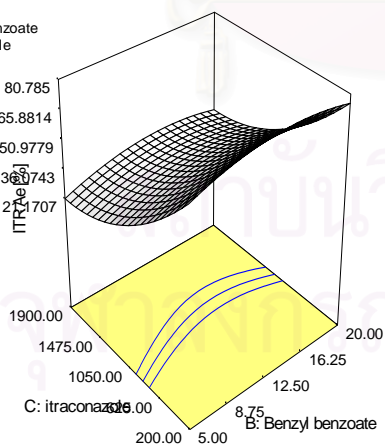
(c)

2.1.4 Multiple Response Optimization

(a) Overlay the Contour Plots for Each Response

Figure 28(a) shows an overlay plot for the 4 responses: 160< the particle size < 190, 0.044< PI< 0.077, 450< ITRAe < 550, and 40< ITRAe [%]< 50. The boundary shown in Figure 28(a) indicates that there are a number of combinations of concentration of IBCA, benzyl benzoate, and itraconazole that will result in a satisfactory process. Figure 28(b) shows an overlay plot for the 4 responses: 160< the particle size < 180, 0.044< PI < 0.077, 450< ITRAe < 550, and 50< ITRAe [%] < 60.   Figure 28(b) shows that there is no boundary that must be met by the process. The encapsulation efficiency was a limiting step of producing itraconazol-loaded PIBCA nanoparticles.

(b) Constrained Optimization and Simultaneous Optimization Technique

Table 26 shows constained optimization of several response data of PIBCA nanoparticles. Using the desirability approach, the target of ITRAe was chosen to be 500 µg/mL, while the lower limit was equal to 450 µg/mL, and the upper limit was 550 µg/mL. The particle size was set in the range from 160 nm to 190 nm. The polydispersity index was set in the range from 0.044 nm to 0.077, and the ITRAe [%] was set in the range from 40% nm to 60%.   Ten solutions having the highest overall desirability (D = 1.00) were found. The desirability function response surface and contour plot of the solution composing of 8.09 µL/mL of IBCA, 10.19 µg/mL of benzyl benzoate , and 1200.77 µg/mL of itraconazole are shown in Figures 29(a) and 29(b), respectively.

Figure 28 Region of the optimum found by overlay the particle size, the polydispersity index (PI), the amount of itraconazole entrapped in nanoparticles (ITRAe), and the encapsulation efficiency (ITRAe [%]) of itraconazole-loaded PIBCA nanoparticles.

(a) 160< particle size< 190, 0.044 < PI < 0.077, 450< ITRAe < 550, and 40< ITRAe[%]<50

(b) 160< particle size< 190, 0.044 < PI < 0.077, 450< ITRAe < 550, and 50< ITRAe[%]<60
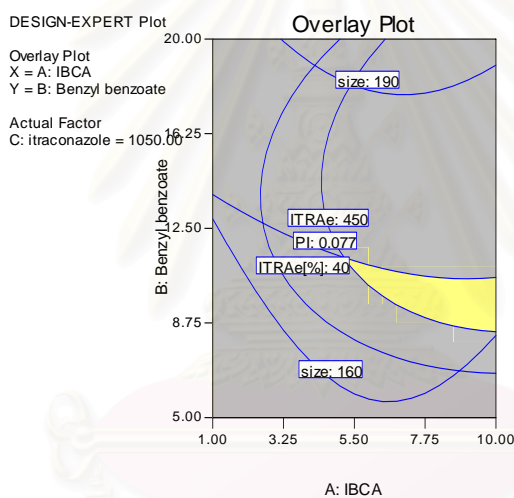
(a)
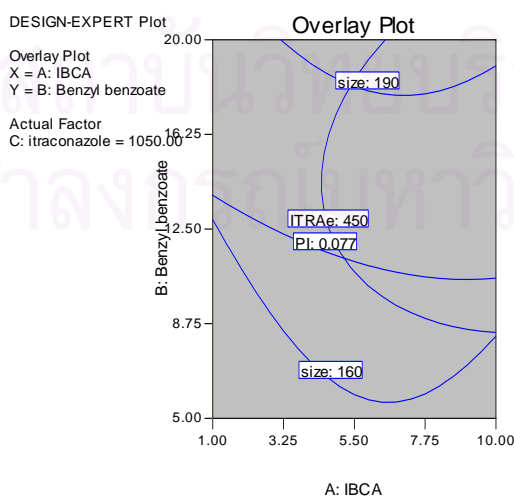
(b)

Table 26 Constrainted optimization of several response data of itraconazole-loaded

PIBCA nanoparticles.

Constraints

Name	Goal	Lower Limit	Upper Limit	Lower Weight	Upper Weight	Importance
IBCA (X_1)	is in range	1	10	1	1	3
Benzyl benzoate(X_2)	is in range	5	20	1	1	3
itraconazole(X_3)	is in range	200	1900	1	1	3
size	is in range	160	190	1	1	3
PI	is in range	0.044	0.077	1	1	3
ITRAe[%]	is in range	40	60	1	1	3
ITRAe	is target = 500	450	550	1	1	3

Solutions

Number	X_1	X_2	X_3	Size	PI	ITRAe[%]	ITRAe	Desira-bility
1	8.09	10.19	1200.77	168.42	0.0762839	40.9422	500.001	1.000
2	7.68	10.14	1224.58	168.723	0.0760225	40.0746	500	1.000
3	7.57	10.32	1218.80	169.213	0.0764319	40.3151	500.001	1.000
4	9.58	10.09	1158.94	165.359	0.0761037	42.489	500.001	1.000
5	8.85	9.72	1203.75	166.15	0.0752108	40.7078	500.001	1.000
6	8.43	10.16	1188.87	167.884	0.0762703	41.3747	500	1.000
7	8.15	10.03	1209.72	167.969	0.0758694	40.5786	500.001	1.000
8	9.74	9.79	1174.76	164.245	0.0753505	41.7865	500.001	1.000
9	7.89	10.10	1217.02	168.437	0.0759828	40.3337	499.999	1.000
10	7.85	10.26	1207.62	168.845	0.076391	40.7065	500	1.000

Figure 29 Desirability function response surface and contour plot for itraconazole-loaded PIBCA nanoparticles.
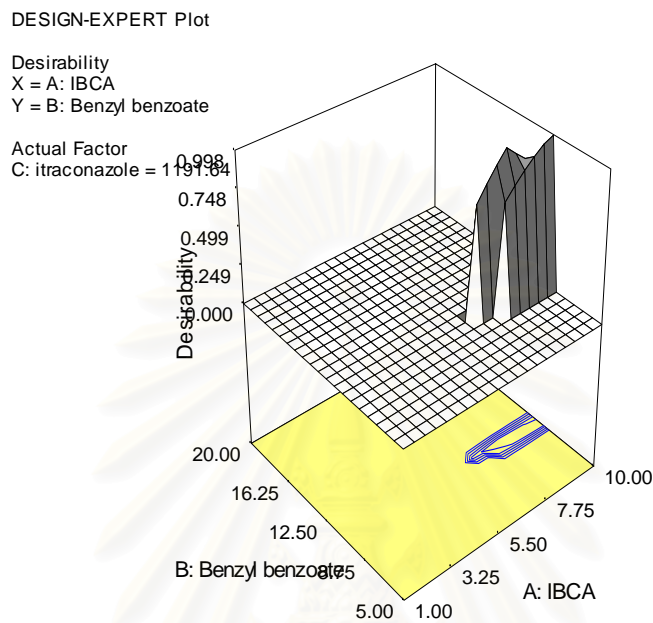
(a) Response surface
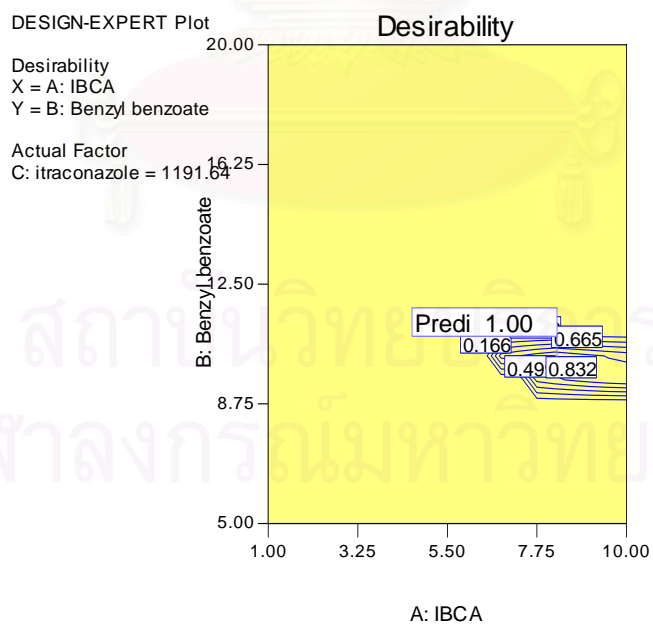
(b) Contour plot

(c) Model and Optimization Verification

Verification of the predicted value was made by using itraconazole-loaded PIBCA nanoparticles prepared using the optimized conditions (solution numbers 1, 2, 6 and 9 in Table 26).   The particle size, amount of itraconazole entrapped in nanoparticles , and encapsulation efficiency are in the 95% prediction interval   (Table 27 and 28). These results therefore corroborate the predicted values, and the effectiveness of the model.

Table 27 Observed and predicted values of particle sizes (nm) and polydispersity index (PI) of itraconazole-loaded PIBCA nanoparticles.

Solution Number	Particle size (nm)			PI		
	Observed response	Predicted value	P-value	Observed response	Predicted value	P-value
1	170.23	168.42	<0.05	0.0761	0.0763	<0.05
2	171.04	168.72	<0.05	0.0753	0.0760	<0.05
6	169.52	167.88	<0.05	0.0760	0.0763	<0.05
9	170.69	168.84	<0.05	0.0754	0.0760	<0.05

Table 28 Observed and predicted values of the amount of itraconazole entrapped in nanoparticles (ITRAe) and the encapsulation efficiency (ITRAe [%]) of itraconazole-loaded PIBCA nanoparticles.

Solution Number	ITRAe (μg/mL)			ITRAe[%]		
	Observed response	Predicted value	P-value	Observed response	Predicted value	P-value
1	509.62	500.001	<0.05	42.44	40.9422	<0.05
2	504.21	500.000	<0.05	41.17	40.0746	<0.05
6	498.32	500.000	<0.05	41.91	41.3747	<0.05
9	497.65	499.999	<0.05	40.89	40.3337	<0.05

2.2 Preparation of Nanoparticles Prepared from PLGA 85:15

2.2.1 Effect of Stirring Rate during Pouring Organic Phase into Water Phase

Table App.C.1, Table App.C.2 and Table App. C.3 show the effect of stirring rate during pouring organic phase into water phase on the particle size, the polydispersity index (PI) and the zeta potential of the nanoparticles formed, respectively. The one-way analysis of variance (ANOVA) demonstrated that the stirring rate did not significantly affect the particle size (Table 29), the polydispersity (Table 30) and the zeta potential (Table 31) of the nanoparticles formed. Since there was no significant difference among the stirring rate of 750, 1000 and 1500 rpm, then the stirring rate of 750 rpm was suitable to use in further study because this stirring rate was the less energy consuming condition which had advantage on cost effective for industrial production.

Table 29 ANOVA Table for particle size of itraconazole-loaded PLGA nanoparticles comparing among different stirring rates.

Source of variables	df	SS	MS	F	P
Stirring rate	2	9.3	4.7	0.31	0.755
Error	3	45.4	15.1		
Total	5	54.7			

Table 30 ANOVA Table for polydispersity index of itraconazole-loaded PLGA

nanoparticles comparing among different stirring rates.

Source of variables	df	SS	MS	F	P
Stirring rate	2	0.000217	0.000109	0.32	0.749
Error	3	0.001023	0.000341		
Total	5	0.001240			

Table 31 ANOVA Table for zeta potential of itraconazole-loaded PLGA

nanoparticles comparing among different stirring rates.

Source of variables	df	SS	MS	F	P
Stirring rate	2	5.11	2.55	0.78	0.532
Error	3	9.77	3.26		
Total	5	14.88			

2.2.2 Effect of Surfactant Concentrations in the Water Phase

Table App.C.4, Table App.C.5 and Table App. C.6 show the effect of surfactant concentration in the water phase on the particle size, the polydispersity index (PI) and the zeta potential of the nanoparticles formed, respectively. The one-way analysis of variance (ANOVA) demonstrated that there was no significant difference among the surfactant concentrations in the particle size (Table 32). For the polydispersity index (Table 33) and zeta potential (Table 34), there were also no significant difference among surfactant concentrations. The suitable surfactant concentration using in the 2^3 factorial design was 0.25% because this concentration was the lowest concentration which gave the same size,

polydispersity index and zeta potential as the other concentrations. The lower concentration of surfactant was used, the safer was gained.

Table 32 ANOVA Table for particle size of itraconazole-loaded PLGA nanoparticles comparing among different surfactant concentrations.

Source of variables	df	SS	MS	F	P
Concentration	3	7.4	2.5	0.09	0.959
Error	4	103.8	25.9		
Total	7	111.1			

Table 33 ANOVA Table for polydispersity index of itraconazole-loaded PLGA nanoparticles comparing among different surfactant concentrations.

Source of variables	df	SS	MS	F	P
Concentration	3	0.000709	0.000236	0.44	0.738
Error	4	0.002151	0.000538		
Total	7	0.002860			

Table 34 ANOVA Table for zeta potential of itraconazole-loaded PLGA nanoparticles comparing among different surfactant concentrations.

Source of variables	df	SS	MS	F	P
Concentration	3	3.295	1.098	1.50	0.342
Error	4	2.920	0.730		
Total	7	6.215			

2.2.3 Factorial design study

A factorial design of type 2^n was used, where n is the number of factors, three in this study and 2 indicated that each factor had two levels of interests. Thus, 8 experimental trials were required to complete the design. Since

there were two replicates, then 16 observations would perform. Five replicates at the center of the design were investigated to allow for an independent estimation of the experimental error and to check the linearity of the factor effects (Montgomery, 2001). Twenty-one observations were randomly performed.

Three factors were considered important for this study. Concentration of PLGA added to the medium was considered important, as it constituted the primary building block of the formed particle and, ultimately, the nanoparticle. The benzyl benzoate was chosen because itraconazole was highly dissolved in benzyl benzoate, thus it could enhance the amount of itraconazole entrapped in nanoparticles. The itraconazole concentration was included as the third design factor because it could enhance encapsulation efficiency.

Influence of Preparation Factors on Particle Size of Itraconazole-Loaded PLGA Nanoparticles

Table App.C.7 shows the particle size of itraconazole-loaded PLGA nanoparticles obtained from the 2^3 factorial design study. Table 35 presents the effect estimates and sums of squares for the 2^3 factorial design of PLGA nanoparticles, using the particle size as the response variable. Factors A, B, C and the AB and AC interaction were important and large effect that together account for nearly 90% of the variability in average particle size. Figure 30(a) shows normal probability plot and half normal probability plot of the factor effect for the 2^3 factorial design study, using the particle size as the response variable. The normal probability plot of these effects that lie along the line are neglible, whereas the large effects are far from the line. The important effects that emerge from this analysis were the main effects of A, B, C and the AB and AC interactions. An alternative to the normal

proability plot of the factor effects is the half-normal plot. This is a plot of the absolute value of the effect estimates against their cumulative normal probabilities. The important effects that emerge from the half-normal plot were also the main effects of A, B, C and the AB and AC. Figure 30(b) presents the half-normal plot of the effects for the particle size experiment.

Table 35 Factor effect estimates and sums of squares for the 2^3 factorial design; response: the particle size.

Model Term	Effect Estimate	Sum of Squares	% Contribution
A	133.075	70835.8	19.894
B	104.175	43409.7	12.1915
C	210.125	176610	49.6005
AB	-9.45	357.21	0.100321
AC	92.6	34299	9.63279
BC	3	36	0.0101105
ABC	2.375	22.5625	0.00633662
Curvature	87.021	30290.6	8.50704

Figure 30 Normal probability plot (a) and half normal probability plot (b)of the effect for the 2^3 factorial design study ; response: the particle size.

(a)   (b)
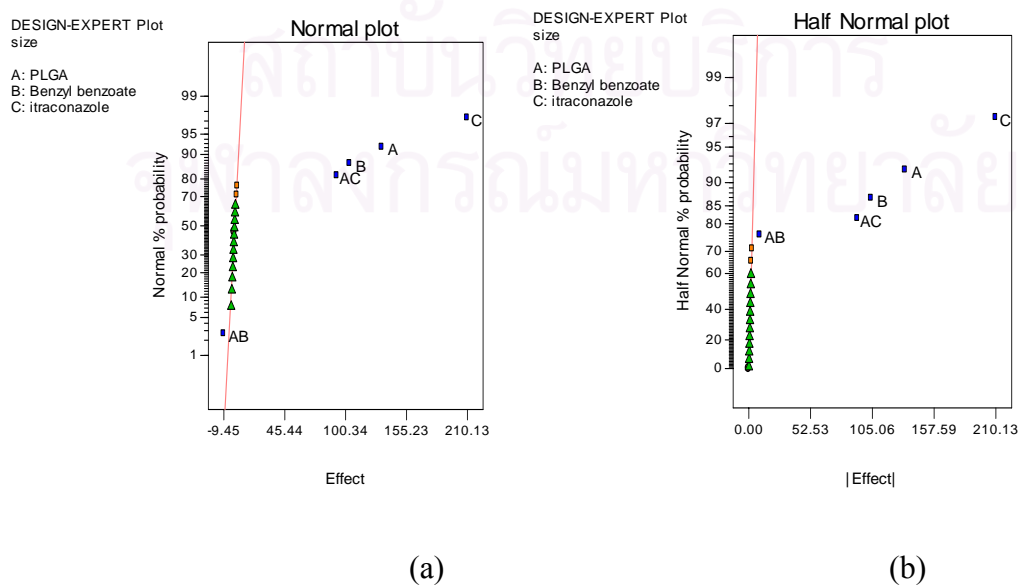
Table 36 shows Design-Expert output analyzing particle size data of itraconazole-loaded PLGA nanoparticles, using the particle size as the response variable in full model. The model F-value of 2731.49 implied the model was significant. Values of "Prob > F" less than 0.0500 indicated model terms were significant. In this case A, B, C, AB and AC were significant model terms. Model reduction was used to improve the model.

Table 36 Design-Expert output analyzing particle size data of itraconazole-loaded PLGA nanoparticles (full model).

Response: Size

ANOVA for Selected Factorial Model
Analysis of Variance Table [Partial Sum of Squares]

Source	Sum of Squares	DF	Mean Square	F Value	Prob > F
Model	3.256E+005	7	46510.06	2731.49	< 0.0001
A	*70835.82*	*1*	*70835.82*	*4160.12*	*< 0.0001*
B	*43409.72*	*1*	*43409.72*	*2549.41*	*< 0.0001*
C	*1.766E+005*	*1*	*1.766E+005*	*10372.15*	*< 0.0001*
AB	*357.21*	*1*	*357.21*	*20.98*	*0.0006*
AC	*34299.04*	*1*	*34299.04*	*2014.35*	*< 0.0001*
BC	*36.00*	*1*	*36.00*	*2.11*	*0.1716*
ABC	*22.56*	*1*	*22.56*	*1.33*	*0.2721*
Curvature	30290.62	1	30290.62	1778.94	< 0.0001
Pure Error	204.33	12	17.03		
Cor Total	3.561E+005	20			

S.D.	4.13	R-Squared	0.9994
Mean	394.98	Adj R-Squared	0.9990
C.V.	1.04	Pred R-Squared	0.9982
PRESS	649.49	Adeq Precision	166.489

Table 36 Design-Expert output analyzing particle size data of itraconazole-loaded

PLGA nanoparticles (full model) (continued).

Factor	Coefficient Estimate	DF	Standard Error	95% CI Low	95% CI High	VIF
Intercept	373.75	1	1.03	371.50	376.00	
A-PLGA	66.54	1	1.03	64.29	68.79	1.00
B-Benzyl benzoate	52.09	1	1.03	49.84	54.34	1.00
C-itraconazole	105.06	1	1.03	102.81	107.31	1.00
AB	-4.73	1	1.03	-6.97	-2.48	1.00
AC	46.30	1	1.03	44.05	48.55	1.00
BC	1.50	1	1.03	-0.75	3.75	1.00
ABC	1.19	1	1.03	-1.06	3.44	1.00
Center Point	89.17	1	2.11	84.56	93.78	1.00

Table 37 shows the analysis of variance summary for the reduced

model that was, the model with the non-significant BC and ABC interactions were

removed. The error or residual sum of squares composed of a pure error component

arising from replicate runs and a lack-of-fit component corresponding to the BC and

ABC interactions. The regression model in terms of both actual and coded variables

was given, along with confidence interval on each model coefficient. The "model F-

value" of 3466.97 implied the model was significant. Values of "Prob > F" less than

0.0500 indicated model terms were significant. In this case A, B, C, AB and AC were

significant model terms. The "curvature F-value" of 1613.10 implied there was

significant curvature (as measured by difference between the average of the center

points and the average of the factorial points) in the design space.

Model adequate checking of PLGA nanoparticles in factorial design

study is shown in Figure 31, where the particle size was used as response variable.

Figure 31(a) is the normal probability plot of the studentized residuals to check for

normality of residuals. The normal probability plot did not reveal anything particularly troublesome. This plot resembled a straight line which indicated that the underlying error distribution was normal. Figure 31(b) shows the plot of studentized residuals versus predicted values to check for constant error. No unusual structure was apparent. Figure 31(c) is the plot of outlier t versus run order to look for outliers, i.e., influential values. All of standardize residuals (d_i) laid in the interval $-3 \le d_i \le 3$ conformed that there was no outlier in this study. Figure 31(d) shows Box-Cox plot for power transformations. The Box- Cox method showed that the tranformation parameter λ was equal to 1, this implied that the data did not need transformation. All the diagnostic plots in Figure 31(a), (b) and (d) were in agree with the assumption of analysis of variance.

Figure 31 Model adequate checking of itraconazole-loaded PLGA nanoparticles in factorial design study, response: the particle size.

(a) Normal probability plot of the studentized residuals

(b) Studentized residuals versus predicted values

(c) Outlier t versus run order　　　　(d) Box-Cox plot
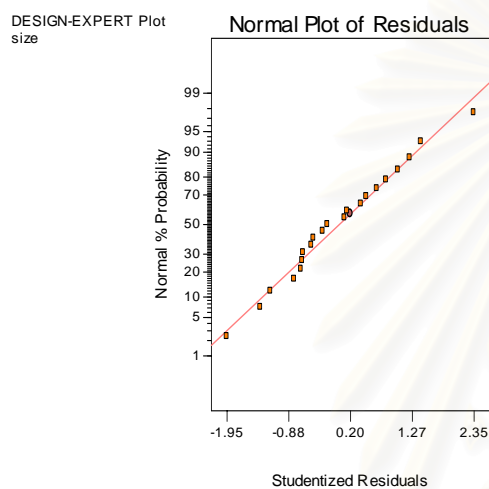
(a)
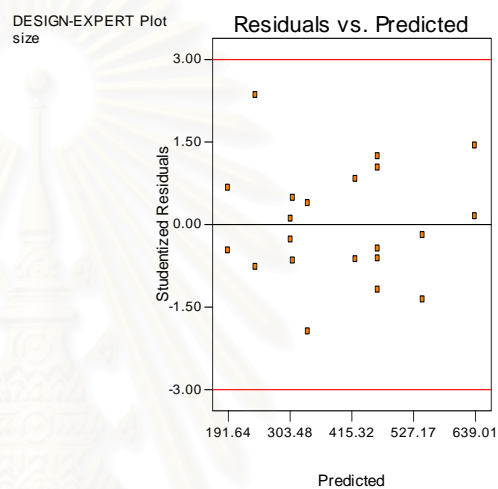
(b)
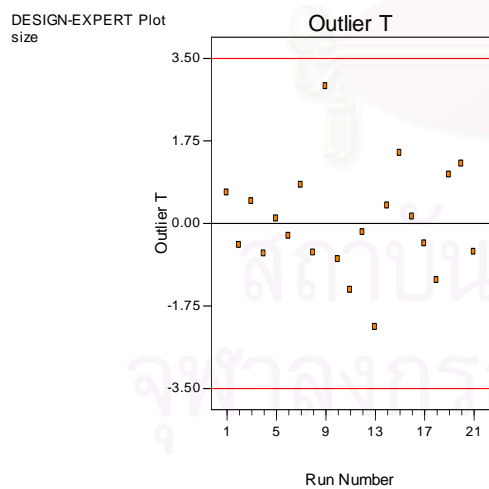
(c)
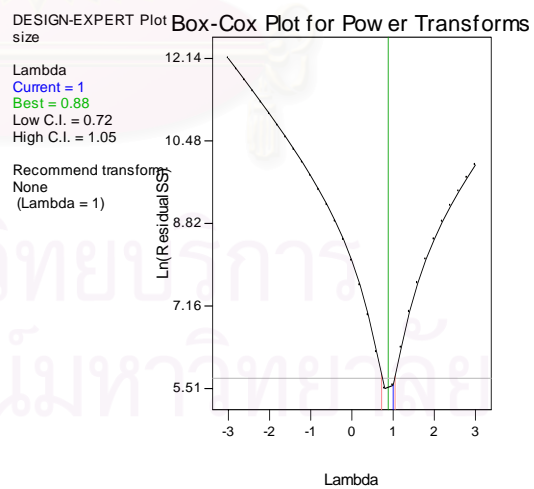
(d)

Table 37 Design-Expert output analyzing particle size data of itraconazole-loaded

PLGA nanoparticles (reduce model).

Response: Size

ANOVA for Selected Factorial Model
Analysis of Variance Table [Partial Sum of Squares]

Source	Sum of Squares	DF	Mean Square	F Value	Prob > F
Model	3.255E+005	5	65102.37	3466.97	< 0.0001
A	*70835.82*	*1*	*70835.82*	*3772.30*	*< 0.0001*
B	*43409.72*	*1*	*43409.72*	*2311.75*	*< 0.0001*
C	*1.766E+005*	*1*	*1.766E+005*	*9405.21*	*< 0.0001*
AB	*357.21*	*1*	*357.21*	*19.02*	*0.0007*
AC	*34299.04*	*1*	*34299.04*	*1826.56*	*< 0.0001*
Curvature	30290.62	1	30290.62	1613.10	< 0.0001
Residual	262.89	14	18.78		
Lack of Fit	*58.56*	*2*	*29.28*	*1.72*	*0.2205*
Pure Error	*204.33*	*12*	*17.03*		
Cor Total	3.561E+005	20			

S.D.	4.33	R-Squared	0.9992
Mean	394.98	Adj R-Squared	0.9989
C.V.	1.10	Pred R-Squared	0.9983
PRESS	604.32	Adeq Precision	178.817

Factor	Coefficient Estimate	DF	Standard Error	95% CI Low	95% CI High	VIF
Intercept	373.75	1	1.08	371.43	376.07	
A-PLGA	66.54	1	1.08	64.21	68.86	1.00
B-Benzyl benzoate	52.09	1	1.08	49.76	54.41	1.00
C-itraconazole	105.06	1	1.08	102.74	107.39	1.00
AB	-4.73	1	1.08	-7.05	-2.40	1.00
AC	46.30	1	1.08	43.98	48.62	1.00
Center Point	89.17	1	2.22	84.41	93.93	1.00

Final Equation in Terms of Coded Factors:

size = + 373.75 + 66.54 * A + 52.09 * B + 105.06 * C - 4.73 * A * B
        + 46.30* A * C

Table 37 Design-Expert output analyzing particle size data of itraconazole-loaded

PLGA nanoparticles (reduce model) (continued).

Final Equation in Terms of Actual Factors:

size = + 135.39687 + 0.36750 * PLGA + 7.71500 * Benzyl benzoate + 0.060592 * itraconazole - 0.014000 * PLGA * Benzyl benzoate + 1.28611E-003 * PLGA * itraconazole

Diagnostics Case Statistics

Standard Order	Actual Value	Predicted Value	Residual	Leverage	Student Residual	Cook's Distance	Outlier t	Run Order
1	193.90	191.64	2.26	0.375	0.660	0.037	0.647	1
2	425.60	422.79	2.81	0.375	0.821	0.058	0.811	7
3	420.60	422.79	-2.19	0.375	-0.639	0.035	-0.624	8
4	539.60	544.29	-4.69	0.375	-1.368	0.160	-1.417	11
5	304.30	305.26	-0.96	0.375	-0.281	0.007	-0.272	6
6	249.60	241.56	8.04	0.375	2.346	0.472	2.902	9
7	306.90	309.16	-2.26	0.375	-0.660	0.037	-0.647	4
8	305.60	305.26	0.34	0.375	0.099	0.001	0.095	5
9	190.00	191.64	-1.64	0.375	-0.478	0.020	-0.464	2
10	310.80	309.16	1.64	0.375	0.478	0.020	0.464	3
11	639.50	639.01	0.49	0.375	0.142	0.002	0.137	16
12	643.90	639.01	4.89	0.375	1.427	0.174	1.487	15
13	337.60	336.29	1.31	0.375	0.383	0.013	0.371	14
14	329.60	336.29	-6.69	0.375	-1.952	0.327	-2.205	13
15	543.60	544.29	-0.69	0.375	-0.201	0.003	-0.194	12
16	461.20	462.92	-1.72	0.200	-0.444	0.007	-0.431	17
17	458.30	462.92	-4.62	0.200	-1.192	0.051	-1.212	18
18	460.50	462.92	-2.42	0.200	-0.624	0.014	-0.610	21
19	467.70	462.92	4.78	0.200	1.233	0.054	1.259	20
20	466.90	462.92	3.98	0.200	1.027	0.038	1.029	19
21	238.90	241.56	-2.66	0.375	-0.777	0.052	-0.766	10

Note: Predicted values of center points include center point coefficient.

On the particle size, the factor effect estimated (and the regression model) indicated that the particle size increased as the concentration of PLGA (A) increased and as the concentration of benzyl benzoate (B) increased, and as the concentration of itraconazole(C) increased. The Fisher F test with a very low probability value ($P_{model} > F$ less than 0.0001) (Table 37) demonstrated a very high

significance for the regression model (Montgomery, 2001). The goodness of fit of the model was checked by the adjusted determination coefficient (adjusted R-Squared). The results show that the value of the determination coefficient (R-Squared = 0.9992) was as high as the value of the adjusted determination coefficient (adjusted R-Squared = 0.9989), which indicated a high significance of the model (Akhnazarova and Kafaro, 1982). A higher value of the correlation coefficient (R = 0.9996) signified an excellent correlation between the independent variables (Box, 1978). At the same time, a relatively low value of the coefficient of variation (C.V. = 1.10) indicated improved precision and reliability of the conducted experiments (Box and Wilson, 1951).

It is obvious that the concentration of PLGA, benzyl benzoate, and itraconazole had significant effect on the particle size of the nanoparticles. Figure 32(a), 32 (b) and 32(c) shows the increasing effect of PLGA, benzyl benzoate, and itraconazole, respectively. A significant antagonistic interaction between PLGA and benzyl benzoate at P < 0.001 was observed. This interaction is reflected by the pattern of the lines of Figure 33(a), 34(a) and 35(a). The two-factor interaction graph shown in Figure 33(a) was helpful in the practical interpretation of the results. This graph was constructed by plotting average particle size versus the concentration of PLGA for each concentration of benzyl benzoate and connecting the points for the low- and high-concentration of benzyl benzoate to give the two curves. Inspection of the interaction graph indicated that changes in the concentration of PLGA produced a much larger change in the particle size at the low concentration of benzyl benzoate than at the high concentration of benzyl benzoate. Figure 34 (a) and Figure 35 (a) are a contour plot and response surface plot of the particle size as a function of the concentration of PLGA and benzyl benzoate. These plots were obtained from the

fitted model. The effect of the strong interaction on this process was very clear since the response surface was a twisted plane.

A significant ($P < 0.001$) synergistic interaction was observed between PLGA and itraconazole. This interaction is reflected by the pattern of the lines of Figure 33(b), 34(b) and 35(b). Inspection of the interaction graph shown in Figure 33 (b) indicated that changes in the concentration of PLGA produced a much larger change in the particle size at the high concentration of itraconazole than at the low concentration of itraconazole. Figure 34 (b), and Figure 35 (b) are a contour plot plot and response surface of the particle size as a function of the concentration of PLGA and itraconazle. These plots were obtained from the fitted model. The effect of the strong interaction on this process was very clear since the response surface was now a twisted plane.

Figure 32 One factor plots of itraconazole-loaded PLGA nanoparticles in factorial design study; response: the particle size.

   (a) PLGA

   (b) Benzyl benzoate
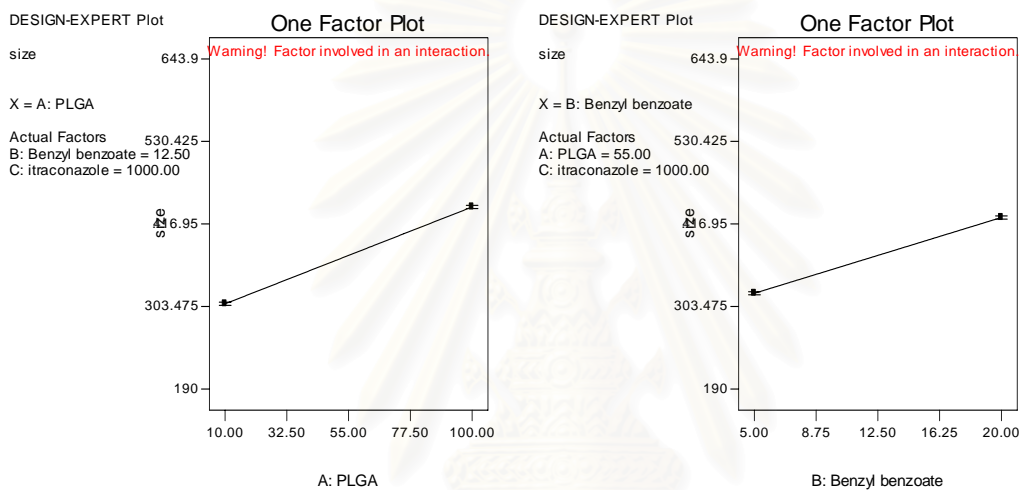
   (c) Itraconazole

(a)

(b)
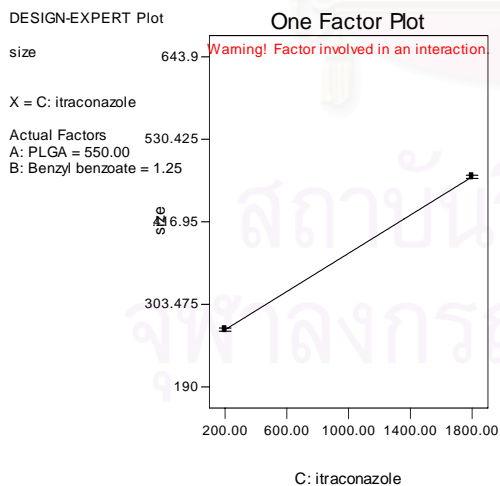
(c)

Figure 33 Interaction plots of itraconazole-loaded PLGA nanoparticles in factorial design study; response: the particle size.

(a)   Interaction of PLGA and benzyl benzoate

(b)   Interaction of PLGA and itraconazole
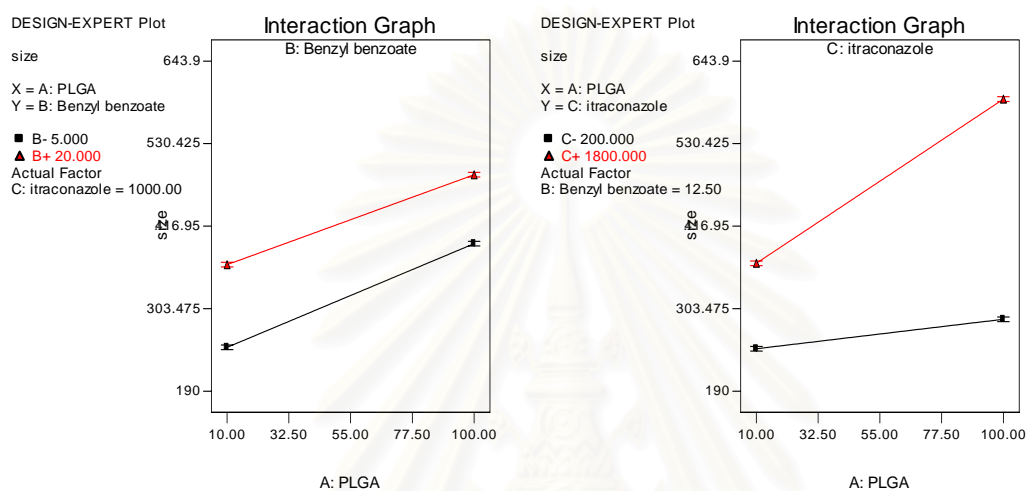
(a)   (b)

Figure 34 Contour plots of itraconazole-loaded PLGA nanoparticles in factorial design study; response: the particle size.

(a) Contour plot of PLGA and benzyl benzoate

(b) Contour plot of PLGA and itraconazole
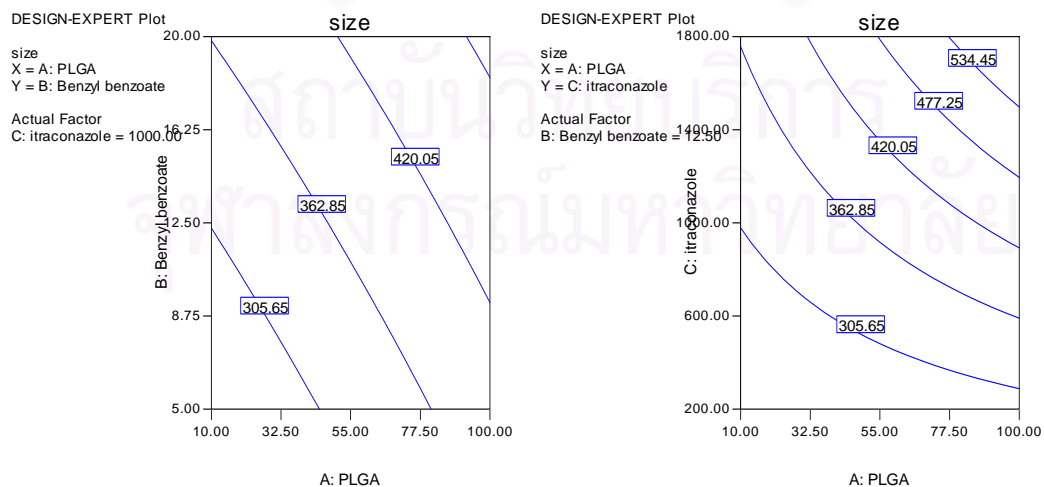
(a)   (b)

Figure 35 Response surface plots of itraconazole-loaded PLGA nanoparticles in factorial design study; response: the particle size.

(a) Response surface plot of PLGA and benzyl benzoate
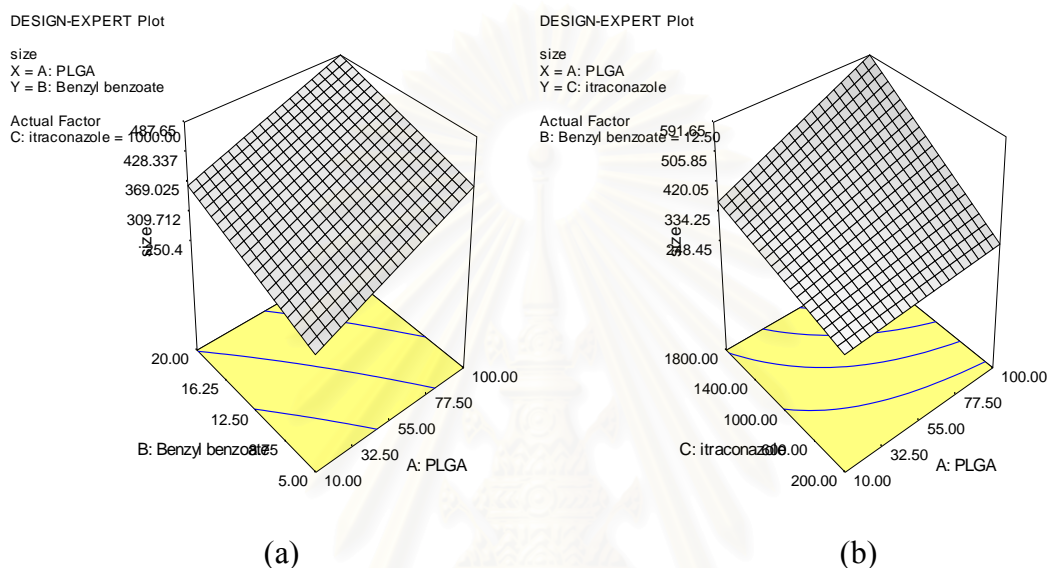
(b) Response surface plot of PLGA and itraconazole

(a)

(b)

Influence of Preparation Factors on Particle Size Distribution of Itraconazole-Loaded PLGA Nanoparticles

Table App.C.8 shows the particle size distribution (PI) of itraconazole-loaded PLGA nanoparticles obtained from the 2^3 factorial design study. Table 38 presents the effect estimates and sums of squares for the 2^3 factorial design of PLGA nanoparticles, using the polydispersity index (PI) as the response variable. Factors A, B, C and AB, AC and BC interaction were not important and little effect that together account for nearly 20% of the variability in average polydispersity index. Figure 36 shows normal probability plot and half normal probability plot of the factor effect for the 2^3 factorial design study, using the polydispersity index as the response variable. The normal probability plot of these effects that lie along the line are neglible, whereas the large effects are far from the line. Figure 36(a) shows that all effects

were neglible. Figure 36 (b) presents the half-normal plot of the effects for the

polydispersity index (PI) experiment. All effects were also neglible.

Table 38 Factor effect estimates and sums of squares for the 2^3 factorial design;

response: the particle size distribution (PI).

Term	Effect Estimate	Sum of Squares	% Contribution
Intercept			
A	0.028375	0.00322056	4.00945
B	0.012875	0.000663063	0.825482
AB	0.032625	0.00425756	5.30047
AC	-0.027625	0.00305256	3.8003
BC	-0.026125	0.00273006	3.3988
ABC	0.029125	0.00339306	4.22421
Curvature	0.00808777	0.000261648	0.3300

Figure 36 Normal probability plot (a) and half normal probability plot (b) of the effect

for the 2^3 factorial design study ; response: the particle size distribution (PI).

(a)   (b)
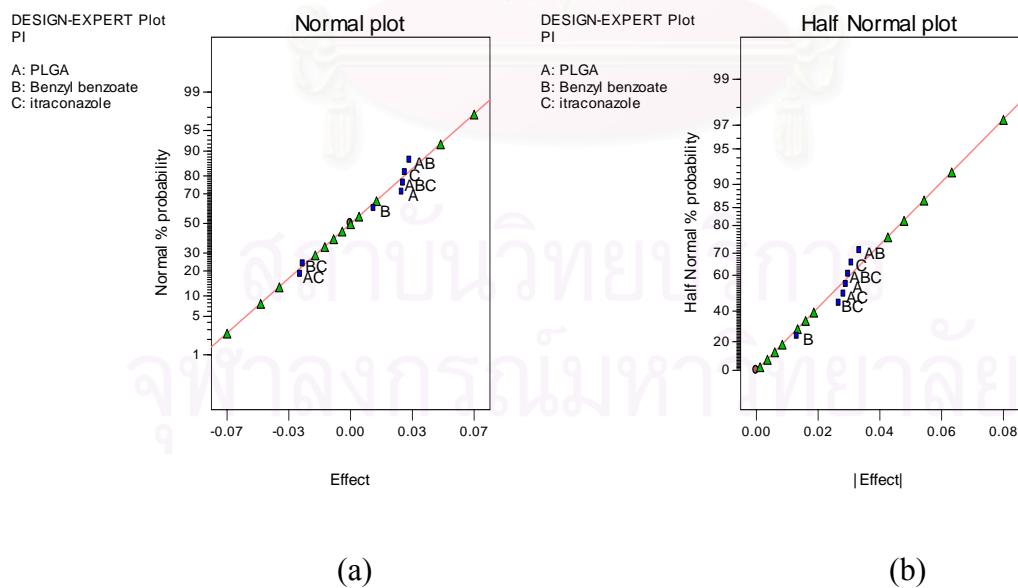
Table 39 shows Design-Expert output analyzing   the polydispersity

index (PI) data of itraconazole-loaded PLGA nanoparticles in full model where the PI

was used as the response variable. The "model F-value" of 0.61 implied the model was not significant . Values of "Prob > F" less than 0.0500 indicated model terms were significant. In this case there were no significant model terms. The "curvature F-value" of 0.05 implied the curvature in the design space was not significant.

Table 39 Design-Expert output analyzing particle size distribution data of itraconazole-loaded PLGA nanoparticles (full model).

Response: PI
ANOVA for Selected Factorial Model
Analysis of variance table [Partial sum of squares]

Source	Sum of Squares	DF	Mean Square	F Value	Prob > F
Model	0.021	7	2.992E-003	0.61	0.7400
A	3.221E-003	1	3.221E-003	0.65	0.4345
B	6.631E-004	1	6.631E-004	0.13	0.7201
C	3.630E-003	1	3.630E-003	0.74	0.4075
AB	4.258E-003	1	4.258E-003	0.86	0.3709
AC	3.053E-003	1	3.053E-003	0.62	0.4464
BC	2.730E-003	1	2.730E-003	0.55	0.4709
ABC	3.393E-003	1	3.393E-003	0.69	0.4228
Curvature	2.616E-004	1	2.616E-004	0.053	0.8216
Pure Error	0.059	12	4.926E-003		
Cor Total	0.080	20			

S.D.	0.070	R-Squared	0.2616	
Mean	0.55	Adj R-Squared	-0.1691	
C.V.	12.71	Pred R-Squared	-1.3408	
PRESS	0.19	Adeq Precision	2.459	

Table 39 Design-Expert output analyzing particle size distribution data of

itraconazole-loaded PLGA nanoparticles (full model) (continued).

Factor	Coefficient Estimate	DF	Standard Error	95% CI Low	95% CI High	VIF
Intercept	0.55	1	0.018	0.51	0.59	
A-PLGA	0.014	1	0.018	-0.024	0.052	1.00
B-Benzyl benzoate	6.438E-003	1	0.018	-0.032	0.045	1.00
C-itraconazole	0.015	1	0.018	-0.023	0.053	1.00
AB	0.016	1	0.018	-0.022	0.055	1.00
AC	-0.014	1	0.018	-0.052	0.024	1.00
BC	-0.013	1	0.018	-0.051	0.025	1.00
ABC	0.015	1	0.018	-0.024	0.053	1.00
Center Point	8.288E-003	1	0.036	-0.070	0.087	1.00

Final Equation in Terms of Coded Factors:

PI = + 0.55 + 0.014* A + 6.438E-003 * B + 0.015 * C + 0.016 * A * B - 0.014 * A * C - 0.013 * B * C + 0.015* A * B * C

Final Equation in Terms of Actual Factors:

PI = + 0.45125 + 7.68981E-004 * PLGA + 3.34352E-003 * Benzyl benzoate

+ 1.04225E-004 * itraconazole - 5.60185E-006 * PLGA * Benzyl benzoate

- 1.05787E-006 * PLGA * itraconazole - 5.14352E-006 * Benzyl benzoate * itraconazole + 5.39352E-008 * PLGA * Benzyl benzoate * itraconazole

Diagnostics Case Statistics

Standard Order	Actual Value	Predicted Value	Residual	Leverage	Student Residual	Cook's Distance	Outlier t	Run Order
1	0.46	0.49	-0.033	0.500	-0.675	0.051	-0.659	1
2	0.45	0.53	-0.074	0.500	-1.501	0.250	-1.595	7
3	0.60	0.53	0.075	0.500	1.501	0.250	1.595	8
4	0.59	0.54	0.046	0.500	0.917	0.093	0.910	11
5	0.50	0.53	-0.029	0.500	-0.584	0.038	-0.568	6
6	0.45	0.54	-0.090	0.500	-1.813	0.365	-2.038	9

Table 39 Design-Expert output analyzing particle size distribution data of itraconazole-loaded PLGA nanoparticles (full model) (continued).

Diagnostics Case Statistics

Standard Order	Actual Value	Predicted Value	Residual	Leverage	Student Residual	Cook's Distance	Outlier t	Run Order
7	0.58	0.60	-0.020	0.500	-0.413	0.019	-0.398	4
8	0.55	0.53	0.029	0.500	0.584	0.038	0.568	5
9	0.52	0.49	0.034	0.500	0.675	0.051	0.659	2
10	0.62	0.60	0.021	0.500	0.413	0.019	0.398	3
11	0.60	0.59	6.000E-003	0.500	0.121	0.002	0.116	16
12	0.58	0.59	-6.000E-003	0.500	-0.121	0.002	-0.116	15
13	0.62	0.58	0.038	0.500	0.776	0.067	0.762	14
14	0.55	0.58	-0.038	0.500	-0.776	0.067	-0.762	13
15	0.50	0.54	-0.045	0.500	-0.917	0.093	-0.910	12
16	0.61	0.56	0.055	0.200	0.882	0.022	0.874	17
17	0.49	0.56	-0.070	0.200	-1.109	0.034	-1.120	18
18	0.48	0.56	-0.081	0.200	-1.284	0.046	-1.323	21
19	0.58	0.56	0.025	0.200	0.405	0.005	0.390	20
20	0.63	0.56	0.069	0.200	1.105	0.034	1.117	19
21	0.63	0.54	0.090	0.500	1.813	0.365	2.038	10

Note: Predicted values of center points include center point coefficient.

Influence of Preparation Factors on the Amount of Itraconazole Entrapped in Nanoparticles (ITRAe) of Itraconazole-Loaded PLGA Nanoparticles

Table App.C.9 shows the amount of itraconazole entrapped in nanoparticles (ITRAe) of itraconazole-loaded PLGA nanoparticles obtained from the 2^3 factorial design study. Table 40 presents the effect estimates and sums of squares for the 2^3 factorial design of itraconazole-loaded PLGA nanoparticles, using the amount of itraconazole entrapped in nanoparticles (ITRAe) as the response variable. Factors A, B, C, AC and BC interaction were important and large effects that together account for nearly 90% of the variability in average ITRAe. Figure 37 shows normal probability plot and half normal probability plot of the factor effect for the 2^3 factorial

design study, using the amount of itraconazole entrapped in nanoparticles (ITRAe) as the response variable. The normal probability plot of these effects that lie along the line are neglible, whereas the large effects are far from the line. The important effects that emerge from this analysis were the main effects of A, B and C and AC and BC interactions(Figure 37(a)). Figure 37(b) presents the half-normal plot of the effects for the amount of itraconazole entrapped in nanoparticles (ITRAe) experiment. The important effects that emerge from the half-normal plot were also the main effects of A, Band C and AC and BC interactions.

Table 40 Factor effect estimates and sums of squares for the 2^3 factorial design; response: the amount of itraconazole entrapped in nanoparticles (ITRAe).

Term	Effect Estimates	Sum of Square	% Contribution
Intercept			
A	146.895	86312.6	2.96997
B	338.12	457301	15.7355
C	666.058	1.77453E+006	61.0607
AB	0.1725	0.119025	4.09559E-006
AC	124.805	62305.2	2.14389
BC	282.98	320311	11.0217
ABC	1.5075	9.09022	0.00031279
Curvature	226.476	205165	7.05964

Figure 37 Normal probability plot (a) and half normal probability plot (b)of the effect

for the 2^3 factorial design study ; response: the amount of itraconazole entrapped in

anoparticles (ITRAe).

(a)   (b)
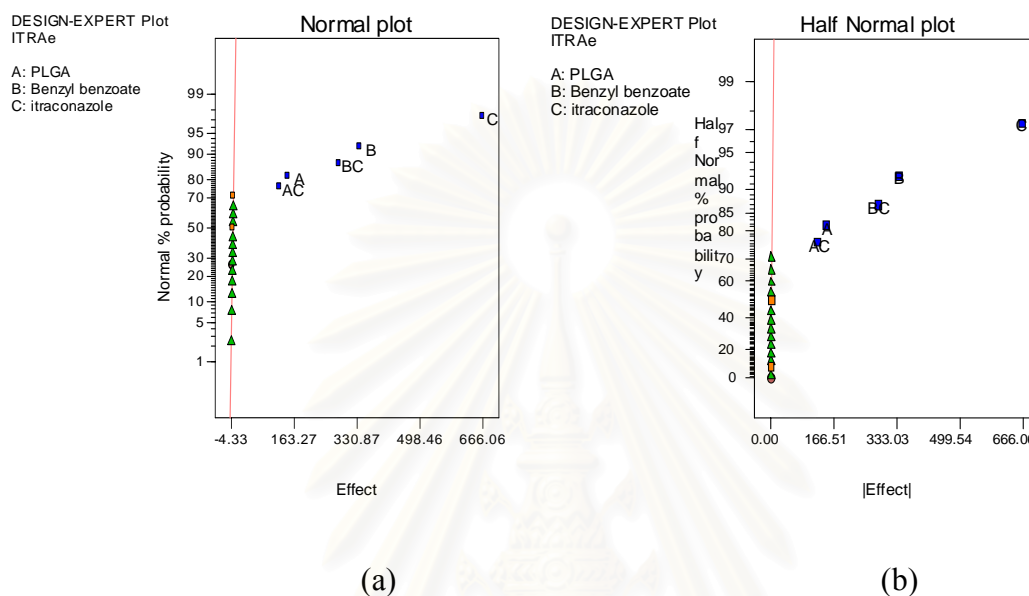
Table 41 shows Design-Expert output analyzing the amount of

itraconazole entrapped in nanoparticles (ITRAe) of itraconazole-loaded PLGA

nanoparticles in full model. The "model F-value"of 19369.93 implied the model was

significant.   Values of "Prob > F" less than 0.0500 indicated model terms were

significant.   In this case A, B, C, AC and BC were significant model terms. Model

reduction was used to improve this model.

Table 41 Design-Expert output analyzing the amount of itraconazole entrapped in

nanoparticles (ITRAe) data of itraconazole-loaded PLGA nanoparticles (full model).

Response: ITRAe

ANOVA for Selected Factorial Model
Analysis of Variance Table [Partial Sum of Squares]

Source	Sum of Squares	DF	Mean Square	F Value	Prob > F
Model	2.701E+006	7	3.858E+005	19369.93	< 0.0001
A	86312.56	1	86312.56	4333.24	< 0.0001
B	4.573E+005	1	4.573E+005	22958.34	< 0.0001
C	1.775E+006	1	1.775E+006	89088.63	< 0.0001
AB	0.12	1	0.12	5.976E-003	0.9397
AC	62305.15	1	62305.15	3127.97	< 0.0001
BC	3.203E+005	1	3.203E+005	16080.90	< 0.0001
ABC	9.09	1	9.09	0.46	0.5121
Curvature	2.052E+005	1	2.052E+005	10300.13	< 0.0001
Pure Error	239.02	12	19.92		
Cor Total	2.906E+006	20			

S.D.	4.46	R-Squared	0.9999
Mean	528.19	Adj R-Squared	0.9999
C.V.	0.84	Pred R-Squared	0.9998
PRESS	698.36	Adeq Precision	394.484

Factor	Coefficient Estimate	DF	Standard Error	95% CI Low	95% CI High	VIF
Intercept	472.93	1	1.12	470.50	475.36	
A-PLGA	73.45	1	1.12	71.02	75.88	1.00
B-Benzyl benzoate	169.06	1	1.12	166.63	171.49	1.00
C-itraconazole	333.03	1	1.12	330.60	335.46	1.00
AB	0.086	1	1.12	-2.34	2.52	1.00
AC	62.40	1	1.12	59.97	64.83	1.00
BC	141.49	1	1.12	139.06	143.92	1.00
ABC	0.75	1	1.12	-1.68	3.18	1.00
Center Point	232.07	1	2.29	227.09	237.05	1.00

Table 42 shows the analysis of variance summary for the reduced model which the non-significant AB and ABC interactions were removed. The error or residual sum of squares was composed of a pure error component arising from replicate runs and a lack-of-fit component corresponding to the AB and ABC interactions. The regression model in terms of both actual and coded variables was given, along with confidence interval on each model coefficient. The "model F-value" of 30463.73 implied the model was significant. In this case A, B, C, AC and BC were significant model terms. The "curvature F-value" of 11571.01 implied there was significant curvature.

Model adequate checking of itraconazole-loaded PLGA nanoparticles in factorial design study is shown in Figure 38, where the particle size was used as response variable. Figure 38(a) is the normal probability plot of the studentized residuals to check for normality of residuals. The normal probability plot did not reveal anything particularly troublesome. This plot resembled a straight line which indicated that the underlying error distribution is normal. Figure 38(b) shows the plot of studentized residuals versus predicted values to check for constant error. No unusual structure was apparent. Figure 38(c) is the plot of outlier t versus run order to look for outliers, i.e., influential values. All of standardize residuals (d_i) lie in the interval $-3 \leq d_i \leq 3$ conformed that there was no outlier in this study. Figure 38(d) shows Box-Cox plot for power transformations. The Box- Cox method showed that the tranformation parameter λ was equal to 1, this implied that the data did not need transformation. All the diagnostic plots in Figure 38(a), (b), (c) and (d) were in agree with the assumption of analysis of variance.

Table 42 Design-Expert output analyzing the amount of itraconazole entrapped in

nanoparticles (ITRAe) data of itraconazole-loaded PLGA nanoparticles (reduce

model).

Response:ITRAe

ANOVA for Selected Factorial Model
Analysis of Variance Table [Partial Sum of Squares]

Source	Sum of Squares	DF	Mean Square	F Value	Prob > F
Model	2.701E+006	5	5.402E+005	30463.73	< 0.0001
A	*86312.56*	*1*	*86312.56*	*4867.90*	*< 0.0001*
B	*4.573E+005*	*1*	*4.573E+005*	*25791.04*	*< 0.0001*
C	*1.775E+006*	*1*	*1.775E+006*	*1.001E+005*	*< 0.0001*
AC	*62305.15*	*1*	*62305.15*	*3513.91*	*< 0.0001*
BC	*3.203E+005*	*1*	*3.203E+005*	*18065.03*	*< 0.0001*
Curvature	2.052E+005	1	2.052E+005	11571.01	< 0.0001
Residual	248.23	14	17.73		
Lack of Fit	*9.21*	*2*	*4.60*	*0.23*	*0.7971*
Pure Error	*239.02*	*12*	*19.92*		
Cor Total	2.906E+006	20			

S.D.	4.21	R-Squared	0.9999
Mean	528.19	Adj R-Squared	0.9999
C.V.	0.80	Pred R-Squared	0.9998
PRESS	530.00	Adeq Precision	473.475

Factor	Coefficient Estimate	DF	Standard Error	95% CI Low	95% CI High	VIF
Intercept	472.93	1	1.05	470.67	475.19	
A-PLGA	73.45	1	1.05	71.19	75.71	1.00
B-Benzyl benzoate	169.06	1	1.05	166.80	171.32	1.00
C-itraconazole	333.03	1	1.05	330.77	335.29	1.00
AC	62.40	1	1.05	60.14	64.66	1.00
BC	141.49	1	1.05	139.23	143.75	1.00
Center Point	232.07	1	2.16	227.44	236.70	1.00

Table 42 Design-Expert output analyzing the amount of itraconazole entrapped in

nanoparticles (ITRAe) data of itraconazole-loaded PLGA nanoparticles (reduce

model) (continued).

Final Equation in Terms of Coded Factors:

ITRAe = + 472.93 + 73.45* A + 169.06* B + 333.03 * C + 62.40* A * C + 141.49* B * C

Final Equation in Terms of Actual Factors:

ITRAe = + 75.21747 - 0.10124 * PLGA - 1.04033 * Benzyl benzoate + 0.026178* itraconazole + 1.73340E-003 * PLGA * itraconazole + 0.023582 * Benzyl benzoate* itraconazole

Diagnostics Case Statistics

Standard Order	Actual Value	Predicted Value	Residual	Leverage	Student Residual	Cook's Distance	Outlier t	Run Order
1	98.28	101.29	-3.01	0.375	-0.903	0.070	-0.897	1
2	976.30	980.66	-4.36	0.375	-1.310	0.147	-1.347	7
3	983.34	980.66	2.68	0.375	0.805	0.056	0.794	8
4	628.87	631.26	-2.39	0.375	-0.718	0.044	-0.705	11
5	159.97	156.43	3.54	0.375	1.064	0.097	1.070	6
6	123.97	123.38	0.59	0.375	0.178	0.003	0.172	9
7	355.60	359.56	-3.96	0.375	-1.190	0.121	-1.209	4
8	154.22	156.43	-2.21	0.375	-0.663	0.038	-0.649	5
9	102.96	101.29	1.67	0.375	0.502	0.022	0.489	2
10	365.20	359.56	5.64	0.375	1.694	0.246	1.831	3
11	1256.80	1252.36	4.44	0.375	1.334	0.152	1.376	16
12	1249.60	1252.36	-2.76	0.375	-0.829	0.059	-0.819	15
13	176.40	178.52	-2.12	0.375	-0.636	0.035	-0.622	14
14	179.30	178.52	0.78	0.375	0.235	0.005	0.227	13
15	631.97	631.26	0.71	0.375	0.213	0.004	0.206	12
16	701.30	705.00	-3.70	0.200	-0.982	0.034	-0.981	17
17	712.60	705.00	7.60	0.200	2.018	0.145	2.309	18
18	706.20	705.00	1.20	0.200	0.319	0.004	0.308	21
19	699.30	705.00	-5.70	0.200	-1.513	0.082	-1.595	20
20	705.60	705.00	0.60	0.200	0.159	0.001	0.154	19
21	124.12	123.38	0.74	0.375	0.223	0.004	0.215	10

Note: Predicted values of center points include center point coefficient.

Figure 38 Model adequate checking of itraconazole-loaded PLGA nanoparticles in

factorial design study ; response: the amount of itraconazole entrapped in

nanoparticles (ITRAe).

(a) Normal probability plot of the studentized residuals

(b) Studentized residuals versus predicted values

(c) Outlier t versus run order

(d) Box-Cox plot
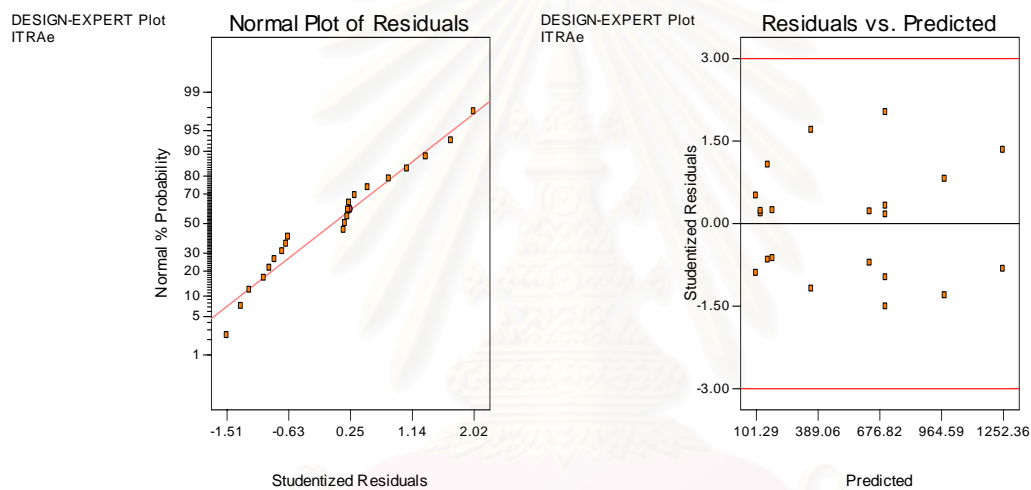
(a)

(b)
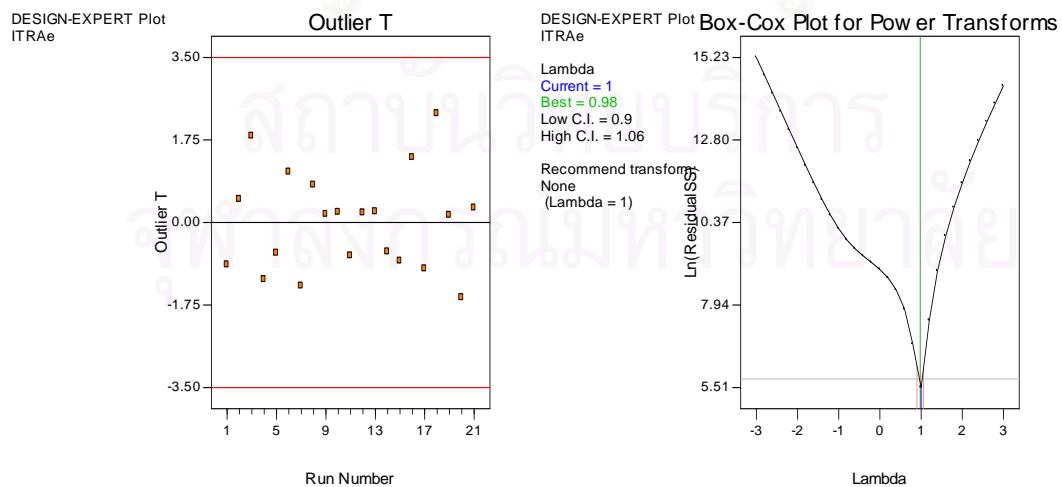
(c)

(d)

On the amount of itraconazole entrapped in the nanoparticles (ITRAe), the factor effect estimated (and the regression model) indicated that the amount of itraconazole entrapped in the nanoparticles (ITRAe) increased as the concentration of PLGA(A) increased and as the concentration of benzyl benzoate(B) increased , and as the concentration of itraconazole(C) increased. The Fisher F test with a very low probability value (P_{model} > F less than 0.0001) (Table 42) demonstrated a very high significance for the regression model. The value of the determination coefficient (R-Squared = 0.9999) was as high as the value of the adjusted determination coefficient (Adjusted R-Squared = 0.9999), which indicated a high significance of the model. A relatively low value of the coefficient of variation (C.V. = 0.80) indicated improved precision and reliability of the conducted experiments.

It is obvious that the concentration of PLGA, benzyl benzoate, and itraconazole also had significant effect on the amount of itraconazole entrapped in the nanoparticles (ITRAe). Figures 39(a), 39(b) and 39(c) show the increasing effect of PLGA, itraconazole and benzyl benzoate, respectively. The increasing effect shown with benzyl benzoate (P < 0.001) was due to itraconazole solubility in benzyl benzoate. The greater the concentration of benzyl benzoate in organic phase, the higher becomes itraconazole dissolved in benzyl benzoate. Since all three effects were positive, and if we considered only these main effects, we would run all three factors at the high level to maximize the amount of itraconazole entrapped in the nanoparticles (ITRAe). However, it was always necessary to examine any interactions that were important.

Figure 39 One factor plots of itraconazole-loaded PLGA nanoparticles in factorial design study; response: the amount of itraconazole entrapped in the nanoparticles (ITRAe).

(a)   PLGA

(b)   Benzyl benzoate
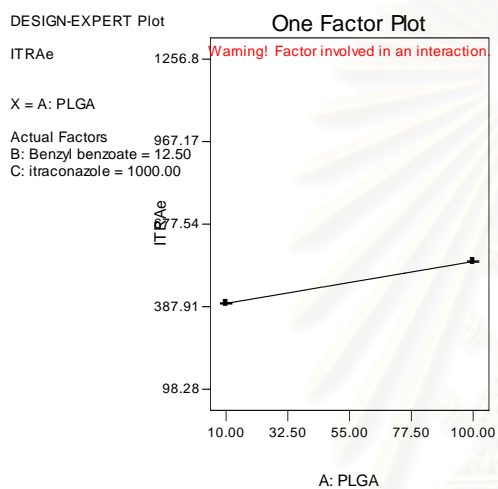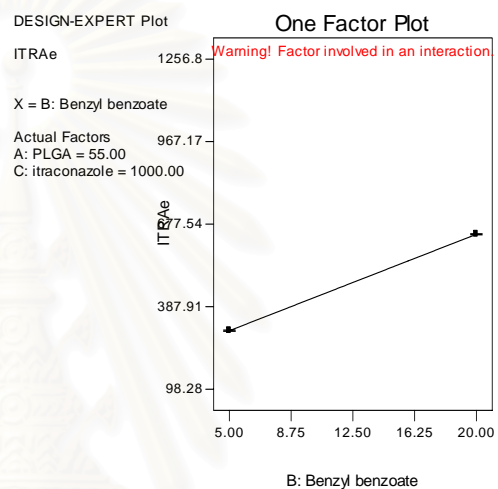
(c)   Itraconazole

(a)

(b)

(c)

A significant synergistic interaction between PLGA and itraconazole at P < 0.001 was observed. This interaction is reflected by the pattern of the lines of Figure 40(a), 41(a) and 42(a). The two-factor interaction graph, Figure 40(a) was helpful in the practical interpretation of the results. Inspection of the interaction graph indicated that changes in the concentration of PLGA produced a much larger change in the amount of itraconazole entrapped in nanoparticles (ITRAe) at the high concentration of itraconazole than at the low concentration of itraconazole. Figure 41 (a), and Figure 42(a) are a contour plot and response surface plot of the amount of itraconazole entrapped in nanoparticles (ITRAe) as a function of the concentration of PLGA and itraconazle. These plots were obtained from the fitted model. The effect of the strong interaction on this process was very clear since the response surface was a twisted plane.

A significant (P < 0.001) synergistic interaction was also observed between benzyl benzoate and itraconazole. This interaction is reflected by the pattern of the lines of Figure 40(b), 41(b) and 42(b). Inspection of the interaction graph Figure 40 (b) indicated that changes in the concentration of benzyl benzoate produced a much larger change in ITRAe at the high concentration of itraconazole than at the low concentration of itraconazole. Figure 41 (b), and Figure 42 (b) are a response surface plot and contour plot of the amount of itraconazole entrapped in nanopaticle (ITRAe) as a function of the concentration of benzyl benzoate and itraconazole. These plots were obtained from the fitted model. The effect of the strong interaction on this process was very clear since the response surface was a twisted plane.

Figure 40 Interaction plots of itraconazole-loaded PLGA nanoparticles in factorial design study; response: the amount of itraconazole entrapped in nanoparticles (ITRAe).　　　　(a) Interaction of PLGA and itraconazole

(b) Interaction of benzyl benzoate and itraconazole
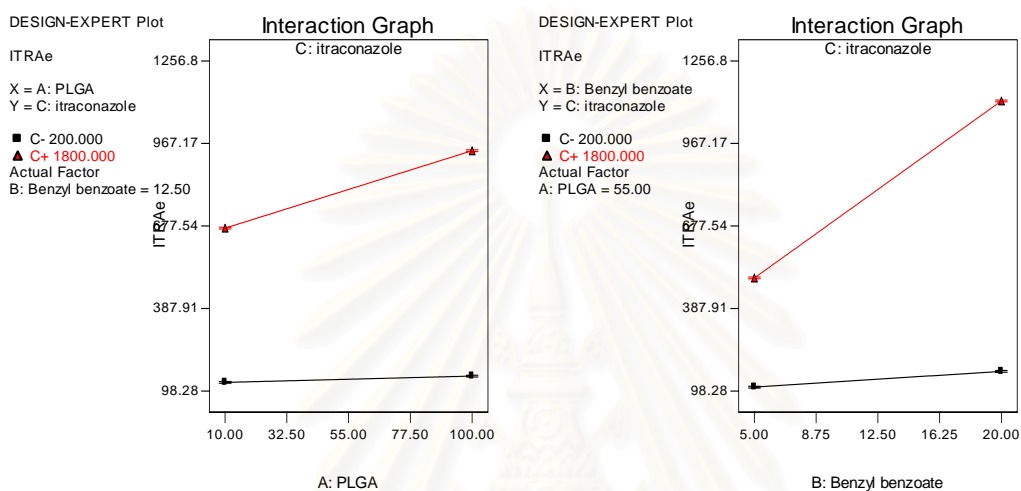
(a)　　　　(b)

Figure 41 Contour plots of itraconazole-loaded PLGA nanoparticles in factorial design study; response: the amount of itraconazole entrapped in nanoparticles (ITRAe).　　(a) Contour plot of PLGA and itraconazole

(b) Contour plot of benzyl benzoate and itraconazole

(a)　　　　(b)

Figure 42   Response surface plots of itraconazole-loaded PLGA nanoparticles in factorial design study ; response : the amount of itraconazole entrapped in nanoparticles (ITRAe).

(a) Response surface plot of PLGA and itraconazole

(b) Response surface plot of benzyl benzoate and itraconazole

(a)

(b)
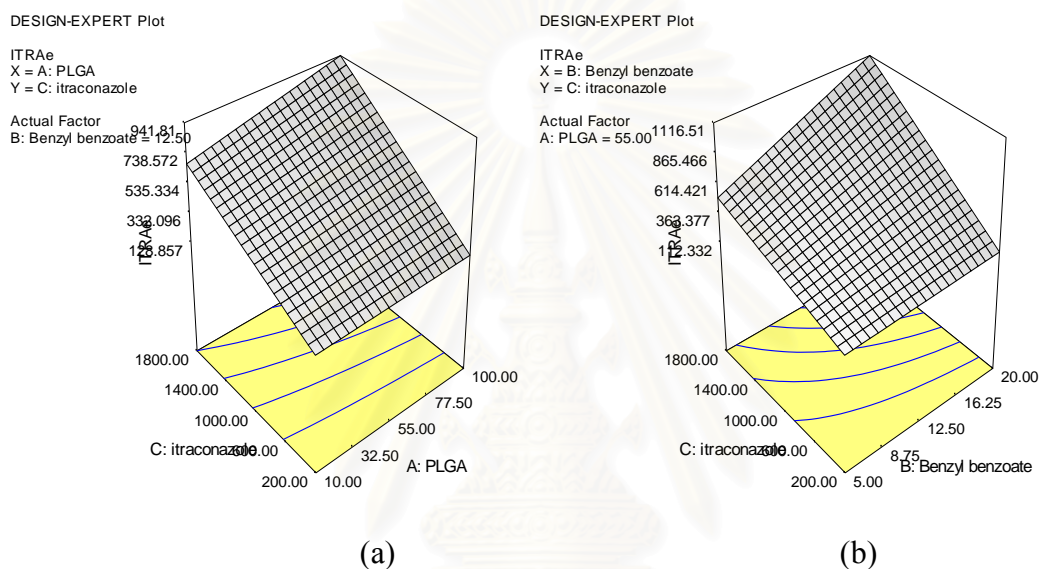
Influence of Preparation Factors on the Encapsulation Efficiency (ITRAe [%]) of Itraconazole-Loaded PLGA Nanoparticles

Table 43 presents the effect estimates and sums of squares for the 2^3 factorial design of PLGA nanoparticles, using the encapsulation efficiency (ITRAe [%]) as the response variable (data shown in Table App.C.10). Figure 46 shows normal probability plot and half normal probability plot of the factor effect for the 2^3 factorial design study, using the encapsulation efficiency (ITRAe [%]) as the response variable. The normal probability plot of these effects that lie along the line are neglible, whereas the large effects are far from the line. The important effects that emerge from this analysis were the main effects of A, B and C and AC and BC

interactions (Figure 43(a)). The important effects that emerge from the half-normal

plot were also the main effects of A, B and C and AC and BC interactions

(Figure 43(b)).

Table 43 Factor effect estimates and sums of squares for the 2^3 factorial design;

response: the encapsulation efficiency (ITRAe [%]).

Term Intercept	Effect Estimates	Sum of Square	% Contribution
A	13.0675	683.038	8.75299
B	31.0375	3853.31	49.3793
C	-25.175	2535.12	32.4871
AB	-0.2875	0.330625	0.00423689
AC	2.025	16.4025	0.210195
BC	3.465	48.0249	0.615429
ABC	0.38	0.5776	0.00740182
Curvature	12.8197	657.375	8.42413

Figure 43 Normal probability plot (a) and half normal probability plot (b) of the effect

for the 2^3 factorial design study ; response: the encapsulation efficiency (ITRAe [%]).

.

(a)   (b)
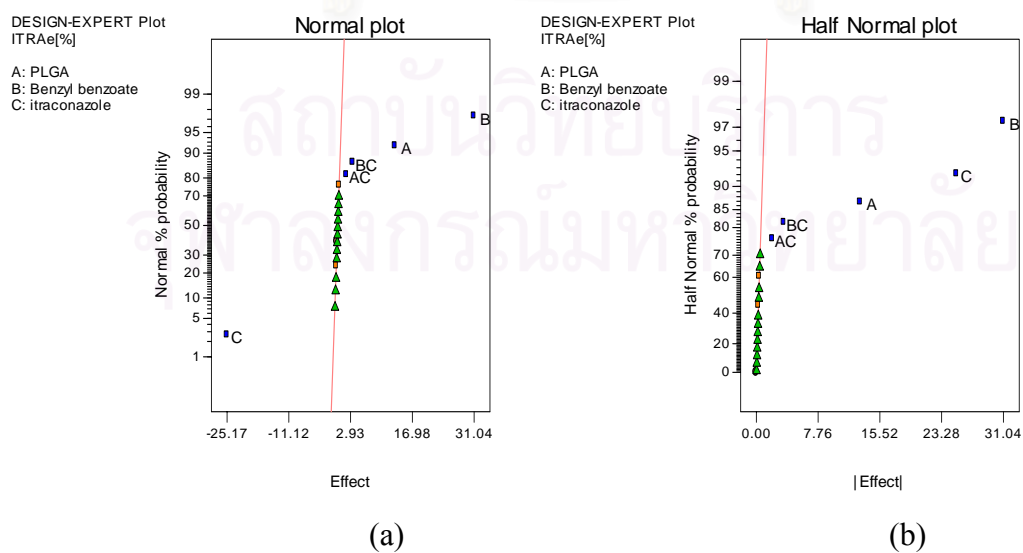
Table 44 shows Design-Expert output analyzing the encapsulation efficiency (ITRAe[%]) data of PLGA nanoparticles in full model, using the encapsulation efficiency (ITRAe [%]) as the response variable. The " model F-value" of 1314.44 implied the model was significant. Values of "Prob > F" less than 0.0500 indicated model terms were significant. In this case A, B, C, AC and BC were significant model terms. Model reduction was used to improve this model.

Table 44 Design-Expert output analyzing the encapsulation efficiency (ITRAe [%]) data of itraconazole-loaded PLGA nanoparticles (full model).

Response:ITRAe[%]
ANOVA for Selected Factorial Model
Analysis of Variance Table [Partial Sum of Squares]

Source	Sum of Squares	DF	Mean Square	F Value	Prob > F
Model	7136.80	7	1019.54	1314.44	< 0.0001
A	*683.04*	*1*	*683.04*	*880.60*	*< 0.0001*
B	*3853.31*	*1*	*3853.31*	*4967.84*	*< 0.0001*
C	*2535.12*	*1*	*2535.12*	*3268.38*	*< 0.0001*
AB	*0.33*	*1*	*0.33*	*0.43*	*0.5261*
AC	*16.40*	*1*	*16.40*	*21.15*	*0.0006*
BC	*48.02*	*1*	*48.02*	*61.92*	*< 0.0001*
ABC	*0.58*	*1*	*0.58*	*0.74*	*0.4051*
Curvature	657.38	1	657.38	847.52	< 0.0001
Pure Error	9.31	12	0.78		
Cor Total	7803.49	20			

S.D.	0.88	R-Squared		0.9987
Mean	60.49	Adj R-Squared		0.9979
C.V.	1.46	Pred R-Squared		0.9956
PRESS	34.65	Adeq Precision		119.502

Table 44 Design-Expert output analyzing the encapsulation efficiency (ITRAe [%])

data of itraconazole-loaded PLGA nanoparticles (full model) (continued).

Factor	Coefficient Estimate	DF	Standard Error	95% CI Low	95% CI High	VIF
Intercept	57.36	1	0.22	56.88	57.84	
A-PLGA	6.53	1	0.22	6.05	7.01	1.00
B-Benzyl benzoate	15.52	1	0.22	15.04	16.00	1.00
C-itraconazole	-12.59	1	0.22	-13.07	-12.11	1.00
AB	-0.14	1	0.22	-0.62	0.34	1.00
AC	1.01	1	0.22	0.53	1.49	1.00
BC	1.73	1	0.22	1.25	2.21	1.00
ABC	0.19	1	0.22	-0.29	0.67	1.00
Center Point	13.14	1	0.45	12.15	14.12	1.00

Table 45 shows the analysis of variance summary for the reduced model, that is, the model with the non-significant AB and ABC interactions were removed. The error or residual sum of squares was composed of a pure error component arising from replicate runs and a lack-of-fit component corresponding to the AB and ABC interactions. The regression model in terms of both actual and coded variables was given, along with confidence interval on each model coefficient. The "Model F-value" of 1955.80 implied the model was significant. Values of "Prob > F" less than 0.0500 indicated model terms were significant. In this case A, B, C, AC and BC were significant model terms. The "curvature F-value" of 900.86 implied there was significant curvature in the design space.

Model adequate checking of PLGA nanoparticles in factorial design study is shown in Figure 44, where the encapsulation efficiency (ITRAe [%]) was used as response variable. Figure 44(a) is the normal probability plot of the studentized residuals to check for normality of residuals. The normal probability plot did not reveal anything particularly troublesome. This plot resembled a straight line which indicated that the underlying error distribution is normal. Figure 44(b) shows the plot of studentized residuals versus predicted values to check for constant error. No unusual structure was apparent. Figure 44(c) is the plot of outlier t versus run order to look for outliers, i.e., influential values. There was one outlier data that |Outlier T| > 3.50 but the others (d_i) laid in the interval $-3 \leq d_i \leq 3$. Figure 44(d) shows Box-Cox plot for power transformations. The Box- Cox method showed that the tranformation parameter λ was equal to 1, this implied that the data did not need transformation. All the diagnostic plots in Figure 44(a), (b), (c) and (d) were in agree with the assumption of analysis of variance.

Figure 44 Model adequate checking of itraconazole-loaded PLGA nanoparticles in factorial design study ; response: the encapsulation efficiency (ITRAe [%]).

(a) Normal probability plot of the studentized residuals

(b) Studentized residuals versus predicted values

(c) Outlier t versus run order

(d) Box-Cox plot
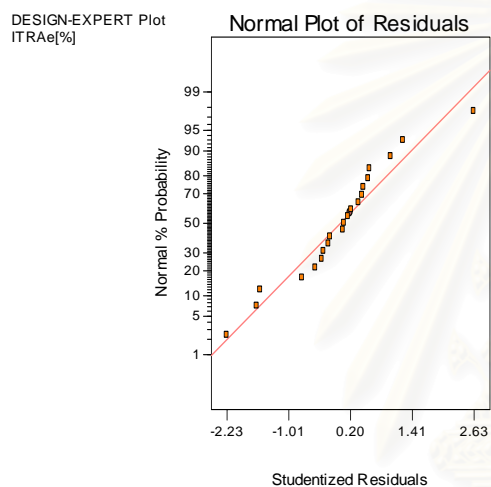
(a)
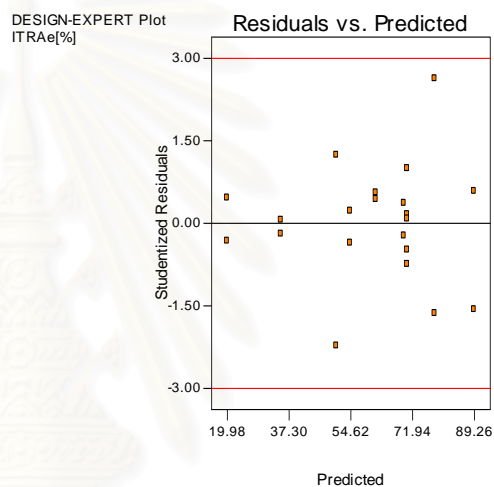
(b)
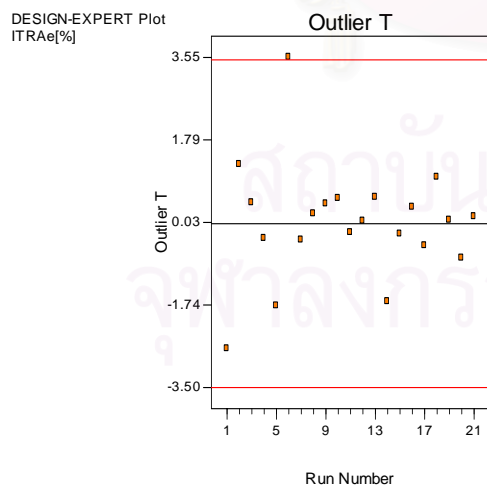
(c)
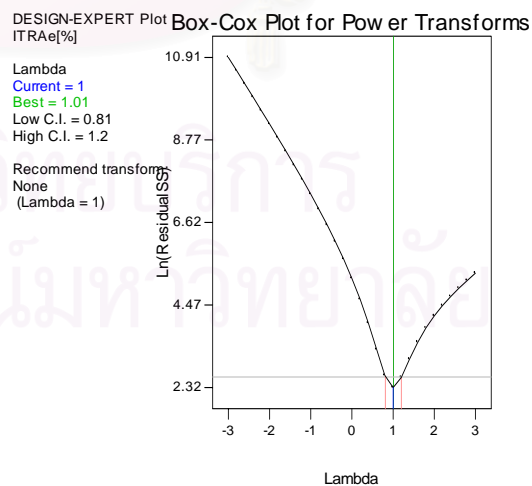
(d)

Table 45 Design-Expert output analyzing the encapsulation efficiency (ITRAe [%])

data of itraconazole-loaded PLGA nanoparticles (reduce model).

Response:ITRAe[%]
  ANOVA for Selected Factorial Model
  Analysis of Variance Table [Partial Sum of Squares]

Source	Sum of Squares	DF	Mean Square	F Value	Prob > F
Model	7135.89	5	1427.18	1955.80	< 0.0001
A	683.04	1	683.04	936.03	< 0.0001
B	3853.31	1	3853.31	5280.55	< 0.0001
C	2535.12	1	2535.12	3474.12	< 0.0001
AC	16.40	1	16.40	22.48	0.0003
BC	48.02	1	48.02	65.81	< 0.0001
Curvature	657.38	1	657.38	900.86	< 0.0001
Residual	10.22	14	0.73		
Lack of Fit	0.91	2	0.45	0.59	0.5720
Pure Error	9.31	12	0.78		
Cor Total	7803.49	20			

S.D.	0.85	R-Squared		0.9986
Mean	60.49	Adj R-Squared		0.9981
C.V.	1.41	Pred R-Squared		0.9968
PRESS	25.10	Adeq Precision		140.473

Factor	Coefficient Estimate	DF	Standard Error	95% CI Low	95% CI High	VIF
Intercept	57.36	1	0.21	56.91	57.82	
A-PLGA	6.53	1	0.21	6.08	6.99	1.00
B-Benzyl benzoate	15.52	1	0.21	15.06	15.98	1.00
C-itraconazole	-12.59	1	0.21	-13.05	-12.13	1.00
AC	1.01	1	0.21	0.55	1.47	1.00
BC	1.73	1	0.21	1.27	2.19	1.00
Center Point	13.14	1	0.44	12.20	14.07	1.00

  Final Equation in Terms of Coded Factors:

ITRAe[%] = + 57.36 + 6.53 * A + 15.52 * B - 12.59 * C + 1.01 * A * C
            + 1.73 * B * C

Table 45 Design-Expert output analyzing the encapsulation efficiency (ITRAe [%])

data of itraconazole-loaded PLGA nanoparticles (reduce model) (continued).

Final Equation in Terms of Actual Factors:

ITRAe[%] = + 44.40410 + 0.11707* PLGA + 1.78042 * Benzyl benzoate - 0.020891 * itraconazole + 2.81250E-005 * PLGA * itraconazole + 2.88750E-004 * Benzyl benzoate * itraconazole

Diagnostics Case Statistics

Standard Order	Actual Value	Predicted Value	Residual	Leverage	Student Residual	Cook's Distance	Outlier t	Run Order
1	49.14	50.64	-1.50	0.375	-2.227	0.425	-2.670	1
2	54.24	54.48	-0.24	0.375	-0.357	0.011	-0.346	7
3	54.63	54.48	0.15	0.375	0.220	0.004	0.213	8
4	34.94	35.07	-0.13	0.375	0.194	0.003	-0.188	11
5	79.99	78.22	1.77	0.375	2.626	0.591	3.554 *	6
6	61.98	61.69	0.29	0.375	0.435	0.016	0.422	9
7	19.76	19.98	-0.22	0.375	-0.324	0.009	-0.313	4
8	77.11	78.22	-1.11	0.375	-1.638	0.230	-1.756	5
9	51.48	50.64	0.84	0.375	1.238	0.131	1.264	2
10	20.29	19.98	0.31	0.375	0.461	0.018	0.448	3
11	69.82	69.57	0.25	0.375	0.365	0.011	0.353	16
12	69.42	69.57	-0.15	0.375	-0.228	0.004	-0.220	15
13	88.20	89.26	-1.06	0.375	-1.568	0.211	-1.664	14
14	89.65	89.26	0.39	0.375	0.579	0.029	0.565	13
15	35.11	35.07	0.039	0.375	0.057	0.000	0.055	12
16	70.13	70.50	-0.37	0.200	-0.484	0.00	-0.471	17
17	71.26	70.50	0.76	0.200	0.995	0.035	0.994	18
18	70.62	70.50	0.12	0.200	0.157	0.001	0.151	21
19	69.93	70.50	-0.57	0.200	-0.746	0.020	-0.734	20
20	70.56	70.50	0.060	0.200	0.079	0.00	0.076	19
21	62.06	61.69	0.37	0.375	0.553	0.026	0.539	10

Note: Predicted values of center points include center point coefficient.

* Case(s) with |Outlier T| > 3.50

On the encapsulation efficiency (ITRAe [%]), the factor effect estimated (and the regression model) indicated that the encapsulation efficiency (ITRAe [%]) increased as the concentration of PLGA (A) increased and as the concentration of benzyl benzoate (B) increased, but ITRA [%] decreased as the concentration of itraconazole (C) increased. The Fisher F test with a very low probability value ($P_{model} > F$ less than 0.0001) (Table 45) demonstrated a very high significance for the regression model. The value of the determination coefficient (R-Squared = 0.9986) was as high as the value of the adjusted determination coefficient (Adjusted R-Squared = 0.9981), which indicated a high significance of the model. A relatively low value of the coefficient of variation (C.V. = 1.41) indicated improved precision and reliability of the conducted experiments.

It is obvious that the concentration of PLGA, benzyl benzoate, and itraconazole also had significant effect on the encapsulation efficiency (ITRAe [%]). Figures 45(a) and 45(b) show the increasing effect of PLGA and benzyl benzoate, respectively. Figure 45(c) shows the deceasing effect of itraconazole. The increasing effect shown with benzyl benzoate ($P < 0.0001$) was due to itraconazole solubility in benzyl benzoate. The greater the concentration of benzyl benzoate in organic phase, the higher becomes itraconazole dissolved in benzyl benzoate. The decreasing effect of itraconazole on the encapsulation efficiency (ITRAe [%]) due to the increasing of itraconazole in the formulas although the amount of itraconazole entrapped in nanoparticle (ITRA) increased.

Figure 45 One factor plots of itraconazole-loaded PLGA nanoparticles in factorial design study; response: the encapsulation efficiency (ITRAe [%]).
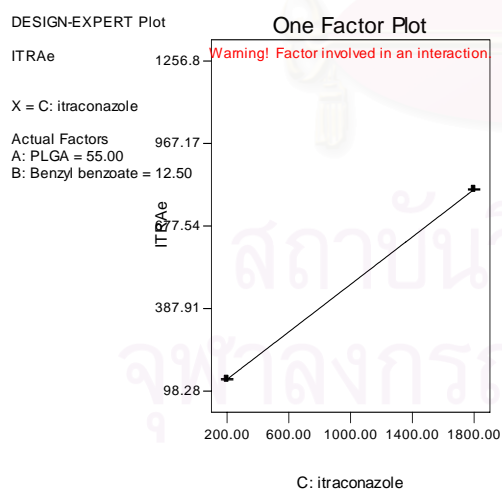
(a)   PLGA

(b)   Benzyl benzoate
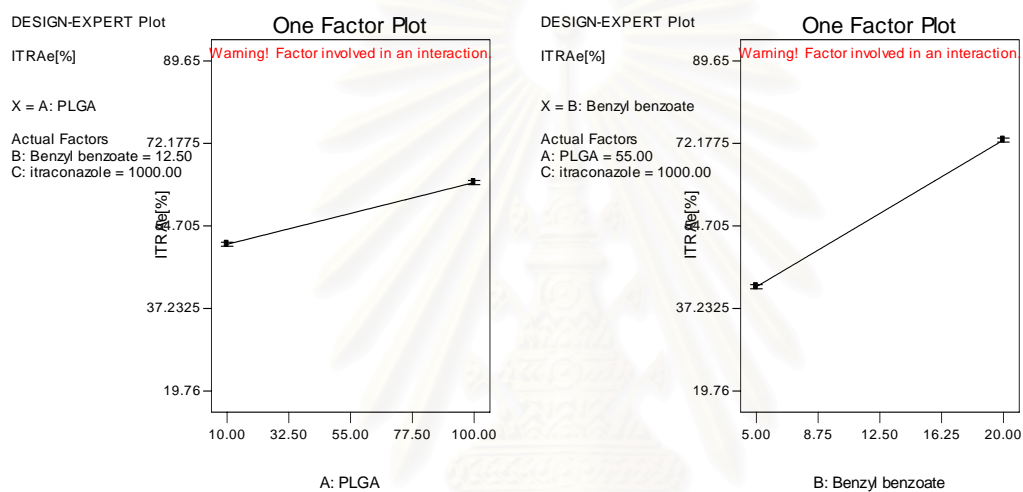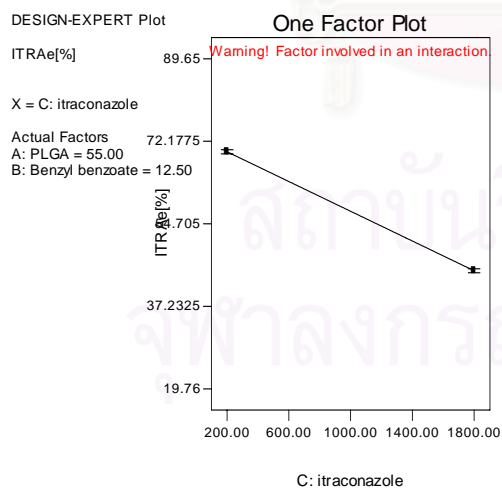
(c)   Itraconazole

(a)

(b)

(c)

A significant synergistic interaction between PLGA and itraconazole at P < 0.001 was observed. This interaction is reflected by the pattern of the lines of Figure 46(a), 47(a) and 48(a). Inspection of the interaction graph (Figure 46 (a)) indicated that changes in the concentration of PLGA produced a much larger change in ITRAe [%] at the low concentration of itraconazole than at the high concentration of itraconazole. Figure 47 (a), and Figure 48(a) are a response surface plot and contour plot of the encapsulation efficiency (ITRAe [%]) as a function of the concentration of PLGA and itraconazole. These plots were obtained from the fitted model. The effect of the strong interaction on this process was very clear because the response surface was a twisted plane (that was the lines in the contour plot were not parallel straight lines).

A significant (P < 0.0001) synergistic interaction also was observed between benzyl benzoate and itraconazole. This interaction is reflected by the pattern of the lines of Figure 46(b), 47(b) and 48 (b). Inspection of the interaction graph (Figure 46 (b)) indicated that changes in the concentration of benzyl benzoate produced a much larger change in ITRAe[%] at the low concentration of itraconazole than at the high concentration of itraconazole. Figure 47(b) and Figure 48(b) are a contour surface plot and response plot of the encapsulation efficiency (ITRAe [%]) as a function of the concentration of benzyl benzoate and itraconazole. These plots were obtained from the fitted model. The effect of the strong interaction on this process was very clear due to the response surface was a twisted plane (that was the lines in the contour plot were not parallel straight lines). Thus the interaction term in the model was a form of curvature.

Figure 46 Interaction plots of itraconazole-loaded PLGA nanoparticles in factorial design study ; response: the encapsulation efficiency (ITRAe[%]) .

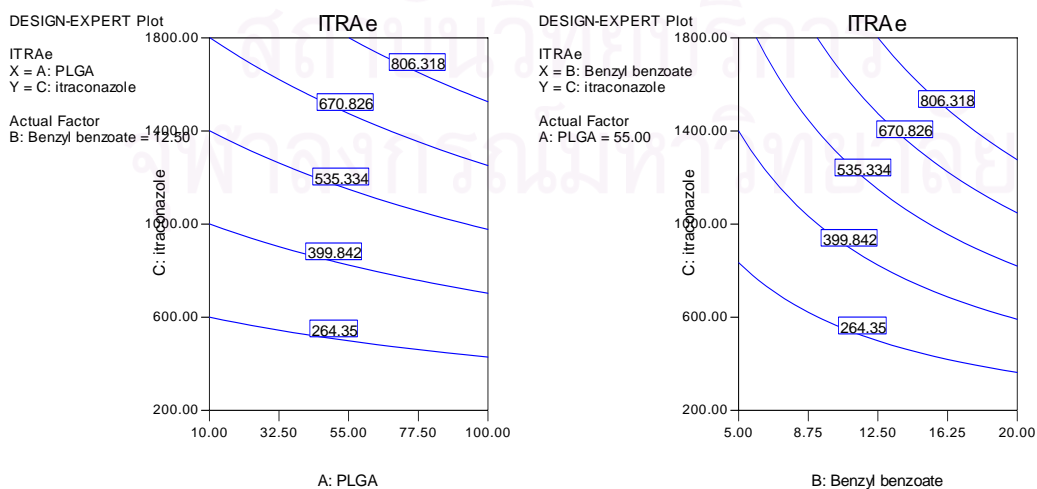(a) Interaction of PLGA and itraconazole

(b) Interaction of benzyl benzoate and itraconazole
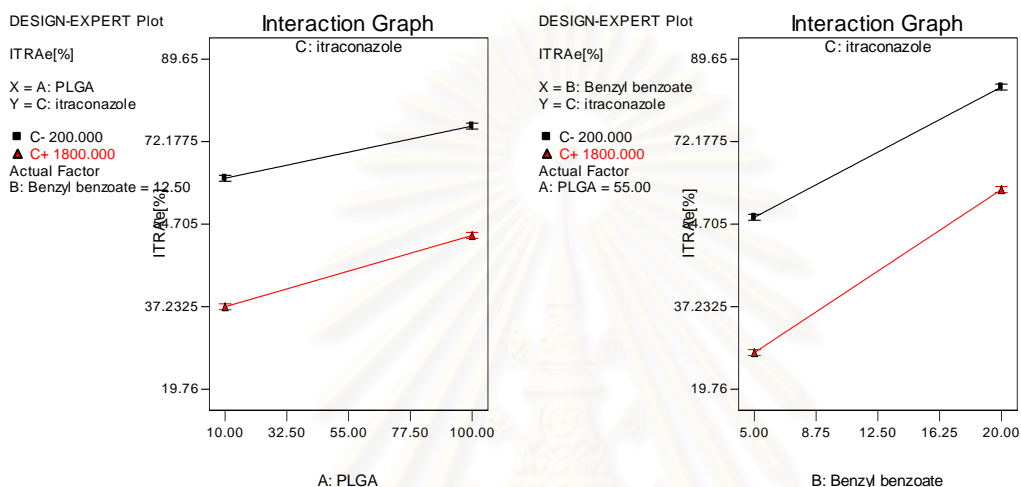
(a)

(b)

Figure 47 Contour plots of itraconazole-loaded PLGA nanoparticles in factorial design study ; response: the encapsulation efficiency (ITRAe [%]).

(a) Contour plot of PLGA and itraconazole

(b) Contour plot of benzyl benzoate and itraconazole
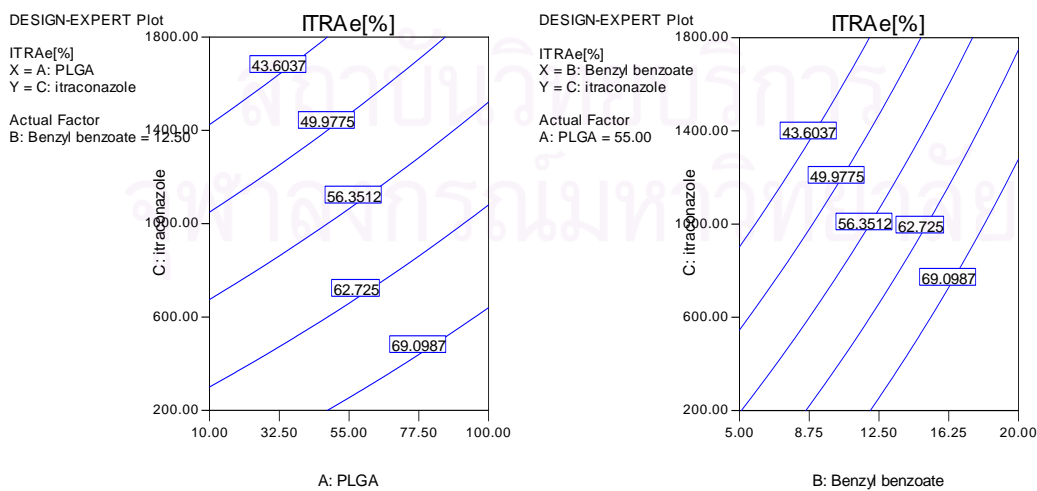
(a)

(b)

Figure 48 Response surface plots of itraconazole-loaded PLGA nanoparticles in factorial design study ; response: the encapsulation efficiency (ITRAe [%]).

  (a) Response surface plot of PLGA and itraconazole

  (b) Response surface plot of benzyl benzoate and itraconazole

(a)   (b)
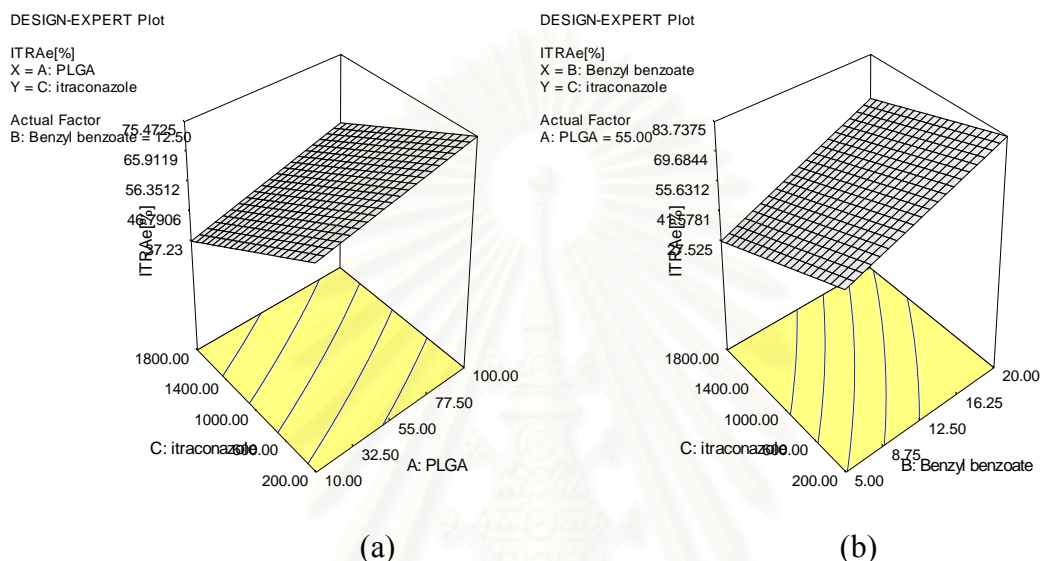
2.2.4 Multiple Response Optimization

(a) Overlay the Contour Plots for Each Response

Figure 49(a) shows an overlay plot for 3 responses; $300 \leq$ the particle size ≤ 400, $0.452 \leq$ PI ≤ 0.632, $450 \leq$ ITRAe ≤ 550, and $60 \leq$ ITRAe [%] ≤ 70. The boundary shown in Figure 49(a) indicates that there are a number of combinations of concentration of PLGA, benzyl benzoate, and itraconazole that will result in a satisfactory process. Figure 49 (b) shows an overlay plot for the 3 responses: $200 \leq$ the particle size ≤ 300, $0.452 \leq$ PI ≤ 0.632, $450 \leq$ ITRAe ≤ 550, and $60 \leq$ ITRAe [%] ≤ 70. Figure 49(b) shows that there is no boundary that must be met by the process. The particle size was a limiting step of producing itraconazol-loaded PLGA nanoparticles.

(b) Constrained Optimization and Simultaneous

Optimization Technique

Table 46 shows constrained optimization of several response data of itraconazole-loaded PLGA nanoparticles. Using the desirability approach, the target of ITRAe was chosen to be 500μg/mL, while the lower limit was equal to 450 μg/mL, and the upper limit was 550 μg/mL. The particle was set equal at a minimum between 300 and 400 nm. The polydispersity index was set in the range from 0.452 to 0.632. Finally, the ITRAe (%) ranged from 60% to 70%. Three solutions were found. The solution having the highest overall desirability ($D = 0.769$) was composed of 10 mg/mL of PLGA, 16.94 μg/mL of benzyl benzoate, and 1001.01 μg/mL of itraconazole. The desirability function response surface and contour plot of the solution having the highest overall desirability is shown in Figures 50 (a) and 50 (b), respectively.

Table 46 Constrainted optimization of several response data of itraconazole-loaded PLGA nanoparticles.

Constraints

Name	Goal	Lower Limit	Upper Limit	Lower Weight	Upper Weigh	Importance
PLGA	is in range	10	100	1	1	3
Benzyl benzoate	is in range	5	20	1	1	3
itraconazole	is in range	200	1800	1	1	3
ITRAe[%]	is in range	60	70	1	1	3
ITRAe	is target = 500	450	550	1	1	3
size	minimize	300	400	1	1	3
PI	is in range	0.452	0.632	1	1	3

Solutions

Number	A	B	C	ITRAe[%]	ITRAe	size	PI	Desirability
1	10.00	16.94	1001.00	60.0001	500	340.915	0.530296	0.769
2	12.80	16.74	1000.78	60.0001	499.999	343.373	0.53201	0.753
3	10.00	19.14	900.51	66.0772	499.999	350.23	0.52683	0.705

Figure 49   Region of the optimum found by overlay the particle size, the polydispersity index (PI), the amount of itraconazole entrapped in nanoparticles (ITRAe), and the encapsulation efficiency (ITRAe [%]) of itraconazole-loaded PLGA nanoparticles.

(a) $300 \leq$ the particle size ≤ 400, $0.452 \leq PI \leq 0.632$, $450 \leq ITRAe \leq 550$, and $60 \leq ITRAe$ [%] ≤ 70

(b) $200 \leq$ the particle size ≤ 300, $0.452 \leq PI \leq 0.632$, $450 \leq ITRAe \leq 550$, and $60 \leq ITRAe$ [%] ≤ 70
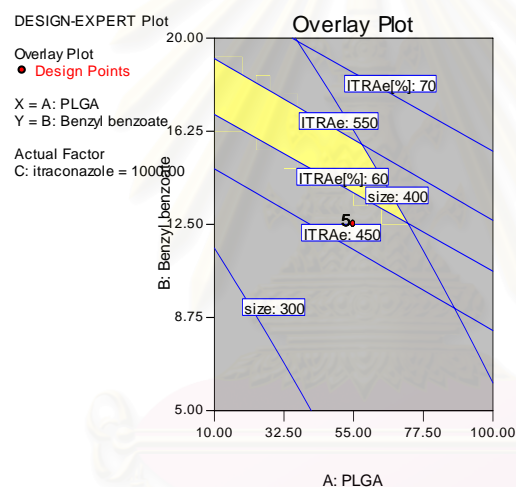
(a)
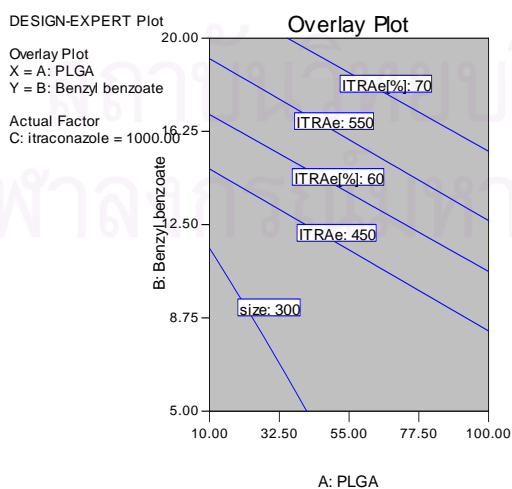
(b)

Figure 50 Desirability function response surface and contour plot for itraconazole-

loaded PLGA nanoparticles.
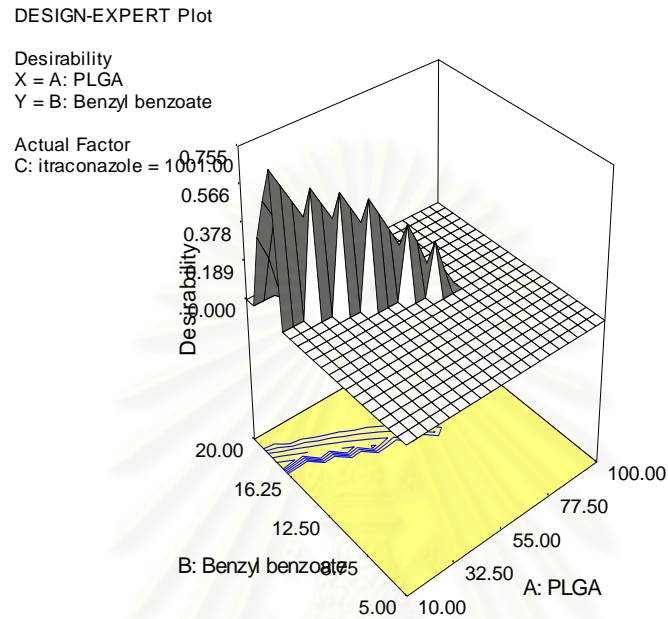
(a) Response surface
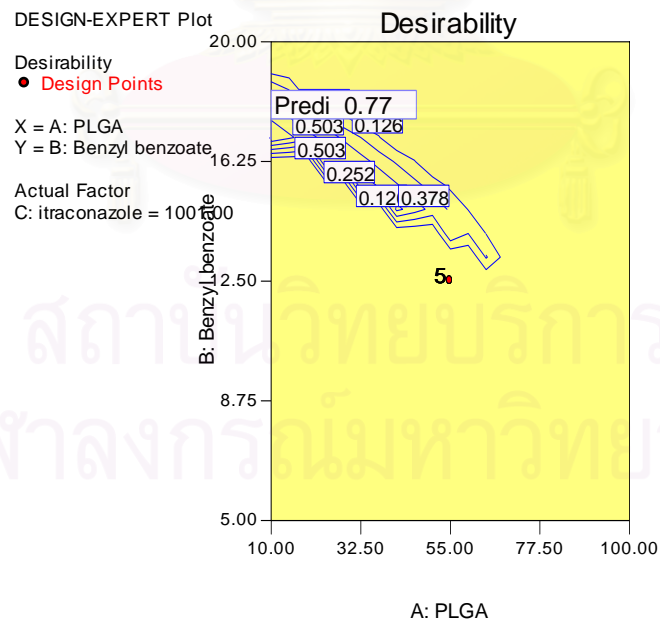
(b) Contour plot

(c) Model and Optimization Verification

Verification of the predicted value was made by using itraconazole- loaded PLGA nanoparticles prepared using the formulas in section 2.3.4. The particle size, amount of itraconazole entrapped in nanoparticles, and encapsulation efficiency are in the 95% prediction interval (Table 47 and 48). These results therefore corroborate the predicted values, and the effectiveness of the model.

Table 47 Observed particle sizes (nm) and predicted values of itraconazole-loaded PLGA nanoparticles.

Formula	Observed response	Predicted value	P-value
1	424.51	425.84	<0.05
2	305.03	307.21	<0.05
3	289.63	288.93	<0.05
4	336.87	340.91	<0.05

Table 48 Observed encapsulation efficiency and predicted values of itraconazole-loaded PLGA nanoparticles.

Formula	ITRAe (µg/mL)		
	Observed response	Predicted value	P-value
1	650.62	641.99	<0.05
2	408.91	399.48	<0.05
3	151.36	150.95	<0.05
4	506.58	499.99	<0.05

3 Characterization of nanoparticles

3.1 Itraconazole-Loaded PIBCA Nanoparticles

The mean particle size of all preparations of itraconazole-loaded PIBCA nanoparticles ranged from 140.6 to 199.6 nm with polydispersity of 0.044 to 0.099. The particle size distribution was monomodal distribution with narrow size distribution (Appendix B) which indicated that nanoparticles prepared by interfacial polymerization had narrow size distribution. Particles were spherical with a smooth surface when view by SEM after freeze fracture. (Figure51). The encapsulation efficiency of itraconazole in PIBCA nanoparticles was ranging from 15.68 % to 81.75% up to component of the preparation.

3.2 Itraconazole-Loaded PLGA Nanoparticles

The mean particle size of all preparations of itraconazole-loaded PLGA nanoparticles ranged from 190.0 to 643.9 nm with polydispersity of 0.452 to 0.628. The particle size distribution was multimodal distribution with wide size distribution (Appendix C) which indicated that itraconazole-loaded PLGA nanoparticles prepared by solvent displacement technique had wide size distribution. Particles were spherical with a smooth surface when view by SEM (Figure 52). The encapsulation efficiency of itraconazole in PLGA nanoparticles was ranging from 19.76 % to 89.65% up to component of the preparation.

Figure 51 Scanning electron micrograph of itraconazole-loaded PIBCA nanoparticles preparing from IBCA 8.09 µL/mL, benzyl benzoate 10.19 µg/mL, and itraconazole 1200.77 µg/mL (15 kv X 10000).
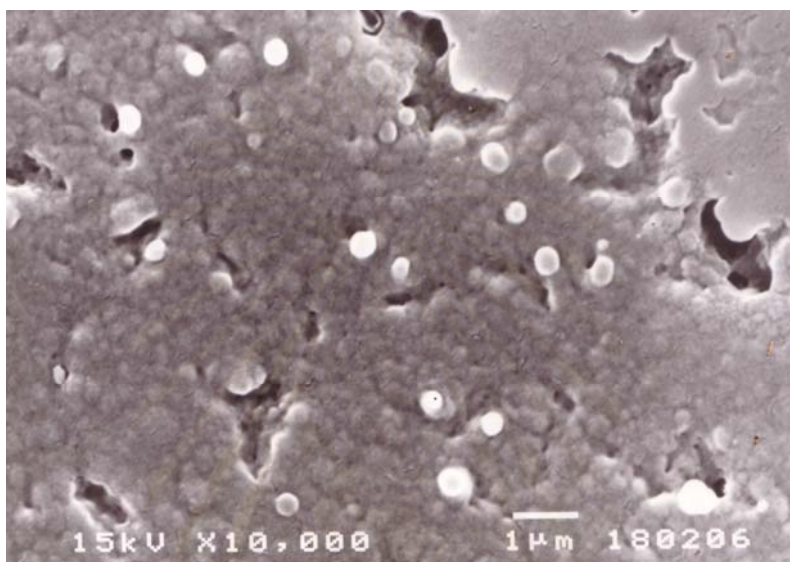
Figure 52 Scanning electron micrograph of itraconazole-loaded PLGA nanoparticles preparing from PLGA 10.00mg/mL, benzyl benzoate 16.94 µg/mL and itraconazole 1001.01 µg/mL (15 kv X 10000).
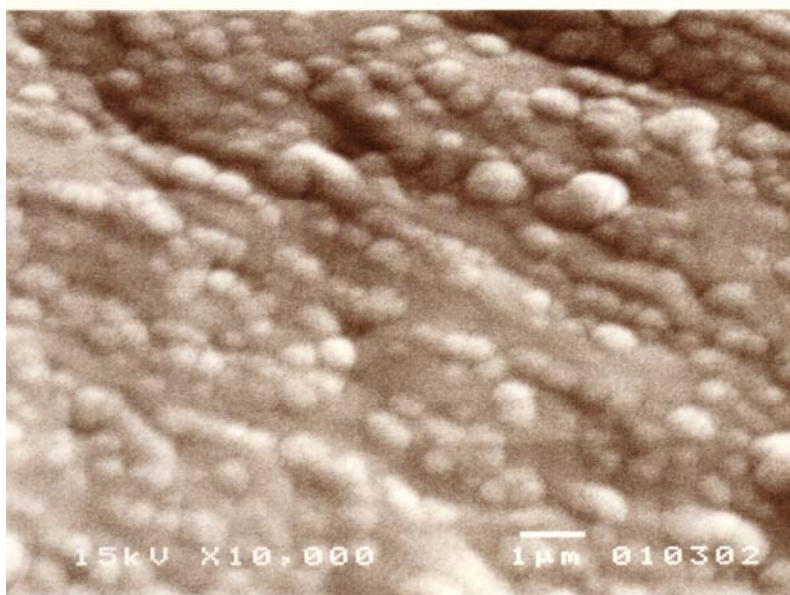
4 High-Performance Liquid Chromatographic Technique for Drug Analysis

Itraconazole was analyzed by reverse phase HPLC and the design chromatographic condition was previously mentioned. Analysis method validation parameters of itraconazole are summarized in Table 49 (The details shown in Appendix D). The results of analytical method validation parameters for itraconazole were accepted which can be determined with acceptable accuracy, precision and linearity.

Table 49 Analysis method validation parameters of HPLC for itraconazole

Parameter	Result value	Limit of acceptability
1. Specificity	No other peak interfere major peak	No other peak interfere major peak [a]
2. Accuracy		
- recovery % (S.D.)	100.24% (1.002)	80-110% [b]
3. Precision		
- RS.D.(%)	1.0	≤ 2 [b]
4. Linearity	0.99992	>0.999 [b]
- the determination coefficient(r^2)		

[a] USP XXIV

[b] Jenke, 1996

5 In Vitro Release Study

The release of itraconazole from itraconazole-loaded PIBCA nanoparticles and itraconazole-loaded PLGA (prepared using PLGA different ratio [85:15, 75:25, 65:35 and 50:50]) are shown in Table 50 and Figure 53. It was found that itraconazole was released in a biphasic manner, characterized by an initial and variable rapid release period followed by a slower release thereafter. The initial burst effect of itraconazole-loaded PIBCA nanoparticle was seen over the first hour, followed by a slower release up to 24 h. The first phase corresponds to the release of the itraconazole located on the surface of the nanoparticles and therefore available for immediate release. PLGA displayed the slower release pattern. The itraconazole-loaded PLGA nanoparticles prepared from the ratio 85:15 showed the slowest release pattern with 30.59 % of the drug remaining in the particles after 168 h (Table 50). In vitro release studies also showed that the release of itraconazole from PLGA nanoparticles was related to the ratio of polylactide/ polyglycolide. In all cases, an initial rapid rate of itraconazole release was observed followed by a period of slow release as shown in Figure 53. The release profiles also showed that the higher ratio of polylactide in PLGA reduced the amount of itraconazole associated with the initial burst release. A closer examination of the release profile during the first hour of the burst phase is shown in Figure 54. The initial release was found to be greatly affected by the type of polymer used. A similar biphasic release pattern has also been reported for PIBCA nanoparticles (Illum et al, 1986; Valero et al., 1996; McCarron et al., 2000) and PLGA nanoparticles (Alejandro et al., 1993; McCarron et al., 2000; Yoo et al., 2000).

Table 50 Percent of itraconazole released from nanoparticles.

Time (h)	Cumulative percentage of itraconazole released				
	PIBCA	PLGA			
		50:50	65:35	75:25	85:15
0.25	20.24	18.75	16.30	16.02	13.04
0.5	35.21	32.56	25.14	24.14	21.10
0.75	44.36	37.25	30.45	28.45	24.98
1	50.13	40.23	34.58	31.25	28.57
2	52.25	47.02	39.59	36.42	32.98
4	56.38	54.68	46.25	43.74	38.51
6	60.98	58.69	48.41	46.95	41.33
12	74.56	65.12	53.65	52.10	45.86
24	99.98	71.26	61.97	57.01	50.18
48	-	82.67	71.89	66.14	58.22
72	-	87.34	75.95	69.87	61.51
96	-	90.42	78.63	72.34	63.68
120	-	92.67	80.58	74.14	65.26
144	-	95.63	83.16	76.50	67.35
168	-	98.56	85.70	78.85	69.41

Attempts had been made to model the release rate of drug from simple monolithic device with spherical geometry to a square-root (Guy et al., 1982) function of time. As the majority of drug was release during the burst phase, the release data over the first hour was fitted to the Higuchi's square root of time model and the goodness of fit estimated from the regression coefficient. Figure 55 shows Higuchi's square root of time plots of itraconazole from itraconazole-loaded PIBCA nanoparticles and itraconazole-loaded PLGA nanoparticles.

Figure 53 Release profiles of itraconazole-loaded PIBCA nanoparticles and itraconazole-loaded PLGA nanoparticles. Values represent means ±S.D., n = 6.
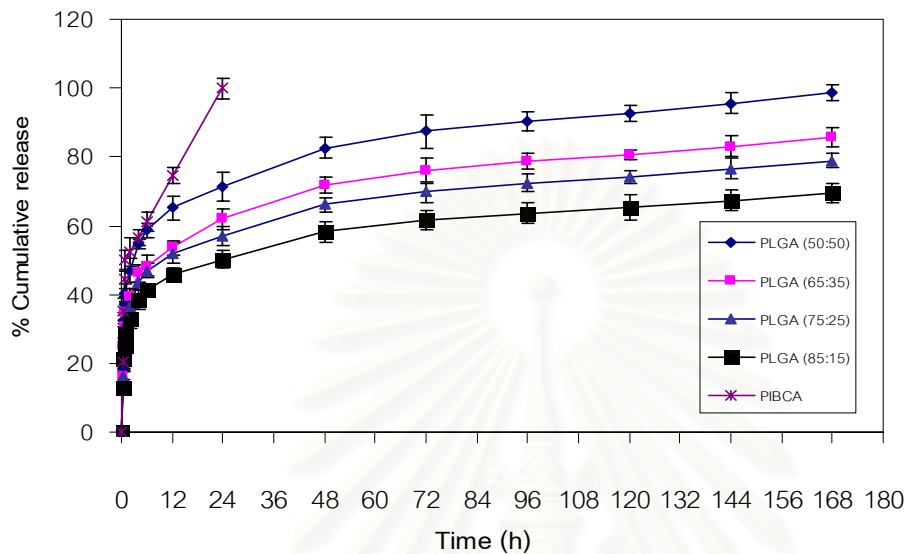
Figure 54 Release profiles of itraconazole-loaded PIBCA nanoparticles and itraconazole-loaded PLGA nanoparticles during the first hour. Values represent means ±S.D., n = 6.
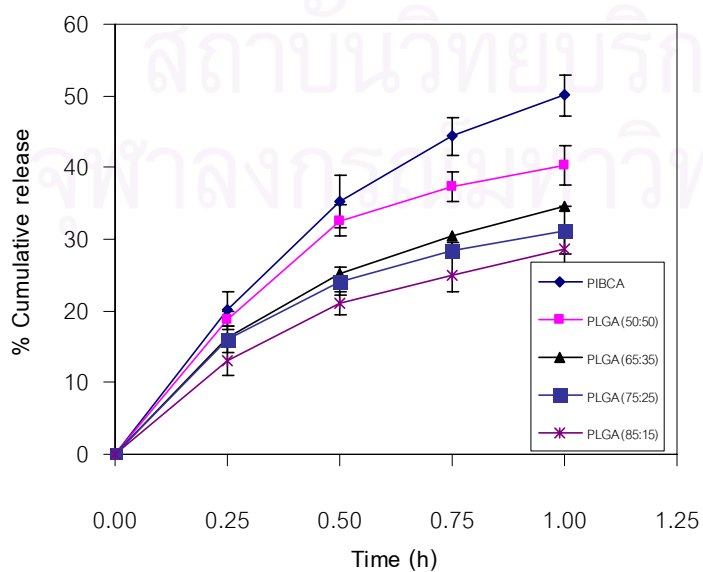
During the first hour, the root-time rate constants of itraconazole release from itraconazole-loaded PIBCA nanoparticles and itraconazole-loaded PIBCA nanoparticles are shown in Table 51. Release data from 2h to 168 h were also fitted to the square root-time model as shown in Table 52. The formulation made from PIBCA gave the rapid release over the burst phase. The root-time rate constant of formulations made from PLGA was also found to decrease with increasing the ratio of polylactide/ polyglycolide (Table 51 and 52).

Table 51 Short-term release data (0-1h) fitted to the root-time model with corresponding regression coefficient. Values represent means, n = 6.

Polymer	Rate constant $(Q/\sqrt{t}\ [\mu gh^{-0.5}])$	R-square
PIBCA	256.94	0.9878
PLGA (50:50)	210.50	0.9844
PLGA (65:35)	175.38	0.998
PLGA (75:25)	160.28	0.9954
PLGA (85:15)	145.19	0.9956

Table 52 Release data (2-168h) fitted to the root-time model with corresponding regression coefficient. Values represent means, n = 6.

Polymer	Rate constant $(Q/\sqrt{t}\ [\mu gh^{-0.5}])$	R-square
PIBCA	69.73	0.9786
PLGA (50:50)	20.92	0.9587
PLGA (65:35)	19.16	0.9588
PLGA (75:25)	16.92	0.9531
PLGA (85:15)	14.75	0.9580

Where Q is the amount of itraconazole released and t is time (h).

Figure 55 Higuchi's square root of time plot of itraconazole-loaded PIBCA

nanoparticles and itraconazole-loaded PLGA nanoparticles. Values represent means,

n = 6.   (a) 0-168 h   (b) 0-1 h   (c) 2-168 h
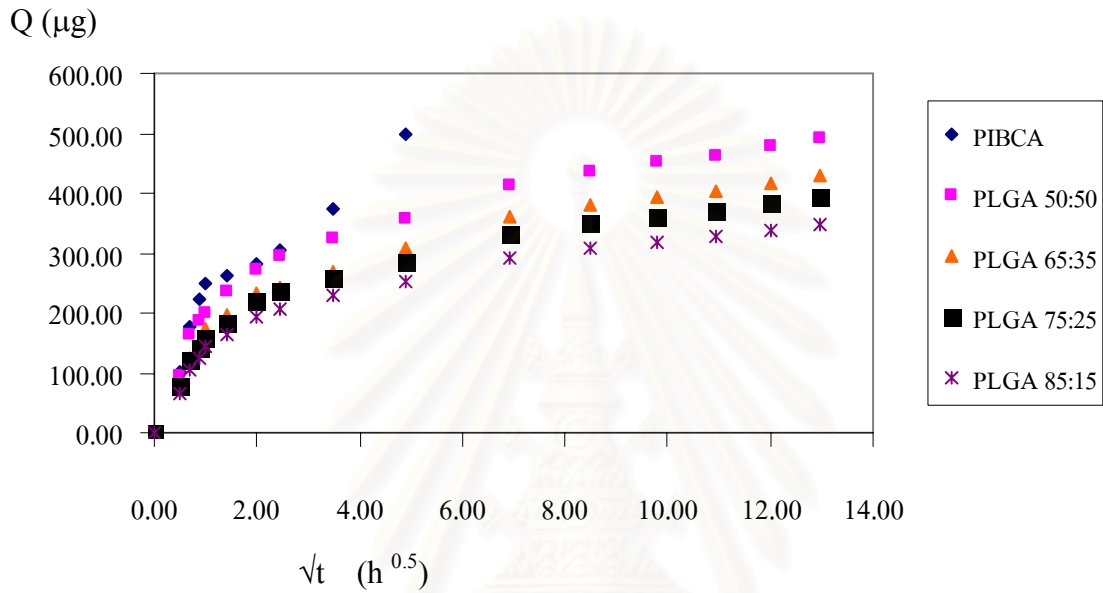
(a)
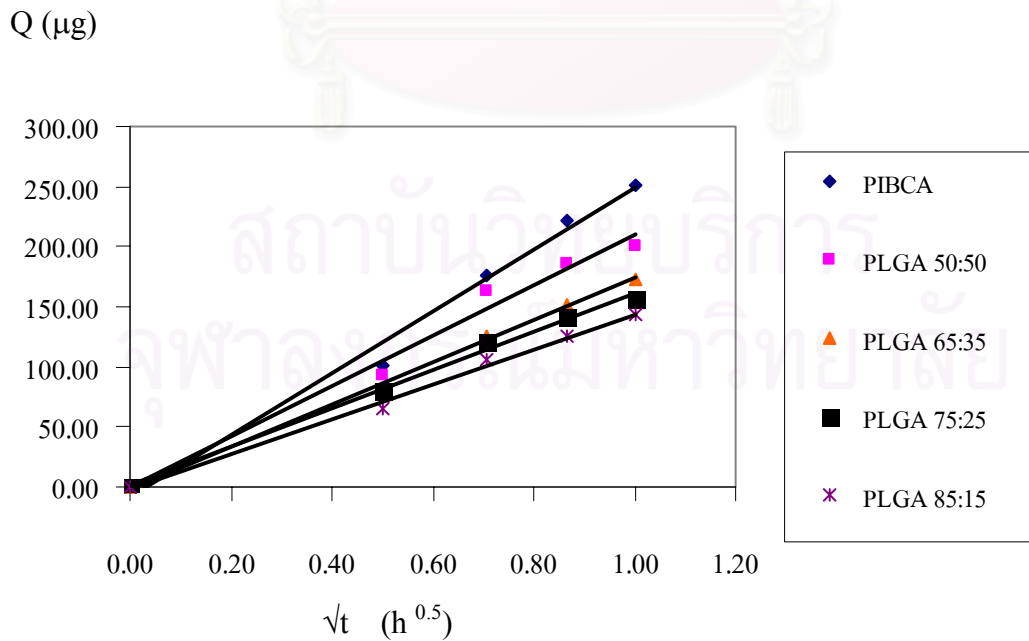
(b)

Figure 55 Higuchi's square root of time plots of itraconazole-loaded PIBCA

nanoparticles and itraconazole-loaded PLGA nanoparticles . Values represent means,

n = 6. (continued)   (a) 0-168 h   (b) 0-1 h   (c) 2-168 h
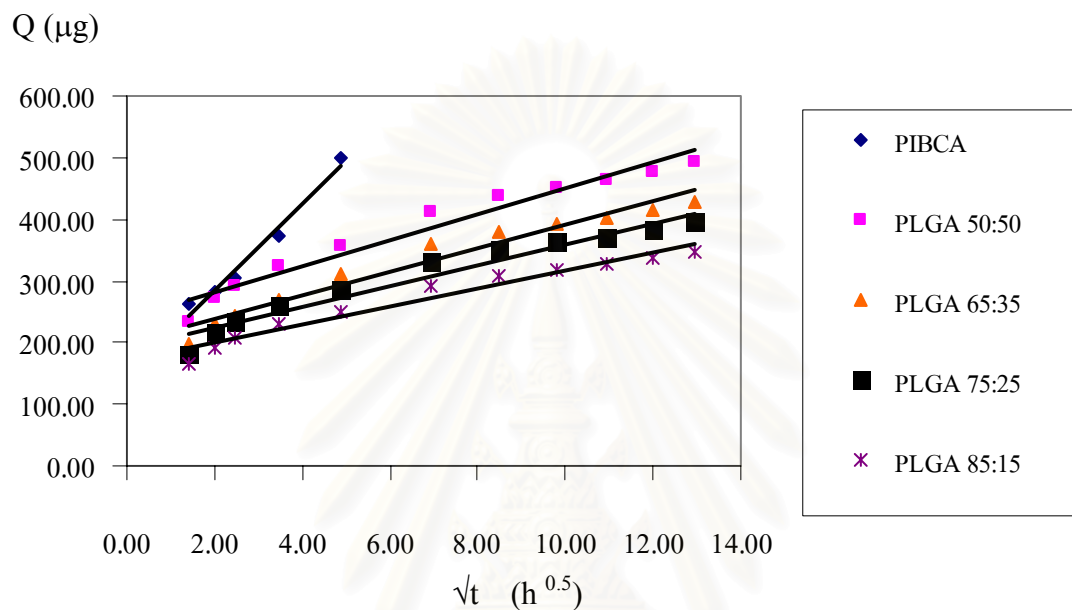
(c)

The apparent dissolution of itraconazole from the nanoparticles could be

explained by Higuchi's square root of time law (Higuchi, 1966). The root-time

rate constant was separated into two parts, during 0-1h and 2-24h for

itraconazole-loaded PIBCA nanoparticles and 2-168 h for itraconazole-loaded

PIBCA nanoparticles. In this case, during the first hour, the polymer

surrounded oily core nanoparticles with the drug dispersed in the polymer

material where diffusion occurred in the intergranular pores, the following

equation held (Desai, et al., 1963)

$$Q = \sqrt{\frac{D \ \varepsilon(2A - \varepsilon C_s)C_s t}{\tau}} \quad = kt^{1/2} \tag{23}$$

where

Q = the amount of drug release after time t per unit exposed area

D = the diffusitivity of the drug in the permeating fluid

τ = the tortuosity factor of the capillary system

A = the total amount of drug present in the matrix per unit

C_S = the solubility of the drug in the permeating fluid

ε = the porosity of the matrix

k = constant

According to this model, the drug molecules could elute out of the polymer wall by dissolution in the permeation liquid and then diffusion through the liquid filled pores and tortuosity. The drug solids in the layer closer to the surface of the polymer wall were the first to release within one hour at the constant rate as shown in Table 51 and when this layer became depleted then the drug solids in the oily core began to dissolute and release. Thus, the root-square rate constants were determined into two parts.

The root-time rate constant was also found to decrease with increasing the ratio of polylactide/ polyglycolide. As the glycolic acid ratio was increased, the rate of degradation was enhanced. Lactic acid had bulky methyl groups on the alpha carbon (--O--CH(CH.sub.3--CH--) which made it difficult for water molecules to access, while glycolic acid had a proton on the alpha carbon(-O-CH.sub.2--CO--), which allowed easier access of water molecules to the ester bonds (Figure 56) resulted in the more permeation of water into the polymer pores.

Figure 56 Structure of lactide and glycolide (Birmingham polymer Inc., 2004)
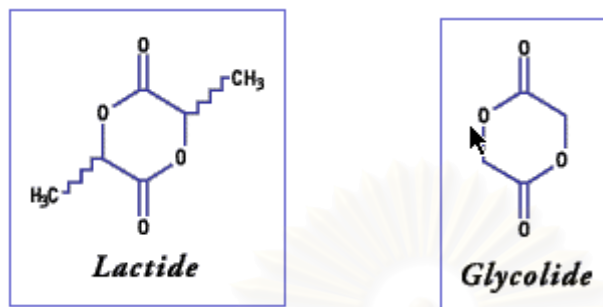
6 Physical Stability

6.1 The Particle Size

Figure 57 shows time course changes in particle size of itraconazole-loaded PIBCA nanoparticles and itraconazole-loaded PLGA nanoparticle. There was no significant change in particle size of both nanoparticles among 0, 30, 60, and 90 days (P > 0.05). On the contrary, there was significant difference in particle size among itraconazole-loaded PIBCA nanoparticles and itraconazole-loaded PLGA nanoparticles.   (P< 0.05) (Table 53). For PLGA, this confirmed the previous finding that PLGA degraded by a bulk erosion mechanism (Reed and Gilding, 1981; Yoo et al., 2000).

Figure 57 Change in particle size of itraconazole-loaded PIBCA nanoparticles and itraconazole-loaded PLGA nanoparticles.
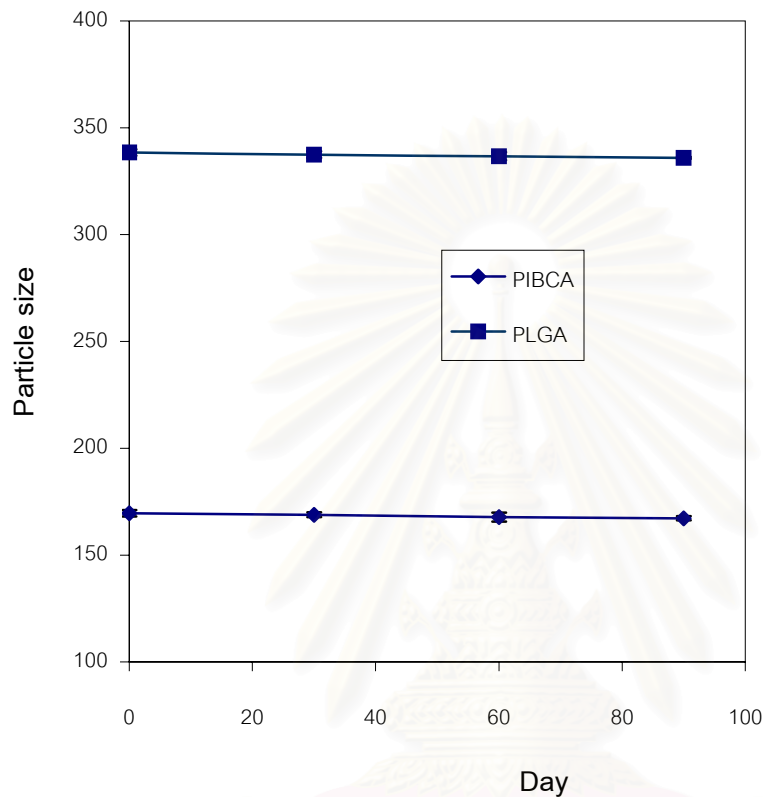
Table 53 ANOVA Table for stability test using the particle size data.

Source of variable	DF	SS	MS	F	P
Polymer	1	170974.1	170974.1	8.1E+04	0.000
Day	3	19.1	6.4	3.01	0.061
Interaction	3	0.2	0.1	0.03	0.991
Error	16	33.8	2.1		
Total	23	171027.3			

6.2 The Encapsulation efficiency

The relative encapsulation efficiency (% encapsulation efficiency at time t = t / % encapsulation efficiency at t = 0) at different time interval is shown in Figure 58. The encapsulation efficiency of itraconazole among 0, 30, 60 and 90 days was significant difference (P< 0.05) as well as the encapsulation efficiency of itraconazole among PIBCA and PLGA (P< 0.05) (Table 54). Itraconazole-loaded PIBCA nanoparticles was more stable than itraconazole-loaded PLGA nanoparticles. The instability of nanoparticles was due to the continuous desorption of itraconazole from nanoparticles. Very low affinity between itraconazole and PLGA was suggested as possible reason for the higher leakage of itraconazole from nanoparticles. On the other hand itraconazole-loaded PIBCA nanoparticles showed noticeable less of itraconazole leakage. These results demonstrated that itraconazole probably existed as a combination of both tightly incorporated and loosely bound drug.

Table 54 ANOVA Table for stability test using the encapsulation efficiency data.

Source of variable	DF	SS	MS	F	P
Polymer	1	4519.09	4519.09	2477.50	0.000
Day	3	10677.14	3559.05	1951.17	0.000
Interaction	3	1754.51	584.84	320.62	0.000
Error	16	29.18	1.82		
Total	23	16979.93			

Figure 58 Change in relative encapsulation efficiency of itraconazole-loaded PIBCA

nanoparticles and itraconazole-loaded PLGA nanoparticles.
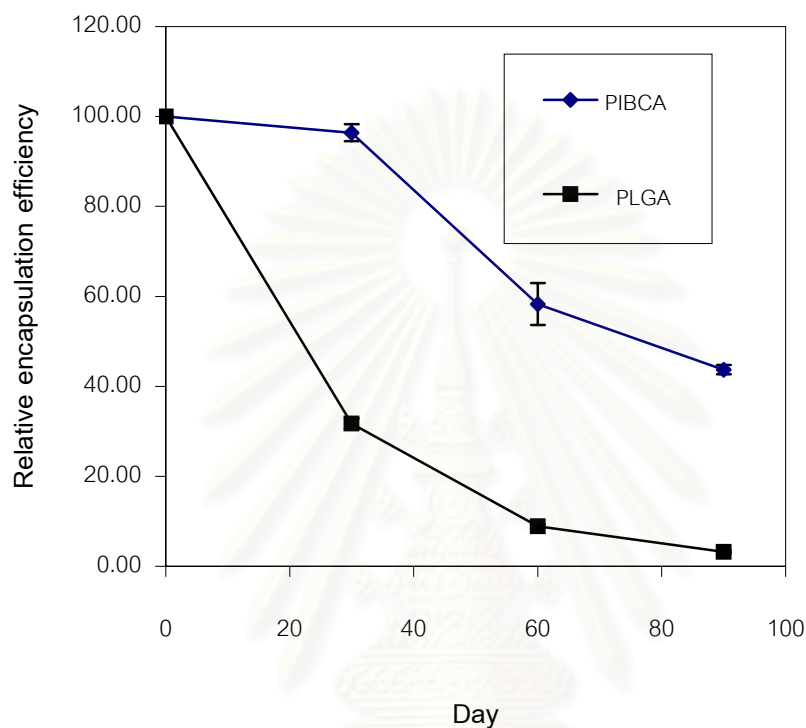
6.3 The Zeta potential

Zeta potential measurements are of great importance because they may
predict the stability of colloidal suspensions (Elimelech and O'Melia, 1990):
generally, it is assumed that the higher the zeta potential, the more stable the
suspension. Here, among the polymer nanoparticles prepared, PIBCA was found to be
the most negatively charged particles. Figure 59 shows time course changes in zeta
potential of itraconazole-loaded PIBCA nanoparticles and itraconazole-loaded PLGA
nanoparticles. There was significant change in zeta potential of both nanoparticles

 (P < 0.05) among 0, 30, 60 and 90 days as well as significant difference in zeta

potential (P < 0.05) among PIBCA and PLGA (Table 55). This may confirm the

instability of both nanopartiles with time, due to drug desorption leading to a

modification of surface properties. It was noteworthy that the zeta potential value, and

hence surface charge, of itraconazole-loaded PIBCA nanoparticles changed less than

that of itraconazole-loaded PLGA nanoparticles, suggesting that itraconazole-loaded

PIBCA nanoparticles remained the most stable with time.

Figure 59 Change in zeta potential of itraconazole-loaded PIBCA nanoparticles and

itraconazole-loaded PLGA nanoparticles.
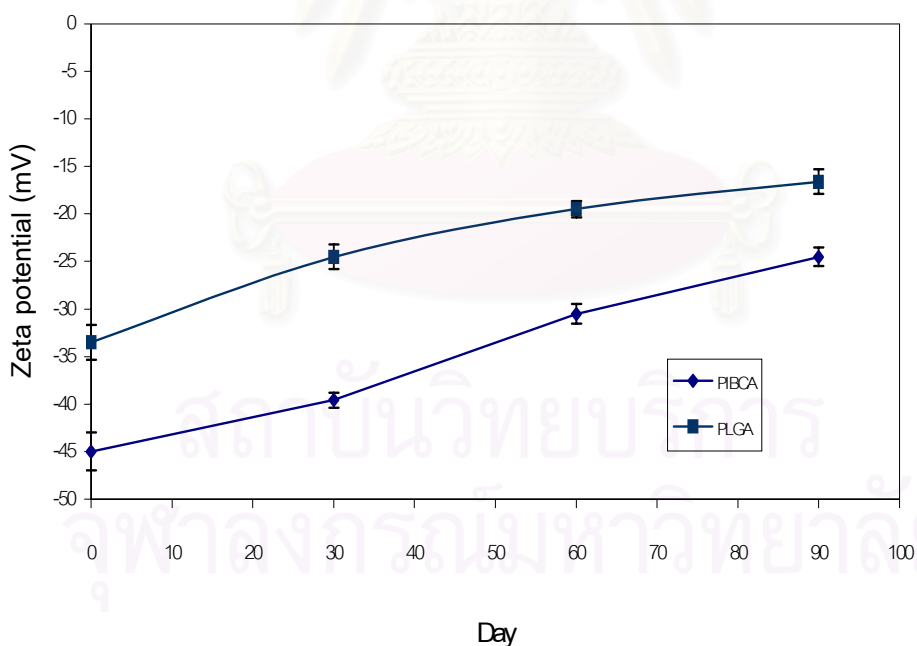
Table 55 ANOVA Table for stability test using the zeta potential data.

Source of variable	DF	SS	MS	F	P
Polymer	1	772.94	772.94	441.47	0.000
Day	3	1206.35	402.12	229.67	0.000
Interaction	3	38.51	12.84	7.33	0.003
Error	16	28.01	1.75		
Total	23	2045.81			

7 Cytotoxic Determination

7.1 Influence of Incubation Times on Cytotoxicity

The cytotoxicity of nanoparticles and the nanoparticle polymerization medium was tested against Vero cell line by crystal violet staining assay. Cells were growth at log phase proliferation. Vero cell line shown in Figure 60 was exposed to 0.5% and 1% of test preparation following the incubation at 1, 2, 3 and 4 h.

At a concentration of 0.5% in the culture medium, all test preparation including itraconazole-loaded PIBCA nanoparticles, plain PIBCA nanoparticles, itraconazole-loaded PLGA nanoparticles, plain PLGA nanoparticles and 0.5% of 0.25% poloxamer in water did not sharply modify the cellular integrity of the Vero cell line (Figure 61). The two-way analysis of variance showed that there was significant change in the viability of Vero cell line among 1,2, 3, and 4 h (P < 0.01) while there was no significant difference in viability of Vero cell line among all

test preparation (P > 0.01) (Table 56).   Using Tukey's pairwise comparisons, the
incubation period of 1 h showed significant difference in viability with 2, 3 and 4 h

(P < 0.01) (Table 57). The viability of Vero cell after incubation for 2 h was
significant difference with 3 and 4h (P< 0.01). There was not significant difference in
viability between incubation period of 3 and 4 h (P > 0.01). The incubation period of
3 and 4 h showed maximum reduction in the viability of Vero cell line.

Figure 60 Vero cell line.

    (a) Contax 167 MT X100   (b) Contax 167 MT X200
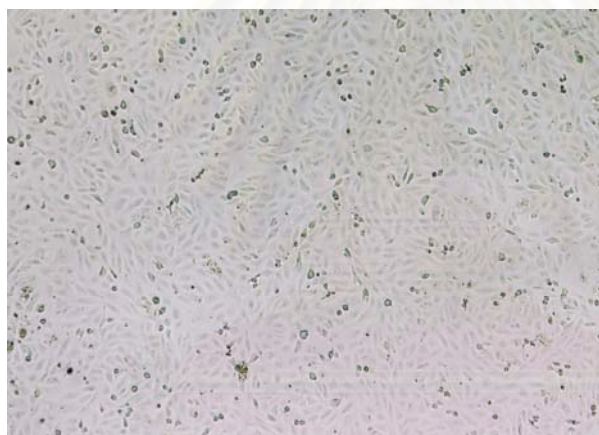
(a) Contax 167 MT X100
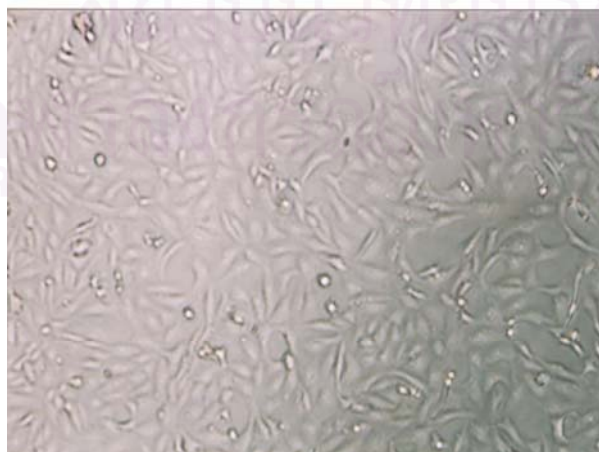
(b) Contax 167 MT X200

Figure 61 Viability of Vero cell line after incubation with 0.5% of 0.25% poloxamer in water in incubated medium , 0.5% plain PLGA nanoparticles in incubated medium, 0.5% itraconazole-loaded PLGA nanoparticles in incubated medium, 0.5% plain PIBCA nanoparticles in incubated medium and 0.5% itraconazole-loaded PIBCA nanoparticles in incubated medium.
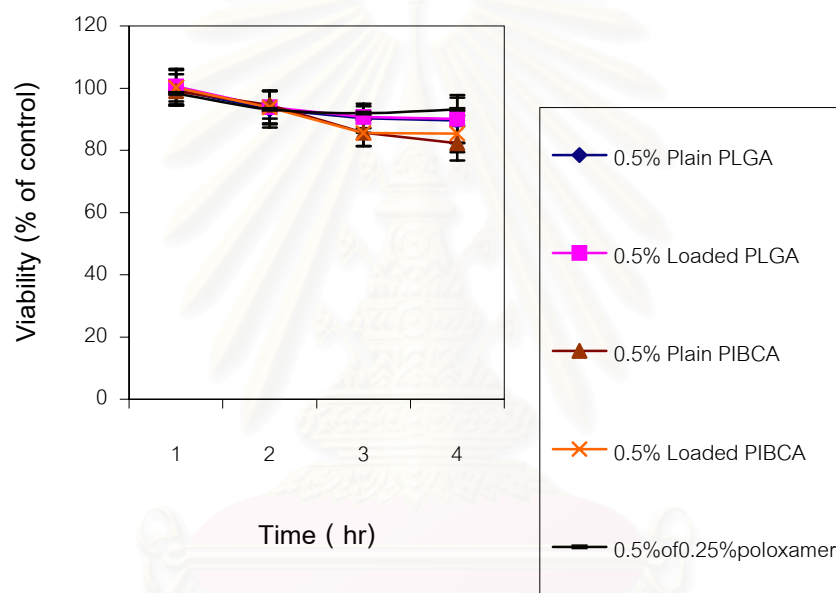
Table 56 ANOVA Table for incubation period using the 0.5% test preparation data.

Source of variable	DF	SS	MS	F	P
Test preparation	4	349.89	87.47	2.79	0.029
Time	3	3336.11	1112.04	35.51	0.000
Interaction	12	569.04	47.42	1.51	0.126
Error	140	4383.87	31.31		
Total	159	8638.91			

Table 57 P-value obtained from Tukey's pairwise comparisons among levels of time using the 0.5% test preparation data.

Time	1h	2h	3h	4h
1h	-	0.0001	0.0000	0.0000
2h	0.001	-	0.0007	0.0001
3h	0.0000	0.0007	-	0.9437
4h	0.0000	0.0001	0.9437	-

At a concentration of 1.0% in the culture medium, the itraconazole-loaded PIBCA nanoparticles and plain PIBCA nanoparticles greatly modified the cellular integrity of the Vero cell line (Figure 62). The two-way analysis of variance showed that there was significant change in the viability of Vero cell line among 1,2, 3, and 4 h (P< 0.01) as well as significant difference in viability of Vero cell line among all test preparation (P< 0.01)(Table 58). Using Tukey's pairwise comparisons, the viability of Vero cell line exposed to 1% of 0.25% poloxamer in water show no significant difference with 1.0 % plain PLGA nanoparticles and 1% itraconazole-loaded PLGA nanoparticles (P> 0.01) (Table 59). One percentage of plain PLGA nanoparticles and 1% itraconazole-loaded PLGA nanoparticles showed the same cytotoxicity (P > 0.01). The viability of Vero cell line exposed to plain PIBCA nanoparticles was not significant difference with that exposed to 1% itraconazole-loaded PIBCA nanoparticles. In case of the 1% final concentration, the PIBCA nanoparticles affected the integrity of Vero cell line; the polymerization medium, on the other hand exerted no effected (Figure 62). The incubation period of 1 h showed significant difference in viability with 2, 3 and 4 h (P< 0.01) (Table 60). The viability

of Vero cell after incubation period for 2 h was significant difference with 4 h (P< 0.01) while there was no significant difference between 2 and 3h (P > 0.01). There was significant difference in viability between incubation period of 3 and 4 h (P< 0.01). Since the incubation period of 4 h showed maximum reduction in the viability of Vero cell line, the incubation 4 h was used to test for further study of the cytotoxicity of nanoparticles.

Figure 62 Viability of Vero cell line after incubation with 1.0% of 0.25% poloxamer in water in incubated medium, 1.0% plain PLGA nanoparticles in incubated medium, 1.0% itraconazole-loaded PLGA nanoparticles in incubated medium, 1.0% plain PIBCA nanoparticles in incubated medium and 1.0% itraconazole-loaded PIBCA nanoparticles in incubated medium.
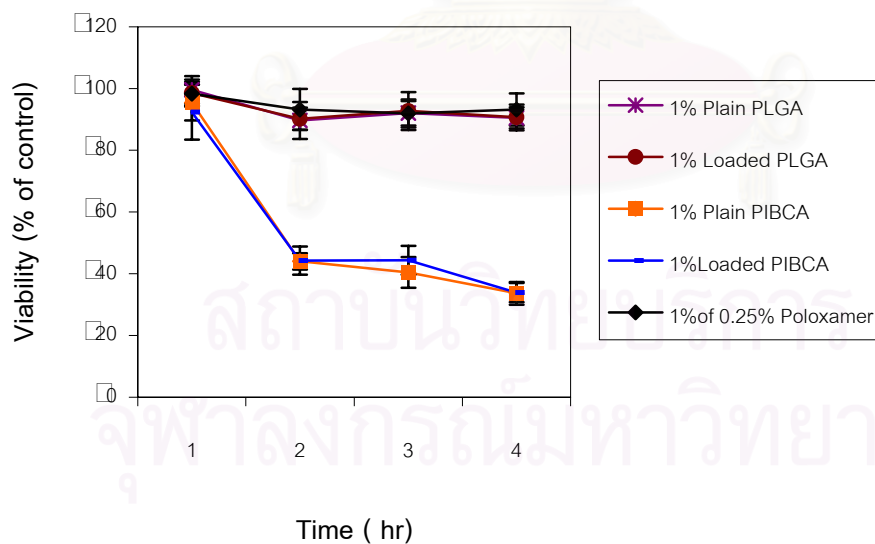
Table 58 ANOVA Table for incubation period using the 1.0% test preparation data.

Source of variable	DF	SS	MS	F	P
Test preparation	4	60919.3	15229.8	620.88	0.000
Time	3	20487.5	6829.2	278.41	0.000
Interaction	12	16370.6	1364.2	55.62	0.000
Error	140	3434.1	24.5		
Total	159	101211.5			

Table 59 P-value obtained from Tukey's pairwise comparisons among levels of test preparation using the 1.0 % test preparation data.

Test preparation (1%)	0.25% poloxamer in water	Plain PLGA nanoparticles	Itraconazole-loaded PLGA nanoparticles	Plain PIBCA nanoparticles	Itraconazole-loaded PIBCA nanoparticles
0.25% poloxamer in water	-	0.8556	0.8873	0.000	0.000
Plain PLGA nanoparticles	0.8556	-	1.000	0.000	0.000
Itraconazole-loaded PLGA nanoparticles	0.8873	1.000	-	0.000	0.000
Plain PIBCA nanoparticles	0.0000	0.0000	0.000	-	0.9990
Itraconazole-loaded PIBCA nanoparticles	0.0000	0.0000	0.000	0.9990	-

Table 60 P-value obtained from Tukey's pairwise comparisons among levels of time using the 1.0 % test preparation data.

Time	1h	2h	3h	4h
1h	-	0.000	0.000	0.000
2h	0.000	-	1.000	0.0034
3h	0.000	1.000	-	0.0033
4h	0.000	0.0034	0.0033	-

7.2 Influence of Concentration on Cytotoxicity

Viability curves generated by treating itraconazole-loaded PIBCA nanoparticles, plain PIBCA nanoparticles, itraconazole-loaded PLGA nanoparticles or plain PLGA nanoparticles with various concentrations are shown in Figure 63 Itraconazole-loaded PLGA nanoparticles and plain PLGA nanoparticles showed less cytotoxicity than itraconazole-loaded PIBCA nanoparticles and plain PIBCA nanoparticles. The two-way analysis of variance showed that there was significant change in the viability of Vero cell line among different kinds of nanoparticles (P< 0.01) as well as significant difference in viability of Vero cell line among various concentration of nanoparticles (P < 0.01)   (Table 61).   Using Tukey's pairwise comparisons, there was not significant difference in viability of Vero cell line exposed to plain PLGA nanoparticles and itraconazole-loaded PLGA nanoparticles (P > 0.01). The viability of Vero cell line exposed to plain PIBCA nanoparticles was not significant difference with that exposed to itraconazole-loaded PIBCA nanoparticles (Table 62). The estimated IC_{50} values of plain PIBCA nanoparticles and itraconazole-

loaded PIBCA nanoparticles were 0.74 %, which corresponded to 114 µg/mL of these nanoparticles (Figure 64). The estimated IC_{50} values of plain PLGA nanoparticles and itraconazole-loaded PLGA nanoparticles were 6.6 %, which correspond to 7.92 mg/mL of these nanoparticles (Figure 65).

Figure 63 Viability of Vero cell line after incubation with various concentrations of plain PIBCA nanoparticles, itraconazole-loaded PIBCA nanoparticles, plain PLGA and itraconazole-loaded PLGA nanoparticles.
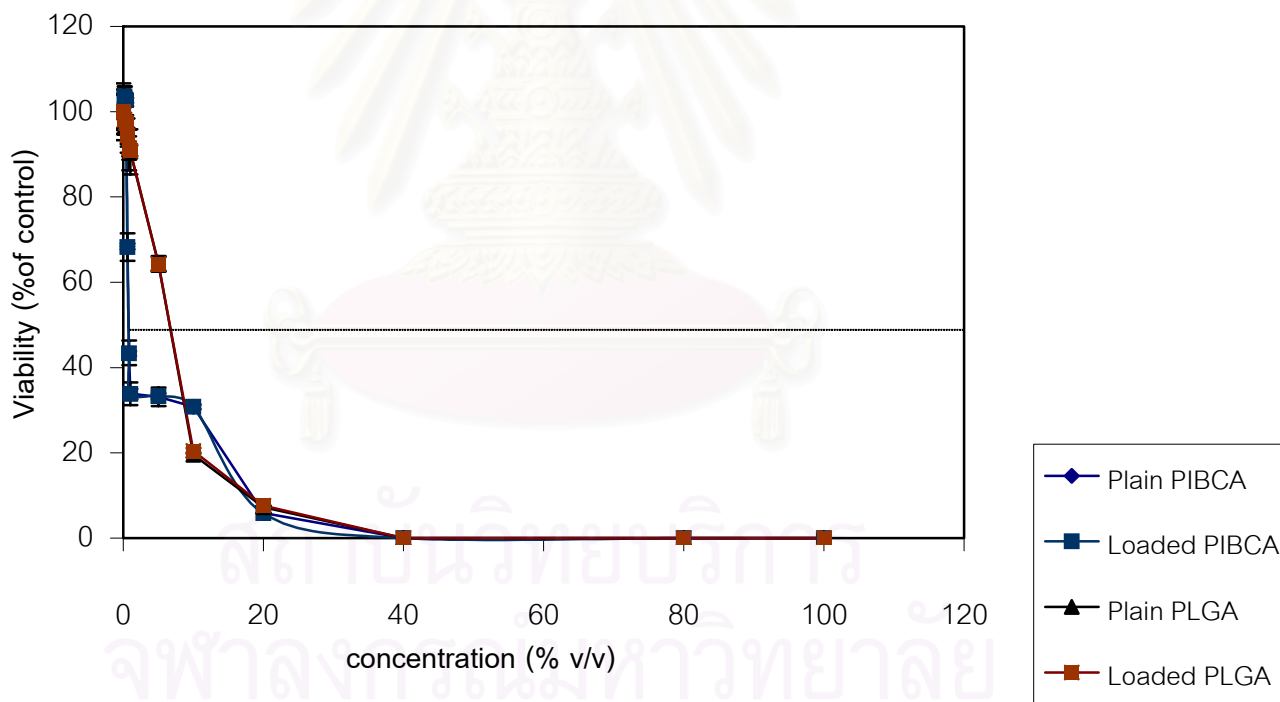
Figure 64 Viability of Vero cell line after incubation with various concentrations of plain PIBCA nanoparticles and itraconazole-loaded PIBCA nanoparticles.
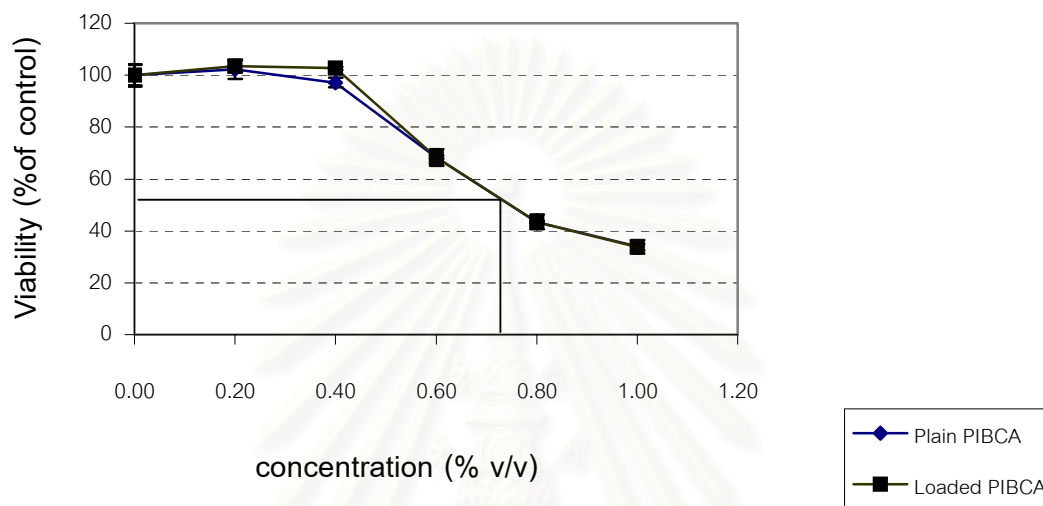
Figure 65 Viability of Vero cell line after incubation with various concentrations of plain PLGA nanoparticles and itraconazole-loaded PLGA nanoparticles.
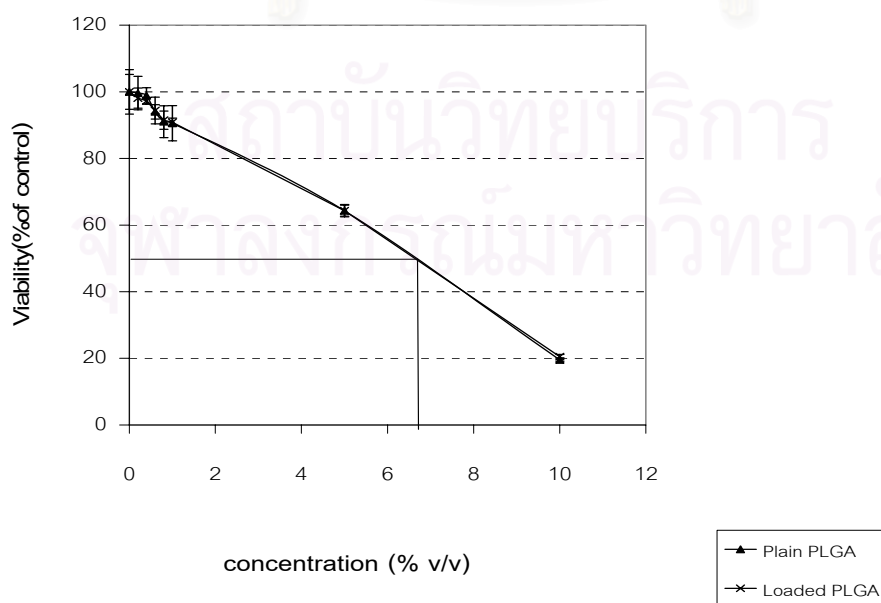
Table 61 ANOVA Table for various concentrations of test preparation.

Source of variable	DF	SS	MS	F	P
Test preparation	3	19124	6375	854.30	0.000
Concentration	8	358614	44827	6007.52	0.000
Interaction	24	39421	1643	220.13	0.000
Error	252	1880	7		
Total	287	419039			

Table 62 P-value obtained from Tukey's pairwise comparisons among levels of test preparation.

Test preparation	Plain PLGA nanoparticles	Itraconazole-loaded PLGA nanoparticles	Plain PIBCA nanoparticles	Itraconazole-loaded PIBCA nanoparticles
Plain PLGA nanoparticles	-	0.9990	0.000	0.000
Itraconazole-loaded PLGA nanoparticles	0.9990	-	0.000	0.000
Plain PIBCA nanoparticles	0.0000	0.000	-	0.3873
Itraconazole-loaded PIBCA nanoparticles	0.0000	0.000	0.3873	-

Since it was found that the estimated IC_{50} values of plain PIBCA nanoparticles and itraconazole-loaded PIBCA nanoparticles were 114 µg/mL, these results confirmed the results of the others. Gonzalea-Martin et al. (2000) found that concentration of unloaded PIBCA nanoparticles greater than 262.9 µg/mL gave 56% cytotoxicity. An IC_{50} of 400 µg/mL for PIBCA nanoparticle suspension was found in hepatocyte cell culture model (Kreuter etal., 1984). The cytotoxicity of PIBCA might be caused by the degradation products as Leonard et al. (1966) and Lehmann et al. (1966) suggestion. Leonard et al. (1966) postulated a degradation mechanism following a Retro-Knoevenagel reaction leading to formaldehyde and cyanoacetate.

The estimated IC_{50} values of plain PLGA nanoparticles and itraconazole-loaded PLGA nanoparticles were higher than the estimated IC_{50} values of plain PIBCA nanoparticles and itraconazole-loaded PIBCA nanoparticles. The reason to explain might be caused by different degradation products. The degradation products of PLGA, monomers and oligomers of lactic acid and glycolic, were known to be well tolerated by various tissues (Wise et al., 1979) and were finally eliminated from the body through the Krebs cycle (Lewis et al.,1990).

CHAPTER V

CONCLUSIONS

In this study, the solubility of itraconazole in four different oils consisting of benzyl benzoate, corn oil, caprylic/capric triglycerides and soybean oil and the solubility of itraconazole in different aqueous media were investigated. It was found that itraconazole solubility in different oils was ranked in the order of soybean oil< caprylic/capric triglycerides < corn oil < benzyl benzoate. Itraconazole solubility in different aqueous medium was ranked in the order of 4% cyclodextrin in water < SGF < 0.25% SLS in PBS since the solubility of itraconazole in water, PBS, 0.25% Poloxamer in PBS, and 0.25% Poloxamer in water were less than 1.25 μg/mL. Then benzyl benzoate and 0.25% SLS in PBS were selected for further studies.

A 3^3 factorial study was used in the study of itraconazole-loaded PIBCA nanoparticles. Concentration of added isobutylcyanoacrylate monomer X_1(1, 5.5, 10 μL/mL), benzyl benzoate X_2 (5, 12.5, 20 μg/mL), and itraconazole X_3 (200, 1050, 1900 μg/mL) were selected as the factors. The particle size (Y_1), polydispersity index (Y_2), amount of itraconazole entrapped in the nanoparticles (Y_3) and encapsulation efficiency (Y_4) were used as responses. Statistical model for the particle size (Y_1), polydispersity index (Y_2), amount of itraconazole entrapped in the nanoparticles (Y_3) and encapsulation efficiency (Y_4) as a function of concentration of the isobutylcyanoacrylate monomer (X_1), benzyl benzoate(X_2), and itraconazole (X_3) were developed. The resulting equations were shown as follows, $Y_1 = 173.983 +$

$5.600X_1 + 18.825X_2 - 0.717X_3 + 1.221X_1X_2 + 0.754X_1X_3 - 0.083X_2X_3 - 9.283 X_1^2 + 3.242X_2^2 + 1.233X_3^2$; $Y_2 = 0.0806 + 0.0044X_1 + 0.0204X_2 - 0.0008X_3 - 0.0031X_1X_2 + 0.0004X_1X_3 - 0.0012X_2X_3 - 0.0033X_1^2 - 0.0032X_2^2 + 0.0007X_3^2$; $Y_3 = 461.82 + 62.19X_1 + 37.10X_2 + 171.02X_3 + 20.96X_1X_2 + 50.67X_1X_3 + 31.77X_2X_3 - 22.46X_1^2 - 66.00X_2^2 - 82.69X_3^2$; $Y_4 = 44.30 + 5.40X_1 + 3.27X_2 - 4.36X_3 + 1.46X_1X_2 + 0.97X_1X_3 + 0.50X_2X_3 - 2.05X_1^2 - 6.85X_2^2 + 11.85X_3^2$. The optimum formulations of the polyisobutylcyanoacrylate nanoparticles containing itraconazole 500 μg/ mL were 8.09 μL/mL of IBCA, 10.19 μg/mL of benzyl benzoate and 1200.77 μg/mL of itraconazole. The particle size, the polydispersity index, the amount of itraconazole entrapped in the nanoparticles, and the encapsulation efficiency of the optimized formula were in agreement with the predictions obtained from the models. Response surface methodology has been successfully used to construct a statistical model for the particle size, the polydispersity index, the amount of itraconazole entrapped in the nanoparticles and the encapsulation efficiency as a function of the formulation variable.

This study also investigated the utility of a 2^3 factorial design and optimization process for polylactic-co-glycolic acid (PLGA) nanoparticles containing itraconazole with 5 replicates at the center of the design. Nanoparticles were prepared by solvent displacement technique with PLGA X_1 (10, 100 mg/mL), benzyl benzoate X_2 (5, 20 μg/mL), and itraconazole X_3 (200, 1800 μg/mL). Particle size (Y_1), the amount of itraconazole entrapped in the nanoparticles (Y_2), and encapsulation efficiency (Y_3) were used as responses. A validated statistical model having significant coefficient figures ($P < 0.001$) for the particle size (Y_1), the

amount of itraconazole entrapped in the nanoparticles (Y_2), and encapsulation efficiency (Y_3) as function of the PLGA (A), benzyl benzoate (B), and itraconazole (C) were developed. The resulting equations were shown as follows, $Y_1 = 373.75 + 66.54A + 52.09B + 105.06C - 4.73AB + 46.30AC$; $Y_2 = 472.93 + 73.45A + 169.06B + 333.03C + 62.40AC + 141.49BC$; $Y_3 = 57.36 + 6.53A + 15.52B - 12.59C + 1.01AC + 1.73BC$. The particle size, the amount of itraconazole entrapped in the nanoparticles, and the encapsulation efficiency of the optimized formula were in agreement with the predictions obtained from the models4 formulas were in agreement with the predictions obtained from the models ($P < 0.05$). An overlay plot for the responses including the particle size, the amount of itraconazole entrapped in the nanoparticles, and the encapsulation efficiency shows the boundary in which a number of combinations of concentration of PLGA, benzyl benzoate, and itraconazole will result in a satisfactory process. Using the desirability approach with the same constraints, the solution composition having the highest overall desirability ($D = 0.769$) was 10 mg/mL of PLGA, 16.94 µg/mL of benzyl benzoate, and 1001.01 µg/mL of itraconazole. This approach allowed the selection of the optimum formulation ingredients for PLGA nanoparticles containing itraconazole of 500 µg/mL.

. Since nanoparticles containing itraconazole 500 µg/mL could be performed, the stability and cytotoxicity of nanoparticles were investigated. The triplicate samples having itraconazole 500 µg/mL prepared by each polymer were used to study the effect of storage (at 4 °C over 3 months). Plain nanoparticles were prepared as previously described but omitting itraconazole. Cell culture experiments

were performed using Vero cell line treated at different concentrations and for different exposure intervals with itraconazole-loaded PIBCA nanoparticles, plain PIBCA nanoparticles, itraconazole-loaded PLGA nanoparticles and plain PLGA nanoparticles. Stability test showed that the itraconazole encapsulation efficiency of itraconazole-loaded PIBCA nanoparticles decreased by 3.58, 41.71, 56.31 % over 30, 60 and 90 days respectively. For itraconazole-loaded PLGA nanoparticles, it decreased by 8.30, 91.11, 96.79% over 30, 60, and 90 days respectively. Both itraconazole-loaded PIBCA and PLGA nanoparticles showed no difference in terms of particle size over the 90-day period ($P < 0.05$). An exposure of 4h was sufficient to induce significant cytotoxic effects. The cytotoxicity between plain and itraconazole-loaded PIBCA nanoparticles was not significant different ($P < 0.05$). The cytotoxicity between plain and itraconazole-loaded PLGA nanoparticles also didn't show significant difference ($P < 0.05$). The estimated IC_{50} values (concentration causing 50% cell death) of PLGA nanoparticles and PIBCA nanoparticles were 79.2 mg/mL and 114 μg/mL, respectively.

Factorial design and response surface methodology has been successfully used to construct a statistical model for the particle size, polydispersity index and encapsulation efficiency as a function of the formulation variable. The optimized formula of itraconazole-loaded PIBCA nanoparticles was more stable than the optimize formula of itraconazole-loaded PLGA nanoparticles. On the contrary, the cytotoxicity of plain and itraconazole-loaded PLGA nanoparticles was less prominent than that of plain and itraconazole-loaded PIBCA nanoparticles. With these preparations, the required concentration of the drug for the treatment of

systemic fungal infections by the intravenous route could be achieved. Nevertheless, findings from the above studies suggested for further study because of the instability of the suspension with time that was due to the continuous desorption of itraconazole from nanoparticles. To optimize the stability of these preparations by means of freeze-drying should be used for further study.

REFERENCES

Adinarayana, K., and Ellaiah, P. 2002. Response surface optimization of the critical medium components for the production of alkaline protease by a newly isolated Bacillus sp. J Pharm. Pharmaceut. Sci. [online] 5(3) : 272-278. Available from: http://www.ualberta.ca/~csps [January 2003].

Akhnazarova, S., and Kafaro ,V.(eds.) 1982.Experiment Optimization in Chemistry and Chemical Engineering. Moscow: Mir House Publications.

Al Khouri Fallouh, N., Roblot-Treupel. L., Fessi, H., Devissaguet, J.P., and Puisieux, F. 1986. Development of a new process for the manufacture of polyisobutylcyanoacrylate nanocapsules. Int. J. Pharm. 28 : 125-132.

Allemann, E., Gurny, R., and Doelker, E. 1993. Drug-loaded nanoparticles-Preparation methods and drug targeting issues. Eur. J. Pharm. Biopharm. 39 : 173-190.

Allemann ,E., and Leroux ,R.G. 1999. Biodegradable nanoparticles of particles of poly(lactic acid) and poly(lactic-co-glycolic acid) for parenteral administration. In G, Gregoridas (ed.), Pharmaceutical Dosage Form. Vol. 3, pp. 163-186.New York: Marcel Dekker.

Arica, B., Kay, H.S., Orman, M.N., and Hincal, A.A. 2002. Biodegradable bromocryptine mesylate microspheres prepared by a solvent evaporation technique. I. Evaluation of formulation variables on microspheres characteristics for brain delivery. J Microencapsul. 19(4) : 473-484.

Armstrong, N.A. and James, K.C. 1990. Understanding Experimental Design and Interpretation in Pharmaceutics . Chichester: Ellis Horwood.

Bakker-Woudenberg, I.A.J.M., and Roerdink, F.H. 1986. Antimicrobial chemotherapy directed by liposomes. J. Antimicrob. Chemother. 17 : 547-548.

Bakker-Woudenberg, I.A.J.M., Lokerse, A.F., ten Kate, M.T., Melissen, P.M.B., Van Vianen, W., and Van Etten, E.W.M. 1993. Liposomes as carriers of antimicrobial agents or immunimulatory agents in the treatment of infections. Eur J. Clin. Microbiol. Infect. Dis. 12 : 61-67.

Bakker-Woudenberg, I.A.J.M, Storm, G., Woodle, M.C. 1994. Liposomes in the treatment of infections. J. Drug Target. 2 : 363-371.

Banakar, U.V. 1992. Dissolution of dosage forms. In U.V. Banakar(ed.), Pharmaceutical Dissolution Testing, pp. 285-589. New York: Marcel Dekker.

Barratt, G.M. 2000. Therapeutic applications of colloidal drug carriers. Pharm. Sci. Technol. Today. 3(5) : 163-171.

Barichello, J.M., Morishita, M., Takayama, K., and Nagai, T. 1999. Encapsulation of hydrophilic and lipophilic drugs in PLGA nanoparticles by the nanoprecipitation method. Drug Dev. Ind.Pharm. 25(4) : 471-476.

Barone, J.A., Koh, J.G., Bierman, R.H., Colaizzi, J.L., Swanson, K.A., Gaffar, M.C., Moskovitz, B.L., Mechlinski ,W., and Van de Velde, V. 1993. Food interaction and steady-state pharmacokinetics of itraconazole capsules in healthy male volunteers. Antimicrob. Agents Chemother. 37(4) : 778-84.

Bindschaedler, C., Gurney, R, and Doelker, E. 1990. United States Patent 4, 968, 350

Birmingham Polymer Inc. 2004. Available from: http://www.birmingham.com. [January 2004].

Bos, C.E., Bolhuis, G.K., and Lerk ,C.F. 1991. Optimization of tablet formulations based on starch/lactose granulations for use in tropical countries. Drug Dev. Ind. Pharm. 17(17) : 2373-2389.

Bouwstra, J.A., and Hofland, H.E.J. in J. kreuter (ed.), Niosomes   , pp. 191-214.

New York : Marcel Dekker.

Box, G.E.P., Hunter, W.G., and Hunter ,J.S.eds. 1978. Statistic for Experiments.

New York: John Wiley and Sons.

Box, G.E.P., and Wilson, K.B. 1951. On the experimental attainment of optimum

conditions. J. Roy. Stat. Soc. B. 13 : 1-45.

Brasseur, R., Goormaghtigh, E., Ruysschaert, J-M, Duquenoy, P-H, Marichal, P., and

Vanden Bossche, H. 1991. Lipid-itraconazole interaction in lipid model

membranes. J. Pharm. Pharmacol. 43 : 167-171.

Calvo, P., Alonso, M., Vila-Jato, J. and Robinson, J., 1996. Improved ocular

bioavailability of indomethacin by novel ocular drug carriers. J. Pharm.

Pharmacol. 48 : 1147–1152.

Cauchetier, E., Deniau, M., Fessi , H., Astier, A., and Paul, A. 2003. Atovaquone-

loaded nanocapsules: influence of the polymer on their in vitro characteristics.

Int. J. Pharm. 250 : 273-281.

Cauwenbergh, G., Degreef, H., Heykants, J., Woestenborghs, R., Van Rooy, P., and

Haeverans, K. 1988. Pharmacokinetic profile of orally administered

itraconazole in human skin. J. Am. Acad. Dermatol. 18 : 263-8.

Ceschel, G.C., Maffei ,P., and Badiello, R. 1999. Optimization of hydrochlorothiazide

tablets. Drug Dev. Ind.Pharm. 25(11) : 1167-1176.

Chasteigner, D.S., Fessi ,H., Devissaguet , J.P., and Puisieux, F. 1996. Comparative

study of the association of itraconazole with colloidal drug carriers. Drug Dev.

Res. 38 : 125-133.

Chouinard, F., Buczkowski, S., and Lenaerts, V. 1994. Poly (alkylcyanoacrylate) nanocapsules : Physicochemical characterization and mechanism of formation. Pharm. Res. 11 : 869-874.

Chowdary, K.P.R., and Srinivasa Rao, S.K. 2000a. A study on the development of dissolution medium for itraconazole. Indian Drugs 37 (6): 291-294.

Chowdary, K.P.R., and Srinivasa Rao, S.K. 2000b. Effect of surfactants on the solubility and dissolution rate of itraconazole. The Eastern Pharmacist September 2000: 113-114.

Chowdary, K.P.R., Srinivasa Rao, S.K. 2000c. Investigation of dissolution enhancement of itraconazole by solid dispersion in superdisintegrants. Drug Dev. Ind. Pharm. 26 (11): 1207-1211.

Clemons, K.V., Homola, M.E., and Stevens, D.A. 1995. Activities of the triazole SCH 51048 against *Coccidioides immitis* in vitro and in vivo. Antimicrob Agents Chemother. 39 : 1169-1172.

Como, J.A., and Dismukes, W.E. 1994. Oral azole drugs as systemic antifungal therapy. New Eng. J. Med. 330 : 263-272.

Couvreur, P., Couarraze, G., Devissaguet, J.P., and Puisieux, F. 1996. Nanoparticles : Preparation and Characterisation. In S.Benita (ed.), Drugs and the Pharmaceutical Sciences vol. 73 : Microencapsulation : Methods and industrial applications. , pp 183-211. New York : Marcel Dekker.

Couvreur, P., Dubernet, C., and Puisieux, F.1995. Controlled drug delivery with nanoparticles : Current possibilities and future trends. Eur. J. Pharm. Biopharm. 41 : 2-13.

Couvreur, P., Kante, B., Roland, M., Guiot, P., Bauduin, P. and Speiser, P. 1979. Polycyanoacrylate nanocapsules as potential lysosomotropic carriers :

preparation, morphological and sorptive properties. J. Pharm. Pharmacol. 31 :

    331-332.

Damge, C., Michel, C., Aprahamian, M., and Couvreur, P. and Devissaguet, J.P.

    1990. Nanocapsules as carriers for oral peptide delivery. J. Controlled

    Release. 13 : 233-239.

Damge, C., Vranckx, P., Balschmidt, P., and Couvreur, P. 1997. Poly

    (alkylcyanoacrylate) nanospheres for oral administration of insulin. J. Pharm.

    Sci. 86 : 1403-1409.

Das, S.K., Tucker, I.G., Hill, D.J.T., and Ganguly N. 1995. Evaluation of poly

    (isobutyl cyanoacrylate) nanoparticles for mucoadhesive ocular drug delivery.

    I. Effect of formulation variables on physicochemical characteristics of

    nanoparticles. Pharm. Res. 12 : 534-540.

Davis, O.L. ed. 1967. The Design and Analysis of Industrial Experiments. 2 nd ed.

    New York: Longaman.

Dawoodbhai, S., Suryanarayan, E.R., Woodruff, C.W., and Rhodes,C.T. 1991.

    Optimization of tablet formulations containing talc. Drug Dev Ind Pharm.

    17(10) : 1343-1371.

Derringer, G., and Suich, R. 1980. Simultaneous optimization of several response

    variables. J. qual. Tech. 28 : 214-219.

Deai, S.J., Singh, P., Simonelli, A.P., and Higuchi, W.I. 1963. Investigation of factors

    influencing release of solid drug dispersed in inert matrices III: quantitative

    studies involving the polyethylene platic matrix. J. Pharm. Sci. 52(12): 1145-

    1149.

Dismukes, W.E. 1988. Azole antifungal drugs : Old and new. Ann. Intern. Med. 109 :

    177-179.

Domb, A.J. 1993. Liposheres for controlled delivery of substances. United States patent 5,188,837.

 Elkheshen, S.A., Badawi, S.S., and Badawi, A.A. 1996. Optimization of a reconstitutable suspension of rifampicin using 24 factorial design**.** Drug Dev Ind Pharm. 22(7) : 623-630.

El-Samaligy, M.S., Rohdewald, P., and Mahmoud, H.A. 1986. Polyalkyl cyanoacrylate nanocapsules. J. Pharm. Pharmacol. 38 : 216-218.

Erden ,N. and Celebi, N. 1996. Factors influencing release of salbutamol sulphate from poly(lactide-co-glycolide) microspheres prepared by water-in-oil-in-water emulsion technique. Int. J. Pharm*.* 137: 57–66.

Fang, L.U., Fang, J., and Chen, C.Q. 2001. TNF receptor-associated factor-2 binding site is involved in TNFR75-dependent enhancement of TNFR55-induced cell dealth. Cell Res. 11(3) : 217-222.

Fattal, E., Lambert, G., and Couvreur, P. 2000. Polyisobutylcyanoacrylate nanocapsules containing an aqueous core as a novel colloidal carrier for the delivery of oligonucleotides. 3rd World Meeting on Pharmaceutics Biopharmaceutics Pharmaceutical Technology. Berlin, April 3-6 : 275-276.

Fessi, H., Puisieux, F., Devissaguet, J.P., Ammoury, N., and Benita, S. 1989. Nanocapsule formulation by interfacial polymer deposition following solvent displacement. Int. J. Pharm. 55 : R1-R4.

Fessi, H., Puisieux, F., and Devissaguet, J.P. 1987. Eur. Patent 274 961.

Medicare and Medicaid programs. 1990. Freedom of information (FOI) guidelines Notice.Fed Regist. 55(240):51342-3.

Floyd, A.G., and Jain, S. 1996. Injectable emulsions and suspensions. In H.A. Lieberman, M.M. Rieger, and G.S. Banker (eds.), Pharmaceutical Dosage forms: Dispersed Systems. Vol.2, 2nd edition, revised and expanded, pp. 261-318. New York: Marcel Dekker.

Florence, A.T., Whateley, T.L. and Wood, and D.A. 1979. Potentially biodegradable microcapsules with poly (alkyl 2-cyanoacrylate) membranes. J. Pharm. Pharmacol. 31 : 422-424.

Freshney, I. 2001. Application of cell cultures to toxicology. Cell Biol Toxicol. 17(4-5) : 213-30.

Fresta, M., Cavallaro, G., Giammona, G., Wehrli, E., and Puglisi, G. 1996. Preparation and characterization of polyethyl 2-cyanoacrylate nanocapsules containing antiepileptic drugs. Biomaterials. 17 : 751-758.

Fresta, M., and Puglisi, G. 1994. Association of netilmicin sulphate to poly (alkylcyanoacrylate) nanoparticles: factors influencing particle delivery behaviors. Drug Dev. Ind. Pharm. 14 : 2227-2243.

Fromtling, R.A. 1988. Overveiw of medically important antifungal azole derivatives. Clin. Microbiol. Rev. 1 : 187-217.

Gallardo, M., Couarraze, G., Denizot, B., Treupel, L., Couvreur, P., and Puisieux, F. 1993. Study of the mechanisms of formation of nanoparticles and nanocapsules of polyisobutyl 2-cyanoacrylate. Int. J. Pharm. 100 : 55-64.

Gasco, M.R., and Trotta, M. 1986. Nanoparticles from microemulsions. Int. J. Pharm. 29 : 267-268.

Gonzalez-Martin, G., Figueroa,C., merino, I., and Osuna, A. 2000. Allopurinol
encapsulated in polycyanoacrylate nanoparticles as potential lysosomatropic
carrier: preparation and trypanocidal activity. Eur. J. Pharm. Biopharm. 49 :
137-142.

Grangier, G.L., Puygrenier, M., Gautier, J.C., and Couvreur, P. 1991. Nanoparticles
as carriers for growht hormone releasing factor. J. Controlled Release. 15 : 3-
13.

Guy, R.H., Hadgraft, J., Kellaway, I. W., and Taylor, M.J. 1982. Calculations of drug
release rates from spherical particles. Int. J. Pharm. 11: 199-207.

Harmia,T., Speisser, P., and Kreuter,J. 1986. Optimization of pilocarpine loading
onto nanoparticles by sorption procedures. Int J. Pharm. 33 : 45-54.

Haskell, R.J. 1998. Characterization of submicron systems via optical methods.
J. Pharm. Sci. 87(2) : 125-9.

Heykants, J., Peer, V., van de Velde, V., Rooy , P.V., Meuldermans ,W., Lavrijsen,
K., Woestenborghs, R., Van , J., and Cauwenbergh ,G. 1989. The clinical
pharmacokinetics of itraconazole: an overview. Mycoses. 32(suppl 1) : 67-68.

Higuchi, T. 1966. Mechanism of sustained-action medication: Theoritical analysis of
rate of release of solid drugs dispersed in solid matrices. J. Pharm. Sci. 55(11)
: 1230-1234.

Hostetler, J.S., Hanson, L.H., and Stevens, D.A. 1992. Effect of cyclodextrin on the
pharmacology of antifungal oral azoles. Antimicrob Agents Chemother. 36 :
477-480.

Illum, L, Khan, M.A., Mak, E., and Davis, D.D. 1986. Evaluation of carrier capacity
and release characteristics for poly(butyl 2- cyanoacrylate) nanoparticles. Int.
J. Pharm. 30 : 17-28.

International Conference on Harmonization guideline residual solvents, 62 Federal registere 67377-67388 (November 7, 1996).

Kaido, T.J., Kash, R.L., Sasnett, M.W., Twa, M., Marcellino, G. and Schanzlin, D. 2002. Cytotoxic and mutagenic action of 193-nm and 213-nm laser radiation. J. Refrac. Sur. 18 : 529-534.

Kante, B., Couvreur, P., Dubois-Krack, G., De Meester, C., Guiot, P., Roland, M., Mercier, M., and Speiser, P. 1982. Toxicity of polyalkylcyanoacrylate nanoparticles I: free nanoparticles. J Pharm. Pharmacol. 71(7) : 786-792.

Kinget, R., and Greef, H. 1995. *In vitro* assessment of drug release from semi-solid lipid matrices. Eur. J. Pharm. Sci. 3: 105-111.

Krause, H.J., Schwarz, A., and Rohdewald, P. 1985. Polylactic acid nanoparticles, a colloidal drug delivery system fo rlipophilic drugs. Int J. Pharm. 27 : 145-155.

Krause, H.J., Schwarz, A., and Rohdewald, P. 1986. Interfacial polymerization, A useful method for the preparation of polymethylcyanoacrylate nanocaprticles. Drug Dev. Ind. Pharm. 12 : 527-552.

Kreuter, J. 1983. Evaluation of nanoparticles as drug-delivery systems I : Preparation methods. Pharm. Acta Helv. 58 : 196-208.

Kreuter, J. 1991. Nanoparticle based drug delivery systems. J. Controlled Relaease. 16 : 169-176.

Kreuter, J. 1994. Nanoparticles. In J. Kreuter (ed.) , Drugs and the Pharmaceutical Science, volume 66 : Colloidal drug delivery system, pp 219-343. New York : Marcell Dekker.

Kreuter, J., and Speiser, P. 1976. In vitro studies of poly(methylmethacrylate) adjuvants. J Pharm. Sci. 65 : 1624-1627.

Kreuter, J.,Wilson, C.G., Fry, J.R., Paterson, P., and Ratcliffe, J.H. 1984.Toxicity and association of polycyanoarylate nanoparticles with hepatocytes. J. Microencapsul. 3 : 253-257.

Law, D., Moore, C.B., and Denning, D.W. 1994. Bioassay for serum itraconazole concentrations using hydroxyitraconazole standards. Antimicrob Agents Chemother. 38 : 1561-1566.

Le Conte, P., Joly, V., Saint-Julien, L., Gillardin, J-M, Carbon, C., and Yeni, P. 1991. Tissue distribution and antifungal effect of liposomal itraconazole in experimental cryptococcosis and pulmonary aspergillosis. Am. Rev. Resp. Dis. 145 : 424-429.

Lehmann, R.A.W., Hayes, G.J., and Leonard, F. 1966. Toxicity of alkyl2-cyanoacrylates. I. Peripheral nerve. Arch. Surg. 93: 441-456.

Leonard,F. Kulkarni, R.K., Brandes, G., Nelso, J., and Cameron, J.J. 1966. Synthesis and degradation of poly(alkyl-cyanoacrylates). J.Appl. Polymer Sci. 10: 259-272.

Leroux, J.C., Allemann, E., Doelker, E., and Gurny, R. 1995. New approach for the preparation of nanoparticles by an emulsification-diffusion method. Eur. J. Pharm. Biopharm. 41 : 14-18.

Leroux, J.C., Cozens, R.M., Roesel, J.L., Galli, B., Doelker, E., and Gurny, R. 1996. pH-sensitive nanoparticles: an effective means to improve the oral delivery of HIV-1 protease inhibitors in dogs. Pharm. Res. 13(3) : 485-7.

Lescure, F., Zimmer, C., Roy, R. and Couveur, P. 1992. Optimization of poly(alkylcyanoacrylate) nanoparticles: influence of sulphur dioxide and pH on nanoparticles characteristics. J. Colloid Interf. Sci. 154 : 77–86.

Leu, D. 1983. Polyacylic nanoparticles as controlled release drug delivery systems. Dissertation No. 7184, ETH-Zurich.

Leung, S.H.S., Robinson, J.R., and Lee, V.H.L. 1987. Parenteral products. In J.R. Robinson, and V.H.L. lee (eds.), Food emulsions, 2nd ed., revised and expaned, pp. 433-480. New York: Marcel Dekker.

Levy, M.Y., and Betina, S. 1990. Drug release from submicronized o/w emulsion: a new *in vitro* kinetic evaluation model. Int. J. Pharm. 66: 29-37.

Lherm, C., Muller, R.H., Puisieux, F., and Couvreur, P. 1992. Alkylcyanoacrylate drug carriers : II. Cytotoxicity of cyanoacrylate nanoparticles with different alkyl chain length. Int.l J. Pharm. 84 : 13-22.

Lopez-Berestein, G. 1987. Liposomes as carriers of antimicrobial agents. Antimicrob Agents Chemother. 31 : 675-678.

Lostritto, R.T., Goei, L., and Silvestri, S.L. 1987. Theoretical considerations of drug release from submicron oil in water emulsions. J. Phar. Sci. Tech. Vol. 41, No.6/November-December: 214-219.

Lowe, P.J., and Temple, C.S. 1994. Calcitonin and insulin in isobutylcyanoacrylate nanocapsules : Protection against proteases and effect on intestinal absorption in rats. J Pharm. Pharmacol. 46 : 547-552.

McCarron, P.A., Woolfson,A.D., and Keating, S.M. 1999. Response surface methodology as a predictive tool for determining the effects of preparation conditions on the physicochemical properties of poly (isobutylcyanoacrylate) nanoparticles. Int. J. Pharm. 193: 37-47.

McCarron, P.A., Woolfson,A.D., and Keating, S.M. 2000. Sustained released of 5-fluorouracil from polymeric nanoparticles. J. Pharm. Pharmacol. 52: 1451-1459.

Montgomery, D.C. ed. 2001. Design and Analysis of Experiments. 5th ed. New York: Wiley & Sons.

Muller, R.H., Lherm, C., Herbort, J., Blunk, T., and Couereur, P. 1992. Alkylcyanoarylate drug carriers I. Physicochemical characterization of nanoparticles with different alkyl chain length. Int. J. Pharm. 84 : 1-11.

Muller, R.H., Mehnert, W., Lucks, J., Schwarz, C. Muhlen, A., Weyhers, H., Freitas, C., and Ruhl,D. 1995. Solid lipid nanoparticles(SLN)- An alternative colloidal carrier system for controlled drug delivery. Eur. J. Pharm. Biopharm. 41(1): 62-69.

Myers, R.H., and Montgomery, D.C. 2002. Response surface methodology. 2nd ed. New York: Wiley & Sons.

Nangia, A., Lam, F., and Hung, C.T. 1990. Formulation optimization of a hydrocolloid dressing. Drug Dev. Ind. Pharm. 16(14) : 2109-2123.

Niwa, T., Takeuchi, H., Hino, T., Kunou, N., and Kawashima, Y. 1993. Preparation of biodegradable nanospheres of water-soluble and insoluble drugs with D,L-lactide/glycolide copolymer by a novel spontaneous emulsificationsolvent diffusion method and the drug release behavior. J. Controlled Release. 25 : 89-98.

Peeters J, Neeskens P, Tollenaere JP, Van Remoortere P,and Brewster ME. 2002. Characterization of the interaction of 2-hydroxypropyl-β-cyclodextrin with itraconazole at pH 2, 4 and 7. J Pharm Sci. 91:1414-1422.

Prankerd, R.J., and Stella, V.J. 1990.The use of oil-in-water emulsions as a vehicle for parenteral drug administration. J. Parenter. Sci. Technol. 44 (3) : 139-49.

Prentice, A.G., Warnock, D.W., Johnson, S.A., Phillips, M.J., and Oliver, D.A. 1994. Multiple dose pharmacokinetics of an oral solution of itraconazole in autologous bone marrow transplant recipients. J. Antimicrob. Chemother. 34(2) : 247-52.

Puglisi, G., Fresta, M., Giammona, G., and Ventura, C.A. 1995. Influence of the preparation conditions on poly(ethyl cyanoacrylate) nanocapsule formation. Int. J. Pharm. 125 : 283-287.

Quintanar-Guerrero, D., Allemann, E., Doelker, E., and Fessi, H. 1998b. Preparation and characterization of nanocapsules from preformed polymers by a new process based on emulsification-diffusion technique. Pharm. Res. 15 : 1056-1062.

Quintanar-Guerrero, D., Allemann, E. Fessi, H., and Doelker, E. 1998a. Preparation techniques and mechanisms of formation of biodegradable nanoparticles from preformed polymers. Drug Dev. Ind. Pharm. 24 : 1113-1128.

Quintanar-Guerrero, D., Allemann, E., Fessi, H., and Doelker, E. 1997. Applications of the ion pair concept to hydrophilic substances with special emphasis on peptides. Pharm. Res. 14 : 119-127.

Quintanar-Guerrero, D., Fessi, H., Allemann, E., and Doelker, E. 1996. Influence of stabilizing agents and preparative variables on the formation of poly (D,L-lactic acid) nanoparticles by an emulsificaton-diffusion technique. Int. J. Pharm. 143 : 133-141.

Renoux, R., Demaziers, J.A., Cardot, J.M., and Aiache, J.M. 1996.Exprimentally designed optimization of direct compression tablets. Drug Dev. Ind. Pharm. 22(2), 103-109.

Rollot, J.M., Couvreur, Roblot-Treupel, L., and Puisieux, F. 1986. Physicochemical and morphological characterization of polyisobutyl cyanoacrylate nanocapsules. <u>J. Pharm. Sci</u>. 75(4) : 361-364.

Saarinen-Savolainen, P., Jarvinen, T., Taipale, H., and Urtti, A. 1997. Method for evaluating drug release from liposomes in sink conditions. <u>Int. J. Pharm.</u> 159: 27-33.

Santos-Magalhaes, N.S., Fessi, H., Puisieux, F., Benita, S., and Sheiller, M. 1995. An in vitro release kinetic examination and comparative evaluation between submicron emulsion and polylactic acid nanocapsules of clofibride. <u>J. Microencapsul.</u> 12 195-205.

Schwartz, J.B. 1990. Optimization techniques in pharmaceutical formulation and processing. In G.S. Banker, and C.T. Rhodes (eds.), <u>Modern pharmaceutics,</u> pp. 803,807. New York : Marcel Dekker.

Seijo, B., Fattal, E., Roblot-Treupel, L. and Couvreur, P. 1990. Design of nanoparticles of less than 50 nm diameter : preparation, characterization and drug loading. <u>Int. J. Pharm.</u> 62 : 1-7.

Shatrov, V.A., Ameyar, M., cai, Z., Bettaieb, A., and Chouaib, S. 1999. Methytransferase inhibitor S-adenosyl-L-homocysteine sensitizes human breast carcinoma MCF7 cells and related TNF-resistant derivatives to TNF-mediated cytotoxicity via the ceramide-independent partway. <u>European Cytokine Network.</u> 10(2) : 247-252.

Siekmann, B., and Westesen, K. 1995. Preparation and physicochemical characterization of aqueous dispersions of coenzyme Q10 nanoparticles. <u>Pharm. Res.</u> 12 (2) : 201-8.

Singh, M., Singh, M.P., Maiti, S.N., Gandhi, A., Micetich, R.G., and Atwal, H. 1993. Preparations of liposomal fluconazole and their in vitro antifungal activity. <u>J. Microencapsul.</u> 10 : 229-236.

Speiser, P.P. 1991. Nanoparticles and liposomes: a state of the art. <u>Methods Find. Exp. Clin. Pharmacol.</u> 13(5) : 337-342.

Stainmesse, S., Orecchioni, A.M., Nakache, E., Puisieux, F., and Fessi, H. 1995. Formulation and stabilization of a biodegradable polymeric colloidal suspension of nanoparticles. <u>Colloid and Polymer Science.</u> 273 : 505-511.

Stetsko, G. 1986. Statistical experimental design and its application to pharmaceutical development problems. <u>Drug Dev Ind Pharm.</u> 12 : 1109-1123.

Tasset,C., barrette,N., Thysman, S., Ketelslegers, J.M., Lemoine, D., and preat,V. 1995. Polybutylcyanoarylate nanoparticles as sustained release system for calcitonin. <u>J. Controlled Release.</u> 33 : 23-30.

The united States Pharmacopeil Convention. 1995. <u>The United States Pharmacopeia, 25th rev. The National Formulary,</u> 15th ed. Rockville : The United States Pharmacopeil Convention .

Thunemann, A.F., and General, S. 2001. Nanoparticles of a polyelectrolyte-fatty acid complex: carriers for Q10 and triiodothyronine. <u>J. Control Release.</u> 75(3) : 237-47.

Thumwanit,V., and Kedjarune, U. 1999. Cytotoxicity of polymerized commercial cyanoacrylate adhesive on cultured human oral fibroblast. <u>Australian Dental J.</u> 44(4) : 248-252.

Tukker, J.J., and de Blaey, C.J. 1983. Membranes in dissolution testing: a good choice?. <u>Drug Dev. Ind. Pharm.</u> 9(3) : 383-398.
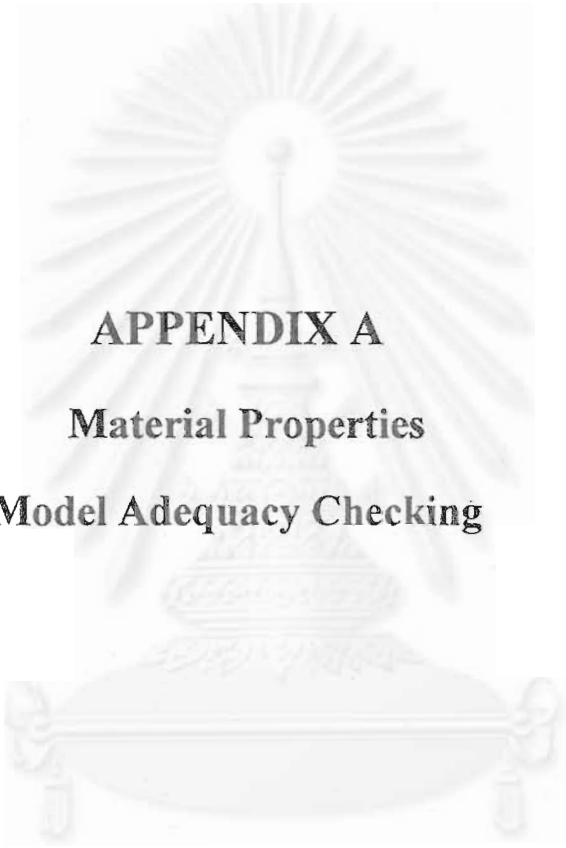
Valero, J., Espina, M., Gamisans, F. and Garcia, M.L. 1996. Effect of polymerization coadjuvants on nanocapsule elaboration and triamcinolone entrapment. <u>Drug Dev. Ind.Pharm.</u>   22 : 167-173 .

Vanderhoff, J.W., El-Aasser, M.S., and Ugelstad. 1979. <u>United States Patent</u> 4, 177, 177.

Vandervoort, J. and Ludwig, A., 2002. Biocompatible stabilizers in the preparation of PLGA nanoparticles: a factorial design study. <u>Int. J. Pharm.</u> 238 : 77–92.

Van Doorne, H., Bosch, E.H., and Lerk, C.F. 1988. Formation and antimicrobial activity of complexes of β-cyclodextrin and some antimycotic imidazole derivatives. <u>Pharm. Weekbl.</u> 10 : 80-85.

Vansnick, L., Couvreur, P., Christiaens-Leyh, D., and Roland, M. 1985. Molecular weights of free and drug-loaded nanoparticles. <u>Pharm. Res.</u> 1 : 36-41.

Vranckx, H., Demoustier, M., and Deleers, M. 1996. A new nanocapsules formulation with hydrophilic core: Application to the oral administration of salmon calcitonin in rats. <u>Eur. J. Pharm. Biopharm.</u> 42 : 345-347.

Wade, A ,and Weller , P.J. 1994. <u>Handbook of Pharmaceutical excipients.</u> The London: Pharmaceutical Press.

Wansan, K.M., and Lopez-Berestein, G. 1995. The past, present, and the future uses of liposomes in treating infectious diseases. <u>Immunopharmacol. Immunotoxicol.</u> 17 : 1-15.

Wasington, C. 1990. Drug release from microdisperse systems: a critical review. <u>Int. J. Pharm.</u> 58: 1-12.

Wise, D.L., Fellmann, T.D., Sanderson, J.E. and Wentworth, R.L. 1979. Lactic/glycolic acid polymers. In G. Gregoridas(ed.), <u>Drug Carriers in Biology and Medicine</u>, pp. 237-270. London : Academic Press.

Yamamoto,Y., Nakajima, M., Yamazaki, H., and Yokoi,T. 2001. Cytotoxicity and apoptosis produced by troglitazone in human hepatoma cells. <u>Life Sciences.</u> 70 : 471-482.

Yamaoka, T., Tabata, Y., and Ikada, Y. 1995. Comparison of body distribution of poly(vinyl alcohol) with other water-soluble polymers after intravenous administration.<u>J. Pharm. Pharmacol. </u> 47(6): 479-486.

Yoncheva,K., Vandervoort, J. and Ludwig, A., 2003. Influence of process parameters of high-pressure emulsification method on the properties of pilocarpine-loaded nanoparticles. <u>J. Microencapsul.</u> 20 : 449–458.

Yoo, H.S., Lee, K.H., Oh., J.E., and Park, T.G. 2000. In vitra and in vivo anti-tumor activities of nanoparticles based on doxorubicin-PLGA conjugates. <u>J. Controlled Release</u>. 68 : 419-431.

Yoo, S.D., Lee, S.H., Kang, E., Jun, H., Jung, J.Y., Park, J.W., and Lee, K.H. 2000. Bioavailability of itraconazole in rats and rabbits after administration of tablets containing solid dispersion particles. <u>Drug Dev Ind Pharm. </u> 26(1) : 27-34.

Zaghloul, A.A., Vaithiyalingam, S.R., Faltinek, J., Reddy, I.K., and Khan, M.A. 2001. Response surface methodology to obtain naproxen controlled release tablets from its microspheres with Eudragit L 100-55. <u>J. Microencapsul.</u> 18(5) : 651-662.

Zambaux, M.F., Bonneaux, F., Gref, R., Maincent, P., Dellacherie E., Alonso, M.J., Labrude, P., and Vigneron, C. 1998. Influence of experimental parameters on the characteristics of poly(lactic acid) nanoparticles prepared by a double emulsion method. <u>J. Controlled Release. </u> 50 : 31-40.

Zimmer, A., Kreuter, J. and Robinson, J., 1991. Studies on the transport pathway of PBCA nanoparticles in ocular tissues. <u>J. Microencapsul. </u> 8 : 497–504.

APPENDICES

APPENDIX A

Material Properties

Model Adequacy Checking

1. Soybean Oil

Synonyms

Calchem IVO-114, Lipex 200: soja bean oil: soya bean oil

Empirical Formula Molecular Weight

A typical analysis of refined soybean oil indicates the composition of the acids, present as glycerides, to be: linoleic acid 50-57%; linolenic acid 5-10%; oleic acid 17-26%; palmitic acid 9-13% and stearic acid 3-6%. Other acids are present in trace quantities.

Functional Category

Oleaginous vehicle; solvent

Applications in Pharmaceutical Formulation or Technology

In pharmaceutical preparations, soybean oil emulsions are primarily used as a fat source in total parenteral nutrition (TPN) regimen. Although other oils, such as peanut oil, have been used for this purpose, soybean oil is now preferred since it is associated with fewer adverse reactions. Emulsions containing soybean oil have also been used as vehicles for oral and intravenous administration of drugs; drug substances that have been incorporated into such emulsions include diazepam, oil soluble vitamin (A, D_2, E and K), poorly water soluble steroids and fluorocarboins. In addition, soybean oil has been included in formulations of liposomes.

Description

Soybean oil is a pale yellow colure, odourless or almost odourless liquid, with a bland taste.

Typical Properties

Density: 0.916-0.922 g/ml at 25° C

Solubility: practically insoluble in ethanol (95%) and water; miscible with carbon disulfide, chloroform, ether and petroleum spirit

Stability and Storage Conditions

Soybean oil is a stable material if protected from atmospheric oxygen. Soybean oil should be stored in a well-filled, airtight, light-resistant container at a temperature not exceeding 25 ° C

Safety

LD_{50} (mouse, IV): 22.1 g/Kg LD_{50} (rat, IV): 16.5 g/Kg

2. Medium Chain Triglycerides

Synonyms

Caprylic/capric triglyceride; Crodamol GTC/C; glyceryl tricaprylate/caprate; Miglyol 812; MCT oil

Empirical Formula Molecular Weight

A The fixed oil extracted from the lard, dried fraction of the endosperm of *Cocos nucifera* L. by hydrolysis, fractionation of the fatty acids obtained and re-esterification. It consists of a mixture of exclusively short or medium chain triglycerides of fatty acids, of which not less than 95 % are the saturated fatty acids octanoic (caprylic) acid and decanoic (capric) acid.

Structural Formula (Figure App.A.1)

$$H-\underset{\underset{H}{|}}{\overset{\overset{H}{|}}{C}}-O-R_1$$

$$H-C-O-R_2$$

$$H-\underset{\underset{H}{|}}{C}-O-R_3$$

Where $R_1 = -\overset{\overset{O}{\|}}{C}-(CH_2)_n CH_3$

$R_2 = -\overset{\overset{O}{\|}}{C}-(CH_2)_n CH_3$

$R_3 = -\overset{\overset{O}{\|}}{C}-(CH_2)_n CH_3$

$n = 6\text{-}8$
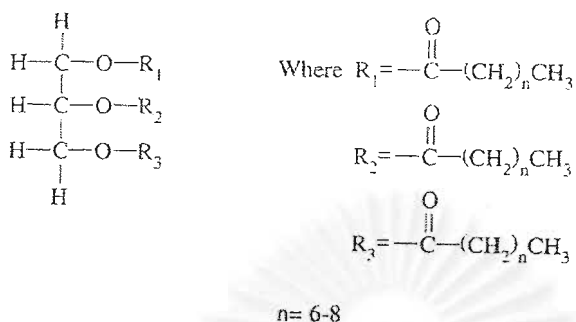
Figure App.A.1 Structural Formula of medium chain triglyceride

(Wade and Weller, 1994).

Functional Category

Emulsifying agent; solvent; suspending agent; therapeutic agent.

Applications in Pharmaceutical Formulation or Technology

Medium chain triglycerides have been used in a variety of pharmaceutical formulations including oral, parenteral and topical preparations.

In parenteral formulations, medium chain triglycerides have similarly been used in the production of emulsion, solutions or suspensions intended for intravenous administration. Medium chain triglycerides have been particularly investigated for their use in total parenteral nutrition (TPN) regimens in combination with long chain triglycerides.

Description
A colourless to slightly yellowish oily liquid which is practically odourless and tasteless. It solidifies at about 0 ° C and has a low viscosity even at temperatures near its solidification point.

Typical Properties

Density: 0.93-0.96 g/ml

Solubility: soluble in acetone, benzene, carbon tetrachloride, chloroform, dichloromethane, ethanol and miscible with long chain hydrocarbons and triglycerides; practical insoluble in water.

Stability and Storage Conditions

Medium chain triglycerides are stable over the wide range of storage temperatures that can be experienced in tropical and temperature climates. Ideally however, they should be stored at temperatures not exceeding 25 ° C and not exposed to temperature above 40° C for long periods of time.

Safety

LD$_{50}$ (mouse, IV): 3.7 g/Kg   LD$_{50}$ (rat, oral): 33.3 g/Kg

3. Benzyl Benzoate

Synonyms

Benzoic acid benzyl ester; benzylbenzenecarboxylate; benzyl phenylformate.

Empirical Formula   **Molecular Weight**

C$_{14}$H$_{12}$O$_2$ 212.24

Structure Formula (Figure App.A.2)
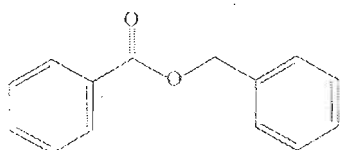
Figure App.A.2 Structural Formula of benzyl benzoate (Wade and Weller, 1994).

Functional Category

Plasticizer; solubilizing agent; solvent; therapeutic agent.

Applications in Pharmaceutical Formulation or Technology

Benzyl benzoate is used as a solubilizing agent and nonaqueous solvent in intramuscular injections at concentrations between 0.01%-46.0 % v/v. It is also used as a solvent and plasticizer for cellulose and nitrocellulose. However, the most widespread pharmaceutical use of benzyl benzoate is a topical therapeutic agent in treatment of scabies.

Description

Benzyl benzoate is a clear, colourless, oily liquid with a slightly aromatic odour. It produces a sharp, burning sensation on the tongue. At temperatures below 17° C it exists as clear, colourless crystals.

Typical Properties

Specific gravity: 1.12

Solubility: practical insoluble in glycerine and water; miscible with chloroform, ethanol (95%) and oils.

Stability and Storage Conditions

Benzyl benzoate is stable when stored in tight, well-filled, light resistant containers. Exposure to excessive heat should be avoided.

Safety

LD_{50} (mouse, oral): 1.47 g/Kg LD_{50} (rat, oral): 0.5 g/Kg

4. Corn Oil

Synonyms

Maize oil; refined maize oil

Empirical Formula   **Molecular Weight**

Corn oil is composed of fatty acid esters with glycerol, known commonly as triglycerides. Typical corn oil produced in the US contains five major fatty acids: linoleic 58.9%, oleic 25.8%, palmitic 11.0%; stearic 1.7%, and linolenic 1.1%. Corn oil also contains small quantities of plant sterols.

Functional Category

Oleaginous vehicle; solvent

Applications in Pharmaceutical Formulation or Technology

Corn oil is used primarily in pharmaceutical formulations as a solvent for intramuscular injections or as a vehicle for topical preparations.

Description

Clear, light yellow coloured, oily liquid with a faint characteristic odor and slightly nutty, sweet taste resembling cooked sweet corn.

Typical Properties

Density: 0.915-0.918 g/ml

Solubility: slightly soluble in ethanol (95%); miscible with benzene, chloroform, ether and hexane.

Stability and Storage Conditions

Corn oil is stable when protected with nitrogen in tightly sealed bottles. Corn oil may be sterilized by dry heat, maintaining it at 150° C for 1 hour.

Safety

No serious toxic manifestations after oral ingestion have been cited in the literature. Corn oil is considered a non-toxic and non-irritant material. Corn oil has an extensive history of usage in food preparation.

5. Poloxamer

Synonyms

Pluronic; poloxalkol;polyethylene-propylene glycol copolymer; polyoxyethylene-polyoxypropylene copolymer; Supronic; Synperonic.

Empirical Formula   Molecular Weight

The poloxamer polyols are a series of closely related block copolymers of ethylene oxide and propylene oxide conforming to the general formula:

HO $(C_2H_4O)_a (C_3H_6O)_b (C_2H_4O)_a$ H
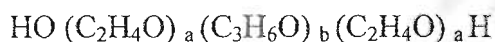
The grades included in the USP are shown below (Table App.A.1):

Table App.A.1: Poloxamer grades

Poloxamer	Physical form	a	b	Average molecular weight
124	liquid	12	20	2090-2360
188*	solid	80	27	7680-9510
237	solid	64	37	6840-8830
338	solid	141	44	12700-17400
407	solid	101	56	9840-14600

* Pluronic F68 is a synonym of poloxamer 188.

Functional Category

Dispersing agent; emulsifying and coemulsifying agent; solubilizing agent; tablet lubricant; wetting agent.

Applications in Pharmaceutical Formulation or Technology

Poloxamers are non-ionic polyoxyethylene-polyoxypropylene copolymers used primarily in pharmaceutical formulations as emulsifying or solubilizing agents. The polyoxyethylene segment is hydrophilic while the polyoxypropylene segment is hydrophobic. All of the poloxamers are chemically similar in composition,differing only in the relative amounts of propylene and ethylene oxides added during manufacture. Their physical and surface-active properties vary over a wide range and a number of different types are commercially available.

Poloxamers are used as emulsifying agents in intravenous fat emulsions, and as solubilizing and stabilizing agents to maintain the clarity of elixirs and syrups. Poloxamers may also be used as wetting agents, in ointments, suppository bases, gel, as tablet binder and coatings.

Description

Poloxamers generally occur as white-colored, waxy, free flowing prilled granules, or as cast solids. They are practically odourless and tasteless.

Typical Properties

Density: 1.06 g/ml at 25 ° C

Solubility: solubility varies according to the poloxamer type.

Stability and Storage Conditions

Poloxamer are stable materials. Aqueous solutions are stable in the presence of acids, alkalis, and metal ions. However, aqueous solutions do support mold growth.

Safety

Poloxamers are used in a variety of oral, parenteral, and topical pharmaceutic formulations and are generally regarded as non-toxic and nonirritanting and nonsensitizing when applied, in 5% w/v and 10 % w/v concentration, to the eyes, gums, and skin.

LD_{50} (mouse, IV): 1/Kg LD_{50} (rat, IV): 7.5 g/Kg

Model Adequacy Checking

It is always necessary to (a) examine the fitted model to ensure that it provides an adequate approximation to the true system and (b) verify that none of the least squares regression assumptions are violated. Proceeding with exploration and optimization of a fitted response surface will likely give poor or misleading results unless the model is an adequate fit.

(I) Residual Analysis

The residuals from the least squares fit, defined by $e_i = y_i - \hat{y}_i$, $i = 1, 2, ..., n$, play an important role in judging model adequacy. A check of the normality assumption may be made by constructing a normal probability plot of the residuals. If the residuals plot approximately along a straight line, then the normality assumption is satisfied. The straight line in this normal probability plot was determined by eye, concentrating on the central portion of the data. When this plot indicates problems with the normality assumption, the transformation of the response variable as a remedial measure is required. It is also useful to plot the residuals in time or run order and versus each of the individual regressors. Nonrandom patterns on these plots would indicate model inadequacy.

(II) Scaling Residuals

❖ *Standardized residual (d_i)*

$$d_i = \frac{e_i}{\hat{\sigma}} \qquad d_i = 1, 2, ..., n \tag{22}$$

$$\hat{\sigma} = \sqrt{MS_E} \tag{23}$$

The standardized residual and studentized residual have mean zero and approximately unit variance; consequently, they are useful in looking for outliers. Most of the standardized residuals should lie in the interval $-3 < d_i < 3$, and any observation with a standardized residual outside of this interval is potentially unusual with respect to its observed response. These outliers should be carefully examined, because they may represent something as simple as a data recording error or something of more serious concern, such as a region of the regressor variable space where the fitted model is a poor approximation to the true response surface. The standardizing process in Equation 16 scales the residuals by dividing them by their average standard deviation. In some data sets, residuals may have standard deviations that differ greatly.

❖ PRESS Residuals

The prediction error sum of squares (PRESS) proposed by Allen (1971, 1974) provides a useful residual scaling. To calculate PRESS, select an observation; for example, i. Fit the regression model to the remaining $n - 1$ observations and use this equation to predict the withheld observation y_i. The PRESS statistic is defined as the sum of squares of the n PRESS residuals as in

$$PRESS = \sum_{i=1}^{n} e_{(i)}^2 = \sum_{i=1}^{n} \left[y_i - \hat{y}_{(i)} \right]^2 \qquad (24)$$

Thus PRESS uses each possible subset of $n - 1$ observations as an estimation data set, and every observation in turn is used to form a prediction data set. PRESS can be used to compute an approximate R^2 for prediction,

$$R_{prediction}^2 = 1 - \frac{PRESS}{SS_T} \qquad (25)$$

This statistic gives some indication of the predictive capability of the regression model.

❖ *R Student*

The studentized residual (r) is often considered an outlier diagnostic. It is customary to use MS_E as an estimate of σ^2 in computing r_i. This is referred to as internal scaling of the residual, because MS_E is an internally generated estimate of σ^2 obtained from fitting the model to all n observations.

$$r_i \;=\; \frac{e_i}{\sqrt{\hat{\sigma}^2 \, (1 - h_{ii})}} \;, \qquad i = 1, 2, \ldots\ldots, n \tag{26}$$

(III)   Influence Diagnostics

Sometimes, parameter estimates or predictions may depend more on the influential subset than on the majority of the data. Some several useful measure of influence are as follows,

❖ *Leverage Points*

The disposition of points in x-space is important in determining model properties. In particular remote observations potentially have disproportionate leverage on the parameter estimates, the predicted values, and the usual summary statistics. The hat matrix $H = X(X'X)^{-1} X'$ is very useful in identifying influential observations., H determines the variances and covariances of $\hat{y}$ and e, because

$Var(\hat{y}) = \sigma^2 H$ and $Var(e) = \sigma^2 (I - H)$. The elements h_{ij} of H may be

interpreted as the amount of leverage exerted by y_j on $\hat{y}_i$. Thus inspection of the

elements of H can reveal points that are potentially influential by virtue of their

location in x-space. Attention is usually focused on the diagonal elements h_{ij}.

Because $\sum_{i=1}^{n} h_{ii} = rank(H) = rank(X) = p$, the average size of the diagonal

element of the matrix H is p/n. As a rough guideline, then, if a diagonal element

h_{ij} is greater than 2 p/n, observation i is a high-leverage point.

❖ Influence on Regression Coefficients

Cook (1977, 1979) has suggested using a measure of the squared distance

between the least squares estimate based on all n points b and the estimate

obtained by deleting the ith point, $b_{(i)}$. This distance measure can be expressed in

a general form as

$$D_i\,(M,c) \;=\; \frac{(b_{(i)} - b)'\, M\, (b_{(i)} - b)}{c}, \quad i = 1, 2, ..., n \tag{27}$$

The usual choices of M and c are $M = X'X$ and $c = pMS_E$, so that Equation 27

becomes

$$D_i\,(M,c) \;\equiv\; D_i \;=\; \frac{(b_{(i)} - b)'\, X'\, X\, (b_{(i)} - b)}{pMS_E}, \quad i = 1, 2, ..., n \tag{28}$$

Points with large values of D_i have considerable influence on the least squares

estimates b. The magnitude of D_i may be assessed by comparing it with $F_{\alpha, p, n-p}$.

If $D_i \cong F_{0.5, p, n-p}$ then deleting point i would move b to the boundary of a 50%

confidence region for β based on the complete data set. This is a large

displacement and indicates that the least squares estimate is sensitive to the i th

data point. Because, $F_{0.5,p,n-p} \cong 1$ points for which $D_i > 1$ are considered to be

influential. Practical experience has shown the cutoff value of 1 works well in

identifying influential points.

(IV) Testing for Lack of Fit

If there are n_i observations on the response at the ith level of the regressors x_i, $i =$

1, 2,..., m. y_{ij} denote the jth observation on the response at x_i , $i = 1, 2, ..., m$,

and $j = 1, 2, ..., n_i$. There are $n = \sum_{i=1}^{m} n_i$ observations together. The test

procedure involves partitioning the residual sum of squares into two components

$$SS_E = SS_{PE} + SS_{LOF} \tag{29}$$

Where SS_{PE} is the sum of squares due to pure error and SS_{LOF} is the sum of

squares due to lack of fit. The test statistic for lack of fit is

$$F_0 = \frac{SS_{LOF} / (m - p)}{SS_{PE}/(n - m)} = \frac{MS_{LOF}}{MS_{PE}} \tag{30}$$

The regression function is not linear if $F_0 > F_{\alpha, m-p, n-m}$. This

test procedure may be easily introduced into the analysis of variance conducted

for significance of regression. If the regression function is not linear, then the

tentative model must be abandoned and attempts made to find a more appropriate

equation.

APPENDIX B

Physicochemical Characterization of PIBCA Nanoparticles:
Particle Size and Distribution, Zeta Potential, Amount of
Itraconazole Entrapped in Nanoparticles (ITRAe)
and Encapsulation Efficiency (ITRAe[%]).

Table App. B.1 Effect of stirring rate on the particle size of itraconazole-loaded PIBCA nanoparticles.

Sirring rate (rpm)	Sample No.	Size (nm)			
		No. 1	No.2	No.3	Mean±S.D.
750	1	175.3	175.3	175.4	175.3±0.06
	2	176.8	176.9	176.9	176.9±0.06
1000	1	176.3	176.2	176.0	176.2±0.15
	2	175.3	175.4	175.8	175.5±0.26
1500	1	175.2	175.6	175.4	175.4±0.20
	2	176.3	176.8	176.7	176.6±0.26

Table App.B.2 Effect of stirring rate on the particle size distribution (PI) of itraconazole-loaded PIBCA nanoparticles.

Sirring rate (rpm)	Sample No.	Polydispersity index(PI)			
		No. 1	No.2	No.3	Mean±S.D.
750	1	0.085	0.080	0.081	0.082±0.0026
	2	0.085	0.083	0.084	0.084±0.0010
1000	1	0.082	0.084	0.086	0.084±0.0020
	2	0.084	0.085	0.082	0.084±0.0015
1500	1	0.081	0.083	0.084	0.083±0.0015
	2	0.083	0.087	0.084	0.085±0.0021

Table App. B.3 Effect of stirring rate on the zeta potential of itraconazole-loaded PIBCA nanoparticles.

Sirring rate (rpm)	Sample No.	Zeta potential			
		No. 1	No.2	No.3	Mean±S.D.
750	1	-46.7	-45.4	-52.1	-48.1±3.55
	2	-42.8	-43.6	-44.5	-43.6±0.85
1000	1	-42.8	-45.0	-43.9	-43.9±1.10
	2	-35.3	-36.2	-36.7	-36.1±0.71
1500	1	-43.6	-44.3	-43.9	-43.9±0.35
	2	-38.6	-37.5	-36.9	-37.7±0.86

Table App.B.4 Effect of surfactant concentrations on the particle size of itraconazole-loaded PIBCA nanoparticles.

Surfactant Concentration %	Sample No.	Size (nm)			
		No. 1	No.2	No.3	Mean±S.D.
0.25	1	175.3	175.3	175.4	175.3±0.06
	2	176.8	176.9	176.9	176.9±0.06
0.50	1	174.9	174.6	175.3	174.9±0.35
	2	176.2	176.9	176.4	176.5±0.36
0.75	1	175.6	175.9	175.4	175.6±0.25
	2	176.9	176.2	176.1	176.4±0.44
1.00	1	175.2	175.8	175.6	175.5±0.31
	2	174.6	174.9	175.0	174.8±0.21

Table App.B.5 Effect of surfactant concentrations on the particle size distribution (PI) of itraconazole-loaded PIBCA nanoparticles.

Surfactant Concentration %	Sample No.	polydispersity index			
		No. 1	No.2	No.3	Mean±S.D.
0.25	1	0.085	0.080	0.081	0.082±0.0026
	2	0.085	0.083	0.084	0.084±0.0010
0.50	1	0.087	0.085	0.080	0.084±0.0036
	2	0.081	0.085	0.083	0.083±0.0020
0.75	1	0.084	0.087	0.083	0.085±0.0021
	2	0.082	0.084	0.086	0.084±0.0020
1.00	1	0.083	0.081	0.089	0.084±0.0042
	2	0.085	0.083	0.084	0.084±0.0010

Table App.B.6 Effect of surfactant concentrations on the zeta potential of itraconazole-loaded PIBCA nanoparticles.

Surfactant Concentration %	Sample No.	Zeta potential			
		No. 1	No.2	No.3	Mean±S.D.
0.25	1	-46.7	-45.4	-52.1	-48.1±3.55
	2	-42.8	-43.6	-44.5	-43.6±0.85
0.50	1	-41.5	-41.4	-42.4	-41.8±0.55
	2	-46.4	-50.5	-51.5	-49.5±2.70
0.75	1	-49.9	-51.6	-51.8	-51.1±1.04
	2	-37.6	-38.6	-40.8	-39.0±1.64
1.00	1	-36.3	-37.8	-38.4	-37.5±1.08
	2	-41.9	-43.9	-42.9	-42.9±1.00

Table App. B. 7 Particle size of itraconazole-loaded PIBCA nanoparticles:

Factorial design study.

Concentration of IBCA monomer in organic phase (μL/mL)	Concentration of benzyl benzoate in organic phase (μg/mL)	Concentration of itraconazole in orgaic phase (μg/mL)	size (nm)			
			No.1	No. 2	No.3	Mean±S.D.
1	5	200	144.1	144.3	144.2	144.2± 0.10
			148.1	148.3	147.9	148.1± 0.20
		1050	144.4	141.8	141.7	142.6± 1.53
			143.9	143.8	144.0	143.9± 0.10
		1900	140.6	140.5	140.7	140.6± 0.10
			145.9	145.7	146.1	145.9± 0.20
	12.5	200	160.8	160.6	161.0	160.8± 0.20
			161.2	163.4	160.6	161.7± 1.47
		1050	159.6	159.7	159.6	159.6± 0.06
			160.9	160.8	161.0	160.9± 0.10
		1900	158.6	158.9	158.3	158.6± 0.30
			160.8	160.9	160.7	160.8± 0.10
	20	200	185.1	185.1	185.2	185.1± 0.06
			182.6	182.7	182.5	182.6± 0.10
		1050	181.5	181.4	181.6	181.5± 0.10
			175.6	175.5	175.7	175.6± 0.10
		1900	184.3	184.4	184.2	184.3± 0.10
			180.6	180.7	180.8	180.7± 0.10
5.5	5	200	160.8	160.8	160.7	160.8± 0.06
			165.0	165.2	165.4	165.2± 0.20
		1050	159.7	159.6	159.6	159.6± 0.06
			160.3	160.4	160.3	160.3± 0.06
		1900	160.2	160.3	160.4	160.3± 0.10
			162.5	162.3	162.1	162.3± 0.20
	12.5	200	179.5	179.6	179.4	179.5± 0.10
			172.6	172.5	172.4	172.5± 0.10
		1050	175.3	175.3	175.4	175.3± 0.06
			176.8	176.9	176.9	176.9± 0.06
		1900	171.6	171.7	171.6	171.6± 0.06
			173.2	173.3	173.2	173.2± 0.06
	20	200	195.8	195.7	195.6	195.7± 0.10
			199.8	199.6	199.4	199.6± 0.20
		1050	195.4	195.6	195.8	195.6± 0.20
			191.8	191.9	191.8	191.8± 0.20
		1900	191.6	191.8	191.4	191.6± 0.20
			193.6	193.8	193.4	193.6± 0.20
10	5	200	154.1	154.3	154.5	154.3± 0.20
			153.2	153.2	153.3	153.2± 0.06
		1050	155.1	155.3	155.5	155.3± 0.20
			149.8	149.7	149.9	149.8± 0.10
		1900	154.3	154.4	154.2	154.3± 0.10
			153.9	154.0	153.8	153.9± 0.10
	12.5	200	170.8	170.6	170.4	170.6± 0.20
			169.3	169.2	169.4	169.3± 0.10
		1050	172.6	172.7	172.5	172.6± 0.10
			167.7	167.8	167.8	167.8± 0.06
		1900	171.1	171.2	171.1	171.1± 0.06
			172.4	172.3	172.3	172.3± 0.06
	20	200	193.6	193.6	193.7	193.6± 0.06
			197.4	197.5	197.6	197.5± 0.10
		1050	194.5	194.6	194.4	194.5± 0.10
			195.7	195.6	195.5	195.6± 0.06
		1900	193.8	193.8	193.7	193.8± 0.06
			199.5	199.6	199.7	199.6± 0.10

Table App.B.8 Particle size distribution (PI) of itraconazole-loaded PIBCA nanoparticles: Factorial design study.

Concentration of IBCA (µL/mL)	Contration of benzyl benzoate (µg/mL)	Concentration of itraconzole (µg/mL)	Polydispersity index (PI)			
			No.1	No. 2	No.3	Mean±S.D.
1	5	200	0.045	0.046	0.044	0.045±0.0010
			0.044	0.046	0.045	0.045±0.0010
		1050	0.048	0.049	0.047	0.048±0.0010
			0.045	0.044	0.043	0.044±0.0010
		1900	0.049	0.054	0.050	0.051±0.0026
			0.049	0.047	0.051	0.049±0.0020
	12.5	200	0.070	0.065	0.069	0.068±0.0026
			0.075	0.077	0.073	0.075±0.0020
		1050	0.077	0.074	0.074	0.075±0.0017
			0.074	0.071	0.068	0.071±0.0030
		1900	0.071	0.076	0.069	0.072±0.0036
			0.075	0.076	0.071	0.074±0.0026
	20	200	0.094	0.096	0.101	0.097±0.0036
			0.103	0.096	0.098	0.099±0.0036
		1050	0.094	0.090	0.089	0.091±0.0026
			0.096	0.089	0.088	0.091±0.0044
		1900	0.093	0.098	0.091	0.094±0.0036
			0.096	0.095	0.091	0.094±0.0026
5.5	5	200	0.058	0.061	0.058	0.059±0.0017
			0.055	0.049	0.052	0.052±0.0030
		1050	0.059	0.052	0.066	0.059±0.0070
			0.055	0.059	0.057	0.057±0.0020
		1900	0.060	0.058	0.056	0.058±0.0020
			0.055	0.058	0.058	0.057±0.0017
	12.5	200	0.082	0.084	0.077	0.081±0.0036
			0.088	0.081	0.077	0.082±0.0056
		1050	0.085	0.080	0.081	0.082±0.0026
			0.085	0.083	0.084	0.084±0.0010
		1900	0.082	0.085	0.088	0.085±0.0030
			0.084	0.081	0.087	0.084±0.0030
	20	200	0.095	0.099	0.093	0.096±0.0035
			0.099	0.102	0.096	0.099±0.0030
		1050	0.099	0.093	0.099	0.097±0.0035
			0.098	0.095	0.098	0.097±0.0017
		1900	0.098	0.096	0.097	0.097±0.0010
			0.096	0.092	0.097	0.095±0.0026
10	5	200	0.059	0.055	0.060	0.058±0.0026
			0.062	0.064	0.063	0.063±0.0010
		1050	0.055	0.058	0.064	0.059±0.0046
			0.063	0.065	0.064	0.064±0.0010
		1900	0.066	0.063	0.060	0.063±0.0030
			0.062	0.065	0.068	0.065±0.0030
	12.5	200	0.078	0.079	0.077	0.078±0.0010
			0.083	0.085	0.078	0.082±0.0036
		1050	0.081	0.079	0.083	0.081±0.0020
			0.081	0.082	0.080	0.081±0.0010
		1900	0.084	0.085	0.080	0.083±0.0026
			0.085	0.081	0.080	0.082±0.0026
	20	200	0.093	0.091	0.098	0.094±0.0036
			0.096	0.102	0.099	0.099±0.0030
		1050	0.103	0.099	0.095	0.099±0.0040
			0.096	0.092	0.091	0.093±0.0026
		1900	0.099	0.102	0.093	0.098±0.0046
			0.097	0.102	0.098	0.099±0.0026

Table App.B.9 The amount of itraconazole entrapped in nanoparticles (ITRAe) of itraconazole-loaded PIBCA nanoparticles: Factorial design study.

Concentration of IBCA (μL/mL)	Contration of benzyl benzoate (μg/mL)	Concentration of itraconzole (μg/mL)	Amount of itraconazole entrapped in nanoparticles (ITRAe)		
			No.1	No. 2	Mean±S.D.
1	5	200	125.90 / 126.90	132.50 / 132.70	129.20±4.67 / 129.80±4.10
		1050	290.60 / 293.60	298.40 / 299.00	294.50±5.52 / 296.30±3.82
		1900	295.60 / 299.60	300.60 / 301.00	298.10±3.54 / 300.30±0.99
	12.5	200	153.60 / 148.90	147.00 / 152.30	150.30±4.67 / 150.60±2.40
		1050	365.20 / 361.20	370.00 / 382.60	367.60±3.39 / 371.90±15.13
		1900	410.30 / 412.30	426.90 / 427.10	418.60±11.74 / 419.70±10.47
	20	200	135.90 / 146.30	145.30 / 139.60	140.60±6.65 / 141.00±4.74
		1050	300.90 / 306.90	320.70 / 324.30	310.80±14.00 / 315.60±12.30
		1900	369.50 / 380.90	391.70 / 398.10	380.60±15.70 / 389.50±12.16
5.5	5	200	135.20 / 135.60	141.60 / 145.20	138.40±4.53 / 140.40±6.79
		1050	352.30 / 350.60	368.70 / 379.60	360.50±11.60 / 365.10±20.51
		1900	410.90 / 416.20	428.30 / 426.80	419.60±12.30 / 421.50±7.50
	12.5	200	158.30 / 159.60	166.70 / 167.40	162.50±5.94 / 163.50±5.52
		1050	471.60 / 479.30	489.80 / 491.70	480.70±12.87 / 485.50±8.77
		1900	562.60 / 579.60	597.80 / 605.80	580.20±24.89 / 592.70±18.53
	20	200	146.90 / 150.60	154.02 / 159.80	150.46±5.03 / 155.20±6.51
		1050	395.60 / 399.80	404.86 / 411.40	400.23±6.55 / 405.60±8.20
		1900	541.60 / 546.30	558.80 / 566.30	550.20±12.16 / 556.30±14.14
10	5	200	144.50 / 146.30	150.30 / 151.70	147.40±4.10 / 149.00±3.82
		1050	339.60 / 345.60	360.80 / 368.80	350.20±14.99 / 357.20±16.40
		1900	440.10 / 441.60	455.10 / 459.00	447.60±10.61 / 450.30±12.30
	12.5	200	156.70 / 159.60	165.30 / 170.80	161.00±6.08 / 165.20±7.92
		1050	510.60 / 528.30	530.40 / 533.10	520.50±14.00 / 530.70±3.39
		1900	650.40 / 649.60	670.60 / 689.20	660.50±14.28 / 669.40±28.00
	20	200	150.60 / 154.00	155.40 / 160.00	153.00±3.39 / 157.00±4.24
		1050	500.60 / 520.60	524.20 / 531.50	512.40±16.69 / 526.05±7.71
		1900	630.40 / 639.60	642.60 / 660.00	636.50±8.63 / 649.80±14.42

Table App.B.10 The encapsulation efficiency (ITRAe [%]) of itraconazole-loaded PIBCA nanoparticles: Factorial design study.

Concentration of IBCA (μL/mL)	Contration of benzyl benzoate (μg/mL)	Concentration of itraconzole (μg/mL)	Encapsulation efficiency (ITRAe [%])		
			No.1	No. 2	Mean±S.D.
1	5	200	62.95	66.25	64.60±2.33
			63.45	66.35	64.90±2.05
		1050	27.68	28.42	28.04±0.53
			27.96	28.48	28.21±0.36
		1900	15.56	15.82	15.68±0.19
			15.77	15.84	15.81±0.05
	12.5	200	76.80	73.50	75.15±2.33
			74.45	76.15	75.30±1.20
		1050	34.78	35.24	35.00±0.32
			34.40	36.44	35.42±1.44
		1900	21.59	22.47	22.03±0.62
			21.70	22.48	22.09±0.55
	20	200	67.95	72.65	70.30±3.32
			73.15	69.80	71.48±2.37
		1050	28.66	30.54	29.60±1.33
			29.23	30.89	30.06±1.17
		1900	19.45	20.62	20.03±0.83
			20.05	20.95	20.50±0.64
5.5	5	200	67.60	70.80	69.20±2.26
			67.80	72.60	70.20±3.39
		1050	33.55	35.11	34.33±1.10
			33.39	36.15	34.77±1.95
		1900	21.63	22.54	22.08±0.65
			21.91	22.46	22.18±0.39
	12.5	200	79.15	83.35	81.25±2.97
			79.80	83.70	81.75±2.76
		1050	44.91	46.65	45.78±1.23
			45.65	46.83	46.24±0.84
		1900	29.61	31.46	30.54±1.31
			30.51	31.88	31.19±0.98
	20	200	73.45	77.01	75.23±2.52
			75.30	79.90	77.60±3.25
		1050	37.68	38.56	38.12±0.62
			38.08	39.18	38.63±0.78
		1900	28.51	29.41	28.95±0.64
			28.75	29.81	29.28±0.74
10	5	200	72.25	75.15	73.70±2.05
			73.15	75.85	74.50±1.91
		1050	32.34	34.36	33.35±1.43
			32.91	35.12	34.02±1.56
		1900	23.16	23.95	23.56±0.56
			23.24	24.16	23.70±0.65
	12.5	200	78.35	82.65	80.50±3.04
			79.80	85.40	82.60±3.96
		1050	48.63	50.51	49.57±1.33
			50.31	50.77	50.54±0.32
		1900	34.23	35.29	34.76±0.75
			34.19	36.27	35.23±1.47
	20	200	75.30	77.70	76.50±1.70
			77.00	80.00	78.50±2.12
		1050	47.68	49.92	48.80±1.59
			49.58	50.62	50.10±0.73
		1900	33.18	33.82	33.50±0.45
			33.66	34.74	34.20±0.76

APPENDIX C

Physicochemical Characterization of PLGA Nanoparticles:
Particle Size and Distribution, Zeta Potential, Amount of
Itraconazole Entrapped in Nanoparticles (ITRAe)
and Encapsulation Efficiency (ITRAe[%]).

Table App.C.1 Effect of stirring rate on the particle size of itraconazole-loaded PLGA nanoparticles.

Stirring rate (rpm)	Sample No.	Size (nm)			
		No. 1	No.2	No.3	Mean±S.D.
750	1	452.6	470.6	477.5	466.9±12.86
	2	458.9	470.6	473.6	467.7±7.77
1000	1	460.9	458.9	470.2	463.3±6.03
	2	452.6	473.6	469.3	465.2±11.09
1500	1	463.3	478.2	470.2	470.6±7.46
	2	460.2	452.3	471.3	461.3±9.54

Table App.C.2 Effect of stirring rate on the particle size distribution (PI) of itraconazole-loaded PLGA nanoparticles.

Stirring rate (rpm)	Sample No.	Polydispersity index (PI)			
		No. 1	No.2	No.3	Mean±S.D.
750	1	0.612	0.639	0.633	0.628 ±0.0142
	2	0.569	0.599	0.584	0.584±0.0150
1000	1	0.603	0.623	0.591	0.606±0.0162
	2	0.567	0.590	0.631	0.596±0.0324
1500	1	0.587	0.652	0.602	0.614±0.0340
	2	0.663	0.604	0.584	0.617±0.0411

Table App. C.3   Effect of stirring rate on the zeta potential of itraconazole-loaded PLGA nanoparticles.

Stirring rate (rpm)	Sample No.	Zeta potential			
		No. 1	No.2	No.3	Mean±S.D.
750	1	-32.5	-35.6	-33.5	-33.9±1.58
	2	-36.5	-36.1	-32.6	-35.1±2.15
1000	1	-33.6	-34.5	-34.7	-34.3±0.59
	2	-30.2	-31.6	-30.1	-30.6±0.84
1500	1	-28.9	-32.1	-33.9	-31.6±2.53
	2	-35.6	-31.2	-34.3	-33.7±2.26

Table App.C.4 Effect of surfactant concentrations on the particle size of itraconazole-loaded PLGA nanoparticles.

Surfactant Concentration %	Sample No.	Size (nm)			
		No. 1	No.2	No.3	Mean±S.D.
0.25	1	452.6	470.6	477.5	466.9±12.86
	2	458.9	470.6	473.6	467.7±7.77
0.50	1	455.6	460.2	471.5	462.4±8.18
	2	452.3	480.9	471.2	468.1±14.54
0.75	1	465.2	472.3	482.3	473.3±8.59
	2	459.5	468.2	458.7	462.1±5.27
1.00	1	476.3	462.5	473.6	470.8±7.31
	2	455.2	468.9	467.2	463.8±7.47

Table App.C.5 Effect of surfactant concentrations on the particle size distribution (PI) of itraconazole-loaded PLGA nanoparticles.

Surfactant Concentration %	Sample No.	polydispersity index (PI)			
		No. 1	No.2	No.3	Mean±S.D.
0.25	1	0.612	0.639	0.633	0.628 ±0.0142
	2	0.569	0.599	0.584	0.584±0.0150
0.50	1	0.623	0.603	0.582	0.603±0.0205
	2	0.559	0.593	0.543	0.565±0.0255
0.75	1	0.603	0.625	0.599	0.609±0.0140
	2	0.562	0.598	0.639	0.600±0.0385
1.00	1	0.614	0.558	0.605	0.592±0.0301
	2	0.644	0.631	0.589	0.621±0.0287

Table App.C.6 Effect of surfactant concentrations on the zeta potential of itraconazole-loaded PLGA nanoparticles.

Surfactant Concentration %	Sample No.	Zeta potential			
		No. 1	No.2	No.3	Mean±S.D.
0.25	1	-32.5	-35.6	-33.5	-33.9±1.58
	2	-36.5	-36.1	-32.6	-35.1±2.15
0.50	1	-32.6	-33.6	-31.5	-32.6±1.05
	2	-35.6	-32.9	-34.6	-34.4±1.37
0.75	1	-33.6	-34.6	-31.6	-33.3±1.53
	2	-32.6	-31.5	-34.5	-32.9±1.52
1.00	1	-33.8	-30.5	-35.6	-33.3±2.59
	2	-33.6	-31.6	-31.6	-32.3±1.15

Table App.C.7 Particle size of itraconazole-loaded PLGA nanoparticles:

Factorial design study.

Concentration of PLGA (mg/mL)	Contration of benzyl benzoate (μg/mL)	Concentration of itraconzole (μg/mL)	Particle size (nm)			
			No.1	No. 2	No.3	Mean±S.D.
10	5	200	195.6	186.6	1995.5	193.9±6.62
			196.3	186.3	187.4	190.0±5.48
		1800	302.6	319.6	310.2	310.8±8.52
			298.6	315.6	306.5	306.9±8.51
	20	200	296.9	314.5	305.4	305.6±8.80
			312.3	299.6	301.0	304.3±6.96
		1800	439.6	419.5	417.7	425.6±12.16
			419.6	430.9	411.3	420.6±9.84
55	12.5	1000	450.6	475.6	457.4	461.2±12.93
			468.7	449.6	456.6	458.3±9.66
			452.6	470.6	477.5	466.9±12.86
			458.9	470.6	473.6	467.7±7.77
			452.8	470.6	458.1	460.5±9.14
100	5	200	256.3	240.6	251.9	249.6±8.10
			246.3	234.6	235.8	238.9±6.44
		1800	529.6	548.6	540.6	539.6±9.54
			536.9	547.9	546.0	543.6±5.88
	20	200	335.6	319.8	333.4	329.6±8.56
			331.6	350.2	331.0	337.6±10.92
		1800	655.6	632.6	643.5	643.9±11.51
			647.8	625.9	644.8	639.5±11.87

Table App.C.8   Particle size distribution (PI) of itraconazole-loaded PLGA

nanoparticles: Factorial design study.

Concentration of PLGA (mg/mL)	Contration of benzyl benzoate (μg/mL)	Concentration of itraconzole (μg/mL)	Polydispersity index (PI)			
			No.1	No. 2	No.3	Mean±S.D.
10	5	200	0.445	0.465	0.458	0.456±0.0101
			0.501	0.546	0.522	0.523±0.0225
		1800	0.602	0.632	0.635	0.623±0.0182
			0.561	0.598	0.587	0.582±0.0190
	20	200	0.544	0.569	0.549	0.554±0.0132
			0.481	0.503	0.504	0.496±0.0130
		1800	0.432	0.462	0.465	0.453±0.0182
			0.619	0.589	0.598	0.602±0.0154
55	12.5	1000	0.622	0.598	0.622	0.614±0.0139
			0.468	0.506	0.493	0.489±0.0193
			0.612	0.639	0.633	0.628±0.0142
			0.569	0.599	0.584	0.584±0.0150
			0.469	0.489	0.476	0.478±0.0101
100	5	200	0.441	0.465	0.450	0.452±0.0121
			0.622	0.642	0.632	0.632±0.0100
		1800	0.564	0.598	0.599	0.587±0.0199
			0.487	0.502	0.499	0.496±0.0079
	20	200	0.532	0.559	0.547	0.546±0.0135
			0.611	0.636	0.622	0.623±0.0125
		1800	0.556	0.598	0.598	0.584±0.0242
			0.585	0.603	0.600	0.596±0.0096

Table App.C.9 The amount of itraconazole entrapped in nanoparticles (ITRAe) of itraconazole-loaded PLGA nanoparticles: Factorial design study.

Concentration of PLGA (μg/mL)	Contration of benzyl benzoate (μg/mL)	Concentration of itraconzole (μg/mL)	Amount of itraconazole entrapped in nanoparticles (ITRAe)		
			No.1	No. 2	Mean±S.D.
10	5	200	90.65	105.91	98.28±10.79
			92.60	113.32	102.96±14.65
		1800	352.60	377.80	365.20±17.82
			345.00	366.20	355.60±14.99
	20	200	149.60	158.84	154.22±6.53
			155.70	164.24	159.97±6.04
		1800	985.72	966.88	976.30±13.32
			995.63	971.05	983.34±17.38
55	12.5	1000	710.58	692.02	701.30±13.12
			724.50	700.70	712.60±16.83
			714.60	696.60	705.60±12.73
			679.63	718.97	699.30±27.82
			710.54	701.86	706.20±6.14
100	5	200	120.54	127.40	123.97±4.85
			120.64	127.60	124.12±4.92
		1800	615.39	642.35	628.87±19.06
			628.96	634.98	631.97±4.26
	20	200	174.89	183.71	179.3±6.24
			173.54	179.26	176.4±4.04
		1800	1220.56	1278.64	1249.6±41.07
			1243.63	1269.97	1256.8±18.63

Table App.C.10 The the encapsulation efficiency (ITRAe [%]) of itraconazole-loaded PLGA nanoparticles: Factorial design study.

Concentration of PLGA (mg/mL)	Contration of benzyl benzoate (μg/mL)	Concentration of itraconzole (μg/mL)	Encapsulation efficiency (ITRAe [%])		
			No.1	No. 2	Mean±S.D.
10	5	200	45.33	52.96	49.14±5.40
			46.30	56.66	51.48±7.33
		1800	19.59	20.99	20.29±0.99
			19.17	20.34	19.76±0.83
	20	200	74.80	79.42	77.11±3.27
			77.85	82.12	79.99±3.02
		1800	54.76	53.72	54.24±0.74
			55.31	53.95	54.63±0.97
55	12.5	1000	71.06	69.20	70.13±1.31
			72.45	70.07	71.26±1.68
			71.46	69.66	70.56±1.27
			67.96	71.90	69.93±2.78
			71.05	70.19	70.62±0.61
100	5	200	60.27	63.70	61.98±2.43
			60.32	63.80	62.06±2.46
		1800	34.19	35.69	34.94±1.06
			34.94	35.28	35.11±0.24
	20	200	87.45	91.86	89.65±3.12
			86.77	89.63	88.20±2.02
		1800	67.81	71.04	69.42±2.28
			69.09	70.55	69.82±1.03

APPENDIX D

High-Performance Liquid Chromatographic

Technique for Drug Analysis

Stability Data

HPLC chromatogram from **Figure App. D.1 - Figure App. D.5** showed that this

method had specificity to measure itraconazole.

Figure App.D.1 HPLC chromatogram of standard itraconazole solution with

internal standard (ketoconazole).

Ketoconazole

Itraconazole

Figure App.D.2   HPLC chromatogram of unloaded PIBCA nanoparticles.

Benzyl benzoate+ PIBCA polymer

Figure App.D.3   HPLC chromatogram of   unloaded PIBCA nanoparticles

with internal standard (ketoconazole).

Ketoconazole
Benzyl benzoate+PIBCA polymer
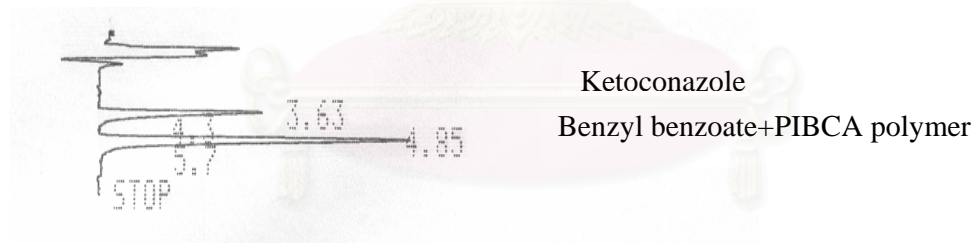
Figure App.D.4 HPLC chromatogram of   standard itraconazole with unloaded

PIBCA nanoparticles and internal standard (ketoconazole).

Ketoconazole
Benzyl benzoate+PIBCA polymer

Itraconazole

Figure App.D.5   HPLC chromatogram of unloaded PLGA nanoparticles.

Benzyl benzoate+ PLGA polymer

Table App. D.1 The Analytical recovery of itraconazole.

Known cocentration (μg/mL)	Calculated concentration from calibration curve (μg/mL)	% Recovery
1.25	1.2693	101.55
	1.2777	102.23
	1.2788	102.31
	1.2646	101.17
	1.2694	101.55
2.50	2.4765	99.06
	2.5153	100.61
	2.4920	99.68
	2.4848	99.39
	2.5136	100.54
5.00	4.9877	99.75
	5.0057	100.11
	4.9716	99.43
	4.9934	99.87
	5.0047	100.09
7.50	7.4688	99.58
	7.5463	100.62
	7.4461	99.28
	7.3856	98.47
	7.4206	98.94
10.00	10.0964	100.96
	10.0019	100.02
	10.0236	100.24
	9.9669	99.67
	10.1059	101.05
Mean		100.25
S.D.		1.00
%C.V.		1.00
95% confidence interval		

The within run and between run coefficient of variation of standard itraconazole in methanol ranged from 0.34-0.70% (**Table App. D.2- Table App.D.4**)

Table App. D.2   Within run precision.

Itraconazole concentration (μg/mL)	Calculated concentration from calibration curve (μg/mL)	Mean	%C.V.
1.25	1.2693	1.2754	0.41
	1.2777		
	1.2788		
2.50	2.4765	2.4946	0.78
	2.5153		
	2.4920		
5.00	4.9877	4.9883	0.34
	5.0057		
	4.9716		
7.50	7.4688	7.4871	0.70
	7.5463		
	7.4461		
10.00	10.0964	10.0406	0.49
	10.0019		
	10.0236		

Table App. D.3   Between run precision.

Itraconazole concentration (μg/mL)	Day	Calculated concentration from calibration curve (μg/mL)	Mean	%C.V.
1.25	1	1.2788	1.2709	0.56
	2	1.2646		
	3	1.2694		
2.50	1	2.4920	2.4968	0.60
	2	2.4848		
	3	2.5136		
5.00	1	4.9716	4.9899	0.34
	2	4.9934		
	3	5.0047		
7.50	1	7.4461	7.4175	0.41
	2	7.3856		
	3	7.4206		
10.00	1	10.0236	10.0321	0.70
	2	9.9669		
	3	10.1059		

The standard curve of peak area ratio against concentration for itraconazole is shown

in **Figure App.D.6**. Linear regression analysis showed the standard curve to be linear

over the concentration range 1.25-10 μg/mL ($r^2 = 0.9999$)

Table App. D.4 Linearity of itraconazole.

Itraconazole concentration (μg/mL)	Peak area ratio	Mean	%C.V.
1.25	0.1261	0.12638	0.51
	0.1270		
	0.1271		
	0.1256		
	0.1261		
2.50	0.2538	0.25592	0.72
	0.2579		
	0.2555		
	0.2547		
	0.2577		
5.00	0.5195	0.52002	0.28
	0.5214		
	0.5178		
	0.5201		
	0.5213		
7.50	0.7820	0.78038	0.82
	0.7902		
	0.7796		
	0.7732		
	0.7769		
10.00	1.0600	1.05392	0.61
	1.0500		
	1.0523		
	1.0463		
	1.0610		

Figure App.D.6. The linearity of itraconazole in standard solution.
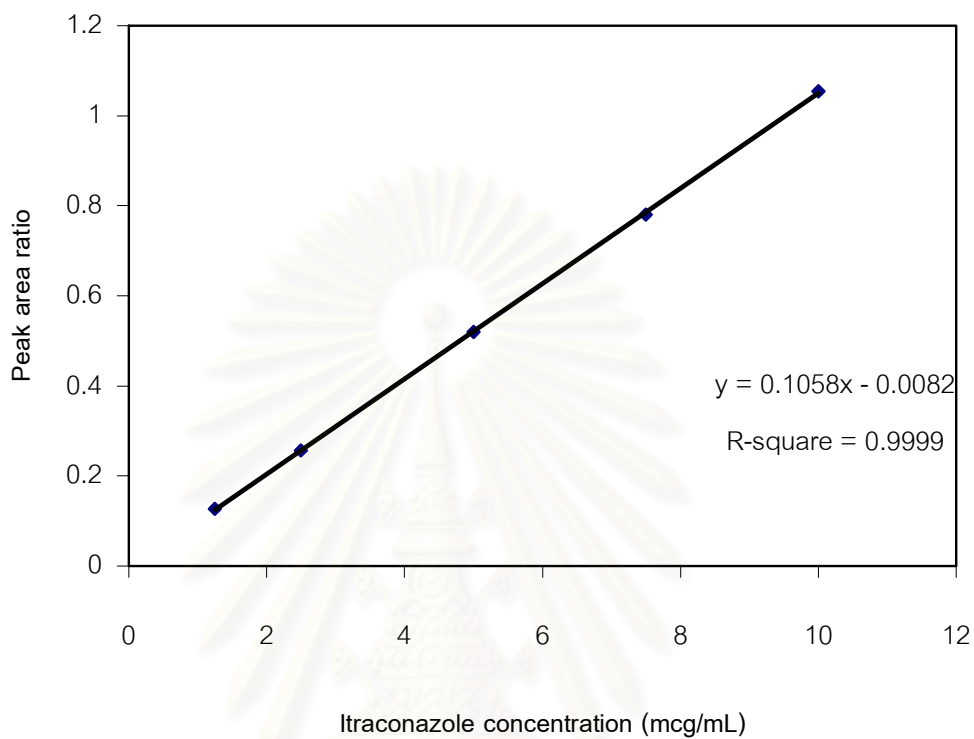
The standard curve of peak area against concentration for itraconazole in different

oils is shown in **Figure App.D.7.** Linear regression analysis showed the standard

curve to be linear over the concentration range 1.25-10 μg/mL ($r^2 > 0.990$)(**Table**

App. D.5)

Figure App.D.7 Standard curve for itraconazole inmethanol as determined by

HPLC (values represent means, n=5).
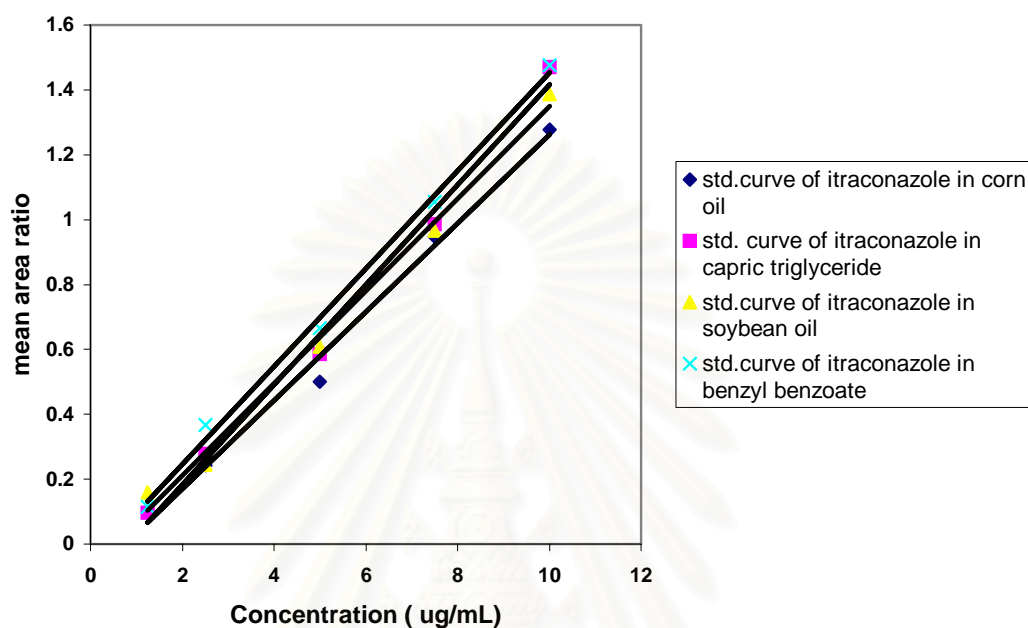
Table App. D.5 Linear regression analysis of standard curve of itraconazole in

different oil.

Standard curve of itraconazole in different oil	Regression equation	R-Square
Benzyl benzoate	y = 0.1511x - 0.0575	0.996
Soybean oil	y = 0.1458x - 0.1033	0.997
Corn oil	y = 0.1367x - 0.1043	0.991
Capric triglyceride	y = 0.1542x - 0.1261	0.992

Table App. D.6   The particle size of itraconazole-loaded PIBCA nanoparticles and itraconazole-loaded PLGA nanoparticles at time 0, 30, 60 and 90 days.

Polymer	Replication	Days			
		0	30	60	90
PIBCA	1	171.04	170.14	169.75	168.25
	2	168.02	167.98	168.25	167.21
	3	169.58	168.50	165.62	166.27
	Mean	169.55	168.87	167.87	167.24
	S.D.	1.510	1.127	2.091	0.990
PLGA	1	336.87	335.82	335.65	335.45
	2	339.87	338.91	335.65	336.45
	3	338.56	337.65	338.94	335.87
	Mean	338.43	337.46	336.75	335.92
	S.D.	1.504	1.554	1.899	0.502

Table App. D.7 The itraconazole encapsulation efficiency of itraconazole-loaded PIBCA nanoparticles and itraconazole-loaded PLGA nanoparticles at time 0, 30, 60 and 90 days.

Poymer	Replication	Days			
		0	30	60	90
PIBCA	1	70.26	68.24	41.83	31.17
	2	70.74	69.92	44.48	31.68
	3	71.03	67.29	37.88	30.27
	Mean	70.67	68.48	41.39	31.04
	S.D.	0.39	1.33	3.32	0.71
PLGA	1	70.34	23.23	5.94	2.04
	2	71.45	21.59	6.54	2.31
	3	70.75	22.45	6.37	2.45
	Mean	70.85	22.42	6.28	2.27
	S.D.	0.56	0.82	0.31	0.21

Table App. D.8 The relative itraconazole encapsulation efficiency of itraconazole-loaded PIBCA nanoparticles and itraconazole-loaded PLGA nanoparticles after storage 0, 30, 60 and 90 days.

Polymer	Replication	Relative encapsulation efficiency		
		30/0	60/0	90/0
PIBCA	1	96.07	58.89	43.88
	2	98.44	62.62	44.60
	3	94.73	53.33	42.61
	Mean	96.41	58.28	43.70
	S.D.	1.87	4.68	1.01
PLGA	1	32.83	8.40	2.88
	2	30.52	9.24	3.27
	3	31.73	9.00	3.46
	Mean	31.69	8.88	3.20
	S.D.	1.16	0.44	0.29

Table App. D.9 The zeta potential of itraconazole-loaded PIBCA nanoparticles and itraconazole-loaded PLGA nanoparticles after storage 0, 30, 60 and 90 days.

Polymer	Replication	Zeta potential			
			30	60	90
PIBCA	1	-46.7	-40.2	-31.5	-25.5
	2	-45.4	-39.9	-30.5	-23.5
	3	-42.8	-38.7	-29.4	-24.6
	Mean	-45.0	-39.6	-30.5	-24.5
	S.D.	1.986	0.794	1.050	1.002
PLGA	1	-32.5	-25.6	-19.2	-17.7
	2	-35.6	-24.9	-20.5	-15.2
	3	-32.4	-23.1	-18.9	-16.9
	Mean	-33.5	-24.5	-19.5	-16.6
	S.D.	1.819	1.290	0.850	1.277

APPENDIX E

Cytotoxic Determination : Optical Density and

% Viability of Vero Cell.

Table App. E.1 Optical density measured at 620 nm after 1 h incubation : 0.5% of test preparations.

No.	Control	0.5% Poloxamer	0.5% Plain PLGA	0.5% Loaded PLGA	0.5% Plain PIBCA	0.5% Loaded PIBCA
1	0.936	0.864	0.935	0.908	0.959	0.954
2	1.007	1.149	1.056	1.055	1.055	1.086
3	0.991	1.084	1.015	1.071	1.028	1.102
4	1.033	1.027	1.083	1.103	0.988	1.014
5	1.000	0.946	1.002	1.015	1.037	1.069
6	1.076	0.994	0.986	1.013	1.028	0.996
7	1.075	1.021	1.079	1.055	1.039	1.036
8	1.070	0.967	0.989	1.016	0.979	0.947
Mean	1.024	1.007	1.018	1.030	1.014	1.026
S.D.	0.050	0.087	0.051	0.058	0.034	0.058
C.V.	4.843	8.615	5.037	5.670	3.365	5.685

Table App. E.2 % Viability of Vero cell after 1 h incubation : 0.5% of test preparations.

No.	0.5% Poloxamer	0.5% Plain PLGA	0.5% Loaded PLGA	0.5% Plain PIBCA	0.5% Loaded PIBCA
1	84.375	91.309	88.672	93.652	93.164
2	112.207	103.125	103.027	103.027	106.055
3	105.859	99.121	104.590	100.391	107.617
4	100.293	105.762	107.715	96.484	99.023
5	92.383	97.852	99.121	101.270	104.395
6	97.070	96.289	98.926	100.391	97.266
7	99.707	105.371	103.027	101.465	101.172
8	94.434	96.582	99.219	95.605	92.480
Mean	98.291	99.426	100.537	99.036	100.146
S.D.	8.467	5.008	5.701	3.333	5.693
C.V.	8.615	5.037	5.670	3.365	5.685

Table App. E.3 Optical density measured at 620 nm after 2 h incubation : 0.5% of test preparations.

No.	Control	0.5% Poloxamer	0.5% Plain PLGA	0.5% Loaded PLGA	0.5% Plain PIBCA	0.5% Loaded PIBCA
1	0.961	0.958	1.087	0.971	1.032	0.946
2	1.073	1.123	1.076	1.099	1.028	1.111
3	1.213	1.082	1.099	1.066	1.140	1.084
4	1.241	1.070	1.144	1.085	1.122	1.107
5	1.257	1.019	1.078	1.107	1.112	1.126
6	1.173	1.049	1.066	1.128	1.155	1.130
7	1.164	1.220	1.122	1.163	1.096	1.110
8	1.137	1.069	0.918	1.029	1.038	1.028
Mean	1.152	1.074	1.074	1.081	1.090	1.080
S.D.	0.097	0.076	0.068	0.060	0.051	0.063
C.V.	8.439	7.121	6.338	5.526	4.674	5.842

Table App. E.4 % % Viability of Vero cell after 2 h incubation : 0.5% of test preparations.

No.	0.5% Poloxamer	0.5% Plain PLGA	0.5% Loaded PLGA	0.5% Plain PIBCA	0.5% Loaded PIBCA
1	83.160	94.358	84.288	89.583	82.118
2	97.483	93.403	95.399	89.236	96.441
3	93.924	95.399	92.535	98.958	94.097
4	92.882	99.306	94.184	97.396	96.094
5	88.455	93.576	96.094	96.528	97.743
6	91.059	92.535	97.917	100.260	98.090
7	105.903	97.396	100.955	95.139	96.354
8	92.795	79.688	89.323	90.104	89.236
Mean	93.207	93.207	93.837	94.651	93.772
S.D.	6.638	5.907	5.185	4.424	5.478
C.V.	7.121	6.338	5.526	4.674	5.842

Table App. E.5   Optical density measured at 620 nm after 3 h incubation : 0.5%

of test preparations.

No.	Control	0.5% Poloxamer	0.5% Plain PLGA	0.5% Loaded PLGA	0.5% Plain PIBCA	0.5% Loaded PIBCA
1	1.215	1.080	1.063	1.111	1.018	1.017
2	1.236	1.173	1.076	1.184	1.111	1.117
3	1.253	1.191	1.062	1.156	0.998	1.003
4	1.248	1.145	1.126	1.113	1.113	0.997
5	1.260	1.058	1.181	1.111	1.110	1.012
6	1.260	1.173	1.163	1.140	1.023	1.104
7	1.228	1.182	1.189	1.084	0.996	1.107
8	1.162	1.063	1.049	1.043	1.077	1.077
Mean	1.233	1.133	1.114	1.118	1.056	1.054
S.D.	0.033	0.057	0.058	0.043	0.052	0.052
C.V.	2.652	4.997	5.217	3.883	4.951	4.914

Table App. E.6 % Viability of Vero cell after 3 h incubation : 0.5% of test

preparations.

No.	0.5% Poloxamer	0.5% Plain PLGA	0.5% Loaded PLGA	0.5% Plain PIBCA	0.5% Loaded PIBCA
1	87.591	86.212	90.105	82.563	82.482
2	95.134	87.267	96.026	90.105	90.592
3	96.594	86.131	93.755	80.941	81.346
4	92.863	91.322	90.268	90.268	80.860
5	85.807	95.783	90.105	90.024	82.076
6	95.134	94.323	92.457	82.968	89.538
7	95.864	96.431	87.916	80.779	89.781
8	86.212	85.077	84.590	87.348	87.348
Mean	91.900	90.318	90.653	85.624	85.503
S.D.	4.592	4.712	3.520	4.240	4.202
C.V.	4.997	5.217	3.883	4.951	4.914

Table App. E.7   Optical density measured at 620 nm after 4 h incubation : 0.5%
of test preparations.

No.	Control	0.5% Poloxamer	0.5% Plain PLGA	0.5% Loaded PLGA	0.5% Plain PIBCA	0.5% Loaded PIBCA
1	1.293	1.297	1.138	1.099	1.225	1.188
2	1.412	1.281	1.325	1.315	1.113	1.203
3	1.397	1.449	1.339	1.363	1.203	1.221
4	1.403	1.319	1.401	1.317	1.112	1.225
5	1.481	1.306	1.258	1.313	1.293	1.105
6	1.433	1.368	1.258	1.350	1.145	1.373
7	1.484	1.264	1.269	1.287	1.114	1.114
8	1.343	1.199	1.089	1.093	1.050	1.166
Mean	1.406	1.310	1.260	1.267	1.157	1.199
S.D.	0.065	0.074	0.103	0.108	0.078	0.083
C.V.	4.602	5.640	8.193	8.538	6.746	6.956

Table App. E.8 % Viability of Vero cell after 4 h incubation : 0.5% of test
preparations.

No.	0.5% Poloxamer	0.5% Plain PLGA	0.5% Loaded PLGA	0.5% Plain PIBCA	0.5%Loaded PIBCA
1	92.248	80.939	78.165	87.127	84.495
2	91.110	94.239	93.528	79.161	85.562
3	103.058	95.235	96.942	85.562	86.842
4	93.812	99.644	93.670	79.090	87.127
5	92.888	89.474	93.385	91.963	78.592
6	97.297	89.474	96.017	81.437	97.653
7	89.900	90.256	91.536	79.232	79.232
8	85.277	77.454	77.738	74.680	82.930
Mean	93.199	89.589	90.123	82.281	85.304
S.D.	5.256	7.340	7.694	5.551	5.934
C.V.	5.640	8.193	8.538	6.746	6.956

Table App. E.9 Optical density measured at 620 nm after 1 h incubation : 1% of test preparations.

No.	Control	1% Poloxamer	1% Plain PLGA	1% Loaded PLGA	1% Plain PIBCA	1% Loaded PIBCA
1	0.936	0.996	0.931	0.904	0.896	0.798
2	1.007	0.956	1.080	1.037	0.962	1.007
3	0.991	1.084	1.022	1.030	1.027	1.051
4	1.033	1.027	1.009	1.029	1.037	0.957
5	1.000	1.011	0.996	1.028	0.937	1.010
6	1.076	0.994	1.026	1.040	1.057	1.003
7	1.075	1.021	1.071	1.007	0.993	0.899
8	1.070	0.967	1.023	0.995	0.913	0.837
Mean	1.024	1.007	1.020	1.009	0.978	0.945
S.D.	0.050	0.040	0.046	0.045	0.060	0.091
C.V.	4.843	3.942	4.519	4.460	6.141	9.647

Table App. E.10 % Viability of Vero cell after 1 h incubation : 1% of test preparations.

No.	1% Poloxamer	1% Plain PLGA	1% Loaded PLGA	1% Plain PIBCA	1%Loaded PIBCA
1	97.266	90.918	88.281	87.500	77.930
2	93.359	105.469	101.270	93.945	98.340
3	105.859	99.805	100.586	100.293	102.637
4	100.293	98.535	100.488	101.270	93.457
5	98.730	97.266	100.391	91.504	98.633
6	97.070	100.195	101.563	103.223	97.949
7	99.707	104.590	98.340	96.973	87.793
8	94.434	99.902	97.168	89.160	81.738
Mean	98.340	99.585	98.511	95.483	92.310
S.D.	3.877	4.501	4.394	5.863	8.905
C.V.	3.942	4.519	4.460	6.141	9.647

Table App. E.11 Optical density measured at 620 nm after 2 h incubation : 1% of test preparations.

No.	Control	1% Poloxamer	1% Plain PLGA	1% Loaded PLGA	1% Plain PIBCA	1% Loaded PIBCA
1	0.961	0.958	0.995	0.973	0.480	0.418
2	1.073	1.123	1.074	1.072	0.548	0.518
3	1.213	1.082	1.033	1.053	0.505	0.542
4	1.241	1.070	1.017	1.079	0.516	0.507
5	1.257	1.019	1.116	1.066	0.489	0.573
6	1.173	1.049	1.121	1.053	0.538	0.555
7	1.164	1.220	0.919	1.041	0.523	0.518
8	1.137	1.069	0.986	0.976	0.458	0.448
Mean	1.152	1.074	1.033	1.039	0.507	0.510
S.D.	0.097	0.076	0.069	0.042	0.030	0.053
C.V.	8.439	7.121	6.671	4.007	5.980	10.342

Table App. E.12 % Viability of Vero cell after 2 h incubation : 1% of test preparations.

No.	1% Poloxamer	1% Plain PLGA	1% Loaded PLGA	1% Plain PIBCA	1%Loaded PIBCA
1	83.160	86.372	84.462	41.667	36.285
2	97.483	93.229	93.056	47.569	44.965
3	93.924	89.670	91.406	43.837	47.049
4	92.882	88.281	93.663	44.792	44.010
5	88.455	96.875	92.535	42.448	49.740
6	91.059	97.309	91.406	46.701	48.177
7	105.903	79.774	90.365	45.399	44.965
8	92.795	85.590	84.722	39.757	38.889
Mean	93.207	89.638	90.202	44.021	44.260
S.D.	6.638	5.980	3.615	2.632	4.577
C.V.	7.121	6.671	4.007	5.980	10.342

Table App. E.13 Optical density measured at 620 nm after 3 h incubation : 1% of test preparations.

No.	Control	1% Poloxamer	1% Plain PLGA	1% Loaded PLGA	1% Plain PIBCA	1% Loaded PIBCA
1	1.215	1.080	1.095	1.035	0.463	0.494
2	1.236	1.173	1.207	1.154	0.537	0.637
3	1.253	1.191	1.189	1.276	0.551	0.545
4	1.248	1.145	1.174	1.047	0.388	0.633
5	1.260	1.058	1.105	1.161	0.532	0.523
6	1.260	1.173	1.113	1.139	0.557	0.533
7	1.228	1.182	1.121	1.185	0.517	0.517
8	1.162	1.063	1.069	1.148	0.440	0.494
Mean	1.233	1.133	1.134	1.143	0.498	0.547
S.D.	0.033	0.057	0.049	0.076	0.061	0.057
C.V.	2.652	4.997	4.364	6.680	12.239	10.431

Table App. E.14   % Viability of Vero cell after 3 h incubation : 1% of test preparations.

No.	1% Poloxamer	1% Plain PLGA	1% Loaded PLGA	1% Plain PIBCA	1%Loaded PIBCA
1	87.591	88.808	83.942	37.551	40.065
2	95.134	97.891	93.593	43.552	51.663
3	96.594	96.431	103.487	44.688	44.201
4	92.863	95.215	84.915	31.468	51.338
5	85.807	89.619	94.161	43.147	42.417
6	95.134	90.268	92.376	45.174	43.228
7	95.864	90.916	96.107	41.930	41.930
8	86.212	86.699	93.106	35.685	40.065
Mean	91.900	91.981	92.711	40.399	44.363
S.D.	4.592	4.014	6.193	4.944	4.628
C.V.	4.997	4.364	6.680	12.239	10.431

Table App. E.15 Optical density measured at 620 nm after 4 h incubation : 1% of test preparations.

No.	Control	1% Poloxamer	1% Plain PLGA	1% Loaded PLGA	1% Plain PIBCA	1% Loaded PIBCA
1	1.293	1.297	1.265	1.324	0.433	0.386
2	1.412	1.281	1.276	1.292	0.503	0.512
3	1.397	1.449	1.256	1.207	0.499	0.500
4	1.403	1.319	1.249	1.277	0.493	0.475
5	1.481	1.306	1.321	1.282	0.493	0.484
6	1.433	1.368	1.237	1.216	0.512	0.528
7	1.484	1.264	1.362	1.220	0.491	0.481
8	1.343	1.199	1.213	1.378	0.360	0.448
Mean	1.406	1.310	1.272	1.275	0.473	0.477
S.D.	0.065	0.074	0.048	0.059	0.052	0.044
C.V.	4.602	5.640	3.764	4.640	10.895	9.227

Table App. E.16 % Viability of Vero cell after 4 h incubation : 1% of test preparations.

No.	1% Poloxamer	1% Plain PLGA	1% Loaded PLGA	1% Plain PIBCA	1% Loaded PIBCA
1	92.248	89.972	94.168	30.797	27.454
2	91.110	90.754	91.892	35.775	36.415
3	103.058	89.331	85.846	35.491	35.562
4	93.812	88.834	90.825	35.064	33.784
5	92.888	93.954	91.181	35.064	34.424
6	97.297	87.980	86.486	36.415	37.553
7	89.900	96.871	86.771	34.922	34.211
8	85.277	86.273	98.009	25.605	31.863
Mean	93.199	90.496	90.647	33.642	33.908
S.D.	5.256	3.406	4.206	3.665	3.129
C.V.	5.640	3.764	4.640	10.895	9.227

Table App. E.17 Optical density measured at 620 nm after 4 h incubation with various concentrations of Plain PLGA nanoparticles.

No.	Control	0.2	0.4	0.6	0.8	1	5	10	20	40	80	100
1	0.940	0.925	0.987	0.975	0.965	0.904	0.645	0.205	0.081	0.000	0.000	0.000
2	1.154	1.058	1.016	0.995	0.934	0.857	0.653	0.214	0.082	0.000	0.000	0.000
3	1.092	1.058	0.931	1.009	0.914	0.977	0.695	0.197	0.081	0.000	0.000	0.000
4	1.033	1.093	1.074	1.021	0.935	0.945	0.679	0.164	0.078	0.000	0.000	0.000
5	1.023	1.067	1.034	0.966	0.977	0.986	0.647	0.214	0.079	0.000	0.000	0.000
6	0.982	1.059	1.086	0.945	0.980	0.977	0.705	0.209	0.068	0.000	0.000	0.000
7	1.088	0.992	1.053	0.974	0.956	1.003	0.689	0.230	0.072	0.000	0.000	0.000
8	1.041	1.072	1.073	0.965	0.947	0.915	0.659	0.204	0.067	0.000	0.000	0.000
Mean	1.044	1.040	1.032	0.981	0.951	0.946	0.672	0.204	0.076	0.000	0.000	0.000
S.D.	0.067	0.055	0.052	0.025	0.023	0.050	0.023	0.019	0.006	0.000	0.000	0.000
C.V.	6.432	5.279	5.088	2.567	2.408	5.276	3.487	9.346	8.019	0.000	0.000	0.000

Table App. E.18 % Viability of Vero cell after 4 h incubation with various concentrations of Plain PLGA nanoparticles.

No.	0.2	0.4	0.6	0.8	1	5	10	20	40	80	100
1	88.554	94.540	93.391	92.385	86.590	61.782	19.588	7.759	0.000	0.000	0.000
2	101.293	97.318	95.307	89.416	82.088	62.548	20.450	7.854	0.000	0.000	0.000
3	101.293	89.176	96.648	87.500	93.582	66.571	18.822	7.759	0.000	0.000	0.000
4	104.646	102.874	97.797	89.511	90.517	65.038	15.661	7.471	0.000	0.000	0.000
5	102.155	99.042	92.529	93.534	94.444	61.973	20.450	7.567	0.000	0.000	0.000
6	101.389	104.023	90.517	93.822	93.582	67.529	19.971	6.513	0.000	0.000	0.000
7	94.971	100.862	93.295	91.523	96.073	65.996	21.983	6.897	0.000	0.000	0.000
8	102.634	102.778	92.433	90.661	87.644	63.123	19.492	6.418	0.000	0.000	0.000
Mean	99.617	98.827	93.989	91.044	90.565	64.320	19.552	7.280	0.000	0.000	0.000
S.D.	5.259	5.028	2.413	2.193	4.778	2.243	1.827	0.584	0.000	0.000	0.000
C.V.	5.279	5.088	2.567	2.408	5.276	3.487	9.346	8.019	0.000	0.000	0.000

Table App. E.19   Optical density measured at 620 nm after 4 h incubation with various concentrations of itraconazole- loaded PLGA nanoparticles.

No.	Control	0.2	0.4	0.6	0.8	1	5	10	20	40	80	100
1	1.094	1.032	1.003	1.000	0.984	0.975	0.670	0.204	0.078	0.000	0.000	0.000
2	1.102	1.074	1.038	1.023	1.034	0.984	0.675	0.203	0.090	0.000	0.000	0.000
3	1.027	1.178	1.098	1.014	0.948	0.983	0.670	0.232	0.076	0.000	0.000	0.000
4	1.048	0.980	1.017	1.032	0.990	0.904	0.701	0.209	0.095	0.000	0.000	0.000
5	1.045	1.039	1.033	1.005	0.892	0.997	0.657	0.211	0.080	0.000	0.000	0.000
6	1.115	0.949	1.039	1.012	0.998	0.979	0.673	0.217	0.075	0.000	0.000	0.000
7	1.075	1.108	1.034	1.004	1.003	0.977	0.677	0.231	0.081	0.000	0.000	0.000
8	1.073	1.059	1.084	1.006	1.000	0.993	0.689	0.254	0.080	0.000	0.000	0.000
Mean	1.072	1.052	1.043	1.012	0.981	0.974	0.677	0.220	0.082	0.000	0.000	0.000
S.D.	0.031	0.072	0.032	0.011	0.043	0.029	0.013	0.018	0.007	0.000	0.000	0.000
C.V.	2.857	6.809	3.075	1.068	4.402	3.007	1.964	8.029	8.548	0.000	0.000	0.000

Table App. E.20 % Viability of Vero cell after 4 h incubation with various concentrations of itraconazole- loaded PLGA nanoparticles.

No.	0.2	0.4	0.6	0.8	1	5	10	20	40	80	100
1	96.222	93.563	93.284	91.744	90.951	63.688	18.983	7.276	0.000	0.000	0.000
2	100.140	96.828	95.429	96.409	91.791	64.163	18.890	8.396	0.000	0.000	0.000
3	109.841	102.425	94.590	88.386	91.698	63.688	21.595	7.090	0.000	0.000	0.000
4	91.371	94.869	96.269	92.304	84.328	66.635	19.450	8.862	0.000	0.000	0.000
5	96.875	96.362	93.750	83.162	93.004	62.452	19.636	7.463	0.000	0.000	0.000
6	88.479	96.922	94.403	93.050	91.325	63.973	20.196	6.996	0.000	0.000	0.000
7	103.312	96.455	93.657	93.517	91.138	64.354	21.502	7.556	0.000	0.000	0.000
8	98.741	101.119	93.843	93.237	92.631	65.494	23.647	7.463	0.000	0.000	0.000
Mean	98.123	97.318	94.403	91.476	90.858	64.306	20.487	7.638	0.000	0.000	0.000
S.D.	6.681	2.992	1.008	4.027	2.732	1.263	1.645	0.653	0.000	0.000	0.000
C.V.	6.809	3.075	1.068	4.402	3.007	1.964	8.029	8.548	0.000	0.000	0.000

Table App. E.21 Optical density measured at 620 nm after 4 h incubation with various concentrations of Plain PIBCA nanoparticles.

No.	Control	0.2	0.4	0.6	0.8	1	5	10	20	40	80	100
1	1.031	1.062	1.016	0.785	0.480	0.323	0.387	0.301	0.074	0.000	0.000	0.000
2	1.081	1.109	1.048	0.765	0.481	0.363	0.363	0.335	0.065	0.000	0.000	0.000
3	1.100	1.144	1.035	0.763	0.476	0.341	0.391	0.307	0.064	0.000	0.000	0.000
4	1.134	1.121	1.049	0.742	0.478	0.426	0.334	0.358	0.066	0.000	0.000	0.000
5	0.965	1.069	1.090	0.745	0.491	0.387	0.345	0.346	0.067	0.000	0.000	0.000
6	1.157	1.129	1.101	0.732	0.468	0.379	0.415	0.367	0.066	0.000	0.000	0.000
7	1.229	1.166	1.135	0.721	0.484	0.389	0.341	0.356	0.068	0.000	0.000	0.000
8	1.114	1.203	1.090	0.769	0.470	0.381	0.345	0.346	0.054	0.000	0.000	0.000
Mean	1.101	1.125	1.070	0.753	0.479	0.373	0.365	0.339	0.066	0.000	0.000	0.000
S.D.	0.080	0.047	0.040	0.021	0.007	0.032	0.029	0.024	0.006	0.000	0.000	0.000
C.V.	7.245	4.184	3.713	2.829	1.548	8.464	8.019	7.057	8.481	0.000	0.000	0.000

Table App. E.22 % Viability of Vero cell after 4 h incubation with various concentrations of Plain PIBCA nanoparticles.

No.	0.2	0.4	0.6	0.8	1	5	10	20	40	80	100
1	96.458	92.234	71.299	43.597	29.292	35.150	27.323	6.721	0.000	0.000	0.000
2	100.727	95.141	69.482	43.688	32.925	32.970	30.411	5.904	0.000	0.000	0.000
3	103.906	93.960	69.301	43.233	30.926	35.513	27.868	5.813	0.000	0.000	0.000
4	101.817	95.232	67.393	43.415	38.647	30.336	32.500	5.995	0.000	0.000	0.000
5	97.094	98.955	67.666	44.596	35.104	31.335	31.410	6.085	0.000	0.000	0.000
6	102.543	99.955	66.485	42.507	34.378	37.693	33.318	5.995	0.000	0.000	0.000
7	105.904	103.043	65.486	43.960	35.286	30.972	32.318	6.176	0.000	0.000	0.000
8	109.264	98.955	69.846	42.688	34.559	31.335	31.410	4.905	0.000	0.000	0.000
Mean	102.214	97.184	68.370	43.460	33.890	33.163	30.820	5.949	0.000	0.000	0.000
S.D.	4.276	3.609	1.934	0.673	2.868	2.659	2.175	0.505	0.000	0.000	0.000
C.V.	4.184	3.713	2.829	1.548	8.464	8.019	7.057	8.481	0.000	0.000	0.000

Table App. E.23 Optical density measured at 620 nm after 4 h incubation with various concentrations of itraconazole- loaded PIBCA nanoparticles.

No.	Control	0.2	0.4	0.6	0.8	1	5	10	20	40	80	100
1	1.127	1.228	1.163	0.754	0.443	0.374	0.367	0.333	0.074	0.000	0.000	0.000
2	1.074	1.186	1.083	0.752	0.522	0.388	0.376	0.342	0.060	0.000	0.000	0.000
3	1.142	1.184	1.169	0.768	0.533	0.370	0.368	0.332	0.058	0.000	0.000	0.000
4	1.150	1.147	1.137	0.756	0.513	0.379	0.343	0.351	0.061	0.000	0.000	0.000
5	1.021	1.123	1.156	0.759	0.439	0.376	0.391	0.349	0.068	0.000	0.000	0.000
6	1.147	1.087	1.156	0.760	0.479	0.373	0.374	0.347	0.066	0.000	0.000	0.000
7	1.167	1.132	1.145	0.764	0.468	0.372	0.378	0.350	0.074	0.000	0.000	0.000
8	1.085	1.141	1.143	0.770	0.465	0.385	0.369	0.342	0.061	0.000	0.000	0.000
Mean	1.114	1.154	1.144	0.760	0.483	0.377	0.371	0.343	0.065	0.000	0.000	0.000
S.D.	0.050	0.044	0.027	0.007	0.036	0.006	0.014	0.007	0.006	0.000	0.000	0.000
C.V.	4.454	3.814	2.348	0.855	7.436	1.706	3.669	2.168	9.649	0.000	0.000	0.000

Table App. E.24 % Viability of Vero cell after 4 h incubation with various concentrations of itraconazole- loaded PIBCA nanoparticles.

No.	0.2	0.4	0.6	0.8	1	5	10	20	40	80	100
1	110.233	104.354	67.684	39.767	33.528	32.944	29.892	6.643	0.000	0.000	0.000
2	106.463	97.172	67.504	46.858	34.785	33.752	30.700	5.386	0.000	0.000	0.000
3	106.284	104.892	68.941	47.846	33.169	33.034	29.803	5.206	0.000	0.000	0.000
4	102.962	102.020	67.864	46.050	33.977	30.790	31.508	5.476	0.000	0.000	0.000
5	100.808	103.725	68.133	39.408	33.707	35.099	31.329	6.104	0.000	0.000	0.000
6	97.576	103.725	68.223	42.998	33.438	33.573	31.149	5.925	0.000	0.000	0.000
7	101.616	102.738	68.582	42.011	33.348	33.932	31.418	6.643	0.000	0.000	0.000
8	102.424	102.558	69.120	41.741	34.515	33.124	30.700	5.476	0.000	0.000	0.000
Mean	103.546	102.648	68.256	43.335	33.808	33.281	30.812	5.857	0.000	0.000	0.000
STD	3.949	2.410	0.584	3.223	0.577	1.221	0.668	0.565	0.000	0.000	0.000
C.V.	3.814	2.348	0.855	7.436	1.706	3.669	2.168	9.649	0.000	0.000	0.000

VITA

Mrs. Mukdavan Prakobvaitayakit was born on May 2, 1964 in Mukdaharn, Thailand. She obtained her Bachelor degree of Science in Pharmacy with 2nd class honors from the Faculty of Pharmaceutical Science, Chulalongkorn University, Bangkok in 1988. In 1992 she earned her second degree in Master of Science in Pharmacy from the Faculty of Pharmaceutical Science, Chulalongkorn University, Bangkok. After graduation, she started working for the Government of Pharmaceutical Organization (GPO), Bangkok in 1995 as Production Supervisor in Mixture Section of Production Department. In 1996 she was promoted to be Head of Penicillin Section 3. In 1995 she got a scholarship form Japanese Internationational Corporation Agency(JICA) for training course of Organic Fine Chemical Technology in Osaka , Japan for 4 months.

Mrs. Mukdavan Prakobvaitayakit joined the graduate program for the Doctor of Philosophy degree in Pharmacy at Chulalongkorn University in 1999.   In 2003 she got poster presentation at 2003 Annual Meeting at Salt Lake City, Utah, USA. Her abstracts were published in AAPS PharmSci Vol. 5, No. 4, Abstract W4175 (2003) , and AAPS PharmSci Vol. 5, No. 4, Abstract W5151 (2003). Her article entitled "Optimization of Polylactic-Co-Glycolic Acid Nanoparticles Containing Itraconazole Using 2^3 Factorial Design" was published in AAPS PharmSciTech Vol4, Issue 4 As Article 71 (2003).

Mrs. Mukdavan Prakobvaitayakit is the member of The Pharmacy Council in Thailand, The American Association of Pharmaceutical Scientist and L'Actim Thailand Club. She is also invited to be one of the reviewers of AAPS PharmSciTech.